ISSN 2518-718X (Print)
ISSN 2663-4872 (Online)

№ 2(94)/2019

ХИМИЯ сериясы
Серия ХИМИЯ
CHEMISTRY Series

ҚАРАҒАНДЫ УНИВЕРСИТЕТІНІҢ ХАБАРШЫСЫ

ВЕСТНИК КАРАГАНДИНСКОГО УНИВЕРСИТЕТА

BULLETIN OF THE KARAGANDA UNIVERSITY

ISSN 2518-718X (Print)
ISSN 2663-4872 (Online)
Индексі 74617
Индекс 74617

ҚАРАҒАНДЫ УНИВЕРСИТЕТІНІҢ ХАБАРШЫСЫ

ВЕСТНИК КАРАГАНДИНСКОГО УНИВЕРСИТЕТА

BULLETIN OF THE KARAGANDA UNIVERSITY

ХИМИЯ сериясы

Серия ХИМИЯ

CHEMISTRY Series

№ 2(94)/2019

Сәуір–мамыр–маусым
28 маусым 2019 ж.

Апрель–май–июнь
28 июня 2019 г.

April–May–June
June, 28, 2019

1996 жылдан бастап шығады
Издается с 1996 года
Founded in 1996

Жылына 4 рет шығады
Выходит 4 раза в год
Published 4 times a year

Қарағанды, 2019
Караганда, 2019
Karaganda, 2019

Редакцияның мекенжайы: 100024, Қазақстан, Қарағанды қ., Университет к-сі, 28
Тел.: (7212) 77-03-69 (ішкі 1026); факс: (7212) 77-03-84.
E-mail: vestnick_kargu@ksu.kz; yelenaminayeva@yandex.ru (*жауапты хатшы*)
Сайты: http://chemistry-vestnik.ksu.kz

Қарағанды университетінің хабаршысы. Химия сериясы.
ISSN 2518-718X (Print). ISSN 2663-4872 (Online).
Меншік иесі: «Академик Е.А. Бөкетов атындағы Қарағанды мемлекеттік университеті» РММ.
Қазақстан Республикасының Мәдениет және ақпарат министрлігімен тіркелген. 23.10.2012 ж. № 13110–Ж тіркеу куәлігі.

Басуға 29.06.2019 ж. қол қойылды. Пішімі 60×84 1/8. Қағазы офсеттік. Көлемі 13,37 б.т. Таралымы 300 дана. Бағасы келісім бойынша. Тапсырыс № 73.
Е.А. Бөкетов атындағы ҚарМУ баспасының баспаханасында басылып шықты.
100012, Қазақстан, Қарағанды қ., Гоголь к-сі, 38. Тел. 51-38-20. E-mail: izd_kargu@mail.ru

Адрес редакции: 100024, Казахстан, г. Караганда, ул. Университетская, 28
Тел.: (7212) 77-03-69 (внутр. 1026); факс: (7212) 77-03-84.
E-mail: vestnick_kargu@ksu.kz; yelenaminayeva@yandex.ru (*отв. секретарь*)
Сайт: http://chemistry-vestnik.ksu.kz

Вестник Карагандинского университета. Серия Химия.

ISSN 2518-718X (Print). ISSN 2663-4872 (Online).

Собственник: РГП «Карагандинский государственный университет имени академика Е.А. Букетова».

Зарегистрирован Министерством культуры и информации Республики Казахстан. Регистрационное свидетельство № 13110–Ж от 23.10.2012 г.

Подписано в печать 29.06.2019 г. Формат 60×84 1/8. Бумага офсетная. Объем 13,37 п.л. Тираж 300 экз. Цена договорная. Заказ № 73.

Отпечатано в типографии издательства КарГУ им. Е.А. Букетова.
100012, Казахстан, г. Караганда, ул. Гоголя, 38, тел.: (7212) 51-38-20. E-mail: izd_kargu@mail.ru

Postal address: 28, University Str., Karaganda, 100024, Kazakhstan

Tel.: (7212) 77-03-69 (add. 1026); fax: (7212) 77-03-84.

E-mail: vestnick_kargu@ksu.kz; yelenaminayeva@yandex.ru (*secretary*)

Web-site: http://chemistry-vestnik.ksu.kz

Bulletin of the Karaganda University. Chemistry series.

ISSN 2518-718X (Print). ISSN 2663-4872 (Online).

Proprietary: RSE «Academician Ye.A. Buketov Karaganda State University».

Registered by the Ministry of Culture and Information of the Republic of Kazakhstan. Registration certificate No. 13110–Zh from 23.10.2012.

Signed in print 29.06.2019. Format 60×84 1/8. Offset paper. Volume 13,37 p.sh. Circulation 300 copies. Price upon request. Order № 73.

Printed in the Ye.A. Buketov Karaganda State University Publishing house.

38, Gogol Str., Karaganda, 100012, Kazakhstan. Tel.: (7212) 51-38-20. E-mail: izd_kargu@mail.ru

МАЗМҰНЫ

ОРГАНИКАЛЫҚ ХИМИЯ

ФИЗИКАЛЫҚ ЖӘНЕ АНАЛИТИКАЛЫҚ ХИМИЯ

БЕЙОРГАНИКАЛЫҚ ХИМИЯ

ХИМИЯЛЫҚ ТЕХНОЛОГИЯ

ХИМИЯНЫ ОҚЫТУ ӘДІСТЕМЕСІ

ҒЫЛЫМИ ЗЕРТТЕУДІ ШОЛУ

СОДЕРЖАНИЕ

ОРГАНИЧЕСКАЯ ХИМИЯ

ФИЗИЧЕСКАЯ И АНАЛИТИЧЕСКАЯ ХИМИЯ

НЕОРГАНИЧЕСКАЯ ХИМИЯ

ХИМИЧЕСКАЯ ТЕХНОЛОГИЯ

МЕТОДИКА ОБУЧЕНИЯ ХИМИИ

ОБЗОР НАУЧНЫХ ИССЛЕДОВАНИЙ

CONTENTS

ORGANIC CHEMISTRY

PHYSICAL AND ANALYTICAL CHEMISTRY

INORGANIC CHEMISTRY

CHEMICAL TECHNOLOGY

METHODS OF TEACHING CHEMISTRY

REVIEW OF RESEARCH

DOI 10.31489/2019Ch2/8-13

UDC 542.9:547

S. Arrous, A. Bolde, I. Boudebouz, M.V. Lyapunova, A.A. Bakibayev

National Research Tomsk State University, Russia
(E-mail: parroussalinkov@yahoo.com)

«Solvent-less» mechanochemical approach to the synthesis of allobetulin and some of its esters

Various significant biological activities have been recently found for allobetulin and its derivatives which in combination with their low toxicities lead to an increased research effort. In the present work allobetulin and some its acyl derivatives have been synthesized by different reactions using a grindstone method. All reactions were carried out at room temperature. Allobetulin (**1a**) and allobetulin 3-O-formate (**1b**) were prepared by reacting betulin with trifluoroacetic acid (TFA) and HCOOH, consecutively. The reactions time was 30–40 min, and the yield of the products was 82 and 98 %, respectively. Allobetulin (**1a**) under the action of TFA for 2 hours affords allobetulin 3-O-trifluoroacetate (**3**) in 95 % yield. Whereas, the treatment of betulin diacetate with TFA for 30 min gives allobetulin 3-O- acetate (**2a**) in 92 % yield. The formation of products was detected by TLC using C_6H_6:CH_2Cl_2:CH_3OH (5:5:1) as eluent and the spots were revealed after spraying the TLC plates with reagent (1 % phosphomolybdic acid-water) followed by heating at 110 ºC for 5 minutes to show a characteristic blue colour. The present procedure is simple, efficient, and environmentally benign. The structures of all products were confirmed by ^{1}H NMR, ^{13}C NMR, and FT-IR spectroscopy.

Keywords: betulin, allobetulin, trifluoroacetic acid, mechanochemistry, grindstone, formic acid, allobetulinformate, betulin diacetate.

Introduction

The organic solvents are volatile and harmful, causing risks to people who inhale them as well as the environment. Thus, development of less hazardous synthetic methods for organic reactions is one of our objectives in current research. One of the methods belonging to such a protocol is a grindstone method. This mechanically activated solvent-free reaction helps in reducing the toxic waste produced, and therefore, becomes less harmful to the environment. Solvent-less organic reactions based on grinding of two macroscopic particles together mostly involves the formation of a liquid phase prior to the reaction, i.e. formation of an eutectic melt of uniform distribution where the reacting components being in close proximity react in a controlled way [1].

The grindstone method has been successfully applied for many reactions like Reformatsky reaction [2], Aldol condensation [3], Dieckmann condensation [4], Knoevenagel condensation [5], Biginelli reaction [6], synthesis of carbamates [7], and others [8]. On the other hand, allobetulin has been utilized as an important precursor in the further transformation of triterpenoids [9–22] and as a sample for biological studies. Recently, considerable attention is paid to the study of their biological activity among which are compounds with anti-inflammatory, antiulcerous [23], antiviral [24, 25], and immunoregulatory activities [26], an antibacterial, hepatoprotective, and antifeedant activity [9, 27, 28].

We report herein a simple and highly efficient method for the synthesis of allobetulin and its derivatives bearing acyl moiety at C-3 by a grindstone method.

Experimental

^{1}H and ^{13}C NMR spectra have been recorded with Bruker AVANCE 400 III HD spectrometer (Bruker, Billerica, MA, USA), 400.17 and 100.63 MHz, respectively. Chemical shifts are reported relative to tetramethylsilane peak set at 0.00 ppm. In the case of multiplets the signals were reported as intervals. Signals were abbreviated as s, singlet; d, doublet; t, triplet; m, multiplet. Coupling constants were expressed in Hz.

TLC was conducted on Sorbfil plates using C_6H_6: CH_2Cl_2: CH_3OH (5:5:1). Spots were detected by spraying TLC plates with 1 % phosphomolybdic acid and heating at 110 ºC for 5 minutes to show a characteristic blue colour.

Infrared spectra were obtained directly from the products using Bruker Tensor 27 FT-IR Spectrometer. The spectra were recorded in the range of 400 to 4000 cm^{-1}. Melting temperatures have been detected in open capillaries using Buchi apparatus. Finely cut birch bark was extracted with hot ethanol to give crude betulin **1** [29].

Synthesis of compound allobetulin **1a**

0.5 g (1.1mmol.) of betulin, 15 ml of TFA were added into a porcelain mortar (8 cm diameter). After few seconds of grinding with the aid of a pestle, the reaction mixture became a dark paste. The mixture was grinded for a period of 40 minutes until totally solidified when a beige solid powder became. At the end of grinding, 10 ml of methanol was added to the mortar (to facilitate the product precipitation) and further well mixed with the product so obtained using the pestle and a spatula to remove the solid from mortar wall. The resulting solid was collected by vacuum filtration on a Büchner funnel. Yield is 98 %. R_f is 0.56 (in system A), mp is 265 ºC (lit., [30] 264–266 ºC). IR spectrum (KBr, ν, cm^{-1}): 3423.4 — OH, 2934.5–2880.7 (-CH_3 and -CH_2), 1451.6, 1381.6 (-CH_3 and -CH_2), 1039.0 (C-O-C). ^{1}H NMR spectrum (400.17 MHz, $CDCl_3$, δ, ppm, *J*/Hz): 0.78 (3H, s, CH_3), 0.81 (3H, s, CH_3), 0.86 (3H, s, CH_3), 0.93 (3H, s, CH_3), 0.95 (3H, s, CH_3), 0.99 (6H, s, CH_3), 1.20–1.73 (24H, m, CH_2, CH), 3.22 (1H, t, C_3H, *J* 5.6 Hz), 3.45 (1H, d, $C_{28}H_2$, *J* 8 Hz), 3.54 (1H, s, $C_{19}H$), 3.78 (1H, dd, $C_{28}H_2$, *J* 7.2 Hz). ^{13}C NMR spectrum (100.63 MHz, $CDCl_3$, δ, ppm): 13.52 (C27), 15.39 (C24), 15.72 (C26), 16.50 (C25), 18.26 (C6), 21.00 (C11), 24.56 (C29 or C30), 26.28 (CH_2), 26.45 (CH_2), 27.43 (C2), 27.99 (C23), 28.83 (C29 or C30), 32.72 (C21), 33.92 (C7), 34.16 (C13), 36.28 (C17), 36.76 (C16), 37.27 (C10), 38.90 (C4), 38.92 (C1), 40.62 (C), 40.72 (C), 41.49 (C), 46.84(C18), 51.09 (C9), 55.49 (C5), 71.29 (C28), 78.99 (C3), 87.94 (C19).

Synthesis of allobetulin 3-O-acetate **2a**

Betulin diacetate 0.5 g (1.1 mmol) and 15 ml of TFA were mixed and placed in a mortar and ground by hand with a pestle. Grinding was continued until the mixture appeared homogeneous and the reaction was complete (TLC), which took 0.5 h. After removal of most solvent, the residue was diluted with methanol, and the white precipitate was collected by filtration to afford white product. Yield is 92 %. R_f is 0.64 (C_6H_6:CH_2Cl_2:CH_3OH / 5:5:1), and mp is 283 ºC (lit., [31] 285–287 ºC). IR spectrum (KBr, ν, cm^{-1}): 2924.4–2856 (-CH_3 and -CH_2), 1726 (C=O), 1247.5 and 1023.3 (C-O-C). ^{1}H NMR spectrum (400.17 MHz, $CDCl_3$, δ, ppm, *J*/Hz): 0.70 (3H, s), 0.74 (3H, s), 0.75 (3H, s), 0.77 (3H, s), 0.83 (3H, s), 0.87 (3H, s), 0.94 (3H, s), 2.08 (3H, s, 3b-$COCH_3$), 3.35 (1H, d, *J*=7.6, 28-H_a), 3.46 (1H, s, 19-H), 3.70 (1H, d, *J*=7.6, 28-H_b), 4.38 (1H, m, 3α-H). ^{13}C NMR spectrum (100.63 MHz, $CDCl_3$, δ, ppm): 13.52 (C27), 15.69 (C24), 15.77 (C26), 16.50 (C25), 18.14 (C6), 20.99 (C11), 21.37, 24.55 (C29 or C30), 26.23 (CH_2), 26.42 (CH_2), 27.93 (C2), 28.36 (C23), 28.80 (C29 or C30), 32.69 (C21), 33.83 (C7), 34.13 (C13), 36.26 (C17), 36.70 (C16), 37.17 (C10), 38.59 (C4), 39.66 (C1), 40.62 (C), 40.71 (C), 41.49 (C), 46.80 (C18), 51.00 (C9), 55.56 (C5), 71.26 (C28), 80.96 (C3), 88.04 (C19), 171.15 ($CH_3\underline{C}OO$).

Synthesis of compound allobetulin 3-O-trifluoroacetate **3**

0.5 g of allobetulin (1.1 mmol), and 50 ml of TFA were added in a mortar and ground continuously. The mixture was ground until completion of the reaction, which was monitored by TLC (2h). 10 ml of methanol was added to the syrupy formed product to give a white precipitate, which filtered through the filtration flask to afford the pure product without further purification. Yield is 95 %, R_f is 0.63 (C_6H_6:CH_2Cl_2:CH_3OH / 5:5:1), and mp is 268 ºC (lit., [24] 265.5–266.8 ºC). IR spectrum (KBr, ν, cm^{-1}): 2944.6–2869.0 (-CH_3 and -CH_2), 1770.1 (C=O), 1219.3, 1188.6 and 1033.0 (C-O-C), 1166.6 (C-F). ^{1}H NMR spectrum (400.17 MHz, $CDCl_3$, δ, ppm, *J*/Hz): 0.72 (3H, s), 0.81 (3H, s), 0.82 (3H, s), 0.84 (3H, s), 0.85 (3H, s), 0.87 (3H, s), 0.91 (3H, s), 3.37 (1H, d, *J*= 7.6, 28-Ha), 3.47 (1H, s, 19a-H), 3.70 (1H, d, *J*=7.6, 28-Hb), 4.63 (1H, m, 3a-H). ^{13}C NMR spectrum (100.63 MHz, $CDCl_3$, δ, ppm): 12.46 (C27), 14.73 (C24), 15.22 (C26), 15.49 (C25),

17.04 (C6), 20.01 (C11), 22.23 (CH2), 23.52 (C29 or C30), 25.49 (CH_2), 26.73 (CH_2), 26.84 (C2), 27.77 (C23), 31.66 (C29 or C30), 32.74 (C21), 33.09 (C7), 35.24 (C13), 35.69 (C17), 36.12 (C16), 37.05 (C10), 37.39 (C4), 39.60 (C1), 39.71 (C), 40.44 (C), 45.77(C18), 49.94 (C9), 54.40 (C5), 70.22 (C28), 85.25 (C3), 86.93 (C19). 115.09 ($\underline{C}F_3COO$), 156.57 ($CF_3\underline{C}OO$).

Synthesis of compound allobetulin 3-O-formate **1b**

Betulin 0.5 g (1.1 mmol) and 25 ml TFA were taken in a pestle; the mixture was grounded till the reaction completion, which was monitored by TLC. The reaction was completed about 30 min at room temperature, after completion 10 ml of methanol was added, the precipitated product was filtered, and recrystallized in ethanol solvent. Yield is 82 %, R_f is 0.63 (C_6H_6:CH_2Cl_2:CH_3OH / 5:5:1), and mp is 314 ºC (lit., [32] 315 ºC). IR (KBr, ν, cm^{-1}): 2925 (=C-H), 1720 (C=O), 1175 (C-O-C).^{1}H NMR (400.17 MHz, $CDCl_3$, δ, ppm): 0.73 (s, 3H, CH3), 0.79 (s, 3H, CH_3), 0.80 (s, 3H, CH_3), 0.84 (s, 3H, CH_3), 0.86 (s, 3H, CH_3), 0.89 (s, 3H, CH_3), 0.97 (s, 3H, CH_3), 3.36 (d, 1H, *J* 7.6, 28-Ha), 3.47 (s, 1H, 19a-H), 3.7 (d, 1H, *J* 7.6, 28-Hb), 4.54 (m, 1H, 3a-H), 8 (s, 1H, 3b-COH). ^{13}C NMR(100.63 MHz, $CDCl_3$, δ, ppm): 13.52 (C27), 15.39 (C24), 15.72 (C26), 16.50 (C25), 18.26 (C6), 21.00 (C11), 23.81, 24.56 (C29 or C30), 26.25(CH_2), 26.42(CH_2), 27.86 (C23), 28.82 (C29 or C30), 32.69 (C21), 33.81 (C7), 34.12 (C13), 36.28 (C17), 36.72 (C16), 37.15 (C10), 37.76 (C4), 38.56 (C1), 40.62 (C), 40.72 (C), 41.48 (C), 46.80 (C18), 50.98 (C9), 55.48 (C5), 71.26 (C28), 81.07 (C3), 87.96 (C19), 161.24 (H$\underline{C}$OH).

Results and Discussion

The combination of solvents and long reaction time, costly chemicals makes this method environmentally hazardous. This provided the stimulus to synthesize allobetulin **1a** and its derivatives **1b**, **2a** and **3** using a grinding technique. In grindstone technique, reaction occurs through generation of heat by grinding of substrate and reagent by a mortar and a pestle.

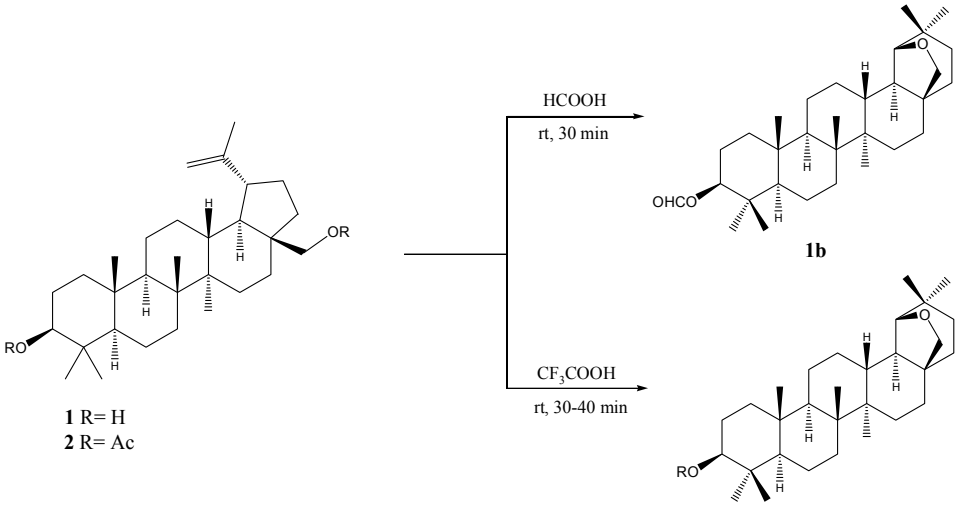

Scheme 1. Synthesis of compounds **1a**, **1b** and **2a**

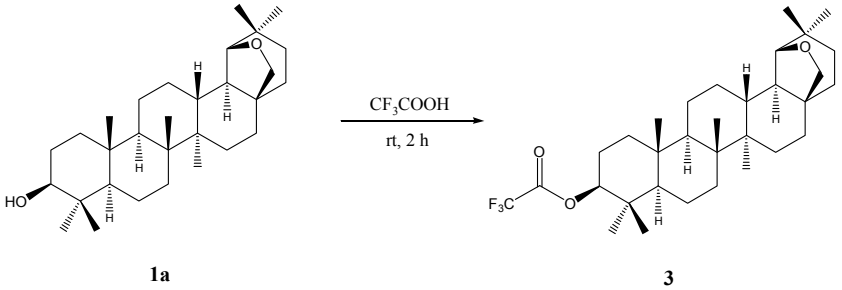

Scheme 2. Synthesis of compound **3**

More recently, a new process for the isomerisation of betulin **1** to allobetulin **1a** using trifluoroacetic acid has been reported by Medvedeva and co-workers [30] by stirring compound **1** with TFA at room temperature for 8 minutes. Whereas, the mechanochemical method required a simple grinding of compound **1** and TFA for 40 min to give allobetulin **1a** in 98 % (Scheme 1). The products obtained by both methods were found to be identical by mp.

The transformation of **1** to **1b** was reported as early as in 1922 by Schulze and Pieroh [32] in which **1** was isomerised by formic acid under reflux during 2 hours to give **1b** in moderate yield. While, the treatment of betulin **1** with formic acid under grinding at 20 ºC for 1h provided **1b** in 82 % isolated yield (Scheme 1).

It should be noted that compound **3** was previously being synthesized starting with betulin using a two-stage method including the stage of 3-monoacetate betulin synthesis that directly reacted with TFA and trifluoroacetic anhydride at 0 ºC for 1.5 hour to afford of allobetulin 3-O-trifluoroacetate. The total yield of allobetulin 3-O-trifluoroacetate **3** was 40 % calculated with reference to betulin [24]. While, in our study the starting compound was allobetulin **1a** which was ground with TFA at room temperature for 2 hours to give allobetulin 3-O-trifluoroacetate **3** in 95 % (Scheme 2).

Compound **2a** was also previously being synthesized from betulin diacetate **2** and formic acid under reflux according to the reported method in trichloromethane at reflux during 1.5 hour [33]. Replacing formic acid by trifluoroacetic acid using a grinding method the compound **2** was converted to allobetulin 3-O-acetate **2a** after 30 min in 92 % (Scheme 1).

Chemical structure of compound **1a** is confirmed using IR spectroscopy, ^{1}H and ^{13}C NMR, and their properties have been compared with literary data [31]. In its IR spectrum we observed the presence of hydroxyl group at 3423.4 cm^{-1} and also the appearance of intense bands at 1039 cm^{-1}, which could be attributed to C–O groups. ^{1}H NMR spectrum of the allobetulin **1a** showed that the signals at 4.59 and 4.69 ppm of the olefinic region were missing, along with the formation of tetrahydrofuran ring which appeared as doublets of protons of $C_{28}H_2$ group (*AB* system) at δ 3.45 and 3.78 ppm, and a singlet of CH group at 3.54 ppm. The ^{13}C NMR spectrum confirmed the absence of two olefinic carbons at 110 and 150 ppm and the presence of new signal at 87.94 ppm corresponding to C-19.

The structures of the synthesized compounds **1b, 2a** and **3** were established by ^{1}H and ^{13}C NMR spectroscopy in comparison with the analogous data published for related triterpenoids [24, 31, 32]. The ^{1}H NMR spectra of allobetulin esters synthesized **1b, 2a** and **3** contain characteristic signals of tetrahydrofuran ring, which appears as doublets of protons of CH_2 group (*AB* system), δ 3.45–3.78 ppm, and a singlet of CH group at 3.53–3.57 ppm. Comparison of the ^{1}H NMR spectra of **1b, 2a, 3** and allobetulin revealed an appreciable downfield shift of the C-3 proton signals as a result of introduction of an acyl group (the very characteristic resonance signal from an unsubstituted derivatives is usually at around 3.22 ppm, while substitution of carbon C-3 shifts this signal downfield by 1.16–1.41 ppm).

The allobetulin esters **1b, 2a** and **3** have been characterized by IR spectra, which display the disappearance of OH band of allobetulin and appearance of new bands such as the C=O group at 1720–1770 cm^{-1} and of the C–O ester group at 1000–1275 cm^{-1}.

Conclusion

We reported simple, faster method for the synthesis of allobetulin and its acyl derivatives by a mechanochemical method. This procedure offers several advantages including time saving, very easy work-up, and it is free from usage of organic solvents. The generality of this method has been demonstrated by the successful conversion with 82–98 % yields in 30–120 minute reaction completion.

References

1 Kumar, S., Sharma, P., Kapoor, K.K., & Hundal, M.S. (2008). An efficient, catalyst- and solvent-free, four-component, and one-pot synthesis of polyhydroquinolines on grinding. *Tetrahedron*, *64*, 536–542.

2 Tanaka, K., Kishigami, S., & Toda, F. (1991). Reformatsky and Luche reaction in the absence of solvent. *J. Org. Chem.*, *56*, 4333–4334.

3 Toda, F., Tanaka, K., & Hamai, K. (1990). Aldol condensations in the absence of solvent: acceleration of the reaction and enhancement of the stereoselectivity. *J. Chem. Soc. Perkin Trans.*, *1*, 3207–3209.

4 Toda, F., Suzuki, T., & Higa, S. (1998). Solvent-free Dieckmann condensation reactions of diethyl adipate and pimelate. *J. Chem. Soc. Perkin Trans.*, *1*, 3521–3522.

5 Ren, Z.J., Cao, W.G., & Tong, W.Q. (2002). The Knoevenagel condensation reaction of aromatic aldehydes with malononitrile by grinding in the absence of solvents and catalysts. *Synth. Commun.*, *32*, 3475–3479.

6 Ren, Z.J., Cao, W.G., Ding, W.Y., & Shi, W. (2004). Solvent-free stereoselective synthesis of cis-1-carbomethoxy-2-aryl-3,3-dicyanocyclopropanes by grinding. *Synth. Commun.*, *34*, 4395–4400.

7 Pathak, P.N., Gupta, R., & Varshney, B. (2008). An efficient, inexpensive Green Chemistry' route to multicomponent biginelli condensation catalyzed by $CuCl_2\,2H_2O$–HCl. *Indian J. Chem.*, *47B*, 434–438.

8 Modarresi-Alam, A.R., Nasrollahzadeh, M., & Khamooshi, F. (2007). Solvent-free preparation of primary carbamates using silica sulfuric acid as an efficient reagent. *ARKIVOC*, *16*, 238–245.

9 Dehaen, W., Mashentseva, A. A., & Seitembetov, T. S. (2011). Allobetulin and its derivatives: synthesis and biological activity. *Molecules*, *16*, 2443–2466.

10 Flekhter, O.B., Boreko, E.I., Nigmatullina, L.R., Pavlova, N.I., Medvedeva, N.I., & Nikolaeva, S.N., et al. (2004). Synthesis and antiviral activity of lupane triterpenoids and their derivatives. *Pharm. Chem. J.*, *38*, 31–34.

11 Lavoie, S., Pichette, A., Garneau, F.X., Girard, M., & Gaudet, D. (2001). Synthesis of betulin derivatives with solid supported reagents. *Synth. Commun.*, *31*, 1565–1571.

12 Pettit, G.R. & Green, B. (1961). Steroids and related natural products. IX. Selective osmium tetroxide oxidation of olefins. *Org. Chem.*, *26*, 4673–4675.

13 Berti, G., Bottari, F., Marsili, A., & Morelli, I. (1971). Boron trifluoride-catalysed rearrangements of some tetrasubstitutedneotriterpene epoxide-I. *Tetrahedron*, *27*, 2143–2152.

14 Berti, G., Marsili, A., & Morelli, I. (1971). Boron trifluoride-catalysed rearrangements of some tetrasubstituted neotriterpene epoxide II: Hopene-II oxide and its analogue in the A: B-neoallobetulin series. *Tetrahedron*, *27*, 2217–2223.

15 Baltina, L.A., Flekhter, O.B., Vasil'eva, E.V. & Tolstikov, G.A. (1996). Stereoselective synthesis of 2-deoxy-α-D-arabino-hexopyranosides of triterpene alcohols. *Russ. Chem. Bull.*, *45*, 2222.

16 Medvedeva, N.I., Flekhter, O.B., Tret'yakova, E.V., Galin, F.Z., Baltina, L.A., & Spirikhin, L.V., et al. (2004). Synthetic transformations of higher terpenoids: XI. Synthesis of A-nor-5bH-19b,28-epoxy-18a-olean-3-one derivatives. *Russian journal of organic chemistry*, *40*, 1140–1145.

17 Kvasnica, M., Tislerova, I., Sarec, J., Sejbal, J., & Cisarova, I. (2005). Preparation of new oxidized 18-α-Oleanane derivatives. *Collect. Czech. Chem. Commun*, *70*, 1447–1464.

18 Medvedeva, N.I., Flekhter, O.B., Kukovinets, O.S., Galin, F.Z., Tolstikov, G.A., & Baglin, I., et al. (2007). Synthesis of 19β,28-epoxy-23,24-dinor-A-neo-18α-olean-4-en-3-one from betulin. *Russian chemical bulletin*, *4*, 835–837.

19 Froelich, A., Kazakova, O.B., Tolstikov, G.A., & Gzella, A.K. (2009). (E)-17β,19-Epoxy-methano-17,23,24-tridemethyl-4-nor-5β,18α-olean-3-one oxime. *Acta Cryst. Section E*, *E65*, 1262.

20 Medvedeva, N.I., Flekhter, O.B., Gzella, A., & Zaprutko, L. (2006). Structure of the minor ozonolysis product of 19β,28-epoxy-A-neo-18α-olean-3(5)-ene. *Chem. Nat. Compd.*, *42*, 618.

21 Kazakova, O.B., Kazakov, D.V., Yamansarov, E.Yu., Medvedeva, N.I., Tolstikov, G.A., & Suponitsky, K.Yu., et al. (2011). Synthesis of triterpenoid-based 1,2,4-trioxolanes and 1,2,4-dioxazolidines by ozonolysis of allobetulin derivatives. *Tetrahedron Lett.*, *52*, 976–979.

22 Kazakova, O.B., Khusnutdinova, E.F., Tolstikov, G.A., & Suponitskii, K.Yu. (2012). Synthesis and molecular structure of 1α,10α:9β,1β:19β,28-triepoxy-A-neo-5β-methyl-25-nor-18α-oleane. *Russian journal of organic chemistry*, *48*, 459–461.

23 Flekhter, O.B., Medvedeva, N.I., Karachurina, L.T., Baltina, L.A., Galin, F.Z., & Zarudii, F.S, et al. (2005). Synthesis and pharmacological activity of betulin, betulinic acid, and allobetulin esters. *Pharm. Chem. J.*, *39*, 400–401.

24 Robert, M.C. (2002). Therapeutic method to treat herpes virus infection. *US patent No. 6369101B1*.

25 Galaiko, N.V., Tolmacheva, I.A., Grishko, V.V., Volkova, L.V., Perevozchikova, E.N., & Pestereva, S.A. (2010). Antiviral activity of 2,3-secotriterpenic hydrazones of the lupane and 19β,28-epoxy-18α-oleanane types. *Russ. J. Bioorg. Chem.*, *36*, 516–521.

26 Gein, S.V., Grishko, V.V., Baeva, T.A., & Tolmacheva, I.A. (2013). Immunoregulatory in vitro/in vivo effects of 2,3-secotriterpene acetylhydrazone. *Int. J. Pharmacol.*, *9*, 74–79.

27 Tolstikov, G.A., Flekhter, O.B., Shults, E.E., Baltina, L.A.,& Tolstikov, A.G. (2005). Betulin and its derivatives. Chemistry and biological activity. *Chemistry for Sustainable Development*, *13*, 1.

28 Krasutsky, P.A., Carlson, R.M., & Raj, K. (2004). Triterpenes having antibacterial activity. *US Pat. No. 6689767 B2*.

29 Tubek, B., Smuga, D., Smuga, M., & Wawrzeńczyk, C. (2012). Synthesis of 28-*O*-(1,2-diacyl *sn*-glycero-3-phospho)-betulin. *Synthetic Communications*, *42*, 3648–3654.

30 Medvedeva, N.I., Flekhter, O.B., Kukovinets, O.S., Galin, F.Z., Tolstikov, G.A., & Baglin, I., et al. (2007). Synthesis of 19β,28-epoxy-23,24-dinor-A-neo-18α-olean-4-en-3-one from betulin. *Russ. Chem. Bull.*, *56*, 835–837.

31 Jorge, A.R. Salvador., Rui, M.A. Pinto., & Rita, C. Santos., et al. (2009). Bismuth triflate-catalyzed Wagner-Meerwein rearrangement in terpenes. Application to the synthesis of the 18a-oleanane core and A-*neo*-18a-oleanene compounds from lupanes. *Org. Biomol. Chem., 7*, 508–517.

32 Schulze, H., & Pieroh, K. (1922). Zur Kenntnis des Betulins. *Chem. Ber*, *55*, 2332.

33 Kazuyoshi, Y. (1957). Isolation and identification of betulin, lupeol, and β-amyrin from the Bird-lime of *Trochodendronaralioides Siebold & Zuccarini*. *Journal of the Agricultural Chemical Society of Japan*, *21*(2), 77–81.

С. Арроус, А. Болде, И. Будебу, М.В. Ляпунова, А.А. Бакибаев

Аллобетулин және оның кейбір күрделі эфирлерінің синтезіне «еріткішсіз» механохимиялық тәсілдеме

Аллобетулин және оның туындылары үшін соңғы кезде биологиялық белсенділік табылған, бұл олардың төмен улылығымен біріккенде ғалымдардың назарын өзіне тартады. Мақалада аллобетулин және оның кейбір ацетил тобы бар туындылары, механохимиялық белендіруге негізделген, әртүрлі әдістермен синтезделді. Барлық реакциялар бөлмелік температурада жүргізілді. Аллобетулин (**1a**) және аллобетулин 3-О-формиат (**1b**) бетулиннің трифторсірке қышқылымен (TFA) және HCOOH әрекеттесу реакциясы арқылы алынды. Реакцияның жүру уақыты 30–40 мин құрды, және өнімдердің шығымы сәйкесінше 82 және 98 % тең болды. Аллобетулин 3-О-трифторацетат (**4**) 95 % шығыммен аллобетулиннің (**1a**) TFA 2 сағаттық реакциясы нәтижесінде алынды. Ал аллобетулиннің 3-О-ацетаты (**2a**) бетулин диацетатының трифторсірке қышқылымен 30 мин ішінде өңделуі нәтижесінде 92 % шығыммен алынды. Өнімдердің түзілуі ЖҚХ әдісімен, элюент ретінде C_6H_6:CH_2Cl_2:CH_3OH (5:5:1) қолданылуымен анықталды, дақтар ЖҚХ пластиналарын реагентпен (1 % фосфомолибден қышқылы – су) бүркіп, соңынан көк түсті бояу пайда болғанша 110 ºС температурада 5 мин қыздырғанда анықталды. Бұл процедура қарапайым, тиімді және экологиялық қауіпсіз. Барлық өнімдердің құрылымдары ^{1}H ЯМР, ^{13}C ЯМР және ИҚ-Фурье-спектроскопия әдістерінің мәліметтерімен дәлелденді.

Кілт сөздері: бетулин, аллобетулин, трифторсірке қышқылы, механохимия, механохимиялық белсендіру, құмырсқа қышқылы, аллобетулиннің формиаты, бетулиннің диацетаты.

С. Арроус, А. Болде, И. Будебу, М.В. Ляпунова, А.А. Бакибаев

Механохимический подход «без растворителя» к синтезу аллобетулина и некоторых его сложных эфиров

Для аллобетулина и его производных не так давно была обнаружена биологическая активность, что, в сочетании с их низкой токсичностью, привлекает внимание ученых. В данной работе аллобетулин и некоторые его производные, содержащие ацетильную группу, синтезируются различными методами, основанными на механохимической активации. Все реакции проведены при комнатной температуре. Аллобетулин (**1a**) и аллобетулин 3-О-формиат (**1b**) были получены реакцией взаимодействия бетулина с трифторуксусной кислотой (TFA) и HCOOH. Время проведения реакции составляло 30–40 мин, выход продуктов составил 82 и 98 % соответственно. Аллобетулин 3-О-трифторацетат (**4**) с выходом 95 % получается реакцией аллобетулина (**1a**) с TFA в течение 2 часов. В то время как 3-О-ацетат аллобетулина (**2a**) получается обработкой диацетатабетулина трифторуксусной кислотой в течение 30 минут с выходом 92 %. Образование продуктов определяли методом ТСХ с использованием C_6H_6:CH_2Cl_2:CH_3OH (5:5:1) в качестве элюента, пятна были обнаружены после опрыскивания пластин ТСХ реагентом (1 % фосфомолибденовая кислота – вода) с последующим нагреванием при 110 ºС в течение 5 минут до появления характерного синего окрашивания. Данная процедура проста, эффективна и экологически безопасна. Структуры всех продуктов были подтверждены данными ^{1}H ЯМР, ^{13}C ЯМР и ИК-Фурье-спектроскопии.

Ключевые слова: бетулин, аллобетулин, трифторуксусная кислота, механохимия, механохимическая активация, муравьиная кислота, формиат аллобетулина, диацетатбетулина.

DOI 10.31489/2019Ch2/14-18

UDC 547. 314. 332. 315. 2

N. Merkhatuly[1], A.N. Iskanderov[1], A.T. Omarova[1], P. Vojtíšek[2], S.K. Zhokizhanova[3]

[1]Ye.A. Buketov Karaganda State University, Kazakhstan;
[2]Charles University, Prague, Czech Republic;
[3]S. Seifullin Kazakh Agrotechnical University, Nur-Sultan, Kazakhstan
(E-mail: merhatuly@ya.ru)

The reaction of C-alkylation of eudesmanolide (–)-α-santonin

This article is concerned with sesquiterpene γ-lactones of the eudesman structure, which is promising class of natural organic compounds and characterized by a wide spectrum of physiological activity. Stereoselective synthesis of new practically significant 4α(ethyl)-3-keto-trans-eudesm-1(2),5(6)-diene-6,12-olide(C_4-α-ethyl-santonin) was carried out at room temperature in argon atmosphere by interaction of eudesmanolide (–)-α-santonin and an organohalide in presence of a strong base: tert-butyl-potassium: dimethylsulfoxide: tert-butyl alcohol. The yield was 50 %. The spatial structure of the synthesized C_4-α-ethyl-santonin was established by ^{1}H NMR-, 2D NMR (COZY, NOESY), mass spectrometry and X-ray analysis. According to the results of X-ray analysis there has been found that the condensed six-membered C_4-α-ethyl-santonin cycles are trans-articulated (CH_3-10, β-oriented), the ethyl group at C-4 has the α-configuration, and the conformation of six-membered eudesmanolide is characterized as distorted chair-chair. Thus, combination of application in the work of modern physico-chemical and spectroscopic research methods allowed characterization of the structure and properties of the compounds obtained.

Keywords: sesquiterpene γ-lactone, cross-conjugated, eudesmanolide, α-santonin, alkylation, keto-eudesmane ester, stereoselectivity, electrophilic rearrangements.

Chemical transformations of plant metabolites, in particular eudesmane sesquiterpene γ-lactones, leading to physiologically active derivatives have become an important field in synthetic and medical chemistry [1–3]. Previously, we have shown that the interaction of natural eudesmanolide (-)-α-santonin (1) with MeOH and EtOH in the presence of sodium alkoxides and the base Me_3COK-DMCO-Me_3COH stereoselectively leads to the formation of practically significant *cis*-condensed 6-keto-eudesman esters (3) and (4) (Fig. 1). In addition, it was suggested that they were formed from enolate ions (5) and (6) with a double bond at C5-C6 [4, 5].

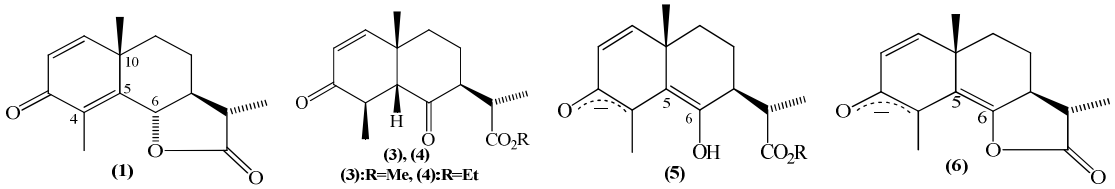

Figure 1. Structure of santonin (1), cis-eudesman esters (3), (4) and enolates (5), (6)

In further research, we studied the alkylation reaction of cross-conjugated (–)-α-santonin (1). Thus, the reaction of eudesmanolide (1) with bromoethane in the presence of base Me_3COK-DMSO-Me_3COH stereoselectively leads to the formation of a new product of C_4-alkylation, namely 4α(Et)-3-keto-trans-eudesma-1(2),5(6)-dien-6,12-olide (7). Yield was 50 % (Fig. 2).

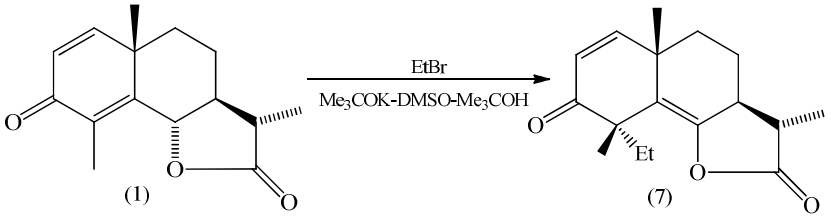

Figure 2. Synthesis of C_4-α-ethyl-eudesmanolide (7)

The spatial structure of eudesmanolide (7) was determined by X-ray analysis. It is shown in Figure 3. As shown in Figure 3, the cycles in the structure of the molecule (7) are trans-articulated (CH3-10, β-oriented), the ethyl group at C-4 has an α-configuration. The configuration of six-membered cycles is characterized as a distorted chair- chair.

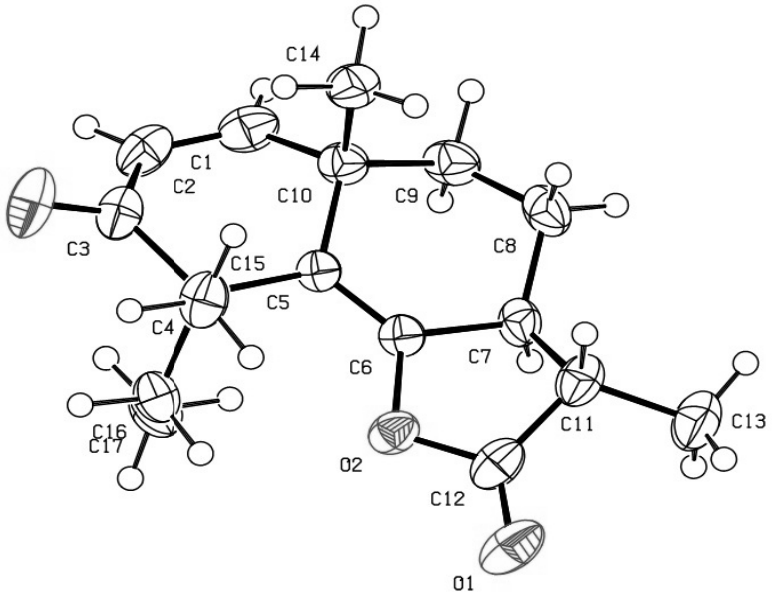

Figure 3. The spatial structure of C4-α-ethyl-eudesmanolide (7)

Two-dimensional NMR (COSY, NOESY) experiments were also carried out with C_4-ethyl eudesmanolide (7). 2D NMR spectra (COSY, NOESY) are shown in Figures 4 and 5.

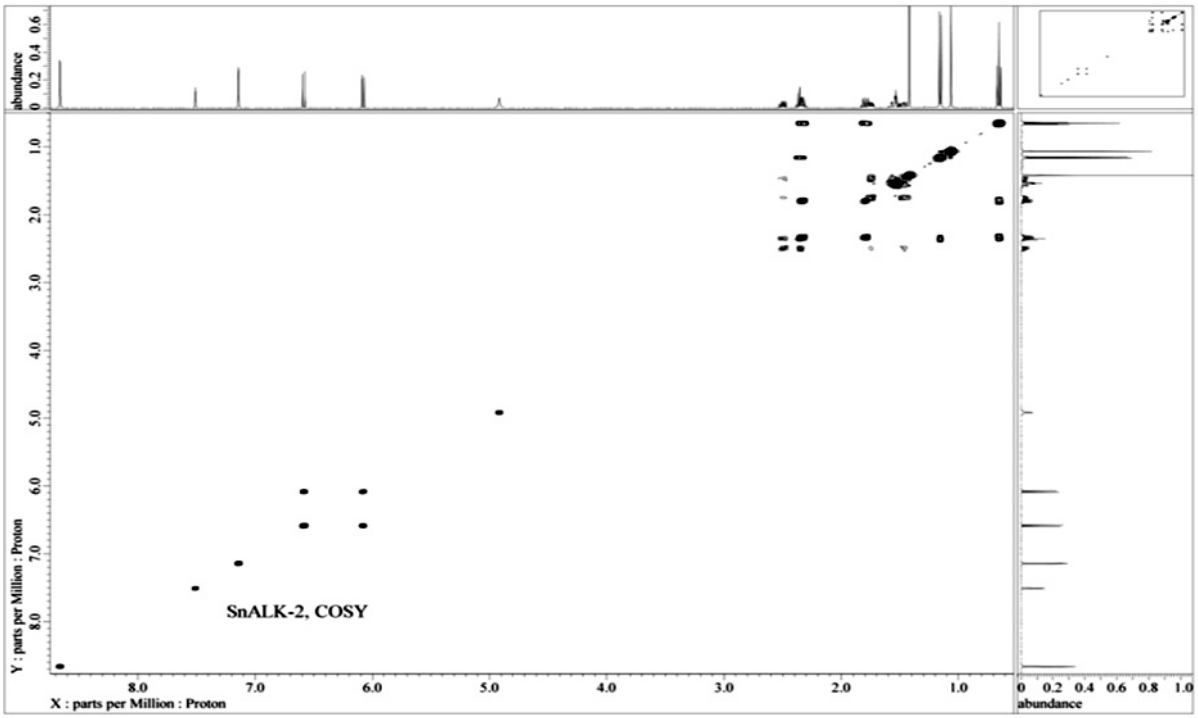

Figure 4. ^{1}H NMR (COSY) spectrum of eudesmanolide (7)

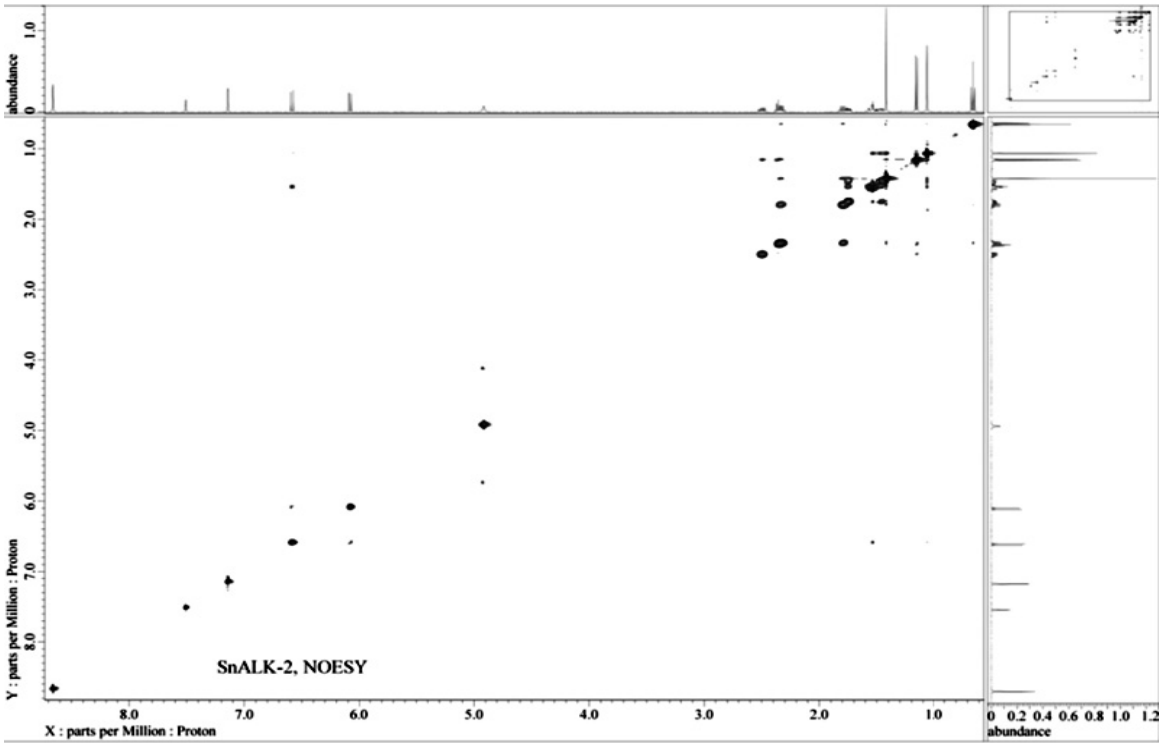

Figure 5. 2D NMR (NOESY) spectrum of eudesmanolide (7)

Considering the structure and stereochemistry of C_4-α-ethyl-eudesmanolide (7), its formation can be represented as shown in Figure 6.

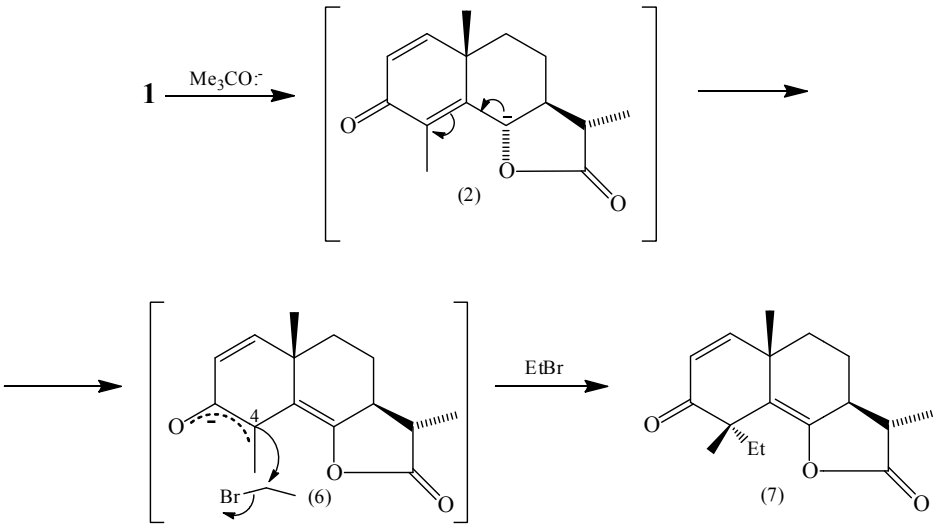

1 — allyl shift; *2* — enolization

Figure 6. Mechanism of C_4-ethyl-eudesmanolide formation (7)

Probably, under the reaction conditions of α-santonin (1) initially stage of the anion (2) formation initiates the subsequent stages of intramolecular electrophilic rearrangements with the formation of enolate-ion (6), which further stereoselectively interacts with organohalide, resulting to 4α-ethyl-eudesmanolide (7) with a double bond at C5-C6. The synthesis of the compound (7) can serve as a confirmation of the proposed mechanism of formation of 6-keto-eudesman esters (3) and (4), which has been described by us in [4, 5].

Experimental

IR spectra (7) were recorded on an Avatar-360 spectrometer in KBr pellets, ^{1}H NMR spectra were registered on a Jeol, ECA-500 spectrometer (operating frequency 500.15 MHz) with a solvent — C_5D_5N. Mass spectra were measured on an Agilent 7890A. X-ray analysis was established on a Nonius Kappa CCD 4-circle automatic diffractometer (Moα, λ = 0,71073 Å, graphite monochromator) at a temperature of 150 K. Specific rotation was determined on a MCP-100 polarimeter, melting points were measured on a M-56 instrument. Sorbfil PTSX-AF-UV plates were used for thin-layer chromatography. Sorbfil PTSKh-AF-UF plates were used for thin layer chromatography.

4α(Et)-3-keto-eudesma-1(2),5(6)-dien-6,12-olide (7). To a solution of potassium tert-butoxide in Me_3COH and DMSO (prepared from 0.06 g of metallic potassium and 1.5 ml of alcohol and 2 ml of DMSO) 0.4 g (1.6 mmol) of compound (1) was added at room temperature under an argon atmosphere. The reaction mixture was stirred at room temperature for 5–7 minutes, and then 0.12 ml (1.62 mmol) of EtBr was added, and kept for 50 minutes. Then the alcohol was distilled off in a vacuum, the residue was dissolved in ethyl acetate, washed with water (3×10 ml), dried with $MgSO_4$. The solvent was evaporated in a vacuum; the residue (0.46 g) was chromatographed on a column with silica gel (eluent — hexane – ethyl acetate, 4:1). Yield was 0.22 g (50 %), colorless crystals, mp 105–106 ºC, R_f 0.60 (hexane – ethyl acetate, 3:2), $[\alpha]_D^{20}$ 43° (*c* 0.003; $CHCl_3$). IR spectrum (ν, cm^{-1}): 1710 (C=O), 1778 (C=O), 1635 (C=C). ^{1}H NMR spectrum (500 MHz, C_5D_5N, δ, m.d, J/Hz): 6.08 (1H, d, J = 9.8, H-1), 6.58 (1H, d, J = 9.8, H-2), 1.42 (3H, s, CH_3-4), 1.06 (3H, s, CH_3-10), 1.15 (3H, d, J = 6.87, CH_3-11), 1.53 (2H, k, J = 5.5, J = 7.52, CH_2-16), 0.65 (3H, t, J = 7.52, CH_3-17). Mass spectrum (EI, 70 eV), *m/z* (I_{rel}, %): 274 (M^+, 45.2).

References

1 Merkhatuly, N., Zhokizhanova, S.K., Balmagambetova, L.T., & Adekenov, S.M. (2006). Reaction of the sesquiterpene γ-lactone α-santonin with alcoholic hydrogen chloride. *Russian Journal of General Chemistry*, *76*(8), 1347–1348.

2 Merkhatuly, N., Zhokizhanova, S.K., Balmagambetova, L.T., & Adekenov, S.M. (2007). Oximation of α-santonin. *Russian Journal of Organic Chemistry*, *43*(1), 150–151.

3 Merhatuly, N., Iskanderov, A.N., Balmagambetova, L.T., & Togizbaeva, B.B. (2013). Reactions of (–)-Estafiatin with Acidic Reagents. *Russian Journal of Organic Chemistry*, *49*(9), 1405–1406.

4 Merkhatuly, N., Abeuova, S.B., Iskanderov, A.N., Omarova, A.T., & Toktarova, L.N. (2015). Stereoselective transformations of (–)-α-santonin in the course of alkaline transesterification. *Russian Journal of Organic Chemistry*, *51*(11), 1664–1665.

5 Merkhatuly, N., Iskanderov, A.N., Zhokizhanova, S.K., Kezdikbaeva, A.T., & Ibraeva, A.K. (2017). Stereoselective synthesis of *cis*-Eudesmane esters based on (–)-santonin. *Chem. Nat. Comp*., *53*, 582–583.

Н. Мерхатулы, А.Н. Искандеров, А.Т. Омарова, П. Войтишек, С.К. Жокижанова

Эвдесманолид (–)-α-сантониннің С-алкилдеу реакциясы

Мақала физиологиялық белсенділіктің кең спектріне ие, табиғи органикалық қосылыстардың маңызды тобы болып табылатын эвдесман типті сесквитерпенді γ-лактондардың құрылысына арналған. Жаңа практикалық маңызды 4α(этил)-3-кето-транс-эвдесм-1(2),5(6)-диен-6,12-олидтің (C_4-α-этил-сантонин) стереоселективті синтезі бөлме температурасында аргон ортасында эвдесманолид (–)-α-сантониннің күшті негіз қатысында (калий трет-бутилаты – диметилсульфоксид – трет-бутил спирті) органикалық галогенидпен әрекеттестіріп жүргізілді. Оптикалық белсенді өнімнің шығымы 50 % құрайды. Синтезделіп алынған С4-α-этил-сантониннің құрылысы мен кеңістіктегі құрылымы протонды магнитті резонанс, екіөлшемді ядролы магнитті резонанс (2D NMR; COSY, NOESY), масс-спектрометрия және рентгенқұрылымдық талдау әдістерімен анықталды. Рентгенқұрылымдық анализ әдісінің нәтижесінде C_4-α-этил-сантониннің конденсирленген алтымүшелі циклдері транс-қосарланған (СН3–10, β-бағытталған), C_4 жағдайындағы этилді топ α-конфигурация күйінде, эвдесманолидтің алтымүшелі циклдерінің конформациясы бұрмаланған кресло-кресло күйінде болатындығы анықталды. Мақалада зерттеудің казіргі заманауи физика-химиялық және спектроскопиялық әдістерді қолдануы алынған заттардың құрылысы мен қасиеттерін сенімді түрде сипаттауға мүмкіндік берді.

Кілт сөздер: сесквитерпенді γ-лактон, *кросс*-қосарлану, эвдесманолид, α-сантонин, алкилдеу, кето-эвдесман эфирі, стереоселективтілік, электрофилді қайтатоптасу.

Н. Мерхатулы, А.Н. Искандеров, А.Т. Омарова, П. Войтишек, С.К. Жокижанова

Реакция С-алкилирования эвдесманолида (–)-α-сантонина

Статья посвящена сесквитерпеновым γ-лактонам эвдесмановой структуры, являющимся перспективным классом природных органических соединений, характеризующихся широким спектром физиологической активности. Стереоселективный синтез нового практически значимого 4α(этил)-3-кето-транс-эвдесм-1(2),5(6)-диен-6,12-олида (C_4-α-этил-сантонина) проводили при комнатной температуре в атмосфере аргона взаимодействием эвдесманолида (–)-α-сантонина с органогалогенидом в присутствии сильного основания (*трет*-бутилат-калия – диметилсульфоксид – *трет*-бутиловый спирт). Выход целевого оптически активного продукта составил 50 %. Строение и пространственная структура синтезированного C_4-α-этил-сантонина установлены методами протонного магнитного резонанса, двумерного ядерно-магнитного резонанса (2DNMR; COSY, NOESY), масс-спектрометрии и рентгеноструктурного анализа. По результатам рентгеноструктурного анализа было установлено, что конденсированные шестичленные циклы C_4-α-этил-сантонина являются транс-сочлененными (CH_3-10, β-ориентирована), этильная группа при С-4 имеет α-конфигурацию, а конформация шестичленных циклов эвдесманолида характеризуется как искаженное кресло-кресло. Таким образом, совокупность применения в работе современных физико-химических и спектроскопических методов исследования позволила надежно и однозначно охарактеризовать строение и свойства полученных соединений.

Ключевые слова: сесквитерпеновый γ-лактон, *кросс*-сопряжение, эвдесманолид, α-сантонин, алкилирование, кето-эвдесмановый эфир, стереоселективность, электрофильные перегруппировки.

DOI 10.31489/2019Ch2/19-28

UDC 547.94 +547.458.68+543.429.2

O.A. Nurkenov[1], T.M. Seilkhanov[2], S.D. Fazylov[1],
A.Zh. Issayeva[1], O.T. Seilkhanov[2], L.M. Vlasova[3]

[1]*Institute of Organic Synthesis and Coal Chemistry of the Republic of Kazakhstan, Karaganda, Kazakhstan;*
[2]*Sh. Ualikhanov Kokshetau State University, Kazakhstan;*
[3]*Karaganda Medical University, Kazakhstan*
(E-mail: nurkenov_oral@mail.ru)

Study of supramolecular inclusion complexes of pseudoephedrine, lupinine, anabasine and cytisine with β-cyclodextrin by NMR spectroscopy

The ^{1}H, ^{13}C and DEPT one-dimensional NMR and two-dimensional spectroscopy methods COSY (^{1}H-^{1}H), HMQC (^{1}H-^{13}C) and TOCSY (^{1}H-^{1}H) were used to study the alkaloids pseudoephedrine, lupinine, anabasine and cytisine and their supramolecular inclusion complexes with cyclic polysaccharide β-cyclodextrin. The proton-proton correlation patterns are presented through three bonds and the proton-carbon correlation patterns through one bond, namely COSY (^{1}H-^{1}H) and HMQC (^{1}H-^{13}C) in the molecules of the alkaloids under study. The use of the capabilities of two-dimensional spectroscopy COSY (^{1}H-^{1}H), HMQC (^{1}H-^{13}C) and TOCSY (^{1}H-^{1}H) to identify the studied alkaloids allowed us to correctly and unambiguously identify the structure of substrates of the supramolecular self-assembly with a cyclic polysaccharide receptor. Homonuclear and heteronuclear correlation NMR COSY (^{1}H-^{1}H) and HMQC (^{1}H-^{13}C) is also used to identify and confirm the structure and structure of the cyclic polysaccharide β-cyclodextrin. The chemical shifts of the aliphatic and hydroxyl protons of the inner and outer surfaces of the receptor were determined. A comparative analysis of the ^{1}H and ^{13}C NMR spectra of pseudoephedrine, lupine, anabasine and cytisine, β-cyclodextrin and their supramolecular inclusion complexes was carried out. Changes in the chemical shifts of ^{1}H and ^{13}C nucleus of pseudoephedrine, lupinine, anabasine, and cytisine, and β-cyclodextrin in inclusion complexes were determined. The proton integral intensities of the substrate and receptor in the ^{1}H NMR spectra determined that the supramolecular interaction of the studied pseudoephedrine, lupinine, anabasine and cytisine with β-cyclodextrin is accompanied by the entry of hydrophobic fragments of 1 substrate molecule into the inner cavity 1 of the receptor molecule.

Keywords: pseudoephedrine, lupinine, anabasine, cytisine, β-cyclodextrin, inclusion complexes, NMR spectroscopy.

Introduction

NMR spectroscopy is currently one of the most informative methods for studying the structure and intermolecular interactions in inclusion complexes [1]. Therefore, this research method was chosen to study the supramolecular inclusion complexes of pseudoephedrine **1**, lupine **2**, anabasine **3** and cytisine **4** with β-cyclodextrin (β-CD). The inclusion of alkaloids **1**–**4** in the cavity of the host molecule will increase the solubility of the substance, improve bioavailability and physico-chemical stability, and protect against biodegradation [2]. Among the currently known biologically active compounds, encapsulating receptors such as cucurbiturils, crown ethers, calixarenes, and others, β-CD [3] has a number of remarkable properties due to its structure. This is a relatively readily available compound derived from a renewable source, namely starch. β-CD is a cyclic oligosaccharide containing 7 glucopyranose units. The β-CD molecule has the shape of a truncated cone, on the inner surface of which hydrophobic binding protons H-3 and H-5 are located, and on the outer surface — H-2 and H-4.

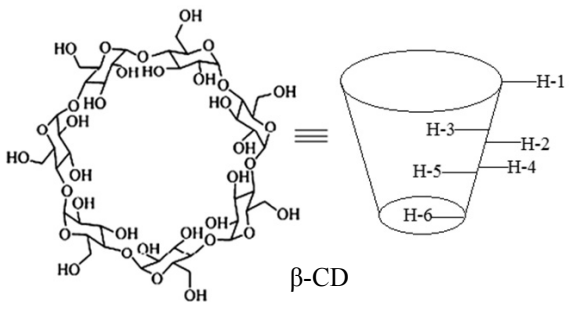

β-CD

The most important feature of β-CD is its ability to hydrophobically bind the guest molecule in its cavity in an aqueous medium.

Results and Discussion

The study by NMR spectroscopy of supramolecular inclusion complexes 5–8 obtained respectively on the basis of alkaloids 1–4 and β-CD is based on determining the difference in the values of chemical shifts of ^{1}H and ^{13}C substrates (1–4) and receptor (β-CD) in free condition and composition of complexes as a result of intermolecular interaction. According to the magnitude of chemical shifts of internal or external protons of β-CD, one can judge the formation of internal or external complexes, respectively. The change in the chemical shifts of ^{1}H and ^{13}C in the spectra of substrates makes it possible to determine the direction of the latter entering the β-CD cavity [4].

Interpretation of the ^{1}H NMR spectrum of the pseudoephedrine 1 molecule in the free state showed the presence of strong-field signals in the form of a three-proton doublet with ^{3}J 6.4 Hz at 0.67 ppm and three-proton singlet at 2.26 ppm, which can be attributed to the protons of the methyl groups H-12, 12, 12 and H-11, 11, 11, respectively.

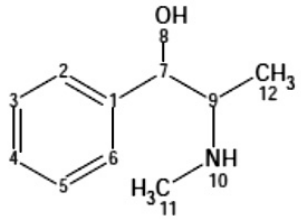

1

One-proton quintet signal at 2.53 ppm from ^{3}J 6.4 Hz can be correlated to protons H-9. One-proton doublet at 4.19 ppm from ^{3}J to 7.2 Hz corresponds to the methane hydrogen atom H-7. Protons of the phenyl radical resonate in the low-field region of the spectrum. Proton H-4 was detected in the form of one-proton multiplet at 7.17–7.22 ppm. The remaining protons of the aromatic nucleus H-2, 6, 3, 5 resonate as multiplet at 7.26–7.27 (4H) ppm. Hydroxyl and imine protons H-8 and H-10 fell into the region of resonance of residual protons of the solvent and appeared along with them as broadened singlet at 3.25 ppm. Similar signals are observed in the PMR spectrum of the pseudoephedrine complex with β-CD 5.

In the carbon NMR spectrum of an individual pseudoephedrine, signals of methyl atoms C-12 and C-13 are observed in the strong field region at 15.77 and 33.90 ppm, respectively. Asymmetric carbon atoms C-9 and C-7 correspond to doublet signals with chemical shifts of 61.10, 61.30 and 76.72–76.94 ppm, respectively. Aromatic carbon atoms resonate at 127.35 (C-3, 5), 128.07 (C-4), 128.44 (C-2, 6) and 144.10 (C-1) ppm. In the supramolecular complexes of pseudoephedrine with β-CD in comparison with the free substrate, the signals of ^{13}C nuclei ($\pm\Delta\delta$) are shifted both to the weak and strong fields (Table 1). This is due to the disshielding and shielding of carbon nuclei during the formation of supra complexes when the interacting nuclei approach each other.

Table 1

Chemical shifts NMR ^{1}H and ^{13}C 1 and β-CD in the free state and in complex 5

Atom number	Group	The value of δ_0 in the free state, ppm		The value of δ in the complex, ppm		Change in chemical shift $\Delta\delta(\delta - \delta_0)$, ppm	
	CH_x	^{1}H	^{13}C	^{1}H	^{13}C	^{1}H	^{13}C
1	2	3	4	5	6	7	8
Pseudoephedrine							
1	=C<	–	144.10	–	144.02	–	-0.08
2	=CH-	7.27	128.44	7.27	128.48	0	0.04
3	=CH-	7.26	127.35	7.26	127.35	0	0
4	=CH-	7.20	128.07	7.20	128.09	0	0.02
5	=CH-	7.26	127.35	7.26	127.35	0	0
6	=CH-	7.27	128.44	7.27	128.48	0	0.04
7	>CH-	4.19	76.94	4.19	76.88	0	-0.06

Continuation of Table 1

1	2	3	4	5	6	7	8
9	>CH-	2.53	61.10	2.53	57.03	0	-4.07
11	$-CH_3$	2.26	33.90	2.26	33.82	0	-0.08
12	$-CH_3$	0.67	15.77	0.67	15.71	0	-0.06
β-cyclodextrin							
1	>CH-	4.77	102.43	4.79	102.68	0.02	0.25
2	>CH-	3.27	72.87	3.29	72.92	0.02	0.05
3	>CH-	3.49	73.54	3.59	73.68	0.10	0.14
4	>CH-	3.30	82.00	3.34	82.14	0.04	0.14
5	>CH-	3.45	72.52	3.55	72.65	0.10	0.13
6	$-CH_2-$	3.57	60.40	3.61	60.57	0.04	0.17

The NMR spectrum of an individual β-CDD (Fig. 1) is characterized by the manifestation of six groups of signals in the region 3.23–3.32; 3.45–3.60; 4.47–4.49; 4.77–4.78; 5.66; 5.71–5.73 ppm.

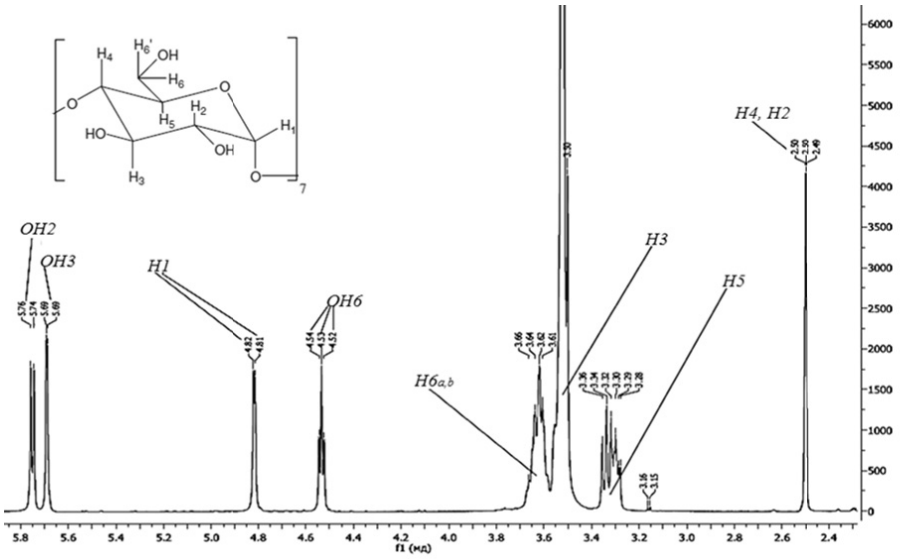

Figure 1. ^{1}H NMR spectrum β-CD

The lowest-field doublet signal in the range of 5.71–5.73 ppm with the splitting of 4 Hz belongs to the proton of the hydroxyl group at the C-2 atom. Also in the weak field region, the proton of the OH group of the neighboring atom (OH-3) resonates in the internal cavity of the β-CD molecule (δ = 5.66 ppm, doublet). The doublet signal in the region of 4.77–4.78 ppm corresponds to the proton H-1 β-CDD. The location of the indicated proton in a weaker field compared to the protons of other CH groups is due to the influence of the oxygen atom. The hydroxyl group OH-6 resonates splitting into a triplet with a center at 4.48 ppm. In the field of a strong field at 3.49–3.60 ppm signals of protons H-6a, b of the methylene group are observed. High intensity signal at 3.45 ppm corresponds to the protons H-3 and H-5 of glucopyranose link. In the range from 3.23 to 3.32 ppm metinic protons H-2 and H-4 appear.

The β-CD NMR spectrum (Fig. 2) consists of six signals from ^{13}C nuclei of the elementary link.

The signal of carbon atom C-6 appears at 60.41 ppm in the high-field part. The signals at 72.49, 72.85 and 7351 ppm resonate due to the C-5, C-2 and C-3 atoms, respectively. Signals of carbon atoms C-4 and C-1, respectively, are observed in the weaker field at 82.02 and 102.41 ppm, which are directly connected with the neighboring glucopyranous unit through the oxygen bridge.

The study of the one-dimensional spectra of β-CD in the free and bound state (Table 1) made it possible to identify the pattern of displacement of all ^{1}H and ^{13}C signals of the host molecule to the weak field, which confirms non-valent binding to the guest. For proton spectra, the greatest difference in the chemical shift values (Δδ=+0.10 ppm) is characteristic of the H-3 and H-5 inner-sphere protons, on the basis of which it can be concluded that an internal (inclusive) complex with pseudoephedrine is formed. In the case of the carbon spectrum, the difference is more significant and ranges from 0.05–0.25 ppm.

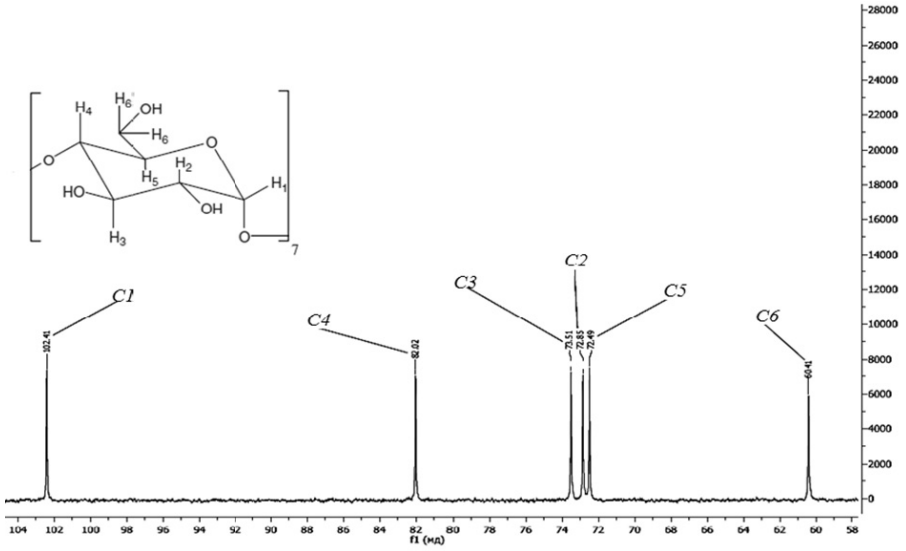

Figure 2. ^{13}C NMR spectrum β-CD

Analysis of two-dimensional NMR spectra in COSY (^{1}H-^{1}H) and HMQC (^{1}H-^{13}C) formats (Fig. 3 and 4) allowed us to establish homo- and heteronuclear interactions in pseudoephedrine molecules in both the free state 1 and in the composition of the supramolecular inclusion complex 5.

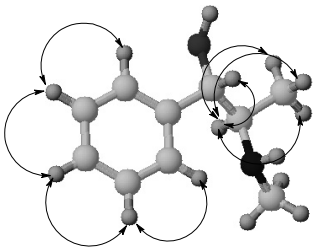

Figure 3. Correlations of COSY (^{1}H-^{1}H) in molecule 1

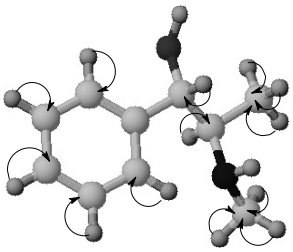

Figure 4. Correlations of HMQC (^{1}H-^{13}C) in molecule 1

Thus, the formation of supramolecular inclusion complexes is confirmed on the basis of changes in the chemical shifts of NMR of the substrate and receptor atoms. Comparison of the integral intensities of the ^{1}H signals of the receptor molecules and the substrate in individual and encapsulated forms showed that there was 1 receptor molecule in the inclusion complexes 5 per 1 substrate molecule. Considering that the greatest displacements of atoms in the substrate molecule are observed for the aliphatic fragment, we can assume the following picture of the inclusion of pseudoephedrine in the internal cavity of β-CD (Scheme 1):

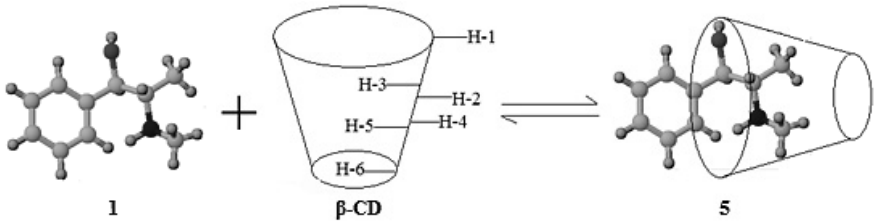

Scheme 1. The formation of the inclusion complex 1 with β-CD

In the spectra of free lupinine in the strong field at 1.03–1.64 and 1.75–1.91 ppm multiplet signals with an intensity of 10H and 4H, respectively, of protons H-6, 4, 4, 3, 3, 8, 8, 5, 7, 7, and H-9, 9, 2, 2 condensed ring systems are observed. The doublet-like multiplet signal at 2.65–2.67 ppm with integral 2H can be attributed to the protons H-10, 10. The two-proton multiplet at 3.47–3.59 ppm belongs to the methylene protons H-11, 11. Hydroxyl protons H-11 resonated with a broad one-proton singlet at 4.23 ppm.

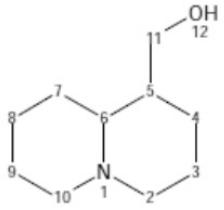

2

Carbon atoms resonate at 21.62 (C-3), 25.40 (C-8), 25.75 (C-6), 27.40 (C-7), 29.35 (C-4), 41.00 (C-5) in the ^{13}C NMR spectrum of substrate 2. The weakest field signals are at 57.28, 60.45 and 64.66 ppm can be attributed to carbon atoms with a nitrogen heteroatom of C-2, 10, C-9 and secondary C-11, respectively.

Analysis of the two-dimensional spectra of COSY (^1H-^1H) and HMQC (^1H-^{13}C) (Fig. 5, 6) allowed us to establish homo- and heteronuclear interactions in the substrate molecule. The COSY correlations carried out through three bonds are determined between the protons of the system of condensed nuclei of the lupinine molecule.

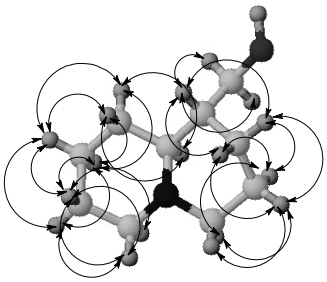

Figure 5. Correlations of COSY (^1H-^1H) in molecule 2

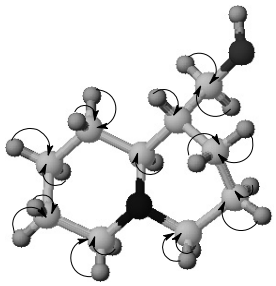

Figure 6. Correlations of HMQC (^1H-^{13}C) in molecule 2

Nonvalent bonding of atoms occurs in the process of supramolecular interaction. This is reflected in the chemical shifts of the interacting nuclei. Equivalent signals of protons of condensed nuclei of lupinine appear in the spectrum of the inclusion complex with β-CD (6) in the ranges 1.00–1.62 and 1.76–1.92 ppm. The signal of the methylene proton in the OH group as a result of complexation shifts to 3.49–3.50 ppm.

For β-CD protons, the formation of an inclusion complex is accompanied by the displacement of all ^1H nuclei into the region of a weak field. The largest difference in chemical shift values (Δδ=+0.10–0.12 ppm) is characteristic of the H-3 and H-5 inner-sphere protons, on the basis of which it can be concluded that an internal β-CD complex is formed lupinine (Table 2).

In the case of carbon spectra of substrate 2, the receptor and their complex 6, a more significant shift of signals is observed. To the carbon atoms of the condensed system, lupinine molecules correspond to signals at 21.59, 25.40, 27.35 and 29.33 ppm. The C-6 signal of the methine group is observed at 25.69 ppm. The weak field signals of the C-2, 10, C-9 and C-11 atoms also underwent slight shifts on the chemical shift scale and appear at 57.28, 64.62 and 60.56 ppm, respectively. The difference in the values of changes in chemical shifts ranges from 0.03–0.25 ppm for carbon atoms of β-CD (Table 2).

Table 2

Chemical shifts NMR ^1H and ^{13}C 2 and β-CD in the free state and as part of complex 6

Atom number	Group	The value of δ_0 in the free state, ppm		The value of δ in the complex, ppm		Change in chemical shift $\Delta\delta(\delta-\delta_0)$, ppm	
	CH_x	^1H	^{13}C	^1H	^{13}C	^1H	^{13}C
1	2	3	4	5	6	7	8
Lupinine							
2	$-CH_2-N$	1.90	57.29	1.92	57.28	0.02	-0.01
3	$-CH_2-$	1.36	21.62	1.34	21.59	-0.02	-0.03
4	$-CH_2-$	1.34	29.35	1.32	29.33	-0.02	-0.02
5	>CH-	1.58	41.01	1.57	41.03	-0.01	0.02
6	>CH-	1.17	25.58	1.20	25.69	0.03	0.11
7	$-CH_2-$	1.65	27.40	1.64	27.42	-0.01	0.02

Continuation of Table 2

1	2	3	4	5	6	7	8
8	-CH_2-	1.37	25.40	1.38	25.40	0.01	0
9	-CH_2-	1.82	64.66	1.83	64.62	0.01	-0.04
10	-CH_2-N	2.66	57.29	2.66	57.28	0	-0.01
11	-CH_2OH	3.56	60.45	3.55	60.49	-0.01	0.04
β-cyclodextrin							
1	>CH-	4.77	102.43	4.79	102.68	0.02	0.25
2	>CH-	3.27	72.87	3.30	72.90	0.03	0.03
3	>CH-	3.49	73.54	3.61	73.69	0.12	0.15
4	>CH-	3.30	82.00	3.33	82.15	0.03	0.15
5	>CH-	3.45	72.52	3.55	72.66	0.10	0.14
6	-CH_2-	3.57	60.40	3.61	60.56	0.04	0.16

Thus, the formation of supramolecular inclusion complexes is confirmed on the basis of changes in chemical shifts of the characteristic atoms of the substrate and receptor. Comparison of the integral intensities of the ^{1}H NMR signals of the receptor molecules and the substrate in the free and encapsulated forms showed that in the 6 per 1 inclusion molecule complexes there is 1 receptor molecule. Taking into account that the greatest displacements of atoms in the substrate molecule are observed uniformly for the atoms of the entire lupinine molecule, the following variants of encapsulating lupinine into the β-CD cavity can be assumed (Scheme 2).

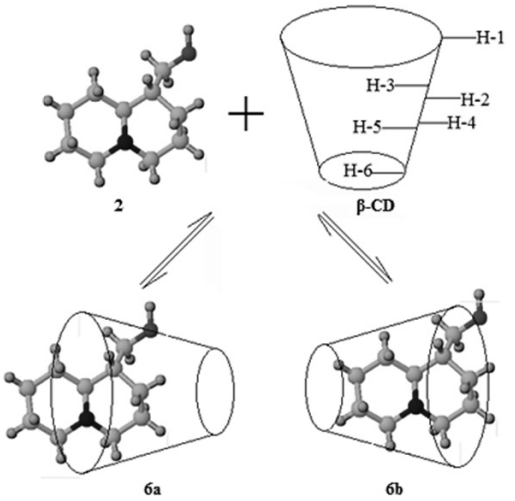

Scheme 2. Possible options for encapsulating 2 in β-CD

In the spectrum of molecular anabasine **3** in the range from 1.25 to 1.52 ppm NMR ^{1}H observed signals 4 protons, which can be correlated to the CH_2-groups with atoms of C-4 and C-5 of the piperidine system. The protons of two neighboring methylene groups of the heterocycle resonate at 1.76 (H-3, multiplet), 2.61 (H-2ax, triplet of doublets, ^{2}J 11.7, ^{3}J .7 Hz) and 2.99 (H-2eq, doublet, ^{2}J 13.7 Hz) ppm. Proton H-6 was manifested by a one-proton doublet of doublets at 3.54 with ^{2}J 10.8 and ^{3}J 2.5 Hz. In the weak-field region of the spectrum, protons of the pyridine cycle at 7.26 (H-11), 7.68 (H-12), 8.38 (H-10) and 8.50 (H-10) ppm manifested themselves in the multiplet signals.

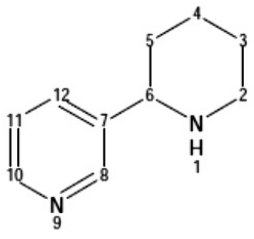

3

In the case of the carbon spectrum of anabasine, a similar picture is noted — the signals of ^{13}C nuclei of the piperidine fragment are observed in the region of a strong field, while the pyridine cycle gives signals in the weak-field part. Methylene atoms C-2, C-3, C-4 and C-5 of a saturated heterocycle are signals with chemical shifts at 47.20, 25.97, 25.81 and 35.38 ppm, respectively. The methine atom C-6 resonates at 59.37 ppm. Carbon atoms in the *o*-position of the pyridine ring give signals in the region of 148.26–148.86 ppm *m*-Atoms C-7 and C-11 resonate at 141.60 and 123.66 ppm, respectively. The carbon atom C-12 appeared at 134.52 ppm. It should be noted that the presence of asymmetric carbon atoms in the molecule 3 leads to the splitting of ^{13}C NMR signals due to the presence of antipodes in the molecules studied.

Homo- and heteronuclear correlations in the anabasine molecule were established using the two-dimensional spectra of COSY (^1H-^1H) (Fig. 7) and HMQC (^1H-^{13}C) (Fig. 8).

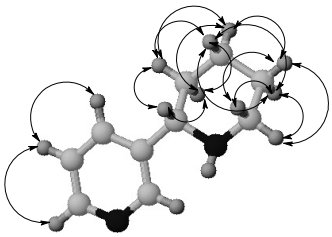

Figure 7. Correlations of COSY (^1H-^1H) in molecule 3

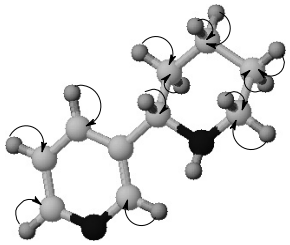

Figure 8. Correlations of HMQC (^1H-^{13}C) in molecule 3

An insignificant strong-field shift was observed ($\Delta\delta$ = –0.01 ppm) for protons of the piperidine ring of molecule 3 during complexation. In the supracomplex, the signals of the protons of the pyridine system are observed at 7.27, 7.68, 8.38 and 8.49 ppm. Since the signals of the piperidine fragment of the substrate underwent the greatest change in the process of complexation, the assumption was made that the protons were bound to the protons of β-CD.

For ^1H cyclodextrin cone nuclei, the formation of a complex is accompanied by a shift of all signals to the weak field region. The largest difference in the chemical shift values ($\Delta\delta$=+0.11–0.12 ppm) is characteristic of the protons of the internal cavity H-3 and H-5, on the basis of which it can be concluded that the formation of the supramolecular inclusion complex 7 of the cyclic polysaccharide with molecule 3 (Table 3).

Table 3

Chemical shifts NMR ^1H and ^{13}C 3 and β-CD in the free state and as part of complex 7

Atom number	Group	The value of δ_0 in the free state, ppm		The value of δ in the complex, ppm		Change in chemical shift $\Delta\delta(\delta-\delta_0)$, ppm	
	CH_x	^1H	^{13}C	^1H	^{13}C	^1H	^{13}C
Anabasine							
2	$-CH_{ax}$	2.61	47.20	2.61	47.16	0	-0.04
	$-CH_{eq}$	2.99		2.99		0	
3	$-CH_2-$	1.76	25.97	1.75	25.95	-0.01	-0.02
4	$-CH_2-$	1.45	25.51	1.44	25.48	-0.01	-0.03
5	$-CH_2-$	1.38	35.24	1.37	35.21	-0.01	-0.03
6	>CH-	3.54	59.37	3.56	59.33	0.02	-0.06
7	>C=	–	141.60	–	141.57	–	-0.03
8	-CH=N	8.50	148.26	8.49	148.28	-0.01	0.02
10	-CH=N	8.38	148.62	8.38	148.62	0	0
11	-CH=	7.26	123.66	7.27	123.70	0.01	0.04
12	-CH=	7.68	134.52	7.68	134.66	0	0.14
β-cyclodextrin							
1	>CH-	4.77	102.43	4.79	102.66	0.02	0.23
2	>CH-	3.27	72.87	3.30	72.96	0.03	0.09
3	>CH-	3.49	73.54	3.61	73.68	0.12	0.14
4	>CH-	3.30	82.00	3.34	82.16	0.04	0.16
5	>CH-	3.45	72.52	3.56	72.65	0.11	0.13
6	$-CH_2-$	3.57	60.40	3.63	60.57	0.06	0.17

Based on the values of the integral intensities of the signals of the protons of CD, consisting of seven glucopyranose units and 6–7 water molecules released during complexation, it can be assumed that one molecule 3 is inserted into the internal cavity of one β-CD molecule with the piperidine fragment of the substrate entering the internal cavity of the receptor (Scheme 3):

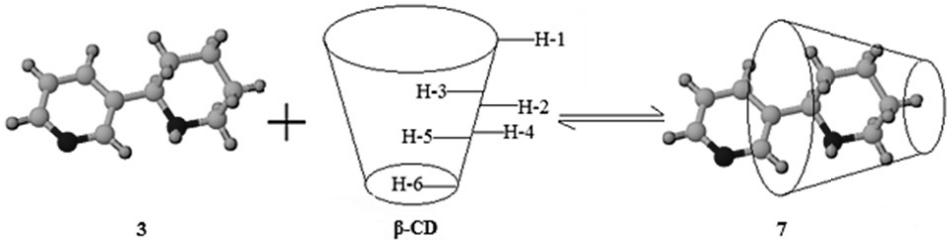

Scheme 3. The formation of the inclusion complex 3 with β-CD

The cytisine 4 alkaloid in the low-field part of the proton spectrum exhibits two doublet at 6.00 (1H, H-5, ^{3}J 6.8 Hz) and 6.16 (1H, H-3, ^{3}J 6.8 Hz) ppm and one triplet signal at 7.27 (1H, H-4, ^{3}J 6.8 Hz) of the pyridine core. In the area of 3.63–3.80 ppm (2H) the resonances of the protons H-10ax and H-10eq are noted, and the signal of the axial proton is shifted to the strong-field part of the spectrum. Four protons H-11, 11, 13, 13 methylene groups associated with the NH-group, and the methine proton H-7 give signals in the range of 2.73–2.90 ppm (5H), splitting under the influence of neighboring atoms into triplets and a multiplet, respectively. Widened singlet signals in the high-field part of the spectrum at 1.77 (2H) and 2.20 (1H) ppm correspond to protons H-8 and H-9.

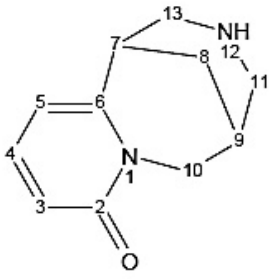

4

Analysis of the DEPT format spectra indicated the presence of four CH_2-signals and five CH-group signals in the carbon spectrum. Spectra at 139.19, 115.60 and 104.36 ppm correspond to the C-4, C-3 and C-5 atoms of the methine groups of the α-pyridine system. Two other signals of tertiary carbon atoms appear in the region of 35.33 and 27.75 ppm and are due to C-7 and C-9 atoms, respectively.

The signals of the methylene groups of the bicyclic system appeared at 26.41 (C-8), 49.98 (C-10), 53.16 (C-11) and 54.07 (C-13) ppm. In the weakest field at 152.95 and 162.85 ppm low-intensity signals of quaternary carbon atoms C-6 and C-2, respectively, appear.

The results of the analysis of two-dimensional spectra in the formats COSY (^{1}H-^{1}H), TOCSY (^{1}H-^{1}H) and HMQC (^{1}H-^{13}C) indicating homo- and heteronuclear interactions in molecule 4 are presented in the diagrams below (Fig. 9–11).

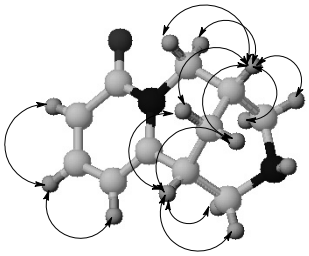

Figure 9. Scheme of the COSY (^{1}H-^{1}H) correlations in molecule 4

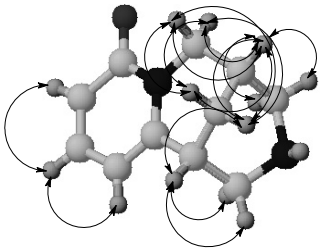

Figure 10. Scheme of TOCSY (^{1}H-^{1}H) correlations in molecule 4

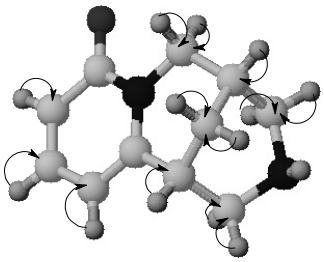

Figure 11. Scheme of HMQC (^{1}H-^{13}C) correlations in molecule 4

According to Table 4, it can be noted that all protons of the glucopyranose β-CDA link in the complex are shifted towards a weaker field compared to similar protons of the individual receptor, with the largest difference in chemical shift values ($\Delta\delta(^1H)$=0.15 m.e.) are observed in the protons of the internal cavity of the toroidal molecule H-3 and H-5. That serves as evidence of the formation of an inclusion complex 8. Comparison of the proton integral intensities of the substrate and receptor indicate the formation of a supramolecular complex of 1:1 composition (Scheme 4).

Table 4

Chemical shifts NMR ^1H and ^{13}C 4 and β-CD in the free state and as part of complex 8

Atom number	Group	The value of δ_0 in the free state, ppm		The value of δ in the complex, ppm		Change in chemical shift $\Delta\delta(\delta-\delta_0)$, ppm	
	CH_x	^1H	^{13}C	^1H	^{13}C	^1H	^{13}C
Cytisine							
2	>C=O	–	162.85	–	162.92	–	0.07
3	=CH-	6.16	115.60	6.17	115.62	0.01	0.02
4	=CH-	7.27	139.19	7.28	139.27	0.01	0.08
5	=CH-	6.00	104.36	6.01	104.51	0.01	0.15
6	>C=	–	152.95	–	152.89	–	-0.06
7	>CH-	2.76	35.33	2.76	35.27	0	-0.06
8	$-CH_2-$	1.77	26.41	1.78	26.35	0.01	-0.06
9	>CH-	2.20	27.75	2.21	27.69	0.01	-0.06
10	$-CH_2-$	3.76	49.98	3.76	49.98	0	0
11	$-CH_2-$	2.84	53.16	2.86	53.08	0.02	-0.08
13	$-CH_2-$	2.80	54.07	2.81	54.01	0.01	-0.06
β-cyclodextrin							
1	>CH-	4.77	102.43	4.79	102.49	0.02	0.06
2	>CH-	3.27	72.87	3.29	72.97	0.02	0.10
3	>CH-	3.45	73.54	3.60	73.60	0.15	0.06
4	>CH-	3.30	82.00	3.31	82.12	0.01	0.12
5	>CH-	3.45	72.52	3.60	72.59	0.15	0.07
6	$-CH_2-$	3.57	60.40	3.62	60.49	0.05	0.09

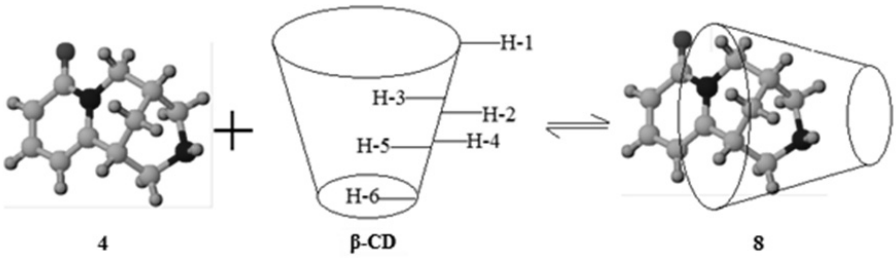

Scheme 4. The formation of the inclusion complex 4 with β-CD

Conclusions

From the above results, it follows that all the alkaloids studied enter supramolecular self-assembly with β-cyclodextrin with the formation of 1:1 inclusion complexes with the occurrence of the hydrophobic part of substrates in the inner region of the receptor. This will increase the solubility of substrates in water. The resulting supra complexes of alkaloids are essentially nanocomplexes of the latter and can be further implemented in nanomedicine.

References

1 Schneider, H.-J., Hacket, F., Rüdiger, V., & Ikeda, H. (1998). NMR Studies of Cyclodextrins and Cyclodextrin Complexes. *Chem. Rev., 98*(5), 1755–1785. DOI 10.1021/cr970019t.

2 Chernykh, E.V., & Brichkin, S.B. (2010). Supramolecular Complexes Based on Cyclodextrins. *High Energy Chemistry*, *44*(2), 83–100. DOI 10.1134/S0018143910020013.

3 Rasheed, A., Kuma, A.S.K., & Sravanthi, V.V. (2008). Cyclodextrins as Drug Carrier Molecule: A Review. *Sci. Pharm.*, *76*(4), 567–598. DOI 10.3797/scipharm.0808–05.

4 Pirnau, A., Floare, C.G., & Bogdan, M. (2014). The complexation of flurbiprofen with β-cyclodextrin: a NMR study in aqueous solution. *J. Incl. Phenom. Macrocycl. Chem., 78*(1–4), 113–120. DOI 10.1007/s10847–012–0277–7.

О.А. Нүркенов, Т.М. Сейлханов, С.Д. Фазылов,
А.Ж. Исаева, О.Т. Сейлханов, Л.М. Власова

Псевдоэфедрин, лупинин, анабазин және цитизиннің β-циклодекстринмен супрамолекулалық қосылу кешендерін ЯМР спектроскопия әдісімен зерттеу

Бірөлшемді ^{1}H, ^{13}C, DEPT және екіөлшемді COSY (^{1}H-^{1}H), HMQC (^{1}H-^{13}C) және TOCSY (^{1}H-^{1}H) ЯМР спектроскопиялары әдістері арқылы псевдоэфедрин, лупинин, анабазин және цитизин алкалоидтары, сонымен қатар құрамында циклдық полисахариды бар β-циклодекстрин қосылу кешендері зерттелді. Зерттеліп отырған алкалоид молекулаларындағы протондармен үш байланыс арқылы біріккен протондардың корреляция сызбасы және COSY (^{1}H-^{1}H) және HMQC (^{1}H-^{13}C) бір байланысты көміртек атомдары протондарының корреляциясы келтірілген. Зерттеліп отырған алкалоидтарды сәйкестендіру кезінде COSY (^{1}H-^{1}H), HMQC (^{1}H-^{13}C) және TOCSY (^{1}H-^{1}H) екіөлшемді спектроскопия мүмкіндіктері циклдік полисахаридты рецепторы бар супрамолекулалық өздік жинақталған субстраттардың құрылымын дұрыс әрі нақты сәйкестендіруге мүмкіндік берді. Сонымен қатар COSY (^{1}H-^{1}H) және HMQC (^{1}H-^{13}C) ЯМР-тың гомо- және гетероядролы корреляциясы β-циклодекстрин циклдік полисахаридтың құрылымы мен құрылысын сәйкестендіруге және растауға қолданылды. Псевдоэфедрин, лупинин, анабазин, цитизин, β-циклодекстриннің және олардың қосылу кешендерінің ЯМР спектрлеріне салыстырмалы талдау жүргізілді. Псевдоэфедрин, лупинин, анабазин, цитизин, β-циклодекстриннің және олардың қосылу кешендеріндегі ^{1}H және ^{13}C ядролардың химиялық жылжу мәндерінің өзгеруі анықталды. ЯМР ^{1}H спектрлеріндегі субстрат пен рецептордың протондық интегралдық қарқындылықтарының мәні бойынша зерттеліп отырған псевдоэфедрин, лупинин, анабазин және цитизиннің β-циклодекстринмен супрамолекулалық әрекеттесуі молекула 1 гидрафобты фрагментінің рецептор молекуласының 1 ішкі қуысына енуімен жүреді.

Кілт сөздер: псевдоэфедрин, лупинин, анабазин, цитизин, β-циклодекстрин, қосылу кешені, ЯМР спектроскопиясы.

О.А. Нуркенов, Т.М. Сейлханов, С.Д. Фазылов,
А.Ж. Исаева, О.Т. Сейлханов, Л.М. Власова

Исследование супрамолекулярных комплексов включения псевдоэфедрина, лупинина, анабазина и цитизина с β-циклодекстрином методом спектроскопии ЯМР

Методами ЯМР одномерной ^{1}H, ^{13}C и DEPT и двумерной спектроскопии COSY (^{1}H-^{1}H), HMQC (^{1}H-^{13}C) и TOCSY (^{1}H-^{1}H) исследованы алкалоиды псевдоэфедрин, лупинин, анабазин и цитизин, а также их супрамолекулярные комплексы включения с циклическим полисахаридом β-циклодекстрином. Представлены схемы корреляций протонов с протонами через три связи и схемы корреляций протонов с углеродными атомами через одну связь COSY (^{1}H-^{1}H) и HMQC (^{1}H-^{13}C) в молекулах исследуемых алкалоидов. Использование при идентификации изучаемых алкалоидов возможностей двумерной спектроскопии COSY (^{1}H-^{1}H), HMQC (^{1}H-^{13}C) и TOCSY (^{1}H-^{1}H) позволило правильно и однозначно идентифицировать строение субстратов супрамолекулярной самосборки с циклическим полисахаридным рецептором. Гомоядерная и гетероядерная корреляция ЯМР COSY (^{1}H-^{1}H) и HMQC (^{1}H-^{13}C) применена также для идентификации и подтверждения строения и структуры циклического полисахарида β-циклодекстрина. Были определены химические сдвиги алифатических и гидроксильных протонов внутренней и внешней поверхности рецептора. Проведен сравнительный анализ спектров ЯМР ^{1}H и ^{13}C псевдоэфедрина, лупинина, анабазина и цитизина, β-циклодекстрина и их супрамолекулярных комплексов включения. Определены изменения значений химических сдвигов ядер ^{1}H и ^{13}C псевдоэфедрина, лупинина, анабазина и цитизина, а также β-циклодекстрина в комплексах включения. По величине протонных интегральных интенсивностей субстрата и рецептора в спектрах ^{1}H ЯМР было определено, что супрамолекулярное взаимодействие исследуемых псевдоэфедрина, лупинина, анабазина и цитизина с β-циклодекстрином сопровождается вхождением гидрофобных фрагментов 1 молекулы субстрата во внутреннюю полость 1 молекулы рецептора.

Ключевые слова: псевдоэфедрин, лупинин, анабазин, цитизин, β-циклодекстрин, комплексы включения, спектроскопия ЯМР.

DOI 10.31489/2019Ch2/29-34

UDC 547.913

Ye.M. Suleimen[1], A.Sh. Zhanzhaxina[1], M.Yu. Ishmuratova[2]

[1]The Institute of Applied Chemistry, L.N. Gumilyov Eurasian National University, Nur-Sultan, Kazakhstan;
[2]Ye.A. Buketov Karaganda State University, Kazakhstan
(E-mail: suleimen_em@enu.kz)

Component composition of *Achillea salicifolia* Besser essential oil and its biological activity

In the present article the component composition and biological activity of the essential oil of *Achillea salicifolia* Besser (*Asteraceae* Family) were studied. The raw material of plant was collected during the flowering period in the Akmola region of the Republic of Kazakhstan. The plant materials were dried at the shade and their essential oils were obtained by hydrodistillation using Clevenger-type device, the yield was 0.34 %. The component composition of essential oil was analyzed using GC/MS Clarus-SQ 8 (Perkin Elmer). Antiradical activity of essential oil was evaluated according to 2,2-diphenyl-1-picrylhydrazyl (DPPH), gallic acid (GA) and butylhydroxyanisole (BHA) were used as comparison reagents. Cytotoxic activity was carried out using test on larvae of *Artemia salina*. Antibacterial effect of EO was evaluated *in vitro* against 3 pathogenic bacteria species, namely gram-positive — *Staphylococcus aureus* 6532, *Bacillus cereus*, gram-negative — *Salmonella enteridis* and microscope fungi *Candida albicans* SC5314. Forty seven components representing 91.2 % composition of the essential oil were characterized. The main components of the oil were α-thujone (43.0 %), 1,8-cineole (11.0 %), terpinen-4-ol (5.3 %), camphor (5.3 %) and sabinene (3.1 %). According to the results of DPPH assay, *A. salicifolia* showed low antiradical activity comparing with BHA and lethal toxicity concerning crustaceans of *Artemia salina* larvae in all tested concentrations (1–10 mg·ml^{-1}).

Keywords: Achillea salicifolia Besser*,* essential oil, gas chromatography–mass spectrometry, antimicrobial, cytotoxic and anti-radical activities, *Artemia salina,* 2,2-diphenyl-1-picrylhydrazyl.

Introduction

Achillea L. is one of the most important genera of the *Asteraceae* (*Compositae*) family, which includes over 120 species. This genus is widely distributed in Europe, Asia and Northern Africa, and is naturalized in other parts of the world [1]. *Achillea* species have been previously reported with pharmaceutical useful properties, such as antioxidant, antimicrobial [2], spasmolytic, antidiabetic, antiulcer, anti-tumor, choleretic, hepatoprotective activity and cytotoxic effects [3–9].

The *Achillea* genus has a wide distributional range, and the differences in oil composition may be affected by different environmental factors such as plant genetic type, seasonality, and developmental stage, because it is a chemically polymorphic and perennial plant. Terpenoids (1,8-cineole, camphor, borneol, pinenes, artemisia ketone, santolina alcohol, farnesane, caryophyllene and its oxides, cubebene, germacrenes, eudesmol, α-bisabolol and oxides, farnesene, γ-gurjunene, γ-muurolene and chamazulene) are the main components of *Achillea*'s essential oils [10].

The component composition and antimicrobial activity of essential oil of *A. salicifolia* Besser (collected from Ardahan between Gole, Turkey) were studied by Turkish researchers. The study showed that the main components of essential oil were camphor (55.3 %), 1,8-cineole (22.8 %), 2,5,5-trimethyl-3,6-heptadien-2-ol (4.4 %), camphene (3.2 %), artemisia alcohol (3.2 %), terpinene-4-ol (3.0 %), α-terpineol (2.5 %) and bornyl acetate (2.0 %). The essential oil showed weak antifungal activity and effectiveness against a wide spectrum of microorganisms and *Candida albicans.* The authors explained this effect to the content the compounds — camphor and 1,8-cineole in the oil, which were known as antimicrobial agents [11].

The aim of present study is to investigate the component composition of essential oil of *A. salicifolia* Besser, collected in Kazakstan, and compare with the results from Turkey; and to make a conclusion how the differences of components have influence on biological activity. Also we included results from antiradical and cytotoxic activity of the essential oil, which have not been reported before.

Experimental

Aerial parts of *Achillea salicifolia* were collected in Akmola region of the Republic of Kazakhstan on August 19, 2017. The voucher specimen was prepared and deposited in Herbarium of the Biological and Geographical Faculty of Buketov Karaganda State University (N1984.08.14.01.01).

The essential oil was extracted from the dried leaves and flowers using a Clevenger-type water distillation apparatus for 2 hours. The yield was 0.34 %. Determination of component composition of *A. salicifolia* essential oil was carried out on the Clarus-SQ 8 (PerkinElmer) Gas Chromatograph equipped with Mass-spectrometer (GC/MS apparatus).

Preparation of sample of essential oil: about 25 mg (exact weight) of essential oil *A. salicifolia* placed into a 25 ml volumetric flask, dissolved in 15 ml of hexane, adjusted to volume and stirred until complete mixing of the oil.

Chromatographic conditions: capillary column — Restek Rxi®-1 ms 0.25 mm × 30 m × 0.25 μm, sample volume: 1.0 μl, carrier gas — He, carrier gas speed: 1 ml min^{-1}, split ratio 1:25, temperature of column: 40 ºC, rise of 2 ºC min^{-1} to 280 ºC, temperature of evaporator — 280 ºC, mass spectrometric detection: temperature — 240 ºC, EI^+ = 70 eV, the scanning time from 4 to 120 minutes, the scan mode ion 39–500 m/z. The percentages of components are automatically calculated based on the total peak areas of the chromatogram of ions (Fig. 1). Components were identified by mass spectra and the retention times, with use of NIST library.

As shown in Table 1 the volatile composition of *A. salicifolia* contains α-thujone — 43.0 %, 1,8-cineole — 11.0 %, camphor — 5.3 %, terpinen-4-ol — 5.3 % as main components. Mostly main components belong to monoterpenoids.

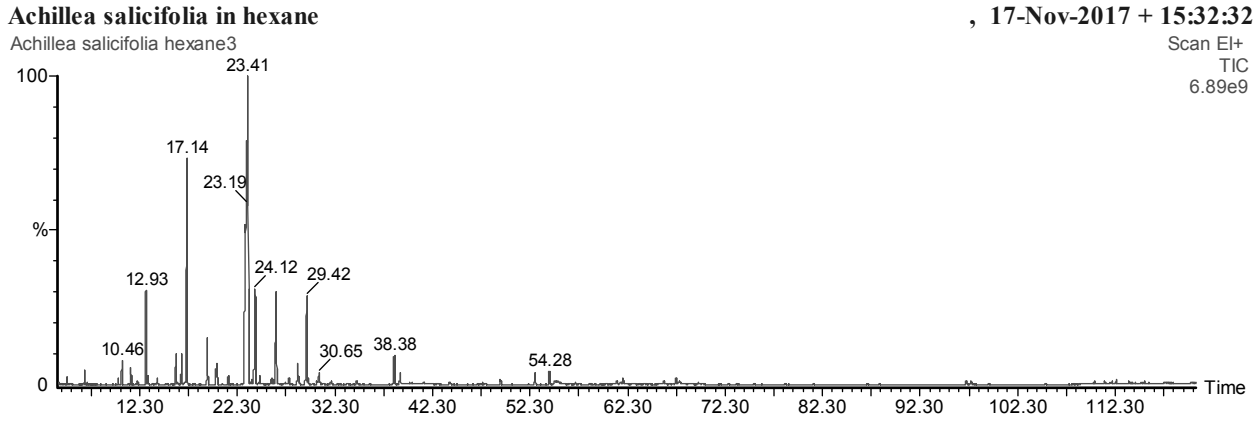

Figure 1. Chromotogram of GC/MS experiment of the essential oil of *A. salicifolia*

Table 1

Component composition of essential oil of *A. salicifolia*

R_{lit}	R_{calc}	Compound	Area, %	R_{lit}	R_{calc}	Compound	Area, %
1	2	3	4	5	6	7	8
800±2	797	*n*-Hexanal	0.1	1167±2	1160	Borneol	1.1
821	842	Cyclopropane, 1,1-dimethyl-2-(2-methyl-2-propenyl)-	0.3	1177±2	1170	**Terpinen-4-ol**	**5.3**
929±2	919	α-Thujene	0.2	1190±N/A	1171	α-Thujenal	0.2
929±7	925	α-Pinene	0.7	1193±3	1181	Myrtenal	0.1
952±2	939	Camphene	0.5	1189±2	1183	α-Terpineol	0.9
962±3	950	Benzaldehyde	0.1	1208±3	1197	*trans*-Piperitol	0.2
974±2	963	**Sabinene**	**3.1**	1239±3	1228	*p*-Isopropylbenzaldehyde	0.2
943	966	β-Pinene	0.3	1285±3	1275	Bornyl acetate	1.5
991±2	980	2,3-Dehydro-1,8-cineole	0.2	1297±N/A	1283	*trans*-Sabinyl acetate	0.5
1017±2	1009	α-Terpinene	1.2	1357±3	1343	Eugenol	0.1
1025±2	1016	*p*-Cymene	1.2	1419±3	1405	Caryophyllene	0.2
1032±2	1023	**1,8-Cineole**	**11.0**	1457±2	1445	*(E)*-β-Famesene	0.6

Continuation of Table 1

1	2	3	4	5	6	7	8
1060±3	1050	γ-Terpinene	1.9	1481±3	1462	Germacrene D	0.7
1070±4	1063	*cis*-Sabinene hydrate	1.6	1471±24	1475	Elixene	0.1
1088±2	1078	Terpinolene	0.4	1509±3	1491	β-Bisabolene	0.1
1103±2	1104	**α-Thujone**	**43.0**	1569 iu	1552	Longipinocarvone	0.2
1107±2	1108	2-Methylbutyl isovalerate	0.2	1576±2	1557	Spathulenol	0.1
1103±2	1112	**α-Thujone**	**5.3**	1581±2	1561	Caryophyllene oxide	0.3
1122±3	1117	*cis*-2-Menthenol	0.4	1637±4	1623	Caryophylladienol II	0.2
1139±2	1130	*trans*-Pinocarveol	0.3	1649±2	1641	β-Eudesmol	0.3
1143±0	1132	*cis*-Sabinol	0.2	1695±N/A	1674	*(1R,7S, E)*-7-Isopropyl-4,10-dimethylenecyclodec-5-enol	0.1
1143±9	1136	Camphor	**5.3**	2092±4	2087	Methyl linoleate	0.2
1164±N/A	1150	Pinocarvone	0.3	2091±7	2096	Methyl oleate	0.2
Total							**91.2**

Determination of antiradical activity of essential oil

Studying antiradical activity of essential oil was performed in regard to 2,2-diphenyl-1-picrylhydrazyl radical (DPPH). Absorbance analytes dependent on the concentration were measured on a spectrophotometer Cary 60 UV-Vis at 520 nm wavelength. Antiradical activity of essential oil was compared with butylhydroxyanisole (BHA). The values of antiradical activity (ARA) were calculated using the formula shown below:

$$ARA\ (\%) = (A_0 - A_t) / A_0 * 100\ \%,$$

where A_0 — is optical density of control; A_t — is the optical density of the working sample [12].

DPPH molecule forms a free radical that is stable in the different environments and wide range temperature, due to the maximum freedom of the electron delocalization over the entire molecule and spatial shielding atoms bearing the greatest spin density as well as the lack of hydrogen atoms in the positions where may occur the isomerization or disproportionation. In addition, delocalization is causing intense violet color of this radical in the aqueous-alcoholic media, the interaction with the antioxidant, capable of donating a proton; there is a restoration of the radical, resulting in the violet color turns into yellow. The results of the experiment showed that the essential oil of *A. salicifolia* has low antiradical activity (Tables 2, 3).

Table 2

The change in optical density depending on the concentration

No	Sample	Values of optical density depending on concentration, mg·ml^{-1}				
		0.1	0.25	0.5	0.75	1.0
1	BHA	0.1362	0.1333	0.1257	0.1202	0.1145
2	*A. salicifolia* (aerial part)	0.7376	0.7106	0.6430	0.6130	0.5870

Table 3

Antiradical activity of essential oil in various concentrations, %

No	Sample	The concentrations of essential oil, mg·ml^{-1}				
		0.1	0.25	0.5	0.75	1.0
1	BHA	80.82	81.23	82.30	83.08	83.88
2	*A.salicifolia* (aerial part)	3.62	7.14	15.99	19.91	23.30

Determination of the cytotoxic activity of essential oil was carried out for the first time.

The 55 ml separator funnel was filled with artificial sea water and added 200 mg eggs of *Artemia salina*. Then, it was kept with a soft supply of air for three days, until the crustaceans hatch from eggs. The one side of funnel was covered with aluminum foil, and after 5 minutes, the larvae, which moved on the bright side of the separator funnel were removed with a Pasteur pipette.

20–40 Larvae were placed into each of the 24 micro titer plates with 990 µl of seawater. Dead larvae were counted under a microscope. 10 µl of dimethylsulfoxide solution per 10 mg·ml^{-1} sample was added. Actinomycin D or staurosporine was used as a standard comparison reagent, and DMSO was a negative con-

trol. After 24 h of incubation and further maintaining micro titer plates for 24 hours (to ensure immobility) the dead larvae were counted under the microscope.

Mortality *P* was determined by the following formula:

$$P = (A - N - B) / Z \times 100\ \%,$$

where *A* is amount of dead larvae after 24 h; *N* is amount of larvae died before the test; *B* is the average amount of larvae died in a negative control; *Z* is the total amount of larvae [13].

Results of the study the cytotoxic activity of essential oils are shown in Table 4.

Table 4

The cytotoxic activity of essential oils of *A. salicifolia*

Parallel	The amount of larvae in the control		The amount of larvae in a sample			The amount of surviving larvae in the control, %	The amount of surviving larvae in sample, %	Mortality, P,%	The percentage of neurotoxicity, %
	survivors	died	survivors	died	paralyzed				
10 mg·ml^{-1}									
1	24	1	0	24	0	96	0	96	0
2	26	2	0	26	0				
3	23	0	0	28	0				
Average	24	1	0	26	0				
5 mg·ml^{-1}									
1	24	1	0	26	0	96	0	96	0
2	26	2	0	23	0				
3	23	0	0	32	0				
Average	24	1	0	27	0				
1 mg·ml^{-1}									
1	24	1	0	21	0	96	0	96	0
2	26	2	0	27	0				
3	23	0	0	27	0				
Average	24	1	0	25	0				

Based on this experiment it can be assumed that the essential oil of *A. salicifolia* in all concentrations tested exhibit acute lethal toxicity — all larvae are died.

The antimicrobial assay was performed a broth microdilution method against 3 bacterial strains; i.e. gram-positive — *Staphylococcus aureus* 6532, *Bacillus cereus*, gram-negative — *Salmonella enteridis* and *Candida albicans* SC5314. Ampicillin and fluconazole standard antibiotics were used as a positive and DMSO as a negative controls. The stock solution was prepared in DMSO and concentration was 50 mg ml^{-1}. The final concentration was varied from 2.5 mg·ml^{-1} till 0.2 mg·ml^{-1} for bacterial strains and from 1.25 mg·ml^{-1} till 0.1 mg ml^{-1} for *Candida albicans*. The lowest concentration that inhibits growth was determined as MIC value.

Table 5

Antimicrobial activity of essential oil of *A. salicifolia*, mg·ml^{-1}

Microorganisms	MIC		
	EO	Ampicillin	Fluconazole
Staphylococcus aureus 6532	1.25	0.25	-
Bacillus cereus	1.25	0.25	-
Salmonella enteritidis	0.63	0.25	-
Candida albicans SC 5314	0.31	-	0.066

The results of antimicrobial activity showed that against gram-positive bacterial strains MIC of essential oil was 1.25 mg·ml^{-1}, against gram-negative 0.63 mg·ml^{-1} and 0.31 mg·ml^{-1} against *Candida albicans* SC 5314 respectively. Thus, the essential oil was effective against *Candida albicans* SC 5314 (0.31 mg·ml^{-1}).

Conclusions

We have investigated the chemical composition, antiradical, cytotoxic and antimicrobial activities of the essential oil of *A. salicifolia* wild growing in Akmola region (Kazakhstan). The essential oil possessed quite different chemical composition as compared with the oil composition of the same species reported in previously published study. The main constitute in the essential oil were α-thujone — 43.0 %, 1,8-cineole — 11.0 %, camphor — 5.3 %, terpinen-4-ol — 5.3 % while the main constitute of the oil from other study was camphor — 55.3 %, 1,8-cineole — 22.8 %, 2,5,5-trimethyl-3,6-heptadien-2-ol — 4.4 %, camphene — 3.2 %, artemisia alcohol — 3.2 %, terpinene-4-ol — 3.0 %, α-terpineol — 2.5 % and bornyl acetate — 2.0 % [11]. The yield of essential oil was 0.34 %, it was higher than essential oil from Turkey (0.08 %). Antimicrobial tests provided information that essential oil had low activity against gram-positive (MIC — 1.25 $mg \cdot ml^{-1}$) and gram-negative (MIC — 0.63 $mg \cdot ml^{-1}$) bacterial strains and significant effective against *Candida albicans* SC 5314 (MIC — 0.31 $mg \cdot ml^{-1}$) as comparing with previous study. It can be assumed that low antimicrobial activity is associated with a low content of camphor and 1,8-cineole.

In present study antioxidant and cytotoxic tests results of the essential oil of *A. salicifolia* were reported for the first time. The essential oil showed lethal toxicity on *Artemia salina* larvae; and low antiradical activity in all concentrations tested. These studies confirmed that the essential oil of the plant can be different in quantity and quality according to geographical and environmental conditions and the period of plant growth and proceeding from this fact the different level biological activity.

Acknowledgements

The authors thank Professor Walter Luyten (KU Leuven, Belgium) for his help in the study of antimicrobial activity and Dr. Zhanar Iskakova (Kazakh University of Business and Technology, Nur-Sultan) for her help in the study of antioxidant activity and cytotoxity of the essential oil.

References

1 Kadereit, J.W., & Jeffrey, C. (Eds.). (2007). *The families and genera of vascular plants. Flowering plants Eudicots, Asterales*. Volume VIII, Berlin, Germany: Springer.

2 Benedec, D., Vlase, L., Oniga, I., Mot, A.C., & Domian, G., et al. (2013). Polyphenolic composition, antioxidant and antibacterial activities for two Romanian subspecies of *Achillea distans* Waldst. et Kit. Ex Willd. *Molecules*, *18*, 8725–8739. DOI 10.3390/molecules18088725.

3 Nemeth, E., & Bernath, J. (2008). Biological activities of yarrow species (Achillea spp.). *Current Pharmaceutical Design*, *14*, 3151–3167. DOI 10.2174/13816120878640428.

4 Si, X.T., Zhang, M.L., Shi, Q.W., & Kiyota, H. (2006). Chemical constituents of the plants in the genus Achillea. *Chemistry and Biodiversity*, *3*, 1163–1179.

5 Kupeli-Akkol, E., Koca, U., Pesin, I., & Yilmazer, D. (2009). Evaluation of the wound healing potential of *Achillea biebersteinii* Afan. (Asteraceae) by in vivo excision and incision models. *Evidence-Based Complementary and Alternative Medicine (eCAM)*, *2011*(6), 1–7. DOI 10.1093/ecam/nep039.

6 Demirci, F., Demirci, B., Gurbuz, I., Yesilada, E., & Baser, K.H.C. (2009). Characterization and biological activity of *Achillea teretifolia* Willd. and *A. nobilis* L. subsp. Neilreichii (Kerner) Formanek essential oils. *Turkish Journal of Biology*, *33*, 129–136. DOI 10.3906/biy-0808–1.

7 Konyalioglu, S., & Karamenderes, C. (2005). The protective effects of Achillea L. species native in Turkey against H_2O_2-induced oxidative damage in human erythrocytes and leucocytes. *Journal of Ethnopharmacology*, *102*(2), 221–227. DOI 10.1016/j.jep.2005.06.018.

8 Iscan, G., Kirimer, N., Kurkcuoglu, M., Arabaci, T., Kupeli, E., & Baser, K.H.C. (2006). Biological activity and composition of the essential oils of *Achillea schischkinii* Sosn. and *Achillea aleppica* DC. subsp. Aleppica. *Journal of Agricultural and Food Chemistry*, *54*(1), 70–173. DOI 10.1021/jf051644z.

9 Karamenderes, C., & Apaydin, S. (2003). Antispasmodic effect of *Achillea nobilis* L. subsp. Sipylea (O. Schwarz) Bässler on the rat isolated duodenum. *Journal of Ethnopharmacology*, *84*(2–3), 175–179. DOI 10.1016/S0378–8741(02)00296–9.

10 Motavalizadehkakhky, A., Shafaghat, A., Zamani, H., Akhlaghi, H., Mohammadhosseini, M., Mehrzad, J., & Ebrahimi, Z. (2013). Compositions and the in vitro antimicrobial activities of the essential oils and extracts of two Achillea species from Iran. *Journal of Medicinal Plants Research*, *7*(19), 1280–1292.

11 Azaz, A.D., Arabaci, T., & Sangun, M.K. (2009). Essential oil composition and antimicrobial activities of *Achillea biserrata* M. Bieb. and *Achillea salicifolia* Besser subsp. salicifolia collected in Turkey. *Asian Journal of Chemistry*, *21*(4), 3193–3198.

12 Sawant, O., Kadam, V.J., & Ghosh, R. (2009). In vitro Free Radical Scavenging and Antioxidant Activity of Adiantum lunulatum. *Journal of Herbal Medicine and Toxicology*, *3*(2), 39–44.

13 Suleimen, Ye.M. (2009). Components of Peusedanum morisonii and their antimicrobial and cytotoxic activity. *Chemistry of Natural Compounds*, *45*(5), 710–711.

Е.М. Сүлеймен, А.Ш. Жанжаксина, М.Ю. Ишмуратова

Achillea salicifolia Besser эфир майының компоненттік құрамы және оның биологиялық белсенділігі

Мақалада *Achilllea salicifolia* Besser (*Asteraceae* тұқымдастығы) өсімдігі эфир майының компоненттік құрамы және биологиялық белсенділігінің зерттеу нәтижелері келтірілген. *Achilllea salicifolia* Besser өсімдік шикізаты гүлдену кезеңінде Қазақстан Республикасының Ақмола облысында жиналған. Эфир майы сулы дистилляция әдісімен алынды, шығымы 0,34 % құрады. Эфир майының компоненттік құрамы Clarus-SQ 8 (PerkinElmer) масс-спектрометриялық детекторымен қамтылған хроматограф көмегімен анықталған. Сонымен қатар эфир майы радикалға, микробқа қарсы және цитоуыттылық белсенділігі зерттелді. Эфир майының цитоуыттылық белсенділігі *Artemia salina* дернәсілдерінде анықталды. Радикалға қарсы белсенділігі 2,2-дифенил-1-пикрилгидразил затына қатысты зерттелді, салыстыру реагенті ретінде галл қышқылы және бутилгидроксианизол қолданылды. Микробқа қарсы белсенділік үш түрлі патогенді бактерияларға: грамоң — *Staphylococcus aureus* 6532, *Bacillus cereus*; грамтеріс — *Salmonella enteridis* және *Candida albicans* SC5314 қолдана анықталды. Зерттеулер нәтижесінде *Achilllea salicifolia* Besser эфир майының негізгі компоненттері (47 компонент) 91,2 % құрайтын, туйон (43,0 %), 1,8-цинеол (11,0 %), терпинен-4-ол (5,3 %), камфора (5,3 %) және сабинен (3,1 %) болды. Эфир майынның *Artemia salina* дернәсілдеріне қатысты барлық сыналған концентрация мәндерінде (1–10 мг·мл$^{-1}$) жоғары улылық және төмен радикалға қарсы белсенділікті көрсетті.

Кілт сөздер: *Achillea salicifolia* Besser*,* эфир майы, газ хроматография–масс-спектрометрия, микробқа қарсы, цитоуыттылық және радикалға қарсы белсенділіктер, *Artemia salina,* 2,2-дифенил-1-пикрилгидразил.

Е.М. Сүлеймен, А.Ш. Жанжаксина, М.Ю. Ишмуратова

Компонентный состав эфирного масла *Achillea salicifolia* Besser и его биологическая активность

В статье даны результаты исследования компонентного состава и биологической активности эфирного масла *Achilllea salicifolia* Besser (семейства *Asteraceae*). Растительное сырье было собрано в период цветения в Акмолинской области Республики Казахстан. Эфирное масло было получено методом гидродистилляции, выход продукта составил 0,34 %. Компонентный состав эфирного масла изучен с помощью газового хроматографа с масс-спектрометрическим детектором Clarus-SQ 8 (Perkin Elmer). Также была изучена антирадикальная, антимикробная и цитотоксическая активность эфирного масла. Определение антирадикальной активности эфирного масла проводили по отношению к 2,2-дифенил-1-пикрилгидразилу, в качестве реагента сравнения использовали галловую кислоту и бутилгидроксианизол. Цитотоксическая активность проведена с использованием теста на личинках рачков *Artemia salina.* Антимикробную активность эфирного масла оценивали против трех видов патогенных бактерий: грамположительные — *Staphylococcus aureus* 6532, *Bacillus cereus*, грамотрицательные — *Salmonella enteridis* и *Candida albicans* SC5314*.* В результате проведенных исследований установлено, что основными компонентами эфирного масла (47 компонентов, составляющих 91.2 %), были α-туйон (43.0 %), 1.8-цинеол (11.0 %), терпинен-4-ол (5.3 %), камфора (5.3 %) и сабинен (3.1 %). Эфирное масло *Achilllea salicifolia* Besser проявляет летальную токсичность в отношении личинок *Artemia salina* во всех испытанных концентрациях (1–10 мг·мл$^{-1}$) и обладает низкой антирадикальной активностью.

Ключевые слова: Achillea salicifolia Besser*,* эфирное масло, газовая хроматография–масс-спектрометрия, антимикробная, цитотоксическая и антирадикальная активности, *Artemia salina,* 2,2-дифенил-1-пикрилгидразил.

DOI 10.31489/2019Ch2/35-44

UDC 541.64:678.744

G. Toleutay[1, 2], A.V. Shakhvorostov[1, 2], S.K. Kabdrakhmanova[1, 2], S.E. Kudaibergenov[1, 2]

[1]*Institute of Polymer Materials and Technology, Almaty, Kazakhstan;*
[2]*K.I. Satpayev Kazakh National Research Technical University, Almaty, Kazakhstan*
(E-mail: skudai@mail.ru)

Solution behavior of quenched or strongly charged polyampholytes in aqueous-salt solutions

Quenched (or strongly charged) polyampholytes based on fully charged anionic monomer — sodium salt of 2-acrylamido-2-methyl-1-propanesulfonic acid (AMPS) and cationic monomer — (3-acrylamidopropyl)-trimethylammonium chloride (APTAC) were synthesized by radical copolymerization and their behavior was studied in aqueous-salt solutions. A series of unbalanced (AMPS-25 and AMPS-75) and balanced (AMPS-50) quenched polyampholytes were characterized by 1H NMR, FTIR, GPC, DLS, viscosity, DSC, TGA. It was established that at the isoelectric point (IEP) the quenched polyampholytes in aqueous solutions are stabilized by cooperative intraionic contacts between strong charged anionic and cationic moieties. The conformational state of AMPS-25 and AMPS-75 in aqueous solution is represented as «core» and «shell» structure. The «core» part behaves polyampholyte character (PA region) while the «shell» part exhibits polyelectrolyte effect (PE region). Increasing of the ionic strength tends to shrink the polyelectrolyte «shell» and to swell the polyampholyte «core». In contrast to AMPS-25 and AMPS-75, the hydrodynamic size of balanced polyampholyte AMPS-50 at the IEP increases upon increasing of the ionic strength demonstrating the antipolyelectrolyte behavior. In aqueous solution the isoelectric points of quenched polyampholytes were found to be pH 6.1±0.1. In the presence of KCl the positions of the IEP shifted to pH 6.5–7.0 due to specific binding of chloride ions by quaternary ammonium groups of «quenched» polyampholytes.

Keywords: quenched polyampholytes, isoelectric point, hydrodynamic size, intrapolyelectrolyte complexes, «core-shell» structure, polyampholyte regime, polyelectrolyte regime, ionic strength.

Introduction

Quenched polyampholytes [1–3] are fully charged polyampholytes prepared from the charged cationic and anionic monomers retaining in contrast to annealed polyampholytes their respective charges over a wide range of pH. Typical examples of quenched polyampholytes are copolymers of 2-acrylamido-2-methyl-propanesulfonate sodium salt (AMPS) and 2-acrylamido-2-methylpropyldimethylammonium chloride (AMPDAC) or (3-acrylamidopropyl)trimethylammonium chloride (APTAC) prepared by microemulsion polymerization [4–8]. The precipitation of charged monomer counterions as silver salt was observed for stoichiometric mixture of 2-methacryloyloxyethyltrimethylammonium iodide (METMAI) and silver salt of 2-methcaryloyloxyethanesulfonate (AgMES) [2]. As a result, the AgI as precipitates and the METMA-MES as ion-pair monomers retains in solution. Polymerization of such ion pairs produces equimolar quenched polyampholyte without inorganic counterions. Quenched polyampholytes prepared in solution have a tendency to be alternative because of the strong electrostatic attractive forces acting between the opposite charged monomers.

McCormick and co. [9–13] synthesized a series of low- and high-charge-density ampholytic copolymers of AMPS and AMPDAC and thoroughly studied their solution properties. In studied systems the sulfonate and quaternary ammonium groups are pH insensitive and the charge balance of these terpolymers is exclusively determined by composition of copolymers.

Amphoteric terpolymers consisting of acrylamide, sodium styrene sulfonate, and acryloxyethyl trimethylammonium chloride monomers, demonstrated excellent thermal-resistance and shear-stability in high-salinity solution [14]. Due to remarkable salinity tolerance, temperature resistance, and shear stability they may be widely applied in drilling fluids and oil recovery.

Low and high molecular weight amphoteric random copolymers of AMPS-APTAC with equimolar composition were prepared via reversible addition-fragmentation chain transfer (RAFT) radical polymerization and conventional free-radical polymerization (FRP) [15]. The copolymer prepared by RAFT was soluble in pure water and formed inter-polymer aggregates while the same copolymer prepared by FRP was insolu-

ble in pure water but dissolved in aqueous solutions of NaCl. Such difference in solubility is connected with formation of intra- and inter-chain interactions that enhanced with increasing the molecular weight.

According to literature survey the quenched polyampholytes are less considered subject in comparison with annealed polyampholytes [16–18] and polymeric betaines [19].

In the present paper the solution properties of linear polyampholytes consisting of fully charged anionic AMPS and cationic APTAC monomers are considered together with their behavior at the isoelectric point where the whole macromolecules are quasineutral.

Experimental

Materials

2-Acrylamido-2-methylpropanesulfonic acid sodium salt (AMPS, 98 wt.%) and (3-acrylamidopropyl)-trimethylammonium chloride (APTAC, 75 wt.% in water), and ammonium persulfate (APS, 99 % purity) were purchased from Sigma-Aldrich Chemical Co. used without further purification.

Methods

^{1}H NMR spectra of AMPS-APTAC in D_2O were registered on impulse Fourier NMR spectrometer Bruker 400 MHz (Bruker, Germany). FTIR spectra were recorded on a Cary 660 FTIR (Agilent, USA). The average molecular weights (M_w and M_n) of aqueous solutions of AMPSNa-APTAC were measured by gel-permeable chromatography (GPC) using Viscotek (Malvern) chromatograph equipped with 270 dual detector (Malvern) and VE 3580 RI detector (Malvern). Two 6000M columns (Malvern) were used and DMF was as mobile phase at 0.7 mL/min flow rate. Polystyrene standard samples (PolyCAL™, Malvern) were used in order to plot the calibration curve. The injection volume of sample was equal to 100 μL. The viscosity of polymers was measured on Ubbelohde viscometer at 25±0.1 ºC. The average hydrodynamic size and zeta-potential of AMPS-APTAC copolymers were determined with the help of Zetasizer Nano ZS90 (Malvern, UK) at 30 ºC. TGA and DSC measurements were performed on «LABSYS evo» (Setaram, France) at heating rate 10 ºC/min. Ionic strength of the solution was adjusted by reagent grade KCl. The pH of the solution was regulated by adding of 0.1M HCl or 0.1M NaOH.

Results and Discussion

Synthesis and characterization of AMPS-APTAC copolymers

Quenched polyampholytes based on AMPS and APTAC were synthesized by free radical (co)polymerization in the presence of APS at 60 ºC during 4 h at various molar ratio of initial monomers [AMPS]:[APTAC] = 75:25, 50:50 and 25:75 mol/mol. Further in dependence of molar fraction of AMPS they are abbreviated as AMPS-25, AMPS-50 and AMPS-75 (Fig. 1).

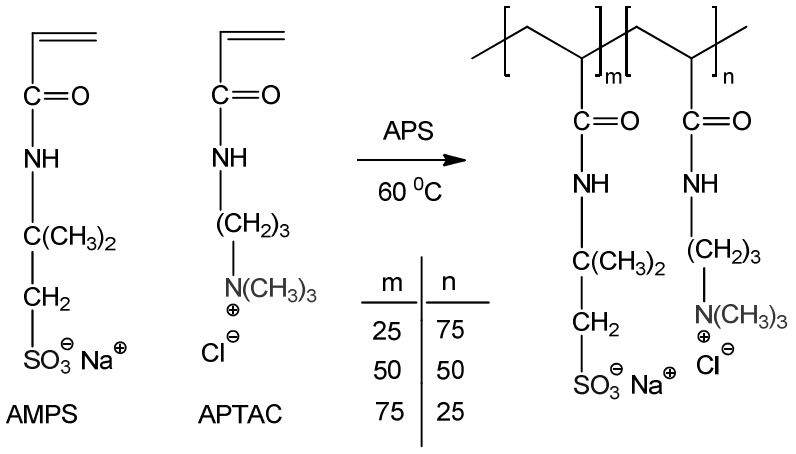

Figure 1. Polymerization protocol of AMPS and APTAC

The obtained copolymers were dissolved in distilled water, dialyzed against deionized water and freeze-dried. ^{1}H NMR spectra of AMPS-75, AMPS-50 and AMPS-25 in D_2O are shown in Figure 2.

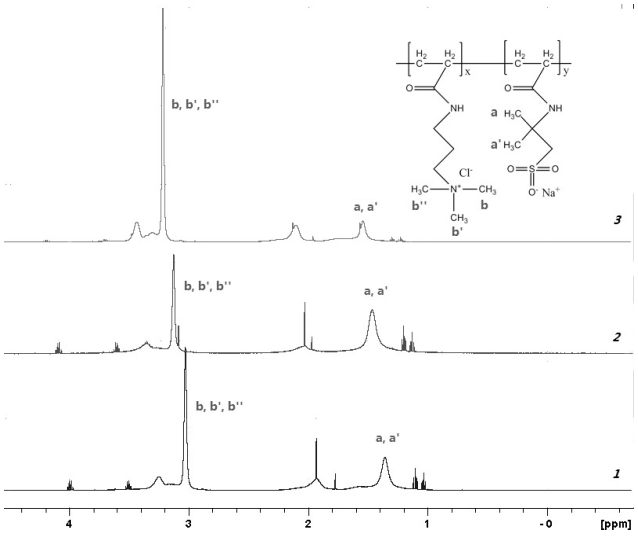

Figure 2. ^{1}H NMR spectra of AMPS-50 (1), AMPS-75 (2) and AMPS-25 (3), in D_2O

The molar composition of AMPS-APTAC copolymers was estimated from the integral peaks of methyl groups (a, a' and b, b', b'') that belong to each monomer as shown in Table 1.

Table 1

Theoretical and experimentally found molar composition of AMPS-APTAC copolymers

No. samples	Molar composition of [AMPS]:[APTAC], mol/mol	
	Theoretically prescribed	Experimentally found from ^{1}H NMR spectra
1	75:25	72:28
2	50:50	53:47
3	25:75	25:75

FTIR spectrum of AMPS-50 together with identification of characteristic bands of functional groups of AMPS-25 and AMPS-75 are presented in Figure 3 and Table 2.

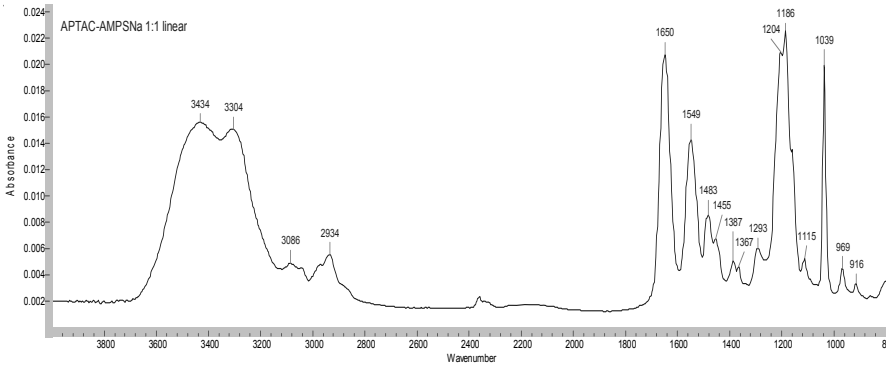

Figure 3. FTIR spectrum of AMPS-50

Table 2

Identification of FTIR spectra of AMPS-25, AMPS-50 and AMPS-75

Functional groups	ν(NH)	ν(CH)	ν(CONH) Amide I,	ν(CONH) Amide II,	δ(CH)	ν(S=O)
Band assignments, cm^{-1}	3434, 3304	2934	1650	1548	1186, 1204	1039

Thus, both ^{1}H NMR and FTIR spectra confirm the compositional closeness of copolymers to that of the monomer feed indicating the formation of homogeneous AMPS-APTAC copolymers in the course of radical

polymerization. The conversion of AMPS-APTAC copolymers found from ^{1}H NMR spectra exceeded 80 %. The weight-average molecular weight (M_w), the number-average molecular weight (M_n), and z-average molecular weight (M_z) together with polydispersity index (PDI) of the AMPS-APTAC copolymers according to GPC measurements are summarized in Table 3.

Table 3

The molecular weights and PDI of AMPS-APTAC copolymers

Copolymers	$M_w \cdot 10^{-5}$	$M_n \cdot 10^{-5}$	$M_z \cdot 10^{-5}$	PDI
AMPS-75	6.40	6.37	6.50	1.01
AMPS-50	3.31	2.01	5.11	1.65

Solution properties of AMPS-APTAC copolymers

Concentration dependence of the reduced viscosity of AMPS-APTAC at different ionic strengths of the solution (μ) expressed as mol·L^{-1} of KCl is demonstrated in Figures 4–6.

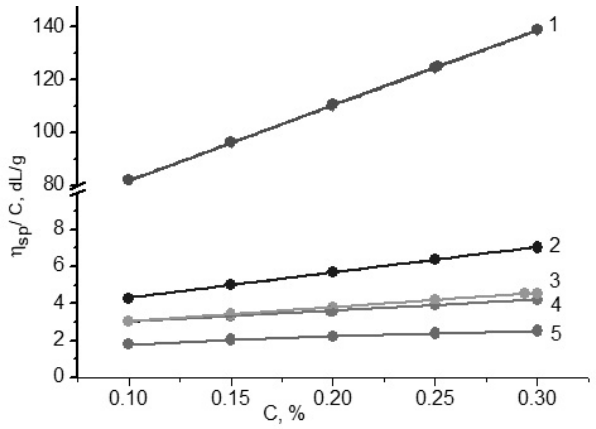

μ (mol·L^{-1}): *1* — 0; *2* — 0.1; *3* — 0.5; *4* — 0.75; *5* — 1.0

Figure 4. Concentration dependence of the reduced viscosity of AMPS-25

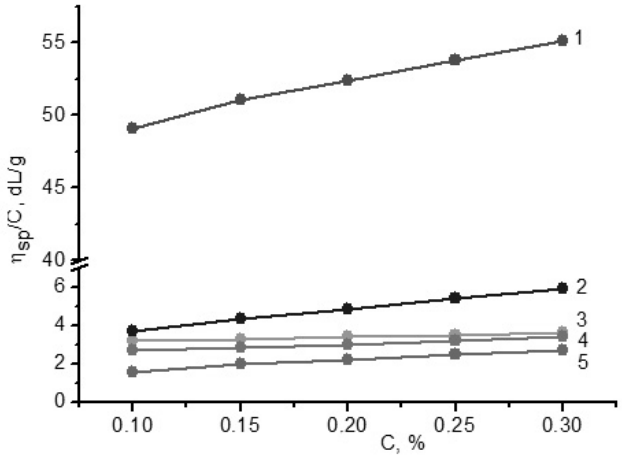

μ (mol·L^{-1}): *1* — 0; *2* — 0.1; *3* — 0.5; *4* — 0.75; *5* — 1.0

Figure 5. Concentration dependence of the reduced viscosity of AMPS-75

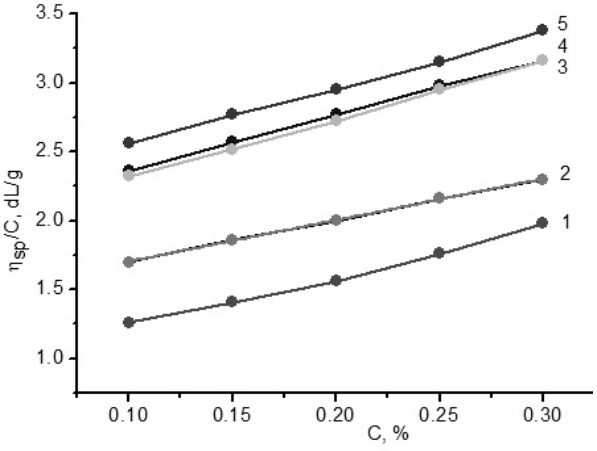

μ (mol·L^{-1}): *1* — 0.05; *2* — 0.1; *3* — 0.75; *4* — 1.0; *5* — 0.5

Figure 6. Concentration dependence of the reduced viscosity of AMPS-50

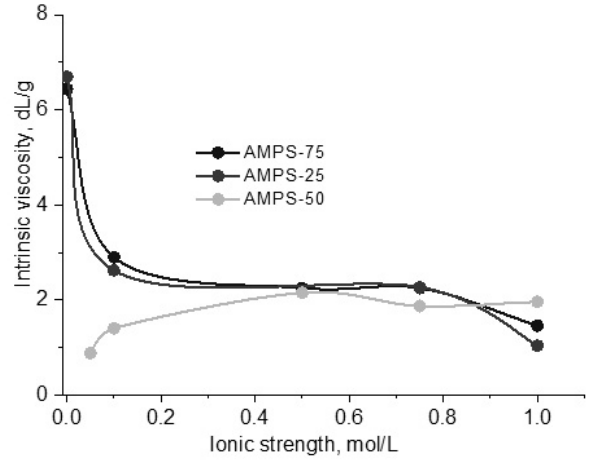

Figure 7. Dependence of the intrinsic viscosity of AMPSNa-APTAC copolymers on the ionic strength of the solution adjusted by KCl

The unbalanced AMPS-APTAC polyampholytes, to whom belong AMPS-25 and AMPS-75, can be considered as a combination of polyampholyte and polyelectrolyte regimes because the charge imbalance causes the increasing of net charge of macromolecules. In that case, the conformational state of AMPS-25 and AMPS-75 in aqueous solution can be represented similar to «core» and «shell» structure. The «core» part containing the equal amount of positive (25 mol.%) and negative (25 mol.%) charges that are mutually compensated can belong to polyampholyte region. The «shell» part of AMPS-25 and AMPS-75 containing the excess of either positive or negative charges is responsible for water solubility and should give to macromolecules polyelectrolyte character. Since the «core» part of AMPS-50 comprising of equal number of positive and negative charges (balanced polyampholyte) has no excess of positive and negative charges in «shell» part, it forms a fine suspension in water but is soluble in salt solution. Surprisingly in pure water AMPS-25 and AMPS-75 do not exhibit polyelectrolyte effect in spite of the excess of positive (Z = +50 mV) and negative (Z = –40 mV) charges. Concentration dependence of the reduced viscosity has a linear character (Figs. 4 and 5). Decreasing of the reduced viscosity upon dilution is probably connected with domination of polyampholyte effect over polyelectrolyte effect. Intramolecular salt bonds (50 mol.%) formed between 25 mol.% positive and 25 mol.% negative charges (polyampholyte effect) prevail the electrostatic repulsion of similar charges (polyelectrolyte effect) in macromolecular chains. In other words, due to counteracting of polyampholyte and polyelectrolyte effects the conformation of macromolecules remains unchanged (or slightly changed) upon dilution in spite of the excess of positive or negative charges. As seen from Figures 4 and 5 the reduced viscosity of AMPS-25 and AMPS-75 decreases with increasing of the ionic strength. In contrast, the reduced viscosity of AMPS-50 increases upon addition of KCl demonstrating antipolyelectrolyte behavior (Figs. 6 and 7). Since AMPS-25 and AMPS-75 contain an excess of positive and negative charges and behave polyelectrolyte character, addition of low-molecular-weight salts shields the electrostatic repulsions. In its turn, addition of low-molecular-weight salts to AMPS-50 shields the electrostatic attraction between the oppositely charges and results in increasing the reduced viscosity. In case of AMPS-25 and AMPS-75 it is expected the simultaneous realization of both polyelectrolyte and polyampholyte behavior. Screening of similar charged monomers by low-molecular-weight salts tends to shrink the «shell» (polyelectrolyte part) while surrounding of oppositely charged monomers by low-molecular-weight salts tends to swell the «core» (polyampholyte part). Such antagonism between polyelectrolyte and polyampholyte effects may cause not dramatically decreasing of the intrinsic viscosity upon increasing of the ionic strength. The plateau observed at $\mu > 0.1$ is likely due to opposite actions of polyelectrolyte and polyampholyte effects. Analogous behavior was observed for AMPS-MADQUAT copolymers with the excess of AMPS monomers at $\mu = 0.5 — 2.0$ [20].

Behavior of AMPS-APTAC at the IEP

In pure water the isoelectric points (IEP) of AMPS-APTAC copolymers corresponding to zero net charge (quasi-electroneutral) of macromolecules are around of pH 6.1±0.1 (Fig. 8). At the IEP the average hydrodynamic size of quenched polyampholytes is minimal due to strong electrostatic attraction of oppositely charged monomers. Increasing of the average hydrodynamic size of amphoteric macromolecules from both sides of the IEP is interpreted in terms of expanding of macromolecular chains due to strong electrostatic repulsion of anionic or cationic groups respectively [16–18].

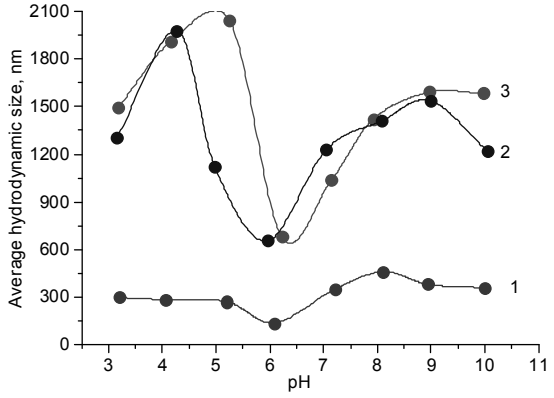

Figure 8. pH dependent average hydrodynamic size of AMPS-50 (1), AMPS-75 (2) and AMPS-25 (3) in aqueous solution

In the presence of KCl the position of the IEP shifts to higher values of pH up to 6.5–7.0. It is connected with specific binding of chloride ions by quaternary ammonium groups that diminishes the amount of positive charges (leading to apparent change of copolymer composition) and increases the value of the IEP in comparison with the nonsalted solution [21].

Different behavior of unbalanced (AMPS-25 and AMPS-75) and balanced (AMPS-50) polyampholytes upon increasing of the ionic strength is illustrated in Figure 9. In aqueous solution AMPS-25 and AMPS-75 have an excess of positive (Z = +50) and negative (Z = –40) charges while AMPS-50 is in electroneutral state (Z = 0).

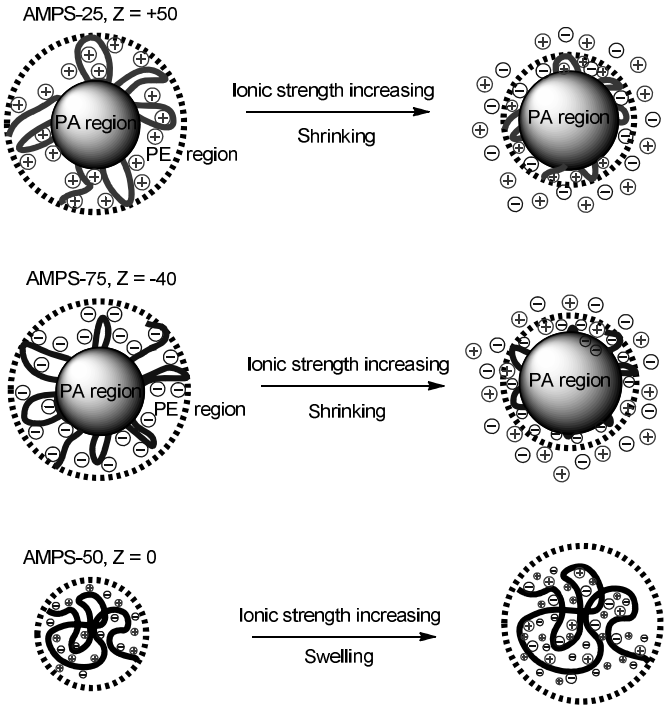

Figure 9. Schematic representation of «core-shell» structure and behavior of AMPS-25, AMPS-50 and AMPS-75 in aqueous-salt solution

Increasing of the ionic strength screens the electrostatic repulsion between uniformly charged groups, if polyelectrolyte effect dominates and shields the electrostatic attraction between oppositely charged monomers, if polyampholyte effect prevails (Table 4). In former case, the macromolecular chain diminishes, whereas in the latter case it expands.

Table 4

Intrinsic viscosities of AMPS-APTAC copolymers in dependence of the ionic strength

Copolymers	Intrinsic viscosity, $dL \cdot g^{-1}$					
	Ionic strength, KCl $mol \cdot L^{-1}$					
	0	0.05	0.1	0.5	0.75	1.0
AMPS-25	46.4	-	2.68	-	2.32	1.12
AMPS-50	-	0.88	1.40	2.15	1.90	1.96
AMPS-75	53.8	-	2.93	-	2.42	1.47

The viscometric data reveal that in aqueous solutions of KCl the intrinsic viscosities of AMPS-25 and AMPS-75 decrease while the intrinsic viscosity of AMPS-50 increases demonstrating antipolyelectrolyte behavior. In aqueous solution the conformation of AMPS-25 and AMPS-75 can be considered as «core» and «shell» structure where the «core» part exists in polyampholyte regime, the «shell» part represents a polyelectrolyte regime. Addition of low-molecular-weight salts tends to shrink the «shell» part (polyelectrolyte region) and to swell the «core» part (polyampholyte region). Such antagonism between polyelectrolyte

(«shell») and polyampholyte («core») effects may cause gradual decreasing of the intrinsic viscosity at relatively high ionic strengths.

According to Lifshiz et al [22] the globular structure of macromolecules can be considered as dense three-dimensional nucleation, consisting of a dense «core» surrounded by loose and open surface or hydrophilic «edge». In our mind, such globular structure can exist at the IEP of quenched polyampholytes as represented schematically in Figure 10. Imaginative structure of «core» consists of 1) high dense globule (r = ~5–10 nm), 2) low-dense globule (r = ~25–50 nm), 3) dense coil (r = ~100 nm), and 4) low-dense coil (r = ~200–500 nm). Radial distribution of macromolecular chains may have whole-number values r_1:r_2:r_3:r_4 = a:b:c:d. Formation of spherical globules with an ~5 nm diameter was directly visualized by Field Emission Scanning Electron Microscope (FE-SEM) images for charge-balanced polyampholyte chains made of sodium 4-vinylbenzenesulfonate (NaSS) and [3-(methacryloylamino)propyl]trimethylammonium chloride (MPTC) denoted as poly(NaSS-*co*-MPTC) [23] (Fig. 11).

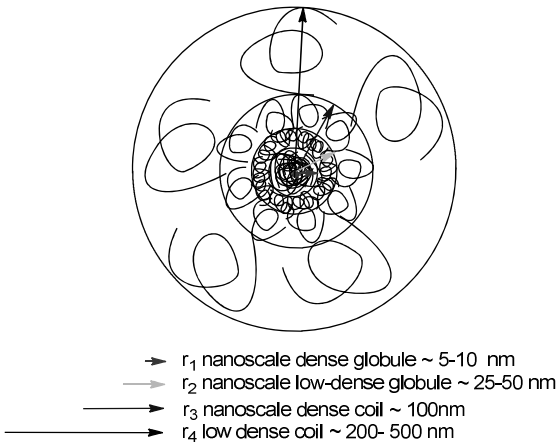

Figure 10. Proposed structure and proposed size of quenched polyampholytes in aqueous solution at the isoelectric point (IEP)

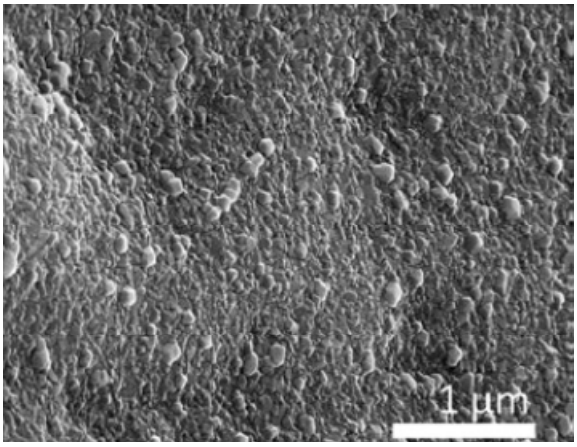

Figure 11. Cross-sectional FE-SEM image of poly(NaSS-*co*-MPTC) at 20 ºC [23]

Thermal properties of solid AMPS-APTAC copolymers

The results of thermogravimetric analysis (TGA) and differential scanning calorimetry (DSC) of quenched polyampholytes are shown in Figure 11. An initial decreasing of sample mass at the interval of temperature 65–120 ºC is due to loosing of the humidity. Intensive mass loose of samples starts at the interval of temperature 308–332 ºC. It is connected with thermal decomposition of polymers.

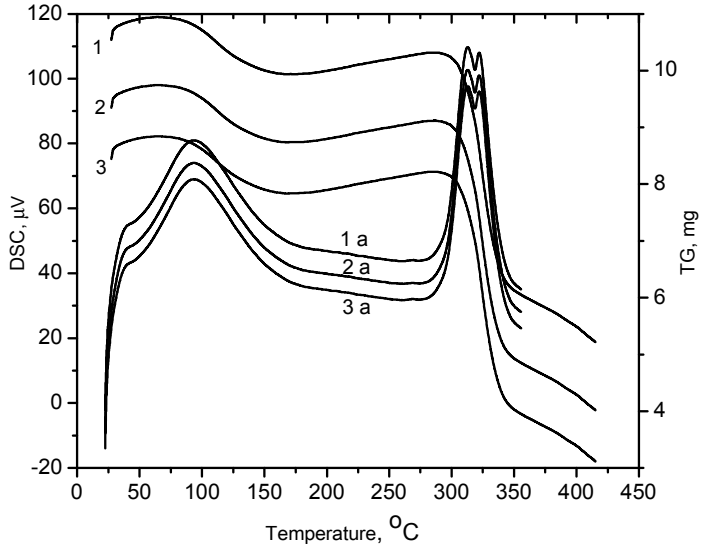

Figure 11. TG (1–3) and DSC (1a-3a) curves of AMPS-50 (1), AMPS-75 (2), AMPS-25 (3)

Conclusions

Quenched (or high-charge-density) polyampholytes were prepared from anionic AMPS and cationic APTAC monomer pairs. Copolymers with large charge asymmetries (AMPS-25 and AMPS-75) exhibited a good solubility in water. Equimolar polyampholyte (AMPS-50) was dispersed in water but soluble in aqueous solutions of KCl. Polyampholytes with excess of anionic (AMPS-75) or cationic (AMPS-25) charges behave as neutral polymers, e.g. at concentration range of 0.05–03 $g \cdot dL^{-1}$ the reduced viscosity linearly diminishes upon dilution. The viscometric data reveal that in aqueous solutions of KCl the intrinsic viscosities of AMPS-25 and AMPS-75 decrease while the intrinsic viscosity of AMPS-50 increases demonstrating *antipolyelectrolyte* behavior. In aqueous solution the conformation of AMPS-25 and AMPS-75 can be considered as «core» and «shell» structure where the «core» part exists in polyampholyte regime, the «shell» part represents a polyelectrolyte regime. Addition of low-molecular-weight salts tends to shrink the «shell» part (polyelectrolyte region) and to swell the «core» part (polyampholyte region). Such antagonism between polyelectrolyte («shell») and polyampholyte («core») effects may cause not dramatically decreasing of the intrinsic viscosity at relatively high ionic strengths. In aqueous solution the positions of the isoelectric points of strongly charged polyampholytes determined by DLS experiments are around of pH 6.3±0.2. In the presence of KCl the position of the IEP shifts to pH 6.5–7.0 due to specific binding of chloride ions by quaternary ammonium groups of APTAC. Imaginative structure of polyampholyte «core» at the IEP consisting of high dense globule, low-dense globule, dense coil, and low-dense coil is suggested. Quenched polyampholytes exhibit thermostability up to 300 ºC.

Acknowledgements

Financial support from the Ministry of Education and Science of the Republic of Kazakhstan (IRN AP05131003, 2018–2020) is greatly acknowledged.

References

1 Salamone, J.C., Tsai, C.C., Watterson, A.C., & Olson, A.P. (1980). Novel ampholytic polymers. A new class of ionomer, in: *Polymeric Amine and Ammonium Salts*. Oxford: Pergamon Press, 105–112.

2 Salamone, J.C., & Rice, W.C. (1987). Polyampholytes. In: *Encycl. of Polym. Sci. Eng*. Edited by H.F. Mark, N.M. Bikales, C.G. Overberger, and G. Menges. New York: Wiley, 514–530.

3 Salamone, J.C., Watterson, A.C., Hsu, T.D., Tsai, C.C., & Mahmud, M.U. (1977). Polymerization of vinylpyridinium salts. IX. Preparation of monomeric salt pairs. *J. Polym. Sci. Polym. Lett. Ed*., *15*, 487–491.

4 Candau, F., & Joanny, J.F. (1996). Polyampholytes (Properties in aqueous solution). In: *Polymeric Materials Encyclopedia*. Edited by J.C. Salamone. New York: CRC Press Boca Raton, 5476–5488.

5 Corpart, J.M., & Candau, F. (1993). Formulation and polymerization of microemulsions containing a mixture of cationic and anionic monomers. *Colloid Polym. Sci*., *271*, 1055–1067.

6 Corpart, J.M., & Candau, F. (1993). Characterization of high charge density ampholytic copolymers prepared by microemulsion polymerization. *Polymer, 34*, 3873–3886.

7 Candau, F. (1995). Recent developments in microemulsion copolymerization. *Macromol. Symp., 92*, 169–178.

8 Ohlemacher, A., Candau, F., Munch, J.P., & Candau, S.J. (1996). Aqueous solution properties of polyampholytes: Effect of net charge distribution. *J. Polym. Sci. Part B: Polym. Phys*., *34*, 2747–2757.

9 McCormick, C.L., & Johnson, C.B. (1998). Water-soluble polymers 28. Ampholytic copolymers of sodium 2-acrylamido-2-methylpropanesulfonate with (2-acrylamido-2-methylpropyl)dimethylammonium chloride: synthesis and characterization. *Macromolecules*, *21*, 686–693.

10 Lowe, A.B., & McCormick, C.L. (2002). Synthesis and solution properties of zwitterionic polymers. *Chem. Rev.*, *102*, 4177–4189.

11 McCormick, C.L., & Salazar, L.C. (2010). Water-soluble copolymers: 44. Ampholytic terpolymers of acrylamide with sodium 2-acrylamido-2-methylpropanesulphonate and 2-acrylamido-2-methylpropanetrimethyl-ammonium chloride. *J. Appl. Polym. Sci*., *48*, 1115–1120.

12 Fevola, M.J., Bridges, J.K., Kellum, M.G., Hester, R.D., & McCormick, C.L. (2004). pH-responsive ampholytic terpolymers of acrylamide, sodium 3-acrylamido-3-methylbutanoate and (3-acrylamidopropyl)trimethylammonium chloride. I. Synthesis and characterization. *J. Appl. Polym. Sci*., *42*, 3236–3251.

13 Fevola, M.J., Kellum, M.G., Hester, R.D., & McCormick, C.L. (2004). pH-responsive ampholytic terpolymers of acrylamide, sodium 3-acrylamido-3-methylbutanoate and (3-acrylamidopropyl)trimethylammonium chloride. II. Solution properties. *J. Appl. Polym. Sci*., *42*, 3252–3270.

14 Dai, C., Xu, Zh., Wu, Y., Zou, Ch., Wu, X., & Wang, T., et all (2017). Design and Study of a Novel Thermal-Resistant and Shear-Stable Amphoteric Polyacrylamide in High-Salinity Solution. *Polymers*, *9*, 296. DOI:10.3390/polym9070296.

15 Nakahata, R., & Yusa, S. (2018). Solution Properties of Amphoteric Random Copolymers Bearing Pendant Sulfonate and Quaternary Ammonium Groups with Controlled Structures. *Langmuir*. DOI: 10.1021/acs.langmuir.7b03785.

16 Kudaibergenov, S.E. (1999). Recent advances in studying of synthetic polyampholytes in solutions. *Adv. Polym. Sci*., *144*, 115–197.

17 Kudaibergenov, S.E. (2002). Polyampholytes: Synthesis, Characterization and Application. New York: Kluwer Academic/Plenum Publishers.

18 Kudaibergenov, S.E. (2008). Polyampholytes. In *Encyclopedia of Polymer Science and Technology*. John Wiley Interscience: Hoboken, NJ, USA, 1–30.

19 Kudaibergenov, S., Jaeger, W., & Laschewsky, A. (2006). Polymeric betaines: Synthesis, characterization and application. *Advances in Polymer Science, 201*, 157–224.

20 Corpart, J.M., & Candau, F. (1993). Aqueous solution properties of ampholytic copolymers prepared in microemulsions. *Macromolecules, 26*, 1333–1343.

21 Alfrey, T., Morawetz, H., Fitzgerald, E.B., & Fuoss. R.M. (1950). Synthetic electrical analog of proteins. *J. Am. Chem. Soc*., *72*, 1864.

22 Lifshits, I.M., Grosberg, A.Y., & Khokhlov, A.R. (1979). Volume interactions in the statistical physics of polymer macromolecule. *Sov. Phys. Rev*., *22*, 123–142.

23 Li, X., Charaya, H., Bernard, G.M., Elliott, J.A.W., Michaelis, V.K., Lee, B., & Chung, H-J. (2018). Low-temperature ionic conductivity enhanced by disrupted ice formation in polyampholyte hydrogels. *Macromolecules*, *51*, 2723–2731.

Г. Төлеутай, А.В. Шахворостов, С.К. Қабдрахманова, С.Е. Құдайбергенов

Quenched, немесе күшті зарядталған, полиамфолиттердің сулы-тұзды ерітіндідегі қасиеті

Радикалды сополимерлеу әдісі көмегімен оң және теріс зарядталған мономерлер натрий 2-акриламид-2-метил-1-пропансульфон қышқылы (AMPS) және (3-акриламидопропил)үшметиламмоний хлориді (АРТАС) негізінде сызықты полиамфолиттер синтезделіп, олардың сулы-тұзды ерітіндідегі физика-химиялық қасиеті зерттелді. Тең емес (AMPS-25 және AMPS-75) және тең (AMPS-50) қатынаста алынған quenched полиамфолиттер ^{1}Н ЯМР- және ИҚ-спектроскопия, термогравиметриялық талдау, дифференциалды-сканирлеуші калориметрия әдістерімен сипатталып, олардың тутқырлықтары анықталды. Quenched полиамфолиттер изоэлектрлік нүкте (ИЭН) жағдайында күшті зарядталған аниондық және катиондық фрагменттер арасындағы ионаралық байланыс көмегімен тұрақталатындығы зерттелді. Сулы ерітіндідегі AMPS-25 және AMPS-75 конформациялық жағдайы «ядро» және «қабық» құрылымынан тұрады. Бұнда «ядро» қабатшасы полиамфолиттік сипатта (ПА аймақ) болса, «қабық» қабатшасы полиэлектролиттік эффект (ПЭ аймақ) көрсететіні белгілі болды. Ертіндінің иондық күшін арттыру полиэлектролиттің «қабық» қабатшасының қысылуына, ал «ядро» қабатшасының ісінуіне әкелетіндігі анықталды. Зарядтары тең емес AMPS-25 және AMPS-75-ке қарағанда, зарядтары тең қатынастағы полиамфолит AMPS-50-тің ИЭН-дегі гидродинамикалық өлшемі ертіндінің иондық күшін арттырғанда өсіп, антиполиэлектролиттік сипатқа ие болады. Сулы ертіндідегі quenched полиамфолиттің ИЭН-сі pH=6,1±0,1 тең. KCl қатысында ИЭН quenched полиамфолиттегі төрттік аммоний тобының хлорид иондарды байлануы нәтижесінде pH=6,5–7,0 аралығына ығысатындығы белгілі болды.

Кілт сөздер: quenched полиамфолиттер, изоэлектрлік нүкте, гидродинамикалық өлшем, полиэлектролитішілік кешен, «ядро-қабық» құрылым, полиамфолиттік жағдай, полиэлектролиттік жағдай, иондық күш.

Г. Толеутай, А.В. Шахворостов, С.К. Кабдрахманова, С.Е. Кудайбергенов

Поведение quenched, или сильно заряженных, полиамфолитов в водно-солевых растворах

Методом свободно-радикальной сополимеризации синтезированы quenched (или сильно заряженные) линейные полиамфолиты на основе отрицательно и положительно заряженных мономеров — натриевой соли 2-акриламидо-2-метил-1-пропансульфоновой кислота (AMPS) и (3-акриламидопропил)триметиламмоний хлорида (АРТАС) и исследованы их физико-химические свойства в водно-солевых растворах. Ряд несбалансированных (AMPS-25 и AMPS-75) и сбалансированных (AMPS-50) quenched полиамфолитов охарактеризованы методами ^{1}Н ЯМР- и ИК-спектроскопии, термогравиметрического анализа и дифференциально-сканирующей калориметрии, а также изучена их вязкость. Установлено, что в изоэлектрической точке (ИЭТ) quenched полиамфолиты стабилизируются с помощью внутриионных контактов между сильно заряженными анионными и катионными фрагментами. Конформационное состояние AMPS-25 и AMPS-75 в водном растворе представлено как структура «ядро» и «оболочка». При этом «ядро» имеет полиамфолитный характер (ПА область), а «оболочка» проявляет полиэлектролитный эффект (ПЭ область). Повышение ионной силы раствора приводит к

сжатию «оболочки» полиэлектролита и набуханию «ядра» полиамфолита. В отличие от AMPS-25 и AMPS-75, гидродинамические размеры сбалансированного полиамфолита AMPS-50 в ИЭТ увеличиваются при повышении ионной силы раствора, демонстрируя *антиполиэлектролитный* характер. Установлено, что в водном растворе ИЭТ quenched полиамфолитов имеют pH=6,1±0,1. В присутствии KCl положение ИЭТ смещается до pH=6,5–7,0 из-за специфического связывания хлорид-ионов четвертичными аммониевыми группами quenched полиамфолитов.

Ключевые слова: quenched полиамфолиты, изоэлектрическая точка, гидродинамический размер, внутриполиэлектролитные комплексы, структура «ядро-оболочка», полиамфолитный режим, полиэлектролитный режим, ионная сила.

DOI 10.31489/2019Ch2/45-50

UDC 543.552

A.S. Gashevskaya[1], A.O. Gusar[1], Ye.V. Dorozhko[1], K.V. Dyorina[1], S.O. Kenzhetayeva[2]

[1]Tomsk Polytechnic University, Russia;
[2]Ye.A. Buketov Karaganda State University, Kazakhstan
(E-mail: asg30@tpu.ru)

Voltammetric determination of carbaryl in some cereals on an impregnated graphite electrode modified with carbon ink

Nowadays, pesticides are an integral part of our lives. These compounds are contained in food, water, soil. Consequently people consume them constantly in significant amounts. Therefore, the control of pesticides content in various objects is the most important problem for human health maintaining. In the present work, the electrochemical oxidation of carbaryl on an impregnated graphite electrode modified with carbon ink was studied for the first time. The optimal conditions of carbaryl extraction from some grain crops were selected, followed by its determination on an impregnated graphite electrode modified with carbon ink by linear sweep anodic voltammetry. A number of cereals, such as wheat, oats and corn, were selected as the objects of study. The determination of carbaryl in the objects was carried out after chromatographic separation by TLC. It is revealed that carbon ink increases the electroactive surface of the impregnated graphite electrode. As a result, the sensitivity of carbaryl determination increases. Therefore, the accuracy of carbaryl trace amounts determination increases. The range of linear dependence of dI/dE on the concentration of carbaryl was from $0 \cdot 10^{-8}$ M to $1.6 \cdot 10^{-8}$ M, the detection limit was $1.2 \cdot 10^{-9}$ M.

Keywords: carbaryl, linear sweep anodic voltammetry, impregnated graphite electrode, carbon ink, food, pesticides, thin-layer chromatography, crops.

Introduction

Today, the problem of pesticide residues determination in food, drinking water and soil is relevant to safety and well being of society. Even a small amount of pesticides in food, water and soil can cause significant harm to human health. Therefore, the monitoring of these residues is one of the most important steps to minimize the potential risks to the health of not only humans, but also animals [1]. In order to avoid hazards to human and animal health caused by pesticide residues, governments of various countries regulate the maximum level of pesticide residues in fruits and vegetables, in drinking water, and in the soil, seeking to limit their effects on the population [2].

Carbamates are a group of pesticides, the derivates of carbamic acid. All pesticides of this group are known as active insectoacaricides, fungicides, and herbicides [3]. The mechanism of carbamates toxic effect on the living organism has been poorly studied. However, it is known that the effect of carbamates on the body disrupts redox processes; there are signs of hypoxia and damage to the central nervous system. In persons working with carbamates, there are lesions of the upper respiratory tract. In contact with the skin there is a pronounced irritant effect. In case of acute intoxication, hemolytic anemia may develop. There is a strong irritant effect of carbamic acid derivatives on mucous membranes [3].

The maximum level of pesticide residues values of carbamates in food products, as established by regulatory authorities, range from 0.01 to 10 mg/kg in relation to acceptable daily intake. In addition, for drinking

water and soil, values were given as indicative limits from 10 μg/l to 90 μg/l [1]. According to the literature, mainly carbamates, namely carbaryl, are determined using chromatographic methods of investigation, such as gas and liquid chromatography, thin layer chromatography [4]. Along with the above methods for the determination of carbamates, inverse voltammetry is also used [5–8]. The advantages of this method are high sensitivity, a wide range of defined elements, and simplicity of measurement techniques, reliability, and low costs [9].

In this work, the electrochemical properties of a carbaryl model compound from the class of carbamates were studied by linear sweep anodic voltammetry on an impregnated graphite electrode modified with carbon ink. The working conditions for the determination of carbaryl in working solutions were the following: the background electrolyte was an alcohol solution of sodium perchlorate, the working electrode was an impregnated graphite electrode, the auxiliary and reference electrode were platinum and silver chloride electrodes. It has been established that the application of carbon ink as an electrode modifier improves the sensitivity of its determination, which is especially important when determining the trace amounts of carbaryl in cereals. The dependence of dI/dE on the carbaryl concentration was linear from $0 \cdot 10^{-8}$ to $1.6 \cdot 10^{-8}$ M, the detection limit was $1.2 \cdot 10^{-9}$ M. The approbation of the method for carbaryl determination in corn, oats, and wheat was carried out.

Experimental

Carbaryl is an organic compound, a carbamate, the α-naphthyl ester of N-methylcarbamic acid, the highly effective insecticide (Fig. 1). It is a solid crystalline substance with a white or slightly yellowish tinge; it has no odor, is poorly soluble in water, and well in organic solvents. Carbaryl is approved to be used in Russia.

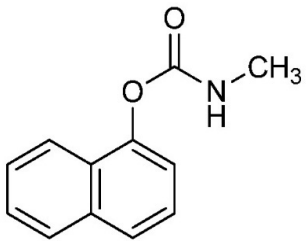

Figure 1. The structural formula of carbaryl

The following reagents were used to study the electrochemical properties of carbaryl, namely sulfuric acid H_2SO_4 (Reahim, Russia), purified ethyl alcohol 96 % C_2H_5OH (Labtech, Russia), potassium chloride KCl (Uralkali, Russia), sodium perchlorate $NaClO_4$ (Merk, Germany), carbaryl $C_{12}H_{11}NO_2$ (Sigma-Aldrich, USA), microcrystalline graphite (<20μm, Sigma-Aldrich, USA), polystyrene (Sigma-Aldrich, USA), 1,2-dichloroethane $C_2H_4C_{l2}$ (Sigma-Aldrich, USA).

All necessary experiments were carried out on a TA — Lab voltammetric station (manufactured by Tomanalit Research and Production Enterprise, Tomsk).

The currents recorded on the anodic voltammogram in the form of a wave were transformed in the mode of the first derivative dI/dE – E, where the analytical signals were observed in the form of peaks.

A sodium perchlorate alcohol solution of 0.1 M was used as the background electrolyte. An impregnated graphite electrode was used as a working electrode, which was obtained by vacuum impregnation of blanks from spectral coal with epoxy resins (Mikroprimesi LLC, Tomsk), the auxiliary and reference electrode were silver and silver chloride electrodes, respectively. Working solutions of carbaryl were prepared by dissolving a certain sample of state standard sample in ethanol.

Modifying carbon ink was a mixture of 0.09 g of microcrystalline graphite and 0.01 g of polystyrene dissolved in 0.5 cm^3 of 1,2-dichloroethane. To create a homogeneous suspension, the mixture was vigorously stirred for 3 minutes using an ElmySkyline shaker. 1 μl of the resulting suspension was placed on the surface of the working electrode and dried in air for 2–3 minutes.

The electrochemical properties of carbaryl on an unmodified and modified carbon ink impregnated graphite electrode were carried out in the potential range from –2.5 to +2.5 V under scan rate ν = 70 mV/s.

Isolation of carbaryl in food

A weighed portion of crushed grain weighing 100 g was filled in with 200 cm^3 *n*-hexane and left overnight with constant stirring under a fume hood. Then, the resulting mass was filtered into a vacuum cup, washing the contents of the flask several times with *n*-hexane, 20 cm^3 each. The filter was also washed with *n*-hexane several times 15 cm^3 each. The contents of the cup were left under a fume hood, to completely volatilize the solvent at room temperature. To extract the carbaryl and remove impurities, 10 ml of 96 % ethanol was added to the dry residue and the residue was triturated with a glass rod. The resulting mixture was filtered through a «Blue Ribbon» filter paper. The filtrate was used to detect carbaryl.

The resulting sample was applied to a Sorbfil chromatographic (aluminum) plate. Chloroform (97.4 %) was chosen as the mobile phase, which is not electrochemically active. The spots were dried in air, and then the plate was introduced into the chamber for chromatography. Then the plate was removed from the chamber, dried in air and irradiated with UV light. When the plate was irradiated with UV light, the spots acquired a red color. R_f for carbaryl was 0.57, the time of chromatography was 3 hours.

Carbaryl was washed off by a method of washing a fixed spot of the development of a spot with ethyl alcohol, in an amount of 3 cm^3 in a glass container. The operation was repeated twice.

Results and Discussion

The voltammetric determination of carbaryl

When studying the electrochemical properties of carbaryl, cyclic voltammograms was recorded on different electrodes (carbon-containing, mercury-film, platinum, modified carbon-containing electrode with carbon ink, impregnated graphite, impregnated graphite electrode, modified with carbon ink) under ν=70 mV/s sodium perchlorate is in the background electrolyte. The analytical signal of carbaryl was detected only on the impregnated graphite electrode in the anodic region of the potentials -2.5V to +2.5V (Fig. 2). When carbon ink was applied to the surface of an impregnated graphite electrode, the sensitivity of the determination of carbaryl in model solutions increased 10 fold.

Figure 2 shows voltammograms of carbaryl oxidation (concentration $0.4 \cdot 10^{-8}$ M) on unmodified and modified graphite carbon ink in electrodes (Fig. 2*a*) and the range of linear dependence of the oxidation current on the concentration of carbaryl (Fig. 2*b*), which amounted to $0 \cdot 10^{-8}$ to $1.6 \cdot 10^{-8}$ M.

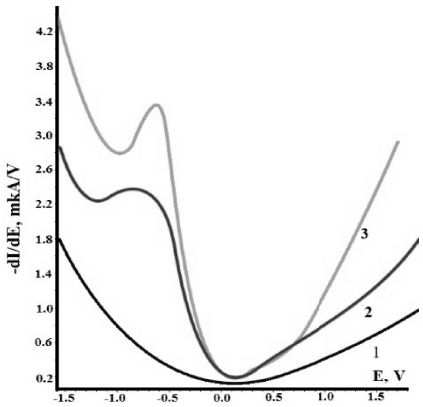

1 — background curve of sodium perchlorate alcohol solution 0.1 M; *2* — carbaryl ($0.4 \cdot 10^{-8}$ M) on the unmodified graphite electrode; *3* — carbaryl ($0.4 \cdot 10^{-8}$M) on a graphite electrode modified with carbon ink

Figure 2*a*. Anodic voltam mograms of carbaryl

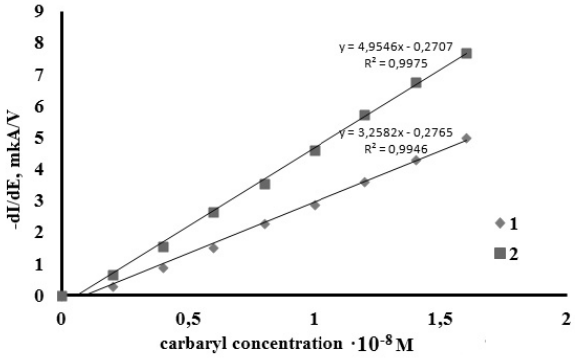

1 — unmodified graphite electrode;
2 — carbon graphite-modified carbon ink

Figure 2*b*. Linear dependence of the carbaryl oxidation current in the concentration range from $0 \cdot 10^{-8}$ to $1.6 \cdot 10^{-8}$M

According to the literature data, the electrochemical oxidation of carbaryl can occur through the oxidation of a carbamate group [7]. The modification of an impregnated graphite electrode with carbon ink leads to the sensitivity increase of carbaryl determination in model solutions due to the possible increase in the area of the electroactive surface of the electrode. A standard technique for evaluating the effectiveness of an electrode modifier is the usage of redox $[Fe(CN)_6]^{3-}/[Fe(CN)_6]^{4-}$ as a standard (Fig. 3).

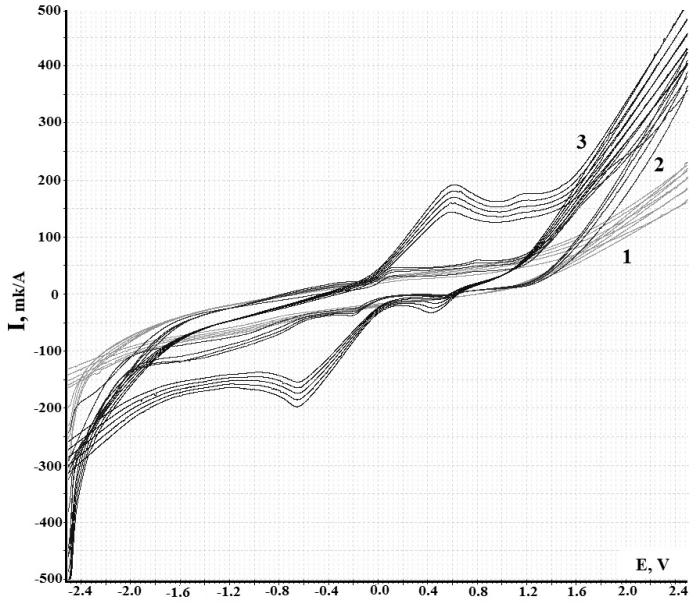

Figure 3. Cyclic voltammograms $1 \cdot 10^{-4}$ M $Fe(CN)_6^{3-}/Fe(CN)_6^{4-}$ on unmodified graphite (2) and graphite electrode modified with carbon ink in graphite electrode (3) at pH=6.86, ν = 70mV/s (1) is the background curve

The Randles-Shevchik equation (1) was used to calculate the electroactive surface area:

$$Ip = 2.69 \times 10^5 Z^{3/2} A D^{1/2} C V^{1/2}, \quad (1)$$

where *Ip* is peak current, A; *Z* is the number of electrons ($n = 1$); *A* is the area of the electroactive surface, cm^2; *D* is diffusion coefficient ($7.60 \cdot 10^{-6}$ cm^2/s), [10]; *C* is concentration of $Fe(CN)_6^{3-}/Fe(CN)_6^{4-}$ in solution ($1 \cdot 10^{-4}$ M); *V* is the sweep speed, mV/s.

The calculated electroactive surface area of the unmodified graphite electrode was 0.013 cm^2, while, after modification, it became 10 times large as 0.103 cm^2. Thus, the efficiency of using carbon ink as a modifier of an impregnated graphite electrode for the voltammetric determination of carbaryl is shown. All further determinations of carbaryl, both in model solutions and in grain crops, were carried out on an impregnated graphite electrode modified with carbon ink.

As a method for isolating carbaryl from the analyzed mixture of components obtained from grain crops, the method of thin layer chromatography was used (the technique is presented in the «experimental part» section). The verification of proposed determination method for carbaryl in model solutions was carried out using the «introduced-found» method. The results are presented in Table 1.

Table 1

Check the correctness of the definition of carbaryl using the «entered-found» method

No.	Is entered, 10^{-8} M	Found, 10^{-8} M	Δ, %
1	0.4	0.33	±4.5
2	0.8	0.79	±4.3
3	1.2	1.12	±4.0

Thus, in the indicated range of carbaryl concentrations, the standard deviation of the found results from the accepted reference values does not exceed 4.5 %.

In the work, the carbaryl was determined by voltammetry on a carbon ink impregnated graphite electrode modified in carbon in corn, oats, and wheat. Sample preparation and chromatographic isolation of carbaryl from grain crops was performed according to the method presented in the section «experimental part». Quantitative determination of carbaryl in the resulting washes was carried out under the following conditions: the anodic region of the signal at a potential of –0.8V, ν=70 mV/s, the background electrolyte was an alcohol solution of sodium perchlorate 0.1 M. The concentration of carbaryl was calculated by the method of calibration curve. The results of the voltammetric determination of carbaryl are presented in Table 2. These results are calculated using the equations presented in Figure 2*b*.

Table 2

The results of the determination of carbaryl in food (n = 3)

Object of study	Found, M	Δ, %
Corn	$0.84 \cdot 10^{-8}$	±0.13
Oats	$0.36 \cdot 10^{-8}$	±0.054
Wheat	–	–

Thus, the selected voltammetric conditions for the determination of carbaryl in model solutions allow the determination of its trace amounts in corn and oats. Carbaryl was not detected in wheat.

Conclusions

In this work, the electrochemical properties of a carbaryl model compound from the class of carbamates were studied by anodic voltammetry on an impregnated graphite electrode modified with carbon ink. The working conditions for the determination of carbaryl in working solutions were selected, namely the background electrolyte is an alcohol solution of sodium perchlorate, the working electrode is an impregnated graphite electrode, the auxiliary and reference electrode is platinum and silver chloride electrodes. It is revealed that when using carbon ink as an electrode modifier, it increases the sensitivity of its determination, which is especially important when determining the trace amounts of carbaryl in grain crops. The range of linear dependence of dI/dE on the concentration of carbaryl was from $0 \cdot 10^{-8}$ to $1.6 \cdot 10^{-8}$ M, the detection limit was $1.2 \cdot 10^{-9}$ M. The approbation of the carbaryl determination method in corn, oats and wheat was carried out.

References

1 ГН 1.2.1323–03 Гигиенические нормативы содержания пестицидов в объектах окружающей среды.

2 Alamgir Zaman Chowdhury M. Detection of the residues of nineteen pesticides in fresh vegetable samples using gas chromatography-mass spectrometry / Alamgir Zaman Chowdhury M., A.M. Fakhruddin, Nazrul Islam M., M. Moniruzzaman, S.H. Gan, Khorshed Alam M. // Food Control. — 2013. — Vol. 34. — P. 457–465.

3 Çelebi M.S. Electrochemical oxidation of carbaryl on platinum and boron-doped diamond anodes using electro-Fenton technology / M.S. Çelebi, N. Oturan, H. Zazou, M. Hamdani, M.A. Oturan // Separation and Purification Technology. — 2015. — Vol. 156. — P. 996–1002.

4 Fan Y. Determination of carbaryl pesticide in Fuji apples using surface-enhanced Raman spectroscopy coupled with multivariate analysis. LWT / Y. Fan, K. Lai, B.A. Rasco, Y. Huang // Food Science and Technology. — 2015. — Vol. 60. — P. 352–357.

5 Van Dyk J.S. Review on the use of enzymes for the detection of organochlorine, organophosphate and carbamate pesticides in the environment / J.S. Van Dyk, B. Pletschke // Chemosphere. — 2011. — Vol. 82. — P. 291–307.

6 Cesarino I. Electrochemical detection of carbamate pesticides in fruit and vegetables with a biosensor based on acetylcholinesterase immobilised on a composite of polyaniline–carbon nanotubes / I. Cesarino, F.C. Moraes, M.V. Lanza, S.S. Machado // Food Chemistry. — 2012. — Vol. 135. — P. 873–879.

7 Moraes F.C. Direct electrochemical determination of carbaryl using a multi-walled carbon nanotube/cobalt phthalocyanine modified electrode / F.C. Moraes, L.H. Mascaro, S.S. Machado, C.A. Brett // Talanta. — 2009. — Vol. 79. — P. 1406–1411.

8 Wei H. Rapid hydrolysis and electrochemical detection of trace carbofuran at a disposable heated screen-printed carbon electrode / H. Wei, J.J. Sun, Y.M. Wang, X. Li, G.N. Chen // Analyst. — 2008. — Vol. 133. — P. 1619–1624.

9 Liu B. Electrochemical analysis of carbaryl in fruit samples on grapheme oxide-ionic liquid composite modified electrode / B. Liu, B. Xiao and L. Cui // Journal of Food Composition and Analysis. — 2015. — Vol. 40. — P. 14–18.

10 Липских О.И. Определение кармуазина в безалкогольных напитках методом вольтамперометрии / О.И. Липских, Е.И. Короткова, Е.В. Дорожко, К.В. Дёрина, О.А. Воронова // Заводская лаборатория. Диагностика материалов. — 2016. — Т. 82, № 6. — С. 22–26.

А.С. Гашевская, А.О. Гусар, Е.В. Дорожко, К.В. Дёрина, С.О. Кенжетаева

Кейбір дәнді дақылдарда ерітінді сіңірілген, көміртектік сиялармен модификацияланған, графит электродында карбарилді вольтамперометриялық анықтау

Пестицидтер бұл күнде біздің өміріміздің ажырамайтын бөлігі болды. Олар күнде біздің ағзамызға тағамдармен, сумен, топырақпен түседі. Сондықтан әртүрлі нысандарда пестицидтердің құрамын бақылау адам өмірі үшін ең маңызды мәселе болды. Мақалада алғаш рет карбарилдің ерітінді сіңірілген, көміртек сияларымен модификацияланған, графит электродында электрохимиялық

тотығуы зерттелген. Карбарилдің кейбір дәнді дақылдардан бөліп алудың оңтайлы жағдайлары табылды, соңынан көміртек сияларымен модификацияланған, ерітінді сіңірілген графит электродында анодтық вольтамперометрия әдісімен анықталды. Зерттеу нысандары болып бидай, сұлы, жүгері сияқты дәнді дақылдар таңдалған. Таңдалған нысандарда карбарилдің анықталуы ЖҚХ әдісімен хроматографиялық бөлуден кейін жүргізілді. Электродтық модификатор ретінде көміртек сияларын қолданғанда ерітінді сіңірілген графит электродының электробелсенді беттерінің аумағы артататыны анықталды. Сол мезгілде карбарилді анықтау сезімталдығы да жоғарлайтыны анықталды, әсіресе бұл карбарилдің дәнді дақылдардағы іздік мөлшерлерін анықтау барысында маңызды. Карбарил концентрациясынан сызықтық тәуелділік диапазоны dI/dE — $0{\cdot}10^{-8}$ М-ден $1{,}6{\cdot}10^{-8}$ М дейін, ал табу шекарасы $1{,}2{\cdot}10^{-9}$ М құрады.

Кілт сөздер: карбарил, анодтық вольтамперометрия, ерітінді сіңірілген электрод, көміртектік сиялар, тағамдар, пестицидтер, жұқақабатты хроматография, дәнді дақылдар.

А.С. Гашевская, А.О. Гусар, Е.В. Дорожко, К.В. Дёрина, С.О. Кенжетаева

Вольтамперометрическое определение карбарила в некоторых зерновых культурах на импрегнированном графитовом электроде, модифицированном углеродными чернилами

Пестициды на сегодняшний день являются неотъемлемой частью нашей жизни. Каждый день они попадают в наш организм с продуктами питания, водой, почвой. Поэтому контроль содержания пестицидов в различных объектах является наиболее важной проблемой для жизни человека. В настоящей работе впервые изучено электрохимическое окисление карбарила на импрегнированном графитовом электроде, модифицированном углеродными чернилами. Подобраны оптимальные условия выделения карбарила из некоторых зерновых культур, с последующим его определением на импрегнированном графитовом электроде, модифицированном углеродными чернилами, методом анодной вольтамперометрии. Объектами исследования были выбраны зерновые культуры, такие как пшеница, овес и кукуруза. Определение карбарила в выбранных объектах исследования проводилось после хроматографического разделения методом ТСХ. Выявлено, что при использовании углеродных чернил в качестве электродного модификатора происходит увеличение площади электроактивной поверхности импрегнированного графитового электрода. При этом увеличивается чувствительность определения карбарила, что особенно важно при определении следовых количеств карбарила в зерновых культурах. Диапазон линейной зависимости dI/dE от концентрации карбарила составил от $0{\cdot}10^{-8}$ М до $1{,}6{\cdot}10^{-8}$ М, предел обнаружения — $1{,}2{\cdot}10^{-9}$ М.

Ключевые слова: карбарил, анодная вольтамперометрия, импрегнированный электрод, углеродные чернила, продукты питания, пестициды, тонкослойная хроматография, зерновые культуры.

References

1 GN 1.2.1323–03 *Hihienicheskie normativy soderzhaniia pestitsidov v obektakh okruzhaiushchei sredy [Hygienic standards for the content of pesticides in environmental objects]* [in Russian].

2 Alamgir Zaman Chowdhury M., Fakhruddin, A.M., Nazrul Islam M., Moniruzzaman M., Gan S.H., & Khorshed Alam M. (2013). Detection of the residues of nineteen pesticides in fresh vegetable samples using gas chromatography–mass spectrometry. *Food Control*, *34*, 457–465.

3 Çelebi, M.S., Oturan, N., Zazou, H., Hamdani, M., & Oturan, M.A. (2015). Electrochemical oxidation of carbaryl on platinum and boron-doped diamond anodes using electro-Fenton technology. *Separation and Purification Technology*, *156*, 996–1002.

4 Fan, Y., Lai, K., Rasco, B.A., & Huang, Y. (2015). Determination of carbaryl pesticide in Fuji apples using surface-enhanced Raman spectroscopy coupled with multivariate analysis. *LWT — Food Science and Technology*, *60*, 352–357.

5 Van Dyk, J.S., & Pletschke, B. (2011). Review on the use of enzymes for the detection of organochlorine, organophosphate and carbamate pesticides in the environment. *Chemosphere*, *82*, 291–307.

6 Cesarino, I., Moraes, F.C., Lanza, M.V., & Machado, S.S. (2012). Electrochemical detection of carbamate pesticides in fruit and vegetables with a biosensor based on acetylcholinesterase immobilised on a composite of polyaniline-carbon nanotubes. *Food Chemistry*, *135*, 873–879.

7 Moraes, F.C., Mascaro, L.H., Machado, S.S., & Brett, C.A. (2009). Direct electrochemical determination of carbaryl using a multi-walled carbon nanotube/cobalt phthalocyanine modified electrode. *Talanta*, *79*, 1406–1411.

8 Wei, H., Sun, J.J., Wang, Y.M., Li, X., & Chen, G.N. (2008). Rapid hydrolysis and electrochemical detection of trace carbofuran at a disposable heated screen-printed carbon electrode. *Analyst*, *133*, 1619–1624.

9 Liu, B., Xiao, B. & Cui, L. (2015). Electrochemical analysis of carbaryl in fruit samples on grapheme oxide-ionic liquid composite modified electrode. *Journal of Food Composition and Analysis*, *40*, 14–18.

10 Lipskikh, O.I., Korotkova, E.I., Dorozhko, E.V., Derina, K.V., Voronova, O.A. (2016). Opredelenie karmuazina v bezalkoholnykh napitkakh metodom voltamperometrii [Determination of carmoisin in soft drinks by voltammetry]. *Zavodskaia laboratoriia. Diahnostika materialov — Factory laboratory. Diagnostics of materials*, *82, 6,* 22–26 [in Russian].

DOI 10.31489/2019Ch2/51-55
UDC 537.531

V.Yu. Chirkova, Ye.A. Sharlayeva, I.Ye. Stas

Altai State University, Barnaul, Russia
(E-mail: varvara.chirkova@gmail.com)

Boiling temperature and the enthalpy of water vaporization exposed to high frequency electromagnetic field

The article is dedicated to the study of the influence of a high-frequency electromagnetic field on the boiling temperature and the enthalpy of water vaporization. It has been established that as a result of exposure to deionized water of the electromagnetic field of ultrahigh frequencies, its boiling point and evaporation enthalpy increase. It has been shown that the effectiveness of electromagnetic exposure depends on the frequency of the field and the exposure time. The maximum increase in the enthalpy of evaporation is observed as a result of exposure to a field with a frequency of 60, 130 and 170 MHz and is 5–10 %. The observed phenomena can be caused by a change in the structural organization of water as a result of electromagnetic interference, effect has a cumulative nature — the value of ΔH_{ev} increases with an increase in the exposure time to 2 hours; the effect of «saturation» is established — an increase in the exposure time over 2 hours does not lead to a further increase in enthalpy. The effect of the electromagnetic field is selective — the properties of water are sensitive to the action of a field of strictly defined frequencies.

Keywords: water, electromagnetic field, frequency, irradiation time, boiling point, evaporation enthalpy.

Introduction

Interest in the study of water and its unique properties has not waned for many decades [1–3]. Numerous studies are focused on changing the properties of water and aqueous solutions under the influence of magnetic and electromagnetic fields [4]. Experimental material accumulates, numerous theories are created to explain the changes in the properties of water and aqueous solutions under the influence of field effects, but there is currently no generally accepted theory about the nature of changes occurring in water as a result of external influences. Numerous experiments on the effects of the electromagnetic field (EMF) of ultrahigh frequencies (30–300 MHz) indicate the sensitivity of the properties of the aquatic environment to this type of exposure [5–8]. Based on the experimental data, it can be assumed that under the influence of the field, the cohesive interaction within the aqueous phase is enhanced, which is manifested in an increase in its surface tension, weakening of the hydration characteristics [6], etc. The enhancement of the intermolecular interaction in the aquatic environment can be fixed by measuring the properties that depend on it. Accurate information on cohesion can be obtained from thermodynamic characteristics related to the energy of vaporization. In the process of evaporation of a substance, a complete rupture of intermolecular bonds occurs; therefore, the work of cohesion is determined by the enthalpy of vaporization (evaporation). The determination of the enthalpy of evaporation of water and its changes as a result of exposure to an electromagnetic field with a variable frequency was the purpose of this study.

Method

Deionized water purified with the deionizer of water WD-301, with an initial specific electric conductivity of $1.4–1.8 \cdot 10^{-4}$ S/m was used in this study.

The source of the electromagnetic field was a high-frequency generator G4–119A, which output power was 1 W and its frequency range was 30–200 MHz. The voltage at the high-frequency electrodes was 20–22 V. The cell consisted of a 50 ml teflon beaker, in the center of which an internal high-frequency electrode was located. The high-frequency electrode was a brass rod isolated with teflon. The outer high-frequency electrode was an aluminum cup, closely fitting to the teflon surface. The electrodes through the bottom of the cup were connected to the generator by means of an high-frequency cable. The field frequency was varied in 10 MHz steps. The time of exposure of the field to water ranged from 1 to 3 hours. It was found that the maximum effect was achieved within 2 hours, but the main changes were observed at an exposure time of 1 hour. In the future, precisely this time was chosen for the experiment.

The determination of T_{boil} and the enthalpies of evaporation were carried out using a standard setup [9]. In a round bottom flask, equipped with a reflux condenser and a thermometer (division price 0.1 ºC), 50 ml

of a predetermined frequency of irradiated field or unirradiated water was poured. In the flask, a vacuum was created using a vacuum pump (minimum pressure 0.1 atm), which was monitored with a pressure gauge (graduation value 0.05 atm). The water was kept at a minimum pressure for 1 hour to remove dissolved gases. Then water was heated to boiling at a given vacuum and the temperature was fixed. The pressure was gradually increased up to atmospheric, determining the boiling point at each pressure value with a step of 0.10 atm. Experimental data on the batch of water at different pressures were compared with the table values [10]. A satisfactory agreement of the results was obtained (the discrepancies did not exceed ± 0.2 ºC). The enthalpy of vaporization ΔH_{ev} was determined from the slope of the line in the coordinates $\ln P - 1000/T$ according to the linear form of the Clausius-Clapeyron equation: $\ln P = \text{const} - 1000\Delta H_{ev}/RT$.

Results and Discussion

Studies have shown that as a result of exposure to electromagnetic fields at certain frequencies (60, 130 and 170 MHz), an increase in the boiling point of water is observed. The use of other EMF frequencies either did not change the batch of water, or the changes were expressed slightly. Figure 1 shows the dependences of T_{boil} on the pressure P for non-irradiated and irradiated EMF frequencies of 170 and 80 MHz of water. In the first case (Fig. 1*a*), in the region of low values of atmospheric pressure, the batch of irradiated water exceeds a similar value for unirradiated water at $P < 0.60–0.75$ atm. A similar pattern is observed for frequencies 60 and 130 MHz. Figure 1*b* shows that the effect of an EMF of 80 MHz slightly changes the boiling point of water only at $P < 0.35$ atm.

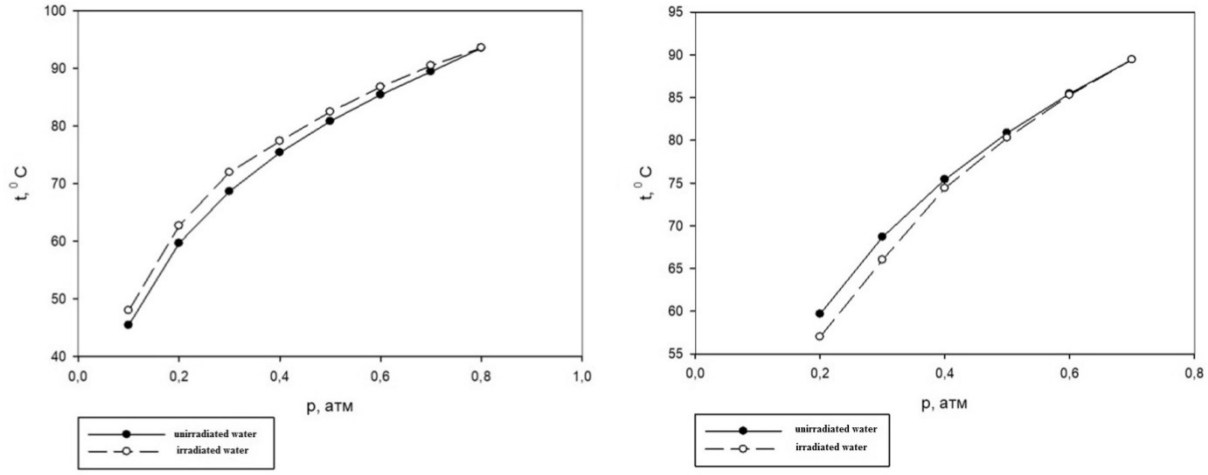

a) f = 170 MHz *b) f* = 80 MHz

Figure 1. Dependence of the boiling point of water exposed to an electromagnetic field of a given frequency *f*, from atmospheric pressure (T = 23 ºC; t_{exp}= 1 hour)

Table 1 shows the T_{boil} values of unirradiated and irradiated EMF of various frequencies of water at $P = 0.20$ atm (average values from 5 parallel experiments).

Table 1

The boiling point T_{boil} of water at $P = 0.20$ atm, depending on the frequency of the electromagnetic field (exposure time 1 hour)

Frequency *f*, MHz	T_{boil}, ºC	ΔT, ºC	Frequency *f*, MHz	T_{boil}, ºC	ΔT, ºC
0	59.8±0.2	–	120	61.0±0.4	1.2
30	59.8±0.2	–	130	61.6±0.3	1.8
40	60.2±0.3	0.4	140	59.6±0.2	0.2
50	59.6±0.3	0.2	150	60.2±0.3	0.4
60	61.0±0.4	1.2	160	59.8±0.1	–
70	59.8±0.1	–	170	61.7±0.3	1.9
80	60.1±0.2	0.3	180	59.4±0.2	0.4
90	59.7±0.1	0.1	190	59.6±0.3	0.2
100	59.9±0.3	0.1	200	59.6±0.2	0.2

From the experimental dependence of $T_{boil} - P$ (in the range of 0.10–0.70 atm, where the differences in boiling points are quite well expressed), the enthalpies of evaporation of water exposed to EMF of different frequencies were calculated using the Clapeyron-Clausius equation. The correlation coefficient of the linear approximation of the experimental data was 0.997–0.999. Table 2 shows the values of ΔH_{ev} at those EMF frequencies at which its significant change is observed — by 5–10 %. The impact of the field of other frequencies in the studied range did not lead to a noticeable change in ΔH.

Table 2

The enthalpy of evaporation of water exposed to an electromagnetic field (exposure time 1 hour)

Frequency f, MHz	ΔH_{ev}, kJ/mol	Δ, %
0	45.3±0.5	–
30	47.6±0.6	5.1
60	48.2±0.9	6.4
130	49.9±0.9	10
170	48.1±0.8	6.5

The determination of the enthalpy of evaporation was carried out immediately after the electromagnetic treatment of water, then after 1, 2 and 7 days. The results are presented in Table 3 for 2 frequencies of EMF (60 MHz and 170 MHz). It can be stated that with time there is a tendency to a slight increase in ΔH_{ev}. The effect of relaxation is absent, i.e. the original properties of water during the week are not restored.

Table 3

The enthalpy of evaporation of water depending on the time elapsed after exposure to an electromagnetic field

Time after exposure to electromagnetic field, day	ΔH_{ev}, kJ / mol (f = 60 MHz)	ΔH_{ev}, kJ / mol (f = 170 MHz)
0	48.2±0.9	48.1±0.8
1	48.3±0.8	48.3±0.9
2	49.0±0.8	47.8±0.9
7	48.7±0.7	49.0±0.6

Conclusions

Thus, as in all previous studies [5–8], it was shown that the effect of EMF is selective — the properties of water are sensitive to the action of a field of strictly defined frequencies. It was also established that the EM effect has a cumulative nature — the value of ΔH_{ev} increases with an increase in the exposure time to 2 hours; the effect of «saturation» is established — an increase in the exposure time over 2 hours does not lead to a further increase in enthalpy. The enhancement of the cohesive interaction in the aqueous phase as a result of exposure to EMF can be due to several reasons: hardening of the hydrogen bonds between water molecules, an increase in the proportion of water bound into clusters, or an enhancement of the van der Waals interaction. The question remains controversial, since the enthalpies of evaporation characterize the intensity of intermolecular interaction, but do not reveal its nature. Nevertheless, the obtained data are consistent with the results of [6] on the increase as a result of the electromagnetic effect of the surface tension of water by 5–10 %, which is also determined by the intensity of the intermolecular interaction.

References

1 Chaplin M.F. A proposal for the structuring of water / M.F. Chaplin // Biophys. Chem. — 2000. — Vol. 83, No. 3. — P. 211–221.

2 Le Bihan D. Water: The Forgotten Biological Molecule / D. Le Bihan, H. Fukuyama. — Singapore: Pan Stanford Publishing Pte. Ltd., 2010. — 399 p.

3 Dack M.R.J. Solvent structure. II. A study of the structure-making and structure-breaking effects of dissolved species in water by internal pressure measurements / M.R.J. Dack // Aust. J. Chem. — 1976. — Vol. 29, No. 4. — P. 771–778.

4 Стехин А.А. Структурированная вода: Нелинейные эффекты / А.А. Стехин, Г.В. Яковлева. — М.: Изд-во ЛКИ, 2008. — 320 с.

5 Стась И.Е. Физико-химические закономерности эволюции коллоидных наносистем в жидкой дисперсионной среде под влиянием электромагнитных полей / И.Е. Стась, Л.Ю. Репейкова. — Барнаул: Изд-во Алт. ун-та, 2013. — 100 с.

6 Стась И.Е. Физико-химические процессы в электромагнитном поле ультравысоких частот / И.Е. Стась, В.Ю. Чиркова, И.А. Штоббе. — Барнаул: Изд-во Алт. ун-та, 2015. — 101 с.

7 Стась И.Е. Влияние электромагнитного поля высокой частоты на критическую концентрацию мицеллообразования водного раствора додецилсульфата натрия / И.Е. Стась, О.П. Михайлова // Журнал физической химии. — 2009. — Т. 83, № 2. — С. 324–325.

8 Стась И.Е. Влияние высокочастотного электромагнитного поля на адсорбционную способность ионогенных ПАВ / И.Е. Стась, Б.П. Шипунов, О.П. Михайлова // Журнал физической химии. — 2010. — Т. 84, № 12. — С. 2128–2132.

9 Практикум по физической и коллоидной химии / под ред. К.М. Евстратовой. — М.: Высш. шк., 1990. — С. 120–124.

10 Краткий справочник физико-химических величин / под ред. К.П. Мищенко, А.А. Равделя. — Л.: Химия, 1974. — 200 с.

В.Ю. Чиркова, Е.А. Шарлаева, И.Е. Стась

Жоғары жиіліктегі электрмагнитті өріс әрекетіне ұшыраған судың қайнау температурасы және булану энтальпиясы

Мақала судың қайнау температурасы мен булану энтальпиясына жоғары жиіліктегі электрмагнитті өрістің әсерін зерттеуге арналған. Деиондалған суға өте жоғары жиіліктегі электрмагнитті өріс әрекет еткенде оның қайнау температурасы мен булану энтальпиясы артатыны анықталған. Электрмагнитті әрекеттің тиімділігі өріс жиілігіне және экспозиция уақытына тәуелді болатыны көрсетілген. Булану энтальпиясының максималды жоғарылау жиілігі 60, 130 және 170 МГц өрістің әрекетінен байқалады және 5–10 % құрайды. Байқалған құбылыстар электрмагнитті әрекет нәтижесінде судың құрылымдық ұйымдасу өзгеруімен түсіндірілуі мүмкін және электрмагнитті әрекет жинақталатын сипатқа ие екені — булану энтальпиясы мөлшері сәулелендіру уақыты 2 сағатқа дейін артқанда жоғарылайтыны — анықталған; «қануғы» эффектісі — экспозиция уақыты 2 сағаттан артық болғанда энтальпия әрі қарай өспейтіні анықталған. Электрмагнитті өрістің әрекеті таңдаулы сипатқа ие болатыны көрсетілген — судың қасиеттері қатаң белгілі жиіліктегі өрістің әрекетіне сезімтал болады.

Кілт сөздер: су, электрмагнитті өріс, жиілік, сәулелендіру уақыты, қайнау температурасы, булану энтальпиясы.

В.Ю. Чиркова, Е.А. Шарлаева, И.Е. Стась

Температура кипения и энтальпия испарения воды, подвергшейся воздействию высокочастотного электромагнитного поля

Статья посвящена изучению влияния высокочастотного электромагнитного поля на температуру кипения и энтальпию испарения воды. Установлено, что в результате воздействия на деионизованную воду электромагнитного поля ультравысоких частот происходит повышение температуры ее кипения и энтальпии испарения. Показано, что эффективность электромагнитного воздействия зависит от частоты поля и времени экспозиции. Максимальное увеличение энтальпии испарения наблюдается в результате воздействия поля частотой 60, 130 и 170 МГц и составляет 5–10 %. Наблюдаемые явления могут быть обусловлены изменением структурной организации воды в результате электромагнитного воздействия. Также установлено, что электромагнитное воздействие имеет накопительный характер — величина энтальпии испарения возрастает при увеличении времени облучения до 2 часов; установлен эффект «насыщения» — увеличение времени экспозиции свыше 2-х часов не приводит к дальнейшему росту энтальпии. Показано, что воздействие электромагнитного поля носит избирательный характер — свойства воды чувствительны к действию поля строго определенных частот.

Ключевые слова: вода, электромагнитное поле, частота, время облучения, температура кипения, энтальпия испарения.

References

1 Chaplin, M.F. (2000). A proposal for the structuring of water. *Biophys. Chem., 83(3)*, 211–221.

2 Le Bihan, D., Fukuyama, H. (2010). *Water: The Forgotten Biological Molecule.* Singapore: Pan Stanford Publishing Pte. Ltd.

3 Dack, M.R.J. (1976). Solvent structure. II. A study of the structure-making and structure-breaking effects of dissolved species in water by internal pressure measurements. *Aust. J. Chem., 29(4)*, 771–778.

4 Stekhin, A.A., Yakovleva, G.V. (2008). *Strukturirovannaia voda: Nelineinye effekty. [Structured Water: Nonlinear Effects]*. Moscow: Izd-vo LKI [in Russian].

5 Stas, I.E., Repeikova, L.Yu. (2013). *Fiziko-khimicheskie zakonomernosti evoliutsii kolloidnykh nanosistem v zhidkoi dispersionnoi srede pod vliianiem elektromahnitnykh polei [Physico-chemical laws of the evolution of colloidal nanosystems in a liquid dispersion medium under the influence of electromagnetic fields]*. Barnaul: Izd-vo ASU [in Russian].

6 Stas, I.E., Chirkova, V.Yu., Shtobbe, I.A. (2015). *Fiziko-khimicheskie protsessy v elektromahnitnom pole ultravysokikh chastot [Physico-chemical processes in the electromagnetic field of ultra-high frequencies]*. Barnaul: Izd-vo ASU [in Russian].

7 Stas, I.E., Mihailova, O.P. (2009). Vliianie elektromahnitnoho polia vysokoi chastoty na kriticheskuiu kontsentratsiiu mitselloobrazovaniia vodnoho rastvora dodetsilsulfata natriia [Effect of high frequency electromagnetic field on the critical micelle concentration of an aqueous solution of sodium dodecyl sulfate]. *Zhurnal fizicheskoi khimii — Russian Journal of Phys. Chem., 83, 2,* 324–325 [in Russian].

8 Stas, I.E., Shipunov, B.P., Mihailova, O.P. (2010). Vliianie vysokochastotnoho ehlektromahnitnoho polia na adsorbtsionnuiu sposobnost ionohennykh PAV [Effect of high-frequency electromagnetic field on the adsorption capacity of ionic surfactants]. *Zhurnal fizicheskoi khimii — Russian Journal of Phys. Chem, 84, 12,* 2128–2132 [in Russian].

9 Evstratova, K.M. (Eds.). (1990). *Praktikum po fizicheskoi i kolloidnoi khimii [Workshop on physical and colloid chemistry]*. Moscow: Vysshaia shkola [in Russian].

10 Mishchenko, K.P., Ravdel, A.A. (Eds.). (1974). Kratkii spravochnik fiziko-khimicheskikh velichin [Quick reference of physico-chemical values]. Leningrad: Khimiia [in Russian].

DOI 10.31489/2019Ch2/56-61

UDC 543.426

A.A. Nikolaeva, E.I. Korotkova, O.I. Lipskikh

Tomsk Polytechnic University, Russia
(E-mail: ivanovaaa@tpu.ru)

Determination of quinine in drugs and beverages by fluorimetric method

A highly sensitive and simple fluorimetric method for the determination of quinine in pharmaceuticals and non-alcoholic beverages is proposed. The optimal conditions for quinine fluorimetric determination in drugs and beverages were found: solvent — 0.01 M sulfuric acid, excitation wavelength 353 nm, luminescence wavelength 452 nm, strobe parameters — signal delay 0.85 μs, signal duration 21.25 μs. To increase the sensitivity of the developed method, quinine luminescence was studied in sulfuric acid of various concentrations — from 0.005 to 1.000 M, and the quantum yield of quinine luminescence was calculated in all studied concentrations of sulfuric acid. It has been established that the highest luminescence intensity, the highest quinine quantum yield and the smallest background signal of the solvent was observed in 0.01 M H_2SO_4. The calibration curve exhibited the linear range from 0.10 to 1.00 mg/l. The limit of detection (LOD) was found to be 0.0029 mg/l for quinine in 0.01 M H_2SO_4. The suggested approach was successfully applied to determine the amount of quinine in tablets «Analgin-quinine» and in the non-alcoholic beverage «Schweppes Bitter Lemon». The proposed method can be used to control the quality of pharmaceuticals and food products.

Keywords: quinine, pharmaceuticals, beverages, fluorimetry, quantum yield, strobe parameters.

Introduction

Quinine is the alkaloid derived from Cinchona bark. Since 1633, quinine has been used as an antimalarial drug [1]. It also has antipyretic and analgesic properties [2]. In addition, due to the bitter taste, quinine is actively used in tonic water with the taste of «bitter lemon» or «bitter lime» [3]. In medicine, quinine is used to increase labor activity [4], but overdosing can lead to abortion [2]. Recent studies in rats have shown that quinine completely blocks ovulation and causes oxidative stress in the ovary of rats [5]. Quinine overdose is dangerous to human health and might be fatal. Therefore, the use of quinine as a food additive is limited up to 83–85 mg/l [6].

Different chromatographic techniques are applied for quinine determination in pharmaceuticals [7–9]. Despite the high prevalence of chromatography, these methods are expensive and toxic solvents are contained in mobile phases in most cases. Electrochemical [10–11], spectrophotometric [12] and fluorimetric [13] methods of analysis are used for quinine determination in beverages. Electrochemical and spectrophotometric methods have lower cost instrumentation, but suffer from less sensitivity. Fluorimetric methods have the highest sensitivity, and often are used as detectors in chromatography for the quinine determination in beverages [14–15].

It is known that quinine has the highest luminescence intensity in sulfuric acid solution. But different concentrations of sulfuric acid are used by researches. Thus, the authors [13] used 0.05 M sulfuric acid to determine quinine in tonic water. In work [12] 0.0005 M H_2SO_4 is used for quinine determination in beverages by capillary electrophoresis. For the determination of quinine in soft drinks by sequential injection analysis (SIA) 0.1 M H_2SO_4 was used [16]. Unfortunately, the authors of these works do not justify the choice of a particular acid concentration.

Qualitative and quantitative determination of quinine in drugs and beverages is a pressing issue in pharmaceutical and food industries, thus the development of highly sensitive methods for quality control is encouraged. The aim of the work is to develop a highly sensitive fluorimetric method for the determination of quinine in drugs and beverages.

Experimental

Reagents. The working solutions of quinine were prepared using the standard quinine substance (95 %; manufactured by Vekton, St. Petersburg, Russia). Quinine working solutions were prepared in 0.01 M H_2SO_4.

The following research objects were selected: 1. Tablets «Analgin-quinine», manufacturer Sopharma (Bulgaria). Ingredients: active ingredients — metamizole sodium 200 mg and quinine hydrochloride 50 mg;

excipients — microcrystalline cellulose, sodium carboxymelitic starch, Coplidon-25, talc and magnesium stearate. 2. Non-alcoholic beverage «Schwepps Bitter Lemon». Ingredients: water, sugar, citric acid, natural flavors, stabilizers, antioxidant ascorbic acid, quinine, carotene dye.

Equipment. All measurements were performed on a Fluorat-02-Panorama spectrofluorimeter fluid analyzer (manufactured by Lumex-Marketing LLC, St. Petersburg, Russia). Spectrophotometric measurements were carried out using Agilent Technology Cary 60 UV-Vis spectrophotometer.

Results and Discussion

As previously noted quinine has good luminescence in sulfuric acid solution [16]. Therefore a synchronous scan of a standard quinine solution (C = 10 mg/l) in sulfuric acid was performed at various monochromator displacements, to reveal the optimal excitation wavelength at which the maximum quinine luminescence occurs (Fig. 1).

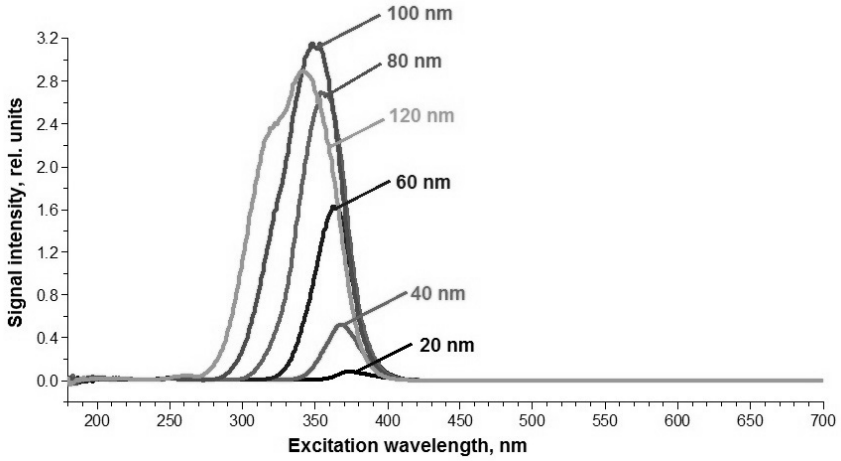

Figure 1. Synchronous scan mode of quinine standard solution (C = 10 mg/l) in sulfuric acid at different shifts of the monochromator

From the synchronous scanning mode an excitation wavelength of 353 nm was established and the maximum quinine luminescence in sulfuric acid at 452 nm was observed (Fig. 2).

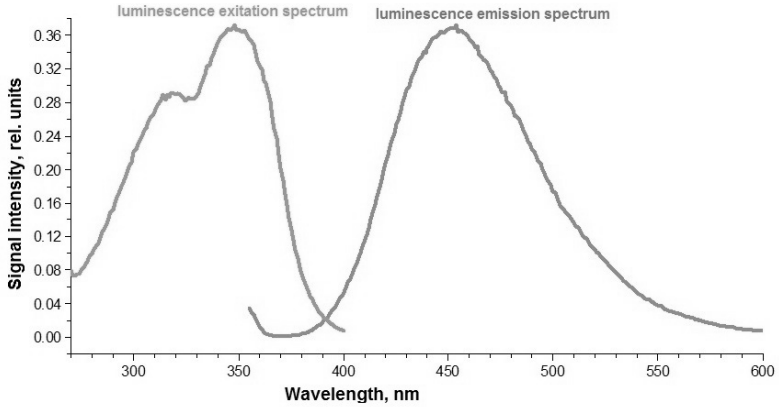

Figure 2. Excitation spectrum and luminescence spectrum of quinine in sulfuric acid

To increase the accuracy and sensitivity of the developed method different concentrations of sulfuric acid were studied, as well as the background and quinine intensity signals and the quantum yield in the studied acid solutions. The results are presented in Table 1.

It is known that quantum yield is one of the most important characteristics of a substance [17]. The quinine quantum yield in sulfuric acid solutions of different concentrations was calculated by the standard method. As a standard we have chosen a solution of fluorescein in 0.1 M NaOH with well-known quantum

yield 0.64 and the luminescence emission of fluorescein at a wavelength of 520 nm. For calculations accuracy the concentrations of the standard (fluorescein) and the test substance (quinine) were selected so that their optical density was lower than 0.1. The areas under the emission spectrum of both the investigated and standard substances (S_i), the optical densities of these substances at the excitation wavelength (D_i) and the refractive indices of solvents (n_i) were measured under the same conditions. The calculation of the quantum yield was carried out according to the formula

$$\varphi_{test} = \frac{\left(1-10^{-D_{st}}\right) * S_{test} * n_{test}^2}{\left(1-10^{-Dtest}\right) * S_{st} * n_{st}^2} * \varphi_{st},$$

where S_{test} is the area under the emission spectrum of the investigated substance; S_{st} is area under the emission spectrum of the standard substance; n_{test} is refractive index of the investigated solvent H_2SO_4; n_{st} is refractive index of the standard solvent NaOH; D_{test} is optical density of the investigated substance quinine at the excitation wavelength; D_{st} is optical density of the standard substance fluorescein at the excitation wavelength; φ_{test} is quantum yield of investigated substance quinine; φ_{test} is quantum yield of standard substance fluorescein.

According to the literature, the quinine quantum yield in 0.1 M H_2SO_4 is 0.58 [18].

Table 1

Investigation of the luminescent properties of quinine in solutions of sulfuric acid of various concentrations

Investigated parameter	Concentration of sulfuric acid, M					
	0.005	0.01	0.05	0.1	0.5	1.0
Background signal intensity (sulfuric acid), rel. units	0.00199	0.00025	0.00327	0.00357	0.00542	0.01626
Quinine signal intensity (C = 100 mg/l) in sulfuric acid, rel. units	16.724	18.928	19.043	19.186	19.438	19.267
Quinine quantum yield, rel. units	0.555	0.609	0.420	0.590	0.608	0.610

As can be seen from the table the highest quantum yield of quinine is observed in 0.01 M and 0.1 M sulfuric acid solutions. With increase sulfuric acid concentration acid, the intensity of the quinine luminescence signal also increases, but rather slightly. Therefore 0.01 M sulfuric acid was chosen for quinine quantitative determination in the studied pharmaceuticals and food products. Furthermore the lowest background signal intensity was observed at a given acid concentration, which will further increase the detection limit.

For sensitivity enhancement of quinine determination, the strobe parameters were selected — delay time (signal intensity versus time) and signal duration (recording time at one wavelength) (Fig. 3).

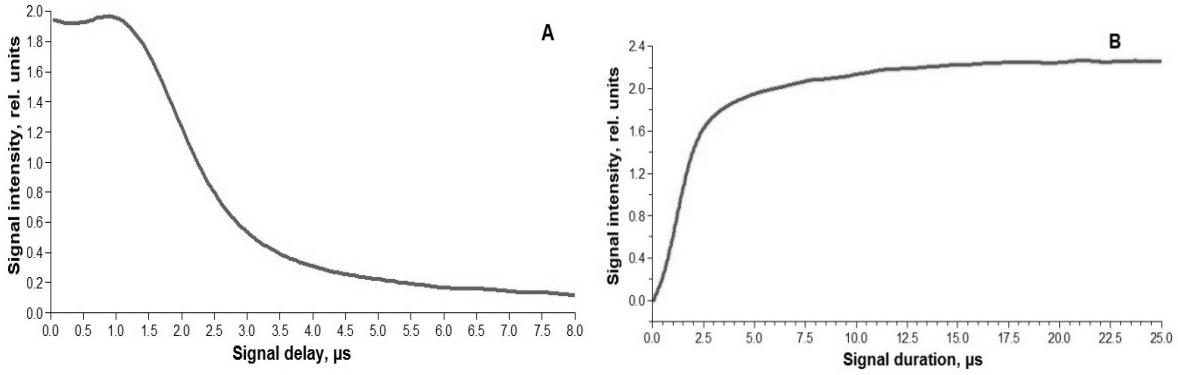

A — signal delay; *B* — signal duration

Figure 3. Dependence of quinine luminescence intensity on strobe parameters

When studying the dependence of the luminescence intensity on the signal delay in the range from 0.05 to 8.00 μs, the optimum value of the signal delay for quinine was set to 0.85 μs. From the signal duration range from 1.00 to 25.00 μs the duration is set to 21.25 μs. The highest quinine luminescence intensity was observed under selected strobe parameters.

Depending on the nature of the excited electronic state the luminescence is divided into two types – fluorescence and phosphorescence. In practice, the processes of fluorescence and phosphorescence differ in temporal characteristics. Instantaneous attenuation of the emission after excitation cessation from 10^{-7} to 10^{-10} s is typical for fluorescence, the continuation of a certain glow time after excitation cessation from 10^{-6} to 10^{-1} s — for phosphorescence. To establish the type of quinine luminescence process the dependence of the luminescence signal intensity on the signal time was plotted (Fig. 4).

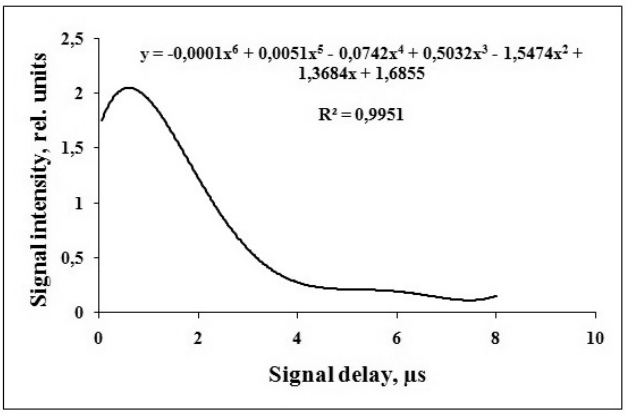

Figure 4. The decay kinetics curve for quinine in 0.01 M H_2SO_4

Using the quinine attenuation curve obtained, the average luminescence lifetime was calculated through the area under the attenuation curve (a definite integral from 0 to 8 μs for the function):

$$\int_0^8 (-0.0001x^6 + 0.0051x^5 - 0.0742x^4 + 0.5032x^3 - 1.5474x^2 + 1.3684x + 1.6855)dx.$$

For quinine the lifetime was $1.505 \cdot 10^{-5}$ s. From the calculations it can be concluded that phosphorescence is characteristic for quinine in 0.01 M H_2SO_4.

Thus, the following working conditions were selected: solvent — 0.01 M H_2SO_4, excitation wavelength 353 nm, luminescence wavelength 452 nm, signal delay 0.85 μs, signal duration 21.25 μs. Under optimized conditions a linear calibration curve of the luminescence intensity on quinine concentration was plotted in the range of 0.10–1.00 mg/l (Fig. 5*A*).

Spectrophotometry was used as a comparison method. Quinine was determined by its own absorption. The dependence of the optical density from the quinine concentration in 0.1 M sulfuric acid at an absorption wavelength 347 nm showed linear response in concentration range of 1.00 to 10 mg/l (Fig. 5*B*).

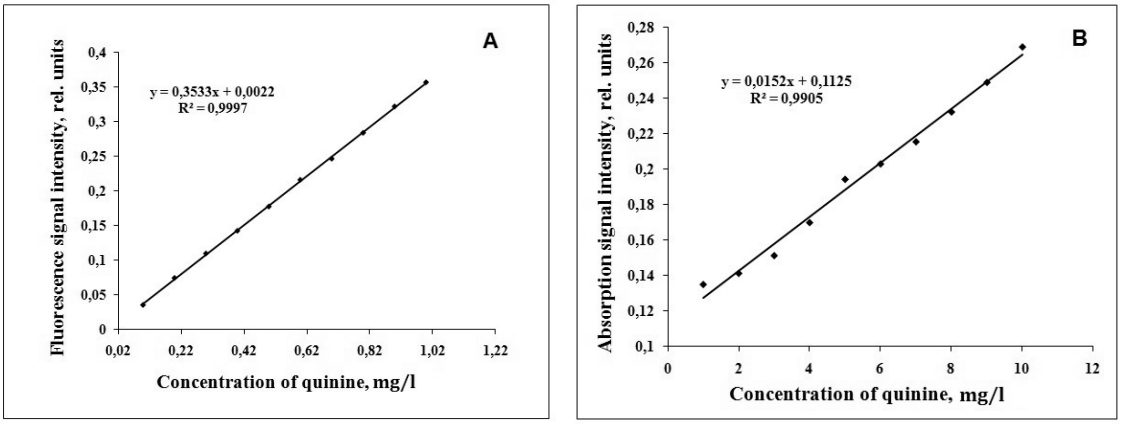

Figure 5. Calibration curves of the intensity of the luminescence (*A*) and absorption (*B*) on the concentration of quinine in 0.01 M sulfuric acid

Sample preparation of the objects was as follows. The tablet was previously dissolved in 20 ml of 0.01 M sulfuric acid. The resulting solution was diluted 10 000 times. The intensity of the diluted solution was

measured and quinine concentration was recalculated into 20 ml of the initial solution. The original sample of the beverage was degassed and diluted 10 times with distilled water. The results of quantitative determination of quinine by two methods are presented in Table 2.

Table 2

The results of the determination of quinine in tablets and soft drinks by fluorimetric and spectrophotometric methods, n = 3, p = 0.95, t_{table} = 2.78

Sample	Fluorimetric method, mg/l	S_r	Spectrophotometric method, mg/l	S_r	t_{exp}
Tablet «analgin-quinine»	51.41±0.43	0.003	52.33±2.74	0.021	0.074
Beverage «Schweppes Bitter Lemon»	53.74±1.86	0.014	54.42±5.25	0.039	0.373

As can be seen from Table 2 there is a good agreement between results obtained by the developed fluorimetric method and spectrophotometric method. The quinine content does not exceed the maximum allowable value of 85 mg/l in a beverage. But it is content in the tablet is slightly higher than the stated amount of 50 mg per tablet, which might have a bearing on human health on scheduled administration.

Additionally the limit of detection of quinine in 0.01 M sulfuric acid was calculated as 0.0029 mg/l. The value of the limit of detection is much lower in comparison with the majority of works [7–8, 11–16].

Conclusions

An effective, highly sensitive, simple and low-cost fluorimetric method for the determination of quinine in pharmaceuticals and soft drinks has been developed. The quantum yield of quinine in sulfuric acid of various concentrations was calculated. Optimal conditions for quinine determination in 0.01 M sulfuric acid were selected. The quinine luminescence process was studied and the quinine phosphorescence process was observed in 0.01 M H_2SO_4. Due to the selected assay conditions the high detection sensitivity and the limit of detection for quinine determination in pharmaceuticals and beverages has been achieved.

References

1 Odoh, U.E., Uzor, P.F., Eze, C.L., Akunne, T.C., Onyegbulam, C.M., & Osadebe, P.O. (2018). Medicinal plants used by the people of Nsukka Local Government Area, south-eastern Nigeria for the treatment of malaria: An ethnobotanical survey. *Journal of Ethnopharmacology*, 218, 1–15. DOI:10.1016/j.jep.2018.02.034.

2 Data-base Pubchem (2019). *pubchem.ncbi.nlm.nih.gov* Retrieved from https://pubchem.ncbi.nlm.nih.gov/compound /Quinine#section=Top.

3 Health line (2019). *www.healthline.com*. Retrieved from https://www.healthline.com/health/quinine-in-tonic-water.

4 Gopi, P., & Sarveswari, S. (2016). Effective water mediated green synthesis of polysubstituted quinolines without energy expenditure. *Monatshefte für Chemie. Chemical Monthly*, *148*(6), 1043–1049. DOI:10.1007/s00706–016–1826–3.

5 Gbotolorun, S.C., Inikori, O., Bamisi, O.D., Osinubi, A.A.A., & Okanlawon, A.O. (2018). Quinine inhibits ovulation and produces oxidative stress in the ovary of cyclic Sprague-Dawley rats. *African Health Sciences, 18*(2), 253–259, DOI:10.4314/ahs.v18i2.8.

6 Donovan, J.L., DeVane, C.L., Boulton, D., Dodd, S., & Markowitz, J.S. (2003). Dietary levels of quinine in tonic water do not inhibit CYP2D6 in vivo. *Food and Chemical Toxicology, 41*(8), 1199–1201. DOI:10.1016/s0278–6915(03)00112–1.

7 Chmurzynski, L. (1997). High-performance liquid chromatographic determination of quinine in rat biological fluids. *Journal of Chromatogaphy. B: Biomedical Applied, 693*(2), 423–429. DOI:10.1016/s0378–4347(97)00074–1.

8 Kluska, M., Marciniuk-Kluska, A., Prukała, D., & Prukała, W. (2015). Analytics of Quinine and its Derivatives. *Critical Reviews in Analytical Chemistry, 46*(2), 139–145. DOI:10.1080/10408347.2014.996700.

9 Reijenga, J.C., Aben, G.V.A., Lemmens, A.A.G., Verheggen, T.P.E.M., De Bruijn, C.H.M.M., & Everaerts, F.M. (1985). Determination of quinine in beverages, pharmaceutical preparations and urine by isotachophoresis. *Journal of Chromatography A, 320*(1), 245–252. DOI:10.1016/s0021–9673(01)90502–3.

10 Dar, R.A., Brahman, P.K., Tiwari, S., & Pitre, K.S. (2012). Electrochemical studies of quinine in surfactant media using hanging mercury drop electrode: A cyclic voltammetric study. *Colloids and Surfaces B: Biointerfaces, 98,* 72–79. DOI:10.1016/j.colsur.

11 Buleandra, M., Rabinca, A.A., Cheregi, M.C., & Ciucu, A.A. (2018). Rapid voltammetric method for quinine determination in soft drinks. *Food Chemistry, 253,* 1–4. DOI:10.1016/j.foodchem.2018.01.130.

12 Mikuš, P., Maráková, K., Veizerová, L., & Piešťanský, J. (2011) Determination of quinine in beverages by online coupling capillary isotachophoresis to capillary zone electrophoresis with UV spectrophotometric detection. *Journal of Separation Science, 34*(23), 3392–3398. DOI:10.1002/jssc.201100633.

13 Lawson-Wood, K., Evans, K. (2019). Determination of Quinine in Tonic Water using Fluorescence Spectroscopy. Retrieved from http://www.perkinelmer.com/labsolutions/resources/docs/APP_Quinine_in_Tonic_Water_014133_01.pdf.

14 Feás, X., Fente, C. A., & Cepeda, A. (2009). Fast and Sensitive New High Performance Liquid Chromatography Laser Induced Fluorescence (HPLC-LIF) Method for Quinine. Comparative Study in Soft Drinks. *Journal of Liquid Chromatography & Related Technologies, 32*(17), 2600–2614. DOI:10.1080/1082607090324.

15 Samanidou, V.F., Evaggelopoulou, E.N. & Papadoyannis, I.N. Simple and Rapid HPLC Method for the Determination of Quinine in Soft Drinks Using Fluorescence Detection. *Journal of Liquid Chromatography and Relative Technology, 27*(15), 2397–2406. DOI:10.1081/jlc-200028156.

16 Infante, C.M.C., & Masini, J.C. (2011). Development of a fluorimetric sequential injection analysis (SIA) methodology for determination of quinine. *Journal of the Brazilian Chemical Society, 22*(10), 1888–1893. DOI:10.1590/s0103–50532011001000009.

17 Mantel, A.I., Irgibayeva, I.S. & Mukatayev, I.R. (2017). Modification of solar batteries by polymer fluorescent films. *Bulletin of the Karaganda University. Ser. Chemistry, 88*(*4*), 39–47.

18 The free encyclopedia (2019). Retrieved from https://en.wikipedia.org/wiki/Quinine.

А.А. Николаева, Е.И. Короткова, О.И. Липских

Дәрілік препараттар мен сусындардағы хининді флуориметрия әдісімен анықтау

Фармацевтикалық препараттар мен алкогольсіз сусындарда хининді анықтаудың жоғары сезімтал және қарапайым флуориметрлік әдісі ұсынылған. Дәрілік заттар мен сусындарда хининді флуориметрлік анықтаудың оңтайлы шарттары табылды: еріткіш — 0,01 М күкірт қышқылы, қозу толқынының ұзындығы 353 нм, люминесценция толқынының ұзындығы 452 нм, строб параметрлері — сигналдың кідірісі 0,85 мкс, дабылдың ұзақтығы 21,25 мкс. Әзірленетін әдістеменің сезімталдығын арттыру үшін 0,005-нан 1,000 М-ге дейін күкірт қышқылының әртүрлі концентрацияларында хининнің люминесценциясына зерттеу жүргізілді, сондай-ақ күкірт қышқылының барлық зерттелетін концентрацияларында хининнің кванттық шығыны есептелді. Хининнің люминесценциясының ең үлкен қарқындылығы, хининнің ең үлкен кванттық шығымы және еріткіштің ең аз фонының сигналы 0,01 М H_2SO_4-те байқалатыны анықталды. Хининді анықтау 0,10-ден 1,00 мг/л дейінгі концентрация аралығында жүргізілді. Табылған жағдайда «Анальгин-хинин» дәрілерінде және «Schweppes Bitter Lemon» алкогольсіз сусынында хининнің мөлшері зерттелді. Салыстыру әдісі ретінде талдаудың спектрофотометриялық әдісі қолданылды. Хининді салыстыру әдісімен анықтау толқын ұзындығы 347 нм кезінде хининді жұтқан кезде 1,00-ден 10,00 мг/л-ге дейінгі концентрация диапазонында жүргізілді. Ұсынылған әдістеме фармацевтикалық препараттар мен тамақ өнімдерінің сапасын бақылау үшін пайдаланылуы мүмкін.

Кілт сөздер: хинин, фармацевтикалық дәрілік заттар, сусындар, квантты шығым, строб параметрлері.

А.А. Николаева, Е.И. Короткова, О.И. Липских

Определение хинина в лекарственных препаратах и напитках методом флуориметрии

Предложен высокочувствительный и простой флуориметрический метод определения хинина в фармацевтических препаратах и безалкогольных напитках. Найдены оптимальные условия флуориметрического определения хинина в лекарствах и напитках: растворитель — 0.01 М серная кислота, длина волны возбуждения 353 нм, длина волны люминесценции 452 нм, параметры строба — задержка сигнала 0.85 мкс, длительность сигнала 21.25 мкс. Для увеличения чувствительности разрабатываемой методики проведены исследования люминесценции хинина при различных концентрациях серной кислоты от 0.005 до 1.000 М, а также подсчитан квантовый выход хинина при всех исследуемых концентрациях серной кислоты. Установлено, что наибольшая интенсивность люминесценции хинина, наибольший квантовый выход хинина и наименьший сигнал фона растворителя наблюдается в 0.01 М H_2SO_4. Определение хинина проводилось в диапазоне концентраций от 0.10 до 1.00 мг/л. Рассчитан предел обнаружения хинина в 0.01 М H_2SO_4 при заданных условиях, который составил 0.0029 мг/л. При найденных условиях исследовано содержание хинина в таблетках «Анальгин-хинин» и в безалкогольном напитке «Schweppes Bitter Lemon». В качестве метода сравнения использован спектрофотометрический метод анализа. Определение хинина методом сравнения проводили в диапазоне концентраций от 1.00 до 10.00 мг/л при поглощении хинина при длине волны 347 нм. Предложенная методика может быть использована для контроля качества фармацевтических препаратов и пищевых продуктов.

Ключевые слова: хинин, фармацевтические препараты, напитки, квантовый выход, параметры строба.

БЕЙОРГАНИКАЛЫҚ ХИМИЯ
НЕОРГАНИЧЕСКАЯ ХИМИЯ
INORGANIC CHEMISTRY

DOI 10.31489/2019Ch2/62-68

UDC 66.021.2

B.K. Kassenov[1], Sh.B. Kassenova[1], Zh.I. Sagintaeva[1], E.E. Kuanyshbekov[1], N.I. Kopylov[2]

[1]Zh. Abishev Chemical-Metallurgical Institute, Karaganda, Kazakhstan;
[2]Institute of Solid State Chemistry and Mechanochemistry, Novosibirsk, Russia
(E-mail: kasenov1946@mail.ru)

Thermal capacity of new nanodimensional cobalt-cuprate-manganite $LaLi_2CoCuMnO_6$ and nickelite-cuprate-manganite $LaLi_2NiCuMnO_6$ in the interval of 298.15–673 K and their thermodynamic properties

The specific thermal capacities of our new obtained nanodimensional cobalt-cuprate-manganite and nickelite-cuprate-manganite of lanthanum and lithium of structures $LaLi_2CoCuMnO_6$ and $LaLi_2NiCuMnO_6$ were first studied with the method of a dynamic calorimetry in the interval of temperatures of 298.15–673 K. Their mole thermal capacities were calculated from specific thermal capacities. It was established that $LaLi_2CoCuMnO_6$ at 398 K and $LaLi_2NiCuMnO_6$ at 373 K and 573 K were subjected to II-type phase transitions. Based on temperature of phase transitions the equations of temperature dependence of thermal capacity were set up. All obtained experimental and calculated data were processed strictly with methods of mathematical statistics. The mean square deviations were measured for average values of specific thermal capacities, as well as random components of an error for mole thermal capacities. The standard entropies of the studied compounds were calculated with method of ionic increments. Referring to the experimental data on thermal capacities and calculated values of standard entropies in the interval of 298.15–675 with step through 50 K the temperature dependences of an enthalpy of $H^o(T)–H^o(298.15)$, entropy of $S^o(T)$ and the specified thermodynamic potential $\Phi^{xx}(T)$ were calculated.

Keywords: thermodynamics, cobalt, nickelite, cuprate, manganite, thermal capacity, calorimetry, lanthanum, lithium.

Introduction

It has been known that cuprates, cobaltites, nickelites and manganites of the rare-earth elements doped with oxides of alkaline and alkaline-earth metals have the unique physical and chemical properties as semiconductor, magnetic, superconducting and they represent as materials of operative memory [1–9]. For several years we have been conducting the systematic and purposeful researches on synthesis and studying the thermodynamic and electrophysical properties of double and threefold manganites, chromites, ferrites, cuprate-manganites, manganite-ferrites, chromite-manganites, cobalt-manganites, nickelite-manganites, ferro-chrome manganites, etc. [10–15].

The certain theoretical and practical interest includes the research of thermodynamic properties of new phases consisting of cobaltites, nickelites, cuprates and manganites. Thus, this paper demonstrates the research results of the thermodynamic properties of new nanodimensional cobalt-cuprate-manganite and nickelite-cuprate-manganite of lanthanum and lithium of structures $LaLi_2CoCuMnO_6$ and $LaLi_2NiCuMnO_6$.

Experimental

$LaLi_2CoCuMnO_6$ and $LaLi_2NiCuMnO_6$ were synthesized with method of the ceramic technology in the interval of 800–1200 ºC by interaction of La_2O_3 (especially pure), CoO (analytically pure), NiO (analytically pure), CuO (analytically pure), Mn_2O_3 (analytically pure) and Li_2CO_3 (analytically pure) with intermediate milling and stirring every 100 ºC for 20 h. Low-temperature annealing for obtaining a stable phase at a low temperature was made at 400 ºC for 10 h. By grinding of polycrystalline samples in a vibration mill of the Retsch (Germany) company of the MM301 brand there have been obtained their nanodimensional (nanocluster) particles, the sizes (40–90 nm) of which were determined on an atomic-force microscope JSPM-5400 Scanning Probe Microscope «JEOL» (Japan). The radiographic research of nanodimensional $LaLi_2CoCuMnO_6$ and $LaLi_2NiCuMnO_6$ was performed on the DRON-2.0 diffractometer at FeK_α — radiation, with Ni-filter. It was established with the indexing of roentgenograms of compounds that they were crystallized in an isometric system with the following parameters of grid: $LaLi_2CoCuMnO_6$ — $a = 11.33\pm0.02$Å; $V^o = 2563.20\pm0.06$Å^3; $Z = 4$; $V^o_{elec.cell} = 640.80\pm0.02$Å^3; $\rho_{roent.} = 4.0$ g/cm^3; $\rho_{pick.} = 3.90\pm0.02$ g/cm^3; $LaLi_2NiCuMnO_6$ — $a = 13.83\pm0.02$Å; $V^o = 2644.16\pm0.06$Å^3; $Z = 4$; $V^o_{elec.cell} = 661.04\pm0.02$Å^3; $\rho_{roent.} = 4.03$ g/cm^3; $\rho_{pick} = 3.99\pm0.01$ g/cm^3 [16, 17].

The thermal capacity of compounds was investigated on IT-S-400 calorimeter in the interval of 298.15–673 K. Calibration of the device was performed using copper standard, and checking operation — measurement of thermal capacity of α-Al_2O_3. The specific thermal capacity ($C_{p(specific)}$) was measured at each temperature every 25 K from which the mole thermal capacity (C^o_p ($_m$)) was calculated. The procedure of experiments is in detail described in [18]. Our similar researches on this calorimeter were performed in [10–15, 19]. Table 1 demonstrates below the results of calorimetric researches.

Table 1

Experimental values of thermal capacities of $LaLi_2CoCuMnO_6$ and $LaLi_2NiCuMnO_6$

[$C_{p(specific)} \pm \overline{\delta}$, J/(g·K); $C^o_{p(m)} \pm \overset{0}{\Delta}$, J/(mol·K)]

T, K	$LaLi_2CoCuMnO_6$		$LaLi_2NiCuMnO_6$	
	$C_{p(specific)} \pm \overline{\delta}$	$C^o_{p(m)} \pm \overset{0}{\Delta}$	$C_{p(specific)} \pm \overline{\delta}$	$C^o_{p(m)} \pm \overset{0}{\Delta}$
298.15	0.6022±0.0056	257±7	0.5962±0.0183	254±22
323	0.7895±0.0077	336±9	0.7704±0.0130	328±15
348	0.8035±0.0081	342±10	0.8730±0.0058	372±7
373	0.8384±0.0077	357±9	0.9014±0.0099	384±12
398	0.8736±0.0072	372±9	0.8199±0.0139	349±16
423	0.8233±0.0204	351±24	0.9554±0.0138	407±16
448	0.9887±0.0084	421±10	0.9975±0.0098	425±12
473	1.0365±0.0107	442±13	1.0553±0.0154	450±18
498	1.0468±0.0108	446±13	1.0689±0.0187	455±22
523	1.0678±0.0141	455±17	1.1006±0.0208	469±25
548	1.0917±0.0130	465±15	1.1132±0.0120	474±14
573	1.1136±0.0082	475±10	1.1465±0.0186	488±22
598	1.1293±0.0112	481±13	1.0405±0.0168	443±20
623	1.1428±0.0078	487±9	1.1089±0.0261	472±31
648	1.1588±0.0127	494±15	1.1314±0.0152	482±18
673	1.1751±0.0052	501±6	1.1691±0.0185	498±22

Results and Discussion

Results of the calorimetric researches in Figure 1 and Table 1 show that there were defined the anomalies changes of thermal capacity probably connected with II-type phase transitions on the curve of dependence $C^o_p \sim f(T)$ for $LaLi_2CoCuMnO_6$ at 398 K, and $LaLi_2NiCuMnO_6$ at 373 K and 573 K. These transitions might be caused with Schottky effects, changes of magnetic resistance, conductivity, dielectric permeability, existence of Curie and Neel points, etc. Including temperatures of phase transitions the equations of temperature dependence of thermal capacity were set up for $LaLi_2CoCuMnO_6$ [J/(mol·K)]:

$$C^o_{p(1)} = (1284\pm37) - (1454.1\pm41.9)\cdot10^{-3}T - (527.7\pm15.2)\cdot10^5T^{-2}, \text{ (298.15–398 K)}; \quad (1)$$

$$C^o_{p(2)} = (714\pm21) - (857.7\pm24.7)\cdot10^{-3}T, \text{ (398–423 K)}; \quad (2)$$

$$C^{o}_{p(3)} = (959\pm28) - (430.6\pm12.4)\cdot10^{-3}T - (761.8\pm21.9)\cdot10^{5}T^{-2}, \text{ (423–673 K)} \quad (3)$$

and for $LaLi_2NiCuMnO_6$ [J/(mol·K)]:

$$C^{o}_{p(1)} = (2402.31\pm105.7) - (3540.0\pm155.76)\cdot10^{-3}T - (971.0\pm42.72)\cdot10^{5}T^{-2}, \text{ (298.15–373 K)}; \quad (4)$$

$$C^{o}_{p(2)} = (902.0\pm39.69) - (1388.80\pm61.11)\cdot10^{-3}T, \text{ (373–398 K)}; \quad (5)$$

$$C^{o}_{p(3)} = (915.07\pm40.26) - (403.53\pm17.76)\cdot10^{-3}T - (641.86\pm28.24)\cdot10^{5}T^{-2}, \text{ (398–573 K)}; \quad (6)$$

$$C^{o}_{p(4)} = (1522.45\pm66.99) - (1804.72\pm79.41)\cdot10^{-3}T, \text{ (573–598 K)}; \quad (7)$$

$$C^{o}_{p(5)} = (635.83\pm27.98) + (70.76\pm3.11)\cdot10^{-3}T - (840.05\pm36.96)\cdot10^{5}T^{-2}. \text{ (598–673 K)}. \quad (8)$$

The standard entropy of $LaLi_2CoCuMnO_6$ and $LaLi_2NiCuMnO_6$ was calculated with system of ionic entropy increments according to [20].

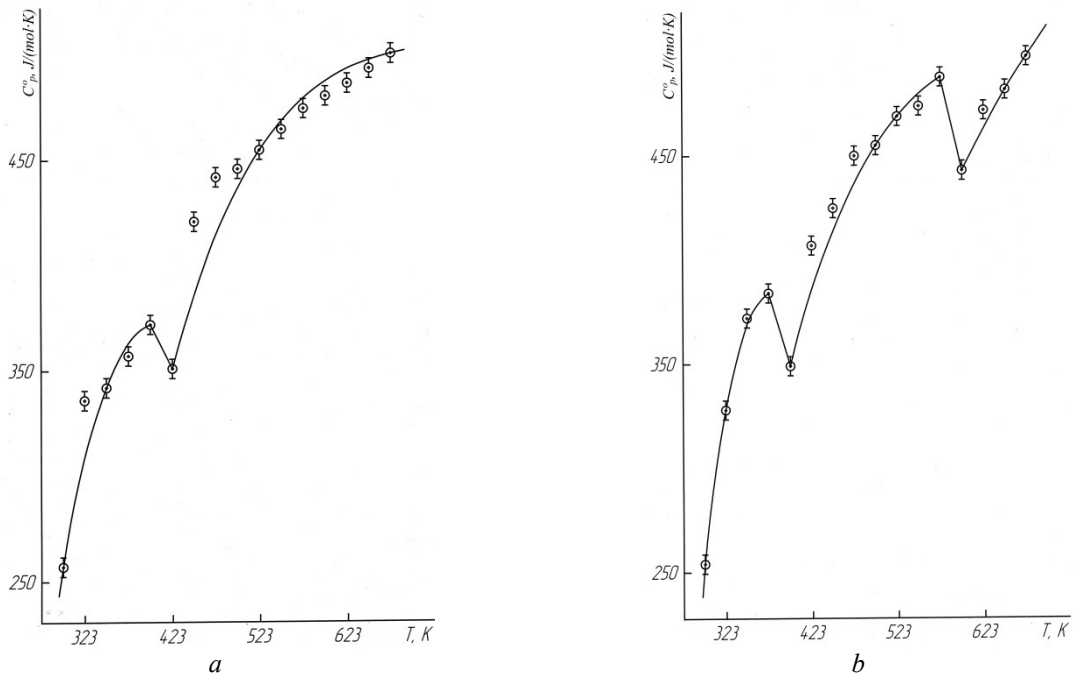

Figure. Dependence of thermal capacity of $LaLi_2CoCuMnO_6$ (*a*) and $LaLi_2NiCuMnO_6$ (*b*) on temperature in the interval of 298.15–673 K

Referring to the experimental data on $C^{o}_{p}(T)$ and calculated values of standard entropies of $S^{o}(298.15)$ the temperature dependences of the thermodynamic functions of $H^{o}(T)–H^{o}(298.15)$, $S^{o}(T)$ and $\Phi^{xx}(T)$ were calculated. Their values are presented in Table 2. Errors of thermodynamic functions were calculated using errors of the experimental data on $C^{o}_{p}(T)$ and calculated values of $S^{o}(298.15)$.

Table 2

Thermodynamic functions of $LaLi_2CoCuMnO_6$ and $LaLi_2NiCuMnO_6$

T, K	$LaLi_2CoCuMnO_6$				$LaLi_2NiCuMnO_6$			
	$C^{o}_{p}(T)$, J/(mol·K)	$S^{o}(T)$, J/(mol·K)	$H^{o}(T)$–$H^{o}(298.15)$, kJ/mol	$\Phi^{xx}(T)$, J/(mol·K)	$C^{o}_{p}(T)$, J/(mol·K)	$S^{o}(T)$, J/(mol·K)	$H^{o}(T)–H^{o}(298.15)$, kJ/mol	$\Phi^{xx}(T)$, J/(mol·K)
298	257±7	248±7	–	248±15	254±11	239±7	–	239±18
300	262±8	250±15	520±15	248±15	261±11	241±18	515±20	239±18
350	345±10	298±18	15970±460	252±15	371±16	291±21	16870±740	243±18
400	373±11	345±20	34070±980	261±15	346±15	341±25	35450±1560	252±19
450	389±11	389±23	52370±1510	273±16	417±18	386±29	54790±2410	265±20
500	439±13	433±25	73160±2107	286±17	457±20	433±32	76700±3370	279±21
550	470±13	476±28	95940±2760	302±18	481±21	477±35	100190±4410	295±22
600	489±14	518±30	107840±3100	318±19	440±19	519±38	123870±5450	312±23
650	499±14	557±33	131160±3780	335±20	483±21	556±41	147100±6470	329±24
675	501±14	576±34	157180±4520	343±20	499±22	574±42	159390±7010	338±25

The standard enthalpies of formation $\Delta_f H^o(298.15)$ of $LaLi_2CoCuMnO_6$ and $LaLi_2CoCuMnO_6$ calculated by the method developed by us are equal to 2934.3 and 2935.3 to kJ/mol, respectively [21].

Conclusions

The isobaric thermal capacity of new nanodimensional (nanocluster) cobalt-cuprate-manganite and nickelite-cuprate-manganite of lanthanum and lithium of structures $LaLi_2CoCuMnO_6$ and $LaLi_2NiCuMnO_6$ was investigated in the interval of 298.15–673 K. Temperatures of II-type phase transitions were determined. The equations describing temperature dependences of thermal capacity compounds were set up with the help of temperatures of phase transitions.

The temperature dependences of the thermodynamic functions $S^o(T)$, $H^o(T)–H^o(298,15)$ and $\Phi^{xx}(T)$ of cobalt-cuprate-manganite and nickelite-cuprate-manganite were calculated on the basis of the experimental data on $C^o_p(T)$ and calculated values of $S^o(298.15)$ in the interval of 298.15–675 K.

Research results are of interest to the physical and chemical modeling of the directed synthesis of obtained and similar compounds, used as basic data for the fundamental reference books and databanks and have an importance for physical chemistry of oxide materials and prediction of valuable physical and chemical properties of cobalt (nickelite)-cuprate-manganites.

Work was performed within the Contract No. 65 dated 23.02.2018 signed between Committee of science of the Ministry of Education and Science of the Republic of Kazakhstan and Abishev Chemical-Metallurgical Institute, the Grant Code of Individual Registration Number: AP05131317; AP05131333).

References

1 Третьяков Ю.Д. Новые поколения неорганических функциональных материалов / Ю.Д. Третьяков, О.А. Брылёв // Журн. Росс. хим. общества им. Д.И. Менделеева. — 2000. — Т. 44, № 4. — С. 10–16.

2 Третьяков Ю.Д. Химические принципы получения металлооксидных сверхпроводников / Ю.Д. Третьяков, Е.А. Гудилин // Успехи химии. — 2000. — Т. 69, № 1. — С. 3–40.

3 Ерин Ю. Найдено вещество с гигантским значением диэлектрической проницаемости / Ю. Ерин // Химия и химики. — 2009. — № 1. — Режим доступа: http://chemistry-chemists.com/N1_2009/16–22.pdf.

4 Sukanti Behera. Synthesis, structure and thermoelectric properties of $La_{1-x}Na_xCoO_3$ perovskite oxides / Sukanti Behera, Vinayak. B. Kamble, Satish Vittac, Arun M. Umarji, C. Shivakumara // Bulletin of Materials Science. — 2017. — Vol. 40, Iss. 7. — P. 1291–1299.

5 Klyndyuk A. Effect of the Cobalt Substitution on the Structure and Properties of the Layered Sodium Cobaltate Derivatives / A. Klyndyuk, N. Krasutskaya, L. Evseeva, E. Chizhova, S. Tanaeva // Universal Journal of Materials Science. — 2015. — No. 3(2). — P. 27–34.

6 Sadykov V. $La_{0.8}Sr_{0.2}Ni_{0.4}Fe_{0.6}O_3$–$Ce_{0.8}Gd_{0.2}O_{2-\delta}$ Nanocomposite as Mixed Ionic–Electronic Conducting Material for SOFC Cathode and Oxygen Permeable Membranes: Synthesis and Properties / V. Sadykov, T. Kharlamova, A. Smirnova // Composite Interfaces. — 2009. — Vol. 16. — P. 407–431.

7 Krohns S. Colossal dielectric constant up to gigahertz at room temperature / S. Krohns, P. Lunkenheimer, Ch. Kant, A.V. Pronin, H.B. Brom, A.A. Nugroho, M. Diantoro, A. Loidl // Appl. Phys. Lett. — 2009. — Vol. 94. — P. 122903.

8 Sen Chen. P_2-type $Na_{0.67}Ni_{0.33-x}Cu_xMn_{0.67}O_2$ as new high-voltage cathode materials for sodium-ion batteries / Chen Sen, Han Enshan, Xu Han, Zhu Lingzhi, Liu Bin, Zhang Guangquan, Lu Min // Internatoinal Journal Ionics. — 2017. — P. 1–10.

9 Archana Singh. Synthesis, Characterization and Gas Sensing Capability of $Ni_xCu_{1-x}Fe_2O_4$ ($0.0 \le x \le 0.8$) Nanostructures Prepared via Sol-GelMethod / Singh Archana, Singh Ajendra, Singh Satyendra, Tandon Poonam, R.R. Yadav. // Journal of Inorganic and Organometallic Polymers and Materials. — 2016. — Vol. 26, Iss. 6. — P. 1392–1403.

10 Касенов Б.К. Двойные и тройные манганиты, ферриты и хромиты щелочных, щелочноземельных и редкоземельных металлов / Б.К. Касенов, Ш.Б. Касенова, Ж.И. Сагинтаева, Б.Т. Ермагамбет, Н.С. Бектурганов, И.М. Оскембеков. — М.: Научный мир, 2017. — 416 с.

11 Касенова Ш.Б. Теплоемкость и термодинамические функции манганито-ферритов NdM^IMnFeO_5 (M^I=Li, Na) в интервале 298,15–673 К / Ш.Б. Касенова, А.Ж. Абильдаева, Ж.И. Сагинтаева, С.Ж. Давренбеков, Б.К. Касенов // ЖФХ. — 2013. − Т. 87, № 5. — С. 739–743.

12 Касенова Ш.Б. Теплоемкость и термодинамические функции наноструктурированных частиц купрато-манганитов $LaM_2^{II}CuMnO_6$ (M^{II} — Mg, Ca) в интервале 298,15–673 К / Ш.Б. Касенова, Б.К. Касенов, Ж.И. Сагинтаева, К.Т. Ермаганбетов, Е.Е. Куанышбеков, А.А. Сейсенова, Д.И. Смагулова // ЖФХ. — 2014. — Т. 88, № 5. — С. 836–840.

13 Касенов Б.К. Теплоемость и термодинамические функции манганитов $NdM^{II}{}_2CoMnO_6$ (M^{II} — Mg, Ca, Sr, Ba) в интервале 298,15–673 К / Б.К. Касенов, Ш.Б. Касенова, Ж.И. Сагинтаева, М.О. Туртубаева, Ш.К. Амерханова, Р.Н. Николов // ТВТ. — 2016. − Т. 54, № 4. — С. 540–544.

14 Касенов Б.К. Теплоемкость и термодинамические функции новых наноразмерных ферро-хромо-манганитов $LaM^{II}_{0,5}FeCrMnO_{6,5}$ (M^{II} — Mg, Ca, Sr, Ba) / Б.К. Касенов, Ш.Б. Касенова, Ж.И. Сагинтаева, М.О. Туртубаева, К.С. Какенов, Г.А. Есенбаева // ЖФХ. — 2017. − Т. 91, № 3. — С. 410–416.

15 Касенова Ш.Б. Калориметрическое исследование теплоемкости никелито-манганитов LaM_2NiMnO_5 (M — Li, Na, K) в интервале температур 298,15–673 К / Ш.Б. Касенова, Ж.И. Сагинтаева, Б.К. Касенов, М.О. Туртубаева, К.Т. Рустембеков, И. Стоев // ТВТ. — 2017. − Т. 55, № 3. — С. 480–483.

16 Сагинтаева Ж.И. Синтез и рентгенография новых наноразмерных (нанокластерных) никелито-купрато-манганитов лантана и щелочных металлов / Ж.И. Сагинтаева, Б.К. Касенов, Ш.Б. Касенова, М.О. Туртубаева, Е.Е. Куанышбеков // Изв. НАН РК. Серия химии и технологии. — 2018. — № 3(429). — С. 73–78.

17 Касенова Ш.Б. Новые наноразмерные (нанокластерные) кобальто-купрато-манганиты лантана и щелочных металлов и их рентгенографическое исследование / Ш.Б. Касенова, Б.К. Касенов, Ж.И. Сагинтаева, М.О. Туртубаева, Е.Е. Куанышбеков // Изв. НАН РК. Серия химии и технологии. — 2018. — № 3(429). — С. 62–72.

18 Техническое описание и инструкции по эксплуатации ИТ-с-400. — Актюбинск: АЗ «Эталон», 1986. — 48 с.

19 Касенов Б.К. Термодинамические и электрофизические свойства феррита $LaSrMnFeO_{5,5}$ / Б.К. Касенов, С.Ж. Даврен-беков, Б.Т. Ермагамбет, Ш.Б. Касенова, Ж.И. Сагинтаева, А.Ж. Абильдаева, Е.Е. Куанышбеков, М.А. Исабаева, М.О. Туртубаева, Е.К. Жумадилов // ТВТ. — 2012. — Т. 50, № 6. — С. 789–792.

20 Кумок В.Н. Прямые и обратные задачи химической термодинамики / В.Н. Кумок. — Новосибирск: Наука, 1987. — С. 108–123.

21 Касенов Б.К. Оценка стандартных термодинамических свойств никелито(кобальто)-купрато-манганитов составов $LaMe^{I}_2Ni(Co)CuMnO_6$ и $LaMe^{II}Ni(Co)CuMnO_6$ (Me^{I} — Li, Na, K) и (M^{II} — Mg, Ca, Sr, Ba) // Химическая термодинамика и кинетика: Сб. науч. тр. Восьмой Междунар. науч. конф. (28 мая – 1 июня 2018 года). — Тверь: Тверской гос. ун-т, 2018. — С. 157–158.

Б.Қ. Қасенов, Ш.Б. Қасенова, Ж.И. Сағынтаева, Е.Е. Қуанышбеков, Н.И. Копылов

298,15–673 К аралығында жаңа наномөлшерлі кобальт-купрат-манганиті $LaLi_2CoCuMnO_6$ мен $LaLi_2NiCuMnO_6$ никелит-купрат-манганитінің жылусыйымдылығы және олардың термодинамикалық қасиеттері

298,15–673 К аралығында динамикалық калориметрия әдісімен алғаш рет синтездеп алған жаңа наномөлшерлі $LaLi_2CoCuMnO_6$ мен $LaLi_2NiCuMnO_6$ құрамды кобальт-купрат-манганит пен никелит-купрат-манганитінің меншікті жылусыйымдылықтары зерттелді. Меншікті жылусыйымдылықтардан олардың мольдік жылусыйымдылықтары есептелінді. $LaLi_2CoCuMnO_6$ 398 К және $LaLi_2NiCuMnO_6$ 373 К мен 573 К температурасында II-ші реттегі фазалық өзгерістер анықталды. Фазалық өзгерістердің температураларын ескере отырып, жылусыйымдылықтардың теңдеулері қорытылып шығарылды. Барлық алынған тәжірибелік және есептеу нәтижелері математикалық статистика әдістерімен нақты түрде өңделді, меншікті жылусыйымдылықтарының орташа мәндері орташі квадраттық ауытқушылықтармен, ал мольдік жылу сыйымдылықтары ауытқушылықтың кездейсоқтық құрамымен анықталды. Иондық инкременттер әдісімен зерттеліп отырған қосылыстардың стандарттық энтропиялары есептелді. Жылусыйымдылықтарының тәжірибелік және стандарттық энтропиялардың есептеу мәндерінің негізінде 298,15–673 К аралығында 50 К сайын энтальпияның $H^o(T)–H^o(298,15)$, энтропияның $S^o(T)$ және келтірілген термодинамикалық потенциалдық $\Phi^{xx}(T)$-тің температураға тәуелділіктері есептелді.

Кілт сөздері: термодинамика, кобальт, никелит, купрат, манганит, жылусыйымдылық, калориметрия, лантан, сілтілік металдар.

Б.К. Касенов, Ш.Б. Касенова, Ж.И. Сагинтаева, Е.Е. Куанышбеков, Н.И. Копылов

Теплоемкость новых наноразмерных кобальто-купрато-манганита $LaLi_2CoCuMnO_6$ и никелито-купрато-манганита $LaLi_2NiCuMnO_6$ в интервале 298,15–673 К и их термодинамические свойства

Методом динамической калориметрии в интервале температур 298,15–673 К впервые исследованы удельные теплоемкости полученных нами новых наноразмерных кобальто-купрато-манганита и никелито-купрато-манганита лантана и лития составов $LaLi_2CoCuMnO_6$ и $LaLi_2NiCuMnO_6$. Из удельных теплоемкостей рассчитаны их мольные теплоемкости. Установлено, что $LaLi_2CoCuMnO_6$ при 398 К и $LaLi_2NiCuMnO_6$ при 373 К и 573 К претерпевают фазовые переходы II-рода. С учетом температур фазовых переходов выведены уравнения температурной зависимости теплоемкости. Все полученные экспериментальные и расчетные данные обработаны строго методами математической статистики, для усредненных значений удельных теплоемкостей рассчитаны среднеквадратичные отклонения, а для мольных теплоемкостей — случайные составляющие погрешности. Методом ионных инкрементов вычислены стандартные энтропии исследуемых соединений. На основе опытных данных по теплоемкостям и расчетных значений стандартных энтропий в интервале 298,15–675 К шагом через 50 К

вычислены температурные зависимости энтальпии $H^o(T)–H^o(298,15)$, энтропии $S^o(T)$ и приведенного термодинамического потенциала $\Phi^{xx}(T)$.

Ключевые слова: термодинамика, кобальт, никелит, купрат, манганит, теплоемкость, калориметрия, лантан, литий.

References

1 Tretyakov, Yu.D., & Brylyov, O.A. (2000). Novye pokoleniia neorhanicheskikh funktsionalnykh materialov [New generations of inorganic functional materials]. *Zhurnal Rossiiskoho khimicheskoho obshchestva im. D.I. Mendeleeva — Journal of the Russian Chemical Society named after D.I. Mendeleev, 44, 4,* 10–16 [in Russian].

2 Tretyakov, Yu.D., & Gudilin, E.A. (2000). Khimicheskiie printsipy polucheniia metallooksidnykh sverkhprovodnikov [Chemical principles of the receiving of metal-oxide superconductors]. *Uspekhi khimii — Russian Chemical Reviews, 69, 1,* 3–40 [in Russian].

3 Erin, Yu. (2009). Naideno veshchestvo s hihantskim znacheniem dielektricheskoi pronitsaemosti [Substance with high value of dielectric capacitivity was found]. *Khimiia i khimiki — Chemistry and Chemists, 1,* Retrieved from http://chemistry-chemists.com/N1_2009/16–22.pdf [in Russian].

4 Behera, S., Kamble, V.B., Vittac, S., Umarji, A.M., & Shivakumara, C. (2017). Synthesis, structure and thermoelectric properties of $La_{1-x}Na_xCoO_3$ perovskite oxides. *Bulletin of Materials Science, 40, 7*, 1291–1299. DOI: 10.1007/s12034–017–1498–6.

5 Klyndyuk, A., Krasutskaya, N., Evseeva, L., Chizhova, E., & Tanaeva, S. (2015). Effect of the Cobalt Substitution on the Structure and Properties of the Layered Sodium Cobaltate Derivatives. *Universal Journal of Materials Science, 3(2),* 27–34.

6 Sadykov, V., Kharlamova, T., & Smirnova, A. (2009). $La_{0.8}Sr_{0.2}Ni_{0.4}Fe_{0.6}O_3$–$Ce_{0.8}Gd_{0.2}O_{2-\delta}$ Nanocomposite as Mixed Ionic–Electronic Conducting Material for SOFC Cathode and Oxygen Permeable Membranes: Synthesis and Properties. *Composite Interfaces, 16,* 407–431. DOI: 10.1163/156855409x450855.

7 Krohns, S., Lunkenheimer, P., Kant, Ch., Pronin, A.V., Brom, H.B., Nugroho, A.A., Diantoro, M., & Loidl, A. (2009). Colossal dielectric constant up to gigahertz at room temperature. *Appl. Phys. Lett., 94,* 122903. DOI: 10.1063/1.3105993.

8 Sen, C., Enshan, H., Han, X., Lingzhi, Z., Bin, L., Guangquan, Zh., & Min, L. (2017). P_2-type $Na_{0.67}Ni_{0.33-x}Cu_xMn_{0,67}O_2$ as new high-voltage cathode materials for sodium-ion batteries. *International Journal Ionics,* 1–10.

9 Archana, S., Ajendra, S., Satyendra S., Poonam. T., Yadav, R.R. (2016). Synthesis, Characterization and Gas Sensing Capability of $Ni_xCu_{1-x}Fe_2O_4$ ($0.0 \le x \le 0.8$) Nanostructures Prepared via Sol-Gel Method. *Journal of Inorganic and Organometallic Polymers and Materials, 26, 6,* 1392–1403. DOI: 10.1007/s10904–016–0428–1.

10 Kasenov, B.K., Kasenova, Sh.B., Sagintaeva, Zh.I., Ermagambet, B.T., Bekturganov, N.S., & Oskembekov, I.M. (2017). *Dvoinye i troinye manhanity, ferrity i khromity shchelochnykh, shchelochnozemelnykh i redkozemelnykh metallov* [*Double and triple manganites, ferrites and chromites of alkali, alkaline earth and rare earth metals*]. Moscow: Nauchnyi mir [in Russian].

11 Kasenova, Sh.B., Abildaeva, A.Zh., Sagintaeva, Zh.I., Davrenbekov, S.Zh., & Kasenov, B.K. (2013). Teploemkost i termodinamicheskie funktsii manhanito-ferritov v intervale 298.15–673 K [Heat capacity and thermodynamic functions of manganite ferrites NdM^IMnFeO_5 (M^I=Li, Na) in the range of 298.15–673 K]. *Zhurnal fizicheskoi khimii — Russian Journal of Physical Chemistry 87, 5,* 739–743. DOI: 10.7868/s0044453713050117 [in Russian].

12 Kasenova, Sh.B., Kasenov, B.K., Sagintaeva, Zh.I., Ermaganbetov, K.T., Kuanyshbekov, E.E., Sejsenova, A.A., & Smagulova, D.I. (2014). Teploemkost i termodinamicheskie funktsii nanostrukturirovannykh chastits kuprato-manhanitov $LaM_2^{II}CuMnO_6$ (M^{II} — Mg, Ca) v intervale 298.15–673 K [Heat capacity and thermodynamic functions of $LaM_2^{II}CuMnO_6$ (M^{II} — Mg, Ca) nanostructured cuprate-manganite particles in the range of 298.15–673 K]. *Zhurnal fizicheskoi khimii — Russian Journal of Physical Chemistry, 88, 5,* 836–840. DOI: 10.7868/s0044453714050112 [in Russian].

13 Kasenov, B.K., Kasenova, Sh.B., Sagintaeva, Zh.I., Turtubaeva, M.O., Amerhanova, Sh.K., & Nikolov, R.N. (2016). Teploemkost i termodinamicheskie funktsii manhanitov $NdM^{II}_2CoMnO_6$ (M^{II} — Mg, Ca, Sr, Ba) v intervale 298.15–673 K [Heat capacity and thermodynamic functions of manganites $NdM^{II}_2CoMnO_6$ (M^{II} — Mg, Ca, Sr, Ba) in the range of 298.15–673 K]. *Teplofizika vysokikh temperatur — High Temperature, 54, 4,* 540–544. DOI: 10.7868/s0040364416040104 [in Russian].

14 Kasenov, B.K., Kasenova, Sh.B., Sagintaeva, Zh.I., Turtubaeva, M.O., Kakenov, K.S., & Esenbaeva, G.A. (2017). Teploemkost i termodinamicheskie funktsii novykh nanorazmernykh ferro-hromo-manhanitov $LaM^{II}_{0,5}FeCrMnO_{6,5}$ (M^{II} — Mg, Ca, Sr, Ba) [Heat capacity and thermodynamic functions of new nanoscale ferro-chromo-manganites $LaM^{II}_{0,5}FeCrMnO_{6,5}$ (M^{II} — Mg, Ca, Sr, Ba)]. *Zhurnal fizicheskoi khimii — Russian Journal of Physical Chemistry, 91, 3,* 410–416. DOI: 10.7868/s0044453717030116 [in Russian].

15 Kasenova, Sh.B., Sagintaeva, Zh.I., Kasenov, B.K., Turtubaeva, M.O., Rustembekov, K.T., & Stoev, I. (2017). Kalorimetricheskoe issledovanie teploemkosti nikelito-manhanitov LaM_2NiMnO_5 (M — Li, Na, K) v intervale temperatur 298,15–673 K [Calorimetric study of the heat capacity of LaM_2NiMnO_5 (M — Li, Na, K) nickelite-manganites in the temperature range 298.15–673 K]. *Teplofizika vysokikh temperatur — High Temperature, 55, 3,* 480–483. DOI: 10.7868/s0040364417030024 [in Russian].

16 Sagintaeva, Zh.I., Kasenov, B.K., Kasenova, Sh.B., Turtubaeva, M.O., & Kuanyshbekov, E.E. (2018). Sintez i renthenohrafiia novykh nanorazmernykh (nanoklasternykh) nikelito-kuprato-manhanitov lantana i shchelochnykh metallov [Synthesis and X-ray of new nanoscale (nanocluster) nickel-cuprate-manganites of lanthanum and alkali metals]. *Natsionalnaia akademiia nauk Respubliki Kazakhstan. Seriia khimii i tekhnolohii — National academy of sciences of the Republic of Kazakhstan informs. Series of Chemistry and technology, 3(429),* 73–78 [in Russian].

17 Kasenova, Sh.B., Kasenov, B.K., Sagintaeva, Zh.I., Turtubaeva, M.O., & Kuanyshbekov, E.E. (2018). Novye nanorazmernye (nanoklasternye) kobalto-kuprato-manhanity lantana i shchelochnykh metallov i ikh renthenohraficheskoe issledovanie [New nanoscale (nanocluster) cobalt-cuprate-manganites of lanthanum and alkali metals and their radiographic examination]. *Natsionalnaia akademiia nauk Respubliki Kazakhstan. Seriia khimii i tekhnolohii — National academy of sciences of the Republic of Kazakhstan informs. Series of Chemistry and technology, 3(429),* 62–72 [in Russian].

18 (1986). *Tekhnicheskoe opisanie i instruktsii po ekspluatatsii IT-S-400* [*Technical specification and manual of instructions for IT-S-400*]. Aktiubinsk: AZ «Etalon» [in Russian].

19 Kasenov, B.K., Davrenbekov, S.Zh., Ermagambet, B.T., Kasenova, Sh.B., Sagintaeva, Zh.I., Abildaeva, A.Zh., Kuanyshbekov, E.E., Isabaeva, M.A., Turtubaeva, M.O., & Zhumadilov, E.K. (2012). Termodinamicheskie i elektrofizicheskie svoistva ferrita $LaSrMnFeO_{5,5}$ [Thermodynamic and electrophysical properties of ferrite $LaSrMnFeO_{5.5}$]. *Teplofizika vysokikh temperatur — High Temperature, 50, 6,* 789–792. DOI: 10.1134/s0018151x12060053 [in Russian].

20 Kumok, V.N. (1987). *Priamye i obratnye zadachi khimicheskoi termodinamiki* [*Direct and Inverse Problems of Chemical Thermodynamics*]. Novosibirsk: Nauka [in Russian].

21 Kasenov, B.K. (2018). *Otsenka standartnykh termodinamicheskikh svoistv nikelito(kobalto)-kuprato-manhanitov sostavov* $LaMe^{I}_{2}Ni(Co)CuMnO_6$ *i* $LaMe^{II}Ni(Co)CuMnO_6$ *(*Me^{I} *— Li, Na, K) i (*M^{II} *— Mg, Ca, Sr, Ba) [Evaluation of the standard thermodynamic properties of nickelite(cobalto)-cuprato-manganite of the compositions* $LaMe^{I}_{2}Ni(Co)CuMnO_6$ *and* $LaMe^{II}Ni(Co)CuMnO_6$ *(*Me^{I} *— Li, Na, K) and (*M^{II} *— Mg, Ca, Sr, Ba)*]. Tver: Tverskii hosudarstvennyi universitet [in Russian].

DOI 10.31489/2019Ch2/69-75

UDC 546.244:65:46:74:541.11+537.226

K.T. Rustembekov, M.S. Kasymova, Ye.V. Minayeva, A.Zh. Bekturganova

Ye.A. Buketov Karaganda State University, Kazakhstan
(E-mail: rustembekov_kt@mail.ru)

Lanthanum-magnesium-nickel tellurite: thermodynamic and electrophysical characteristics

Lanthanum-magnesium-nickel tellurite with composition of $La_2MgNiTeO_7$ was synthesized from La_2O_3, NiO, TeO_2 oxides and $MgCO_3$ with the help of the ceramic technology. The temperature dependences of the isobaric heat capacity of tellurite $La_2MgNiTeO_7$ were studied on an IT-S-400 calorimeter using an experimental method of dynamic calorimetry in the range of 298.15–673 K. The operation of the calorimeter was checked by measuring the standard heat capacity of α-Al_2O_3. The specific heat capacities were measured, and then the molar heat capacities of the synthesized tellurite were calculated using them. In the study of the dependence of the heat capacity of tellurite $La_2MgNiTeO_7$ on temperature at 423 K, a sharp anomalous λ-shaped jump was found, probably related to a second-order phase transition. This transition can be associated with cationic redistribution, changes in the coefficient of thermal expansion and magnetic moment, as well as changes in dielectric constant and electrical resistivity. The equation of the temperature dependence of the heat capacity of the compound is derived on the basis of the experimental data, taking into account the phase transition temperature of the second kind. The temperature dependences of the heat capacity C_p^0(T) and thermodynamic functions, namely, the entropy $S^0(T)$, the enthalpy $H^0(T) - H^0(298.15)$ and the reduced thermodynamic potential $\Phi^{xx}(T)$ were calculated based on the experimental data on heat capacities and the calculated standard entropy value $S^0(298.15)$ in the interval 298.15–673 K. For the first time, the temperature dependences of the dielectric constant and electrical resistance of tellurite $La_2MgNiTeO_7$ in the temperature range of 293–483 K were studied on the LCR-800 instrument. There are maxima and minima on the curves of lgε~$f(T)$ and lgR~$f(T)$, which confirm the λ-shaped effect on the C_p^0~$f(T)$ curve of a successful compound, related to the second-order phase transition. The data obtained show that the tellurite studied has semiconductor properties.

Keywords: lanthanum-magnesium-nickel tellurite, heat capacity, thermodynamic functions, dielectric constant, electrical resistance.

The study of complex oxides of 3*d*- and 4*f*-elements with a perovskite structure is important for inorganic materials science [1]. In this regard, the purpose of this work is to study the thermodynamic and electrophysical characteristics of new lanthanum-magnesium-nickel tellurite $La_2MgNiTeO_7$. Ceramic technology was used to synthesize lanthanum-magnesium-nickel $La_2MgNiTeO_7$ tellurite from oxides La_2O_3, NiO («high pure»), TeO_2 («reagent grade») and carbonate $MgCO_3$ («reagent grade»). The method of synthesis and X-ray study of this compound are described in detail in our previous work [2]. The proposed structure of the synthesized tellurite is perovskite with the space group P_m3_m.

The isobaric heat capacity of $La_2MgNiTeO_7$ was studied by dynamic calorimetry on an IT-C-400 instrument in the temperature range 298.15–673 K. The operation of the calorimeter was checked by measuring the standard heat capacity of α-Al_2O_3. The value of C_p(298.15) α-Al_2O_3 found experimentally was 76.0 J/(mol K), which fully satisfies the reference value (79 J/(mol K)) [3]. At each temperature, the estimation of standard deviation ($\bar{\delta}$) was carried out for the averaged values of specific heat capacity, and the random error component ($\bar{\delta}$) [4] was calculated for the molar heat capacity. The measurement errors of the heat capacity at all temperatures are within the accuracy of the instrument (± 10 %) [5]. The specific heat capacities of tellurite were studied, then its molar heat capacities were calculated from the experimental values obtained [6]. The experimental values of the heat capacity of the tellurite under study are listed in Table 1.

When studying the dependence of the heat capacity of $La_2MgNiTeO_7$ tellurite on temperature at 423 K, a sharp anomalous λ-shaped jump (Fig. 1) was found, probably related to a second-order phase transition. This transition can be associated with cationic redistribution, changes in the coefficient of thermal expansion and magnetic moment, as well as changes in dielectric constant and electrical resistivity.

Table 1

Experimental values of the heat capacities of $La_2MgNiTeO_7$

T, K	$C_p \pm \bar{\delta}$, J/(g K)	$C_p^0 \pm \overset{0}{\Delta}$, J/(mol K)
298.15	0.5337±0.0124	332±21
323	0.5562±0.0173	334±29
348	0.6225±0.0155	374±26
373	0.7365±0.0201	442±34
398	0.8892±0.2277	534±38
423	1.0677±0.0100	641±17
448	1.0231±0.0119	614±20
473	0.9651±0.0266	580±44
498	0.8953±0.0248	538±41
523	0.8070±0.0134	485±22
548	0.7252±0.0189	435±32
573	0.7813±0.0177	469±30
598	0.8532±0.0145	512±24
623	0.9263±0.0191	556±32
648	1.0213±0.0111	613±19
673	1.1270±0.0291	677±49

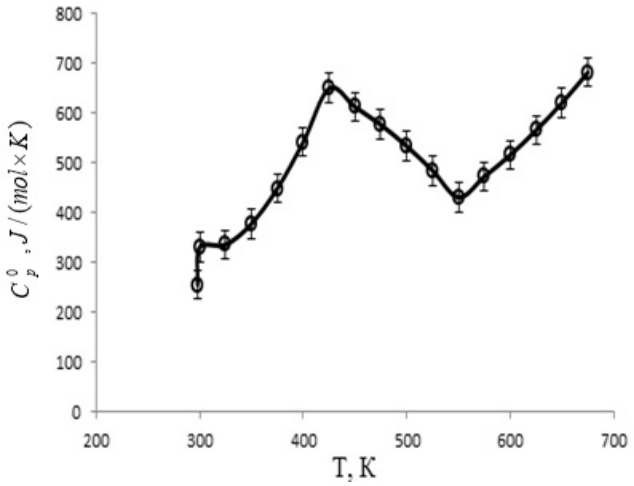

Figure 1. Temperature dependence of the heat capacity of $La_2MgNiTeO_7$

The equation of the temperature dependence of the heat capacity of the compound is derived On the basis of experimental data (Table 1), taking into account the temperature of a phase transition of the second kind,

$$C_p^0, \text{J/(mol×K)} = a + bT + cT^{-2}, \quad (1)$$

coefficients are given in Table 2.

Table 2

The coefficients of equation (1) in the range of 298.15 — 673 K

ΔT, K	a	$b\times10^3$	$c\times10^{-5}$
298–423	–(3174±191)	7542.7±454.8	1118.15±67.43
423–548	2643±159	–(3428.5±206.7)	–(986.92±59.51)
548–673	–(2534±153)	4010.5±241.8	2317.69±139.76

We used the mean random error values for the temperature ranges under consideration to determine the error of the coefficients in the $C_p^0 \sim f(T)$ dependency equations.

The temperature dependences of the functions $S^0(T)$, $H^0(T) - H^0(298.15)$ and $\Phi^{xx}(T)$ have been calculated based on the known relations [6], using the experimental data on $C_p^0 \sim f(T)$ and the calculated value

S^0(298.15). The results are shown in Table 3. Due to the fact that the technical characteristics of the device do not directly calculate the standard entropy of S^0(298.15) tellurite from experimental data on $C_p^0(T)$, it was estimated using the ion increment method [7].

Table 3

Thermodynamic functions of tellurite $La_2MgNiTeO_7$ in the range of 298.15 — 673 K

T, K	$C_p^0(T) \pm \overset{\circ}{\Delta}$, J/(mol × K)	$S^0(T) \pm \overset{\circ}{\Delta}$, J/(mol×K)	$H^\circ(T) - H^\circ(298.15) \pm \overset{\circ}{\Delta}$, J/mol	$\Phi^{xx}(T) \pm \overset{0}{\Delta}$, J/(mol×K)
298.15	255±15	251±8	–	251±8
300	331±20	253±23	660±40	251±23
325	336±20	279±25	8900±540	252±23
350	378±23	306±28	17760±1070	255±23
375	449±27	334±30	28050±1690	259±23
400	542±33	366±33	40390±2440	265±24
425	650±39	402±36	55260±3330	272±25
450	613±37	438±40	70930±4280	280±25
475	577±35	470±42	85820±5180	289±26
500	534±32	498±45	99720±6010	299±27
525	485±29	523±47	112460±6780	309±28
550	431±26	545±49	123920±7470	319±29
575	473±29	565±51	135290±8160	330±30
600	516±31	586±53	147630±8900	340±31
625	566±34	608±55	161140±9720	350±32
650	621±38	631±57	175970±10610	360±33
675	682±41	656±59	192240±11590	371±34

The average random components and errors were estimated for all values of heat capacity and enthalpy over the entire temperature range, and the accuracy of entropy calculation (± 3 %) was included in the error estimate for the values of entropy and reduced thermodynamic potential. The presence of a phase transition of the second kind on the plot of $C_p^0 \sim f(T)$ for the tellurite under study suggests that this compound may have unique electrophysical properties.

In this connection, the temperature dependences of the dielectric constant and electrical resistance of tellurium $La_2MgNiTeO_7$ in the temperature range 293–483 K were investigated. The study of electrophysical properties was carried out by measuring the electrical capacitance of samples on an LCR-800 instrument (Taiwan) at a working frequency of 1 kHz continuously in dry air in a thermostat mode with an exposure time at each fixed temperature.

Previously, plane-parallel samples were made in the form of discs with a diameter of 10 mm and a thickness of 1–5 mm with a binding additive (~1.5 %). Pressing was carried out under a pressure of 20 kg/cm^2. The resulting discs were fired in a silica oven at 1000 for 6 hours.

The samples were kept for 8 hours at a temperature of 600 ºC in order to impart sufficient strength for the experiment they were thoroughly double-sided polished. The two-electrode system is applied; the electrodes are applied by firing silver paste.

The dielectric constant was determined from the electrical capacity of the sample for known values of the sample thickness and the surface area of the electrodes. The Sawyer-Tower circuit was used to obtain the relationship between the electric induction D and the electric field strength E. A visual observation of D (E hysteresis loop) was carried out on a C1–83 oscilloscope with a voltage divider consisting of a resistance of 6 MΩ and 700 kΩ and a reference capacitor of 0.15 μF. The frequency of the generator is 300 Hz. In all temperature studies, the samples were placed in a furnace, the temperature was measured with a chromel-alumel thermocouple connected to a B2–34 voltmeter with an error of ± 0.1 mV. The rate of temperature change is ~5 K/min. The value of the dielectric constant at each temperature was determined by the formula:

$$\varepsilon = \frac{C}{C_0}, \qquad (2)$$

where $C_0 = \frac{\varepsilon_0 \cdot S}{d}$ is the capacitance of the capacitor without the test substance (air).

Since ceramic materials have certain inertia, the change in electrical properties, the data on the integral electrical resistance and electrical capacity were determined only after preliminary exposure for ~0.5 hours at a fixed temperature. This is especially important in the area of abnormal changes in the above characteristics., measurements are also carried out by the method of direct deflection using an E6–13A thermometer to compare the data on the electrical conductivity.

Experimental data on the study of the electrophysical properties of $La_2MgNiTeO_7$ ternary tellurite are given in Table 4 and in Figures 2, 3.

Table 4

Dependence of electric capacitance (C), dielectric constant (ε) and electrical resistance (R) of tellurite $La_2MgNiTeO_7$ on temperature

T, K	*C*, μF	ε	lg ε	*R*, Ohm	lg *R*
293	9.24	52	1.71	366300	5.56
303	9.23	52	1.71	230100	5.36
313	9.17	51	1.71	114100	5.06
323	9.49	53	1.73	30340	4.48
333	9.87	55	1.74	395300	5.60
343	10.17	57	1.76	647600	5.81
353	10.60	60	1.77	1043000	6.02
363	10.07	57	1.75	2389000	6.38
373	10.63	60	1.78	2905000	6.46
383	11.07	62	1.79	3115000	6.49
393	11.27	63	1.80	3210000	6.51
403	10.52	59	1.77	2508000	6.40
413	8.85	50	1.70	612800	5.79
423	8.70	49	1.69	436500	5.64
433	8.89	49	1.69	562200	5.75
443	8.89	50	1.70	760500	5.88
453	9.08	51	1.71	1021000	6.01
463	9.29	52	1.72	1179000	6.07
473	9.40	53	1.72	1241000	6.09
483	9.57	54	1.73	1397000	6.15

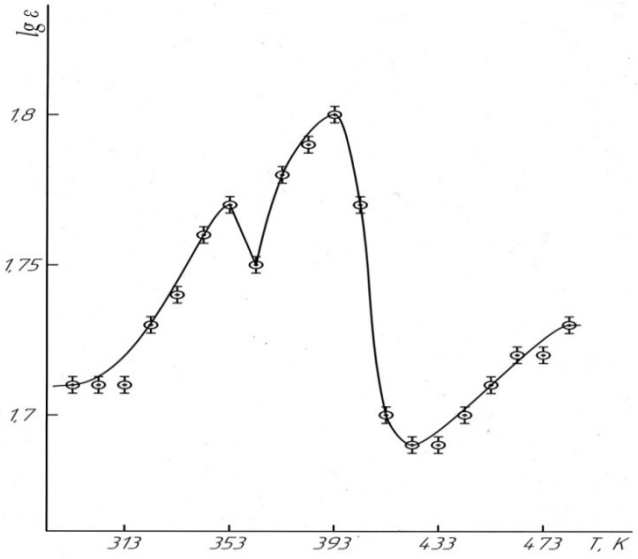

Figure 2. Temperature dependence of dielectric constant of $La_2MgNiTeO_7$

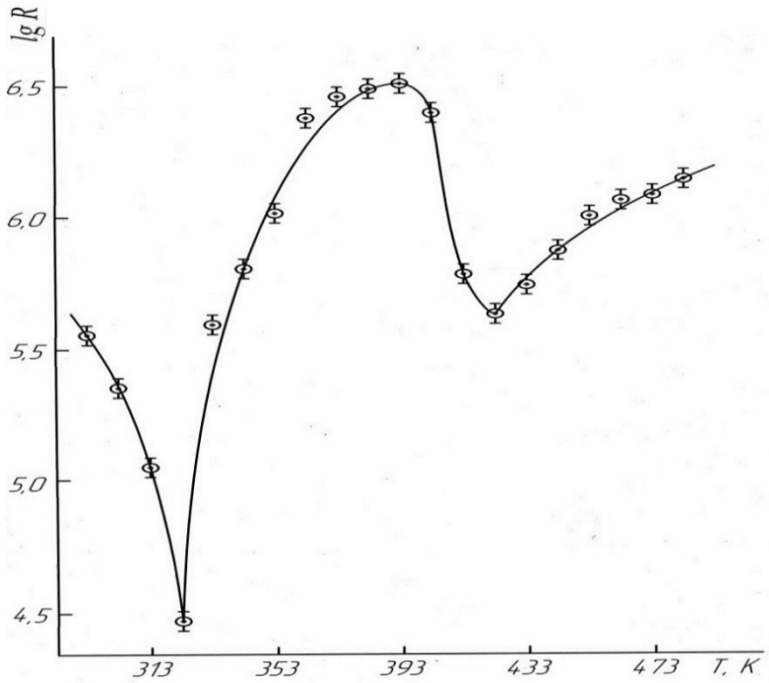

Figure 3. Temperature dependence of the electrical resistance of $La_2MgNiTeO_7$

Analysis of the data in Table 4 and Figures 2 and 3 shows that $La_2MgNiTeO_7$ compound in the range of 293–323 K exhibits semiconductor, at 323–393 K — metallic, at 393–423 K — semiconductor and at 433–483 K — metallic conductivity.

The calculation of the width of the forbidden zone was calculated by the formula

$$\Delta E = \frac{2kT_1T_2}{T_2 - T_1} \ln\frac{R_1}{R_2}, \qquad (3)$$

where k is the Boltzmann constant; R_1 and R_2 are resistances at temperatures T_1 and T_2, respectively.

The width of the forbidden zone (ΔE), calculated by the formula (3), in the interval 293–323 K is 1.57 eV, and it is 2.56 eV in the interval 393–423 K. The research results given in Table 4 and in Figures 2 and 3 shows that the new tellurite $La_2MgNiTeO_7$ exhibits semiconductor properties.

Thus, for the first time, the isobaric heat capacity of lanthanum-magnesium-nickel tellurite $La_2MgNiTeO_7$ was experimentally investigated by dynamic calorimetry in the temperature range 298.15–673 K. The temperature dependences of the heat capacity for the compound under study are derived based on the experimental values. The standard heat capacity of ternary tellurite was determined experimentally. The temperature dependences of the thermodynamic functions $S^0(T)$, $H^0(T) - H^0(298.15)$ and $\Phi^{xx}(T)$ are calculated in the range of 298.15–673 K. There is a λ-shaped peak related to a second-order phase transition on the $C_p^0 \sim f(T)$ dependence curve of lanthanum-magnesium-nickel tellurite $La_2MgNiTeO_7$ at a temperature of 423 K.

For the first time, the temperature dependences of the dielectric constant and electrical resistance of tellurite $La_2MgNiTeO_7$ have been studied on the LCR instrument. The curves $\lg\varepsilon \sim f(T)$ and $\lg R \sim f(T)$ have maxima and minima, which confirm the λ-like effect on the $C_p^0 \sim f(T)$ dependence curve of the indicated compound, related to the phase transition of the second kind.

The obtained data showed that the $La_2MgNiTeO_7$ tellurite had semiconductor properties and was of interest for electronic technology.

The obtained new thermochemical and thermodynamic data serve as initial information files for fundamental data banks and reference books; they are of theoretical and practical interest for inorganic materials science in the field of directional synthesis of compounds with multifunctional properties.

References

1 Третьяков Ю.Д. Новые поколения неорганических функциональных материалов / Ю.Д. Третьяков, О.А. Брылев // Журнал Российского химического общества им. Д.И. Менделеева. — 2000. — Т. 45, № 4. — С. 10.

2 Бектурганова А.Ж. Синтез и рентгенографическое исследование новых никелито-теллуритов $La_2MNiTeO_7$ (M — Mg, Ca, Sr, Ba) / А.Ж. Бектурганова, Ж.И. Сагинтаева, К.Т. Рустембеков и др. // Известия НАН РК. Серия химии и технологии. — 2017. — № 2(422). — С. 99.

3 Robie R.A. Thermodynamic Properties of Minerals and Related Substances at 298.15 and (10^5 Paskals) Pressure and at Higher Temperatures / R.A. Robie, B.S. Hewingway, I.R. Fisher // Washington: United States Government Printing Office, 1978. — 456 p.

4 Спиридонов В.П. Математическая обработка экспериментальных данных / В.П. Спиридонов, Л.В. Лопаткин. — М.: Изд-во МГУ, 1970. — 221 с.

5 Техническое описание и инструкции по эксплуатации ИТ-С-400. — Актюбинск: Актюбинский завод «Эталон», 1986. — 48 с.

6 Rustembekov K.T. X-ray Diffraction and Thermodynamic Characteristics for Tellurite of the Composition Li_2CeTeO_5 / K.T. Rustembekov, A.Zh. Bekturganova // Russian Journal of Physical Chemistry A. — 2017. — Vol. 91, № 4. — P. 622–626.

7 Кумок В.Н. Прямые и обратные задачи химической термодинамики / В.Н. Кумок. — Новосибирск: Наука, 1987. — С. 108.

К.Т. Рүстембеков, М.С. Қасымова, Е.В. Минаева, А.Ж. Бектұрғанова

Лантан-магний-никель теллуриті: термодинамикалық және электрфизикалық сипаттамалары

Керамикалық технология әдісімен La_2O_3, NiO, TeO_2 оксидтері мен $MgCO_3$ карбонатынан $La_2MgNiTeO_7$ құрамды лантан-магний-никель теллуриті синтезделді. ИТ-С-400 калориметрінде динамикалық калометрияның тәжірибелік әдісімен 298,15–673 К аралығында $La_2MgNiTeO_7$ теллуритінің изобаралық жылусыйымдылығы зерттелді. Калориметрдің жұмысы α-Al_2O_3 стандартты жылусыйымдылығын өлшеумен тексерілді. Меншікті жылусыйымдылық өлшенді, кейін олар бойынша синтезделген теллуриттің мольдік жылусыйымдылығы есептелді. $La_2MgNiTeO_7$ теллуриті жылусыйымдылығының температурадан тәуелділігін зерттеу барысында 423 К күрт аномальді λ-тәрізді секіріс байқалды, оның II-ші текті фазалық ауысуға сәйкес келуі мүмкін. Бұл ауысу катиондардың қайта бөлінулерімен, термиялық ұлғаю коэффициенттерінің және магниттік моментінің өзгерістерімен, сол сияқты диэлектрлік өткізгіштігі және электрлік кедергісінің өзгерістерімен байланысты болуы мүмкін. Тәжірибелік мәліметтерінің негізінде, II-ші текті фазалық ауысу температурасын ескере отырып, қосылыстың жылусыйымдылығының температуралық тәуелділік теңдеулері шығарылды. Жылусыйымдылықтарының тәжірибелік мәліметтерінің және стандартты энтропияның $S^0(298{,}15)$ есептелген мәнінің негізінде 298,15–673 К аралығында жылусыйымдылықтың $C_p^0(T)$ және термодинамикалық функциялардың: энтропияның $S^0(T)$, энтальпияның $H^0(T) - H^0(298{,}15)$ және келтірілген термодинамикалық потенциалдың $\Phi^{xx}(T)$ температуралық тәуелділіктері есептелді. LCR-800 құрылғысында алғаш рет 293–483 К температура аралығында $La_2MgNiTeO_7$ теллуритінің диэлектрлік өткізгіштігі мен электрлік кедергісінің температуралық тәуелділігі зерттелді. $\lg\varepsilon \sim f(T)$ және $\lg R \sim f(T)$ тәуелділік қисықтарында максимумдар мен минимумдардың болуы, бұл қосылыстың $C_p^0 \sim f(T)$ тәуелділік қисығындағы, II-ші фазалық ауысуға тиесілі λ-тәрізді эффектіні дәлелдеді. Алынған мәліметтер зерттеліп отырған теллуриттің жартылайөткізгіштік қасиеттерге ие болатындығын көрсетті.

Кілт сөздер: лантан-магний-никель теллуриті, жылусыйымдылық, термодинамикалық функциялар, диэлектрлік өткізгіштік, электркедергісі.

К.Т. Рустембеков, М.С. Касымова, Е.В. Минаева, А.Ж. Бектурганова

Теллурит лантана-магния-никеля: термодинамические и электрофизические характеристики

Методом керамической технологии из оксидов La_2O_3, NiO, TeO_2 и карбоната $MgCO_3$ синтезирован теллурит лантана-магния-никеля состава $La_2MgNiTeO_7$. На калориметре ИТ-С-400 экспериментальным методом динамической калориметрии в интервале 298,15–673 К исследованы температурные зависимости изобарной теплоемкости теллурита $La_2MgNiTeO_7$. Проверку работы калориметра проводили измерением стандартной теплоемкости α-Al_2O_3. Измерены удельные, а затем по ним рассчитаны мольные теплоемкости синтезированного теллурита. При исследовании зависимости теплоемкости теллурита $La_2MgNiTeO_7$ от температуры при 423 К обнаружен резкий аномальный

λ-образный скачок, связанный, вероятно, с фазовым переходом II рода. Этот переход может быть связан с катионным перераспределением, с изменениями коэффициента термического расширения и магнитного момента, а также с изменениями диэлектрической проницаемости и электросопротивления. На основании экпериментальных данных, с учетом температуры фазового перехода II рода выведено уравнение температурной зависимости теплоемкости соединения. На основании опытных данных по теплоемкостям и расчетного значения стандартной энтропии $S^0(298{,}15)$ в интервале 298,15–673 К вычислены температурные зависимости теплоемкости $C_p^0(T)$ и термодинамических функций: энтропии $S^0(T)$, энтальпии $H^0(T) - H^0(298{,}15)$ и приведенного термодинамического потенциала $\Phi^{xx}(T)$. Впервые на приборе LCR-800 исследованы температурные зависимости диэлектрической проницаемости и электросопротивления теллурита $La_2MgNiTeO_7$ в диапозоне температуры 293–483 К. На кривых зависимостях $\lg\varepsilon \sim f(T)$ и $\lg R \sim f(T)$ имеются максимумы и минимумы, которые подтверждают λ-образный эффект на кривой зависимости $C_p^0 \sim f(T)$ удачного соединения, отнесенный к фазовому переходу II рода. Полученные данные показали, что исследуемый теллурит обладает полупроводниковыми свойствами.

Ключевые слова: теллурит лантана-магния-никеля, теплоемкость, термодинамические функции, диэлектрическая проницаемость, электросопротивление.

References

1 Tretyakov, Yu.D., & Brylev, O.A. (2000). Novye pokoleniia neorhanicheskikh funktsionalnykh materialov [New generations of inorganic functional materials]. *Zhurnal Rossiiskoho khimicheskoho obshchestva im. D.I. Mendeleeva — Journal of the Russian Chemical Society, named after D.I. Mendeleev*, *Vol. 45, 4,* 10 [in Russian].

2 Bekturganova, A.Zh., Sagintaeva Zh.I., & Rustembekov K.T. et al. (2017). Sintez i renthenohraficheskoe issledovanie novykh nikelito-telluritov $La_2MNiTeO_7$ (M — Mg, Ca, Sr, Ba) [Synthesis and X-ray study of new nickelite-tellurites $La_2MNiTeO_7$ (M — Mg, Ca, Sr, Ba). *Izvestiia NAN RK. Seriia Khimiia i tekhnolohii — News of the National Academy of Sciences of Kazakhstan. A series of chemistry and technology, 422, 2*, 99 [in Russian].

3 Robie, R.A., Hewingway, B.S., & Fisher, I.R. (1978). *Thermodynamic Properties of Minerals and Related Substances at 298.15 and (105 Paskals) Pressure and at Higher Temperatures.* Washington: United States Government Printing Office.

4 Spiridonov, V.P., & Lopatkin, L.V. (1970). *Matematicheskaia obrabotka eksperimentalnykh dannykh [Mathematical processing of experimental data]*. Moscow: Izd-vo MHU [in Russian].

5 *Tekhnicheskoe opisanie i instruktsii po ekspluatatsii IT-S-400 [Technical description and operating instructions for IT-C-400]*. Aktiubinsk: Aktiubinskii zavod «Etalon». (1986) [in Russian].

6 Rustembekov, K.T., & Bekturganova, A.Zh. (2017). Diffraction and Thermodynamic Characteristics for Tellurite of the Composition Li_2CeTeO_5. *Russian Journal of Physical Chemistry A*, *91*(4), 622–626.

7 Kumok, V.N. (1987). *Priamye i obratnye zadachi khimicheskoi termodinamiki [Direct and inverse problems of chemical thermodynamics]*. Novosibirsk: Nauka [in Russian].

DOI 10.31489/2019Ch2/76-80

UDC 66.10167.7642

E.S. Mustafin, A.A. Ainabayev, D.T. Sadyrbekov, A.M. Pudov,
D.A. Kaikenov, I.M. Pudov, A.S. Borsynbayev

Ye.A. Buketov Karaganda State University, Kazakhstan
(E-mail: edigemus@mail.ru)

Production of syngas from agricultural wastes by plasma-chemical method

A promising technology for utilization of agricultural waste is chemical plasma technology based on high-temperature plasma-chemical effects and the decomposition of hydrocarbon products to produce synthesis gas. Emulsified mixture of cow dung and water was placed into the reactor for producing synthesis gas. On entering the emulsion is exposed to flame of a gas burner with a combustion temperature of two thousand degrees. The plasma-chemical reactor was regularly tested in different modes to find the best mode for the production of synthesis gas and its composition. The stability of the voltage at the output of the electric generator was monitored at various loads. As a result, a stable operation of the gas generator was achieved. Chemical characteristics of syngas obtained appeared to be high: gas was pure and without dust, CO_2 content was low, but content of hydrogen and CO was high, namely 31.62 % and 37.28, respectively. Gas quality was checked by visual observation of the burner flame and the temperature of the burning gas using an infrared pyrometer. The stability of the flame and the stability of the temperature of combustion characterize the quality of synthesis gas. It is shown experimentally that the plasma-chemical treatment of hydrocarbons and agricultural wastes is a highly effective method for producing synthesis gas.

*Keywords***:** plasma chemistry, synthesis gas, hydrogen, carbon monoxide, agricultural waste, recycling.

The development of power industry is based on the use of renewable energy sources and stimulated by the lack of traditional fuel and energy resources and environmental problems. Currently, there is an increasing interest in creating new environmentally friendly technologies based on plasma processes. One of the most promising substitutes for classic fuels is synthesis gas, which is formed in the processing and recycling of oil and gas, coke-chemical, energy industries and agriculture waste [1, 2]. Due to modern developments, synthesis gas is obtained by gasifying not only coal and oil, but also more unconventional carbon sources, up to household and agricultural waste.

Synthesis gas is mainly a mixture of carbon monoxide and hydrogen. It is produced industrially by steam reforming of methane, partial oxidation of methane, plasma gasification of waste and raw materials, coal gasification [3, 4]. The ratio of components in the synthesis gas varies in a wide range, because it depends both on the raw materials used and on the type of conversion — by water vapor or by oxygen. Depending on the method of producing synthesis gas, the ratio of CO: H_2 in it varies from 1: 1 to 1: 3. Typically, the percentage of substances in raw crude synthesis gas is as follows, %: CO — 15–18; H_2 — 38–40; CH_4 — 9–11; CO_2 — 30–32.

The most promising technology for the disposal of agricultural waste is a plasma-chemical technology. It is based on a high-temperature plasma-chemical effect on the recyclables to produce synthesis gas and the complete decomposition of the recyclable waste [5, 6]. The schematic diagram of the laboratory setup is shown in Figure 1.

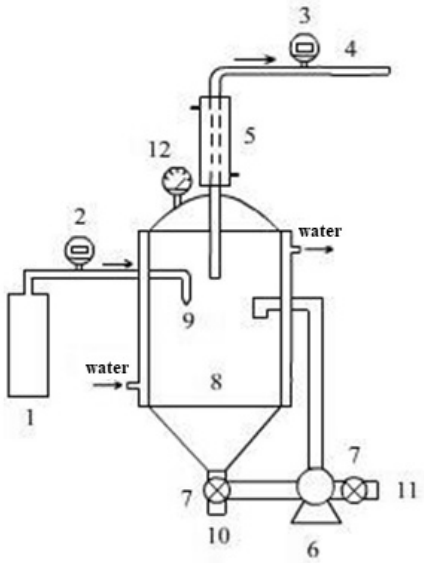

1 — cylinder (propane-butane); *2, 3* — gas meters; *4* — gas outlet; *5* — dephlegmator; *6* — circulation pump; *7* — valve; *8* — reactor; *9* — gas burner; *10* — drain; *11* — loading of raw materials; *12* — pressure gauge

Figure 1. Laboratory set-up of plasma-chemical waste processing into synthesis gas

An emulsified mixture of cow manure and water was fed into a 8 L metal cell (reactor) to produce synthesis gas. The incoming emulsion was affected by the flame of a gas burner (domestic propane-butane gas) with a temperature of up to 2000 ºC. During the reaction for 15 minutes, the volume of evolved gas amounted to 0.176 m^3. The volume of consumed domestic gas in the burner was 0.036 m^3.

In this technology, cattle manure was the main material used in the production of synthesis gas. The composition of manure is greatly influenced by the specific gravity of concentrated feed in the diet and by the quantity and quality of litter. Manure contains up to 80 percent of water (source of water vapor) and up to 20 percent of organic matter (source of carbon) [7, 8]. The chemical composition of manure is given in Table 1.

Table 1

The chemical composition of the feedstock

Cattle manure	Chemical composition (%)							
	Water	Organic matter	Nitrogen (common)	(P_2O_5)	(K_2O)	(CaO)	(MgO)	Iron oxide and Aluminum oxide (R_2O_3)
Cattle	77.3	20.3	0.45	0.23	0.50	0.40	0.11	0.05

The resulting mixture of gases was collected in plastic containers every five minutes for investigation (burning temperature, composition, humidity, etc.). The analysis carried out on the Kristall Lux 4000-M gas chromatograph with a thermal conductivity detector showed a stable gas composition for a long time of 2–5 days. The composition and quantitative ratios between the components of the mixture obtained by means of a plasma-chemical set-up correspond to the composition of synthesis gas. The composition and volume fractions of the components of the evolved gas mixture are shown in Table 2.

Table 2

The composition of the synthesis gas, depending on the operating time of the reactor

The operating time of the reactor, min	Composition of the output gas, %				
	H_2	O_2	CO_2	N_2	CO
10	14	8.6	3.6	55.0	17
15	25	4.0	4.5	15	23
20	45	0.0	6.5	0.5	43

As it seen from Table 2, an increase in the operating time of the reactor leads to improving qualitative composition of the output gas, because the content of CO_2, O_2, N_2 decreases, and the content of CO and H_2 increases.

Figure 2 shows the program window of the NetChrome chromatograph, where one of the results of the chromatographic analysis of the output gas is shown.

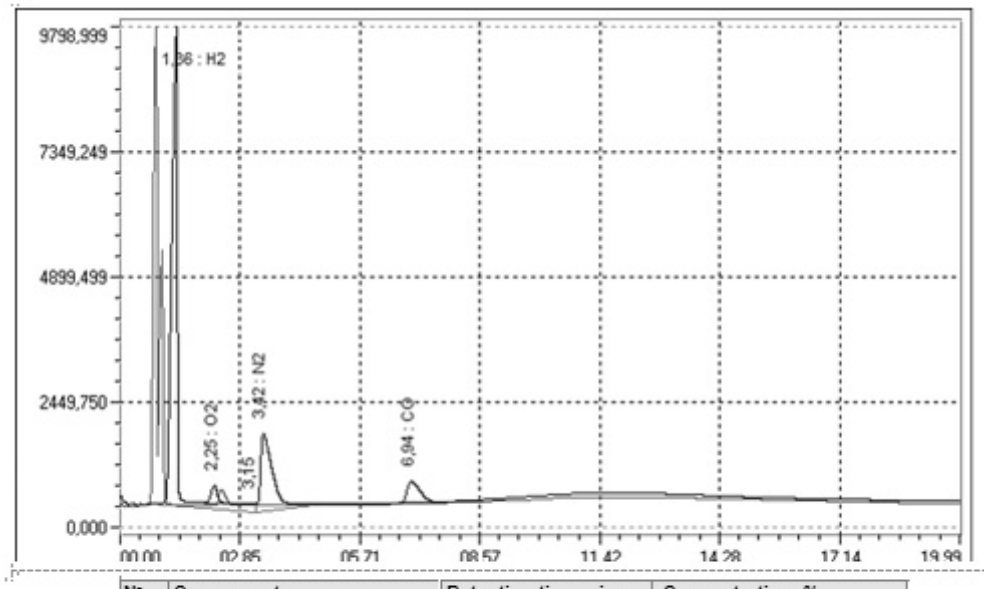

№	Component	Retention time,min	Concentration, %
1	H2	1,36	4,575E+01
2	O2	2,25	0,00
3	CO2	2,42	6,572E+00
4	N2	3,42	5,579E-01
5	CO	6,94	4,300E+01
			1,181E+02

Figure 2. Synthesis Gas Chromatogram

The plasma-chemical reactor was regularly tested in different modes to find the best mode for the production of synthesis gas and its composition. The stability of the voltage at the output of the electric generator was monitored at various loads. Gas quality was checked by visual observation of the burner flame and the temperature of the burning gas using an infrared pyrometer. The stability of the flame and the stability of the temperature of combustion characterize the quality of synthesis gas. The presence of water vapor, mechanical impurities at various burner modes with different ratios of air supplied and synthesis gas was constantly monitored. As a result, a stable operation of the gas generator was achieved. The composition and volume fractions of gas obtained in a steady mode of operation are presented in Table 3.

Table 3

The composition and volume fraction of the gas mixture obtained by the plasma-chemical method from cattle manure

No.	Gas components	Processing time, min	
		3	15
		gas composition, %	
1	H_2	25.04	31.62
2	O_2	0.18	0.74
3	CO	35.69	37.28
4	CO_2	1.23	11.75
5	N_2	5.99	4.91

The gas mixture obtained processing of 15 minutes contained 31.6 hydrogen and 37.28 carbon monoxide (1: 1 ratio). During this time, the ratio of consumed and obtained synthesis gas amounted to 1:30. The

amount of both consumed and released gas was measured by gas meters. The released synthesis gas was burned with an tranquil flame and had a good caloric effect (burning temperature in air 2500 K).

The synthesis gas was pumped out by a pump-compressor. The compressor pumps synthesis gas into the tank-gasholder (2000 L) until pressure reaches 8 atmospheres. The pressure in the gas-holders is controlled by gas manometers; the gas tanks are equipped with gas reducers and gas cranes. The quality of the synthesis gas was checked using an electric generator, which operated in the gas fuel mode. After filling the gasholders, the synthesis gas was supplied to the gas generator «Interskol EBG-5500» to generate electrical energy. It worked steadily for 1 hour, with a load capacity of 2 kilowatts.

As a result, a method for producing synthesis gas from agricultural waste was proposed with the help of processing cattle manure by a plasma chemical method. It has been experimentally shown that plasma-chemical processing of hydrocarbon and agricultural wastes is a highly efficient method for producing synthesis gas, which will be used as a fuel for heating and producing electricity at a gas power station. The developed plasma-chemical set allows processing not only agricultural waste, but also any waste containing organic components.

Advantages of the technology are follows:

– there are no polluting emissions compared with direct combustion methods;

– high velocity gasification and the availability of liquefied gas and electricity at power stations;

– utilization of hydrocarbon waste and production of fertilizer from agricultural waste.

References

1 Петров С.В. Управление процессом плазменной переработки твердых органических отходов / С.В. Петров, С.Г. Бондаренко, Е.Г. Дидык, А.А. Дидык // Вісник НТУУ «КПІ» Хімічна інженерія, екологія та ресурсосбереження. Науковий сбірник. — 2009. — Т. 3, № 3. — С. 29–38.

2 Beychok M.R. Process and environmental technology for producing SNG and liquid fuels, U.S. EPA, report EPA-660/2–75–011, May 1975. — P. 12.

3 Жуков М.Ф. Новые технологии сжигания топлива / М.Ф. Жуков, Б.И. Михайлов и др. // Энергетика страны и регионов. Теория и методы управления. — Новосибирск: Наука. Сиб. отд., 1988. — С. 176−190.

4 Мустафин Е.С., Касенов Р.З., Пудов И.М., Айнабаев А.А., Дюсекеева А.Т., Кездикбаева А.Т. Переработка углеводородных и сельскохозяйственных отходов в синтез-газ методом плазмохимии / ЭКСПО-2017: Технологии будущего: материалы Республиканской научно-практической конференции (21–22 октября 2016 года). — Караганда, 2016. — С. 92–95.

5 Тухватуллин А.М., Засыпкин И.М. Плазмохимическая технология переработки углеводородного сырья, обезвреживания и утилизации токсичных отходов // Генерация низкотемпературной плазмы и плазменные технологии. Проблемы и перспективы. (Низкотемпературная плазма. Т. 20). — Новосибирск: Наука. Сиб. отд. РАН, 2004. — С. 307−327.

6 Патон Б.Е., Чернец А.В., Маринский Г.С., Коржик В.Н., Петров С.В. Перспективы применения плазменных технологий для уничтожения и переработки медицинских и других опасных отходов. Ч. 1 // Современная электрометаллургия. — 2005. — № 3. — С. 54–63.

7 Пархоменко В.Д., Сорока П.И., Моссэ А.Л. и др. Плазмохимическая технология. Низкотемпературная плазма. — Новосибирск: Наука. Сиб. отд., 1991. — Т. 4. — С. 8–10.

8 Мамченков И.П. Навоз // Большая советская энциклопедия: в 30 т. — Т. 17 / И.П. Мамченков; гл. ред. А.М. Прохоров. — М.: Сов. энцикл., 1974. — С. 1969–1978.

Е.С. Мустафин, А.А. Айнабаев, Д.Т. Садырбеков, А.М. Пудов,
Д.А. Кайкенов, И.М. Пудов, А.С. Борсынбаев

Плазмахимиялық әдіспен ауылшаруашылық қалдықтарынан синтез-газ алу

Ауылшаруашылық қалдықтарын толықтай ыдырату арқылы синтез-газ ала отырып, жоюдың перспективті әдісі жоғарытемпературалы плазмохимиялық әсерге негізделген технология болып табылады. Синтез-газды алу үшін реакторға сиырдың көңі мен су қоспасының эмульсиясы салынды. Эмульсияға екі мың градус температурамен әсер етілді. Алынған синтез-газдың химиялық сипаты жоғары болды: газ таза, шаңсыз, құрамында CO_2 аз, ал сутегі мен CO мөлшері жоғары сәйкесінше 31,62 % және 37,28 %. Синтез-газды өндіруді және оның құрамын жақсарту үшін плазмахимиялық реакторға әртүрлі режимдерде сынақ жүргізілді. Электргенераторындағы кернеудің тұрақтылығы түрлі жүктемелерде бақыланды. Нәтижесінде газ генераторының тұрақты жұмысына қолжеткізілді. Зерттеу жұмысының нәтижесі бойынша көмірсутек пен ауылшаруашылық қалдықтарын плазмахимиялық өңдеу синтез-газ алудың жоғары әрі тиімді әдісі болып табылады.

Кілт сөздер: плазмохимия, синтез-газ, сутегі, көміртегі тотығы, ауылшаруашылық қалдықтары, қайта өңдеу.

Е.С. Мустафин, А.А. Айнабаев, Д.Т. Садырбеков, А.М. Пудов,
Д.А. Кайкенов, И.М. Пудов, А.С. Борсынбаев

Получение синтез-газа из сельскохозяйственных отходов плазмохимическим методом

Перспективной технологией утилизации сельскохозяйственных отходов является плазмохимическая технология, основанная на высокотемпературном плазмохимическом воздействии и полном разложении углеводородных продуктов с получением синтез-газа. Для получения синтез-газа в реактор подавали эмульгированную смесь коровьего навоза и воды. На поступающую эмульсию воздействовали пламенем газовой горелки с температурой горения до двух тысяч градусов. Регулярно проводили испытания плазмохимического реактора в разных режимах для поиска лучшего режима производства синтез-газа и его состава. Проводился контроль стабильности напряжения тока на выходе электрогенератора при различных нагрузках. В результате был достигнут устойчивый режим работы газогенератора. Химические характеристики полученного синтез-газа оказались высокими: газ чистый и без пыли, содержание CO_2 — низкое, а водорода и CO — высокое, а именно 31, 62 % и 37,28 % соответственно. Качество газа проверялось при визуальном наблюдении за пламенем горелки и температурой горящего газа с помощью инфракрасного пирометра. Устойчивость пламени и стабильность температуры горения характеризуют качество синтез-газа. Таким образом, экспериментально показано, что плазмохимическая обработка углеводородных и сельскохозяйственных отходов является высокоэффективным методом получения синтез-газа.

Ключевые слова: плазмохимия, синтез-газ, водород, монооксид углерода, сельскохозяйственные отходы, переработка.

References

1 Petrov, S.V., Bondarenko, S.G., Didyk, E.G., & Didyk, A.A (2009). Upravlenie protsessom plazmennoi pererabotki tverdykh orhanicheskikh otkhodov [Managing the process of plasma processing of solid organic waste]. *Visnik NTUU «KPI» Khimichna inzheneriia, ekolohiia ta resursosberezhennia. Naukovii sbirnik. — Herald STU «KPI» Chemical Engineering and Resource Saving Ecology. Scientific collection, 3, 3,* 29–38 [in Russian].

2 *Beychok, M.R.* Process and environmental technology for producing SNG and liquid fuels, U.S. EPA, report EPA-660/2–75–011, May 1975. — P. 12.

3 Zhukov, M.F., & Mikhailov, B.I. et al. (1988). Novye tekhnolohii szhihaniia topliva [New technologies of fuel combustion]. *Energetika strany i regionov. Teoriia i metody upravleniia. — Energy of the country and regions. Theory and methods of management.* Novosibirsk: Nauka, Sibirskoe otdelenie RAN*,* 176–190 [in Russian].

4 Mustafin, E.S., Kassenov, R.Z., Pudov, I.M., Ainabaev, A.A., Dyusekeeva, A.T., & Kezdikbaeva, A.T. (2016). Pererabotka uhlevodorodnykh i selskokhoziaistvennykh otkhodov v sintez-haz metodom plazmokhimii [Processing of hydrocarbon and agricultural wastes into synthesis gas using the plasma-chemical method]. Proceedings from: «EXPO-2017: Technologies of the future»: *Respublikanskaia nauchno-prakticheskaia konferentsiia (21–22 oktiabria 2016 hoda) — the Republican scientific and practical conference.* (pp. 92–95). Karaganda [in Russian].

5 Tukhvatullin, A.M., & Zasypkin, I.M. (2004). Plazmokhimicheskaia tekhnolohiia pererabotki uhlevodorodnoho syria, obezvrezhivaniia i utilizatsii toksichnykh otkhodov [Plasma-chemical technology of hydrocarbon raw materials processing, neutralization and utilization of toxic waste]. *Heneratsiia nizkotemperaturnoi plazmy i plazmennye tekhnolohii. Problemy i perspektivy (Nizkotemperaturnaia plazma. T. 20). — Generation of low-temperature plasma and plasma technologies. Problems and prospects. (Low-temperature plasma. Vol. 20).* Novosibirsk: Nauka, Sibirskoe otdelenie RAN, 307–327 [in Russian].

6 Paton, B.E., Chernets, A.V., Marinsky, G.S., Korzhik, V.N., & Petrov, S.V. (2005). Perspektivy primeneniia plazmennykh tekhnolohii dlia unichtozheniia i pererabotki meditsinskikh i druhikh opasnykh otkhodov. Chast 1 [Prospects for the use of plasma technology for the destruction and processing of medical and other hazardous waste. Part 1]. *Sovremennaia elektrometallurhiia. — Modern electrometallurgy, 3,* 54–63 [in Russian].

7 Parkhomenko, V.D., Soroka, P.I., & Mosse, A.L. et al. (1991). *Plazmohimicheskaia tehnolohiia. Nizkotemperaturnaia plazma [Plasma-chemical technology. Low-temperature plasma]*. (Vol. 4). Novosibirsk: Nauka, Sibirskoe otdelenie RAN [in Russian].

8 Mamchenkov, I.P. (1974). Navoz [Manure]. *Bolshaia sovetskaia entsiklopediia — Big Soviet Enciclopedia*. A.M. Prokhorov (Ed.). (Vols. 1–30; Vol. 17). Moscow: Sovetskaia Entsiklopediia [in Russian].

ХИМИЯНЫ ОҚЫТУ ӘДІСТЕМЕСІ
МЕТОДИКА ОБУЧЕНИЯ ХИМИИ
METHODS OF TEACHING CHEMISTRY

DOI 10.31489/2019Ch2/81-87

UDC 378.1

S.B. Abeuova[1], D.D. Naushabekova[1], D.M. Muslimova[1],
E.B. Abeuova[2], E.K. Tussupbekova[3], A.T. Dyussekeyeva[1]

[1]Ye.A. Buketov Karaganda State University, Kazakhstan;
[2]102 school-gymnasium, Karaganda, Kazakhstan;
[3]Karaganda State Technical University, Kazakhstan
(E-mail: abeuova.salta@gmail.com)

Application of technology of problem-based learning in the discipline «Methodology of carrying out school chemical experiment»

The article presents the results of an experiment on the application of problem-based learning technology in teaching chemistry. Problem learning is aimed at the independent search for new knowledge and ways of action, and also involves a consistent and purposeful promotion of cognitive problems, through the resolution of which students actively learn new knowledge. Technology of problem-based learning was used in the discipline «Methodology of carrying out of school chemical experiment» with the students of the third course. Two demonstration experiences in chemistry were chosen as problem situations in our case. Updating of knowledge was carried out before the experiment. Then there was the creation of a problem situation and the formulation of the problem. The chemical experiment was shown by a teacher. The situations were considered by students. Then conclusions were drawn. The questionnaire of A.A. Rean and V.A. Yakunin was used for diagnostics of educational motivation of students. Knowledge of problem situations was tested with the test method before and after the experiment. To identify opinions of students on the technology of problem-based learning the individual interviews were conducted. As a result of application of technology of problem-based learning cognitive and research interest, search features and abilities were created, opportunities for cooperation of the teacher with students were opened that promoted deeper and strong assimilation of material. Despite the disadvantages of problem learning, including high time costs, the presence of the necessary «starting» level of knowledge of students, today the idea of problem learning has been successfully implemented in the systems of developmental education.

Keywords: problem-based learning, problem situations, new technologies of teaching chemistry, chemical experiment, methods of teaching chemistry.

Introduction

Currently, problem learning is widely used in many disciplines, as one of the techniques of modern learning technologies [1–3]. It involves the creation of teacher-led problem situations and active independent activity of students to resolve them. This type of training is aimed at independent search of students for new concepts and methods of action. The main purpose of the technology of problem learning is the development of thinking and abilities of students, the assimilation of their knowledge and skills obtained in the active search and independent problem solving. As a result, such knowledge is stronger than traditional training. In the learning process, students are put forward cognitive problems, the resolution of which (under guidance of a teacher) leads to the active assimilation of new knowledge. Problem learning provides a special way of thinking, strength of knowledge and their creative application in practice.

It is possible to create problem situations and solve them with the help of various methods, with the involvement of visual and technical means of training, as well as with the appliction of chemical experiment [4, 5]. For example, in the production of demonstration and laboratory experiments, the results of which students cannot explain using their knowledge, because these results usually contain new information, which requires new knowledge to understand. Such experiments are carried out before the study of a new topic or a separate issue, as well as before the generalization of all the material. First, students simply observe the phenomena, and then, when a problem arises, consider their essence deeply and comprehensively. Demonstration and laboratory experiments in the process of problem training can serve as a material for creating problem situations, and used to solve them.

Chemical experiment is a source of knowledge, promotion and testing of hypotheses, a means of securing knowledge and control. Through laboratory and demonstration experiments, the teacher creates certain organizational conditions for the activation of mental activity of students, stimulating the search for missing knowledge to resolve cognitive contradictions.

Experimental

Pedagogical experiment was conducted in the classes on the discipline «Methodology of carrying out of school chemical experiment» among third-year students. The experiment involved 8 students (female), who are trained in the specialty «chemistry-education» and are future teachers. They can apply the acquired knowledge in their future professional activity. During the class, students worked in groups.

Diagnostics of educational motivation of the respondents (before and after experiment) was carried out according to the method of A.A. Rean and V.A. Yakunin [6].

Knowledge of students about problem situations was evaluated by testing. The test consisted of 30 questions on the following topics, namely properties of nonmetal oxides, bases, acids, salts; electrolytic dissociation; monobasic carboxylic acids; double bond; chemical properties of ethylene. Testing was conducted twice, namely before the experiment (pre-test) and after the experiment (post-test).

We conducted an individual interview after the experiment in order to identify the views of students about the problem-based learning.

Two demonstration experiences were selected to create a problem situation. Depending on the level of training of students problem situations are analyzed by students under the guidance of a teacher or independently. Then students find ways to solve the problem and draw conclusions.

Demonstration experiment No. 1

Preparation of carbon dioxide and testing its properties

Purpose: Show the dependence of the properties of carbon dioxide on its composition and structure.

Reagents and equipment: Pieces of marble or limestone, solutions of hydrochloric acid and universal indicator, lime or barite water, highly diluted sodium hydroxide solution; gas discharge tube for carbon dioxide, laboratory tripod, test tubes.

Updating of existing knowledge: Students know the general properties of non-metal oxides. They also understand the properties of bases, acids and salts from the point of view of the theory of electrolytic dissociation. During the introductory conversation, they restore the properties of these substances in memory.

The creation of problem situation and statement of the problem: The composition of carbon dioxide refers to non-metal oxides. Considering the electronic formula of carbon dioxide, the saturation of carbon bonds with oxygen and their strength (covalent nonpolar bonds) are noted. Hence, carbon dioxide is a compound in which there was a complete oxidation of the carbon atom. This gives you the opportunity to claim that the carbon dioxide is able to demonstrate general properties of non-metals oxides. The problem is to test experimentally whether carbon dioxide will interact with water and alkalis.

The nomination of hypothesis: Students assume that carbon dioxide exhibits chemical properties similar to the general properties of non-metal oxides.

The solution to the problem and conclusions: The experiments were demonstrated by a teacher, or they were performed by students.

1. Pieces of marble or limestone are lowered into the carbon dioxide device and a solution of hydrochloric acid (1:4) is added. There is a release of gas bubbles-carbon dioxide.

2. Carbon dioxide is passed into the test tube with water colored with a solution of the universal indicator. There is a change in the color of the indicator.

3. Carbon dioxide is passed firstly in a test tube with lime water, and then in a test tube with a highly diluted solution of sodium hydroxide, which wetted with a universal indicator. In the first test tube there is turbidity of the solution, in the second is discoloration.

Students explain the nature of the observed experiments, make the reaction equations and come to the conclusion that carbon dioxide exhibits the general properties of nonmetal oxides and get it as well as most gaseous oxides.

Demonstration experiment No. 2

The ratio of oleic acid to bromine water and potassium permanganate solution

Purpose: To show the dependence of unsaturated properties of oleic acid on its composition and structure.

Reagents and equipment: Oleic acid, bromine water, potassium permanganate solution, test tubes.

Updating of existing knowledge: Students revise in memory the structure of the double bond, its characteristics and chemical properties of ethylene and its homologues. They also recall the chemical properties of monobasic carboxylic acids.

The creation of problem situation and statement of the problem: According to the molecular formula of oleic acid $C_{18}H_{34}O_2$ students make its structural formula and determine the structure, note the presence in the oleic acid molecule of one double bond and one functional carboxyl group. Students characterize this acid as a substance exhibiting the properties of carboxylic acids and unsaturated compounds. They suggest the properties of oleic acid due to double bond. The problem is posed: to test experimentally the possibility of interaction of oleic acid with bromine water and potassium permanganate solution.

The nomination of hypothesis: Students assume that oleic acid exhibits properties similar to ethylene due to the presence of a double bond in molecule of the oleic acid.

The solution to the problem and conclusions: The experiments were demonstrated by a teacher, or they were performed by students.

1. 2 cm^3 of oleic acid and bromine water is poured into a test tube. The tube is closed with a stopper and is shaken. There is discoloration of bromine water.

2. 2 cm^3 of oleic acid and potassium permanganate solution is poured into a test tube. The tube is closed with a stopper and also is shaken. There is discoloration of potassium permanganate solution.

Students write the reaction equations, explain the essence of the experiments and come to the conclusion that oleic acid along with the properties of carboxylic acids also shows the properties of unsaturated compounds, which indicates its dual nature.

Results and Discussion

Questionnaire consisted of 34 questions [6]. Students evaluated on a 5-point system given the motives of educational activity on the importance for them: 1 point corresponds to the minimum significance of the motive, 5 points — the maximum.

Scale 1. Communicative motives — 7, 10, 14, 32 questions;

Scale 2. Avoiding Motives — 6, 12, 13, 15, 19 questions;

Scale 3. Prestige motives — 8, 9, 29, 30, 34 questions;

Scale 4. Professional motives — 1, 2, 3, 4, 5, 26 questions;

Scale 5. Motives of creative self-realization — 27, 28 questions;

Scale 6. Educational and cognitive motives — 17, 18, 20, 21, 22, 23, 24 questions;

Scale 7. Social motives — 11, 16, 25, 31, 33 questions.

When processing the test results, the average for each scale of the questionnaire was calculated.

Diagnostics of educational motivation of students according the questionnaire of A.A. Rean and V.A. Yakunin showed the increase of communicative, professional, educational and cognitive motives (Table 1).

The results of students on the scales of motives of avoiding and prestige remained unchanged. This shows that before and after the study, the desire of students to keep up with fellow students, to be among the best students and to get approval from parents and others remains at the same level (not changed).

Table 1

Diagnostics of educational motivation of students (before and after the experiment)

No.	Scales of motives	Values of respondents (before and after experiment)															
		1		2		3		4		5		6		7		8	
		Before	After	Before	After	Before	After	Before	After	Before	After	Before	After	Before	After	Before	After
1	Communicative motives	3.5	4.5	3.8	4.5	4	4.3	3.8	4.3	3.3	4	3.8	4.3	3	4	3.8	4.8
2	Avoiding Motives	3	3	3.2	3.2	3	3	3	3	2.8	2.8	3.2	3.2	2.8	2.8	2.8	2.8
3	Prestige motives	4	4	4.6	4.6	4.4	4.4	3.8	3.8	4	4	4.4	4.4	3.2	3.2	3.8	3.8
4	Professional motives	5	5	5	5	5	5	4.3	5	5	5	4.2	4.7	3.5	4.7	4.5	5
5	Motives of creative self-realization	4	4	4	4	4	4	4.5	4.5	4	4	3.5	3.5	3	3	3	3
6	Educational and cognitive motives	4	4.6	4.1	4.7	4.1	4.6	3.9	4.7	3.9	4.6	3.4	4.7	3.3	4.4	3.4	4.6
7	Social motives	4.4	4.4	4.6	4.6	4.2	4.2	4	4	3.8	3.8	3.8	3.8	3.8	2.8	3.2	3.2

Testing for knowledge of problem situations showed that the number of students with good results increased (Table 2, Fig.).

Table 2

Testing results for knowledge of problem situations

Number of correct answers	Number of students	
	Before experiment	After experiment
High index (23–30)	2	4
Average index (15–22)	4	3
Low index (1–14)	2	1

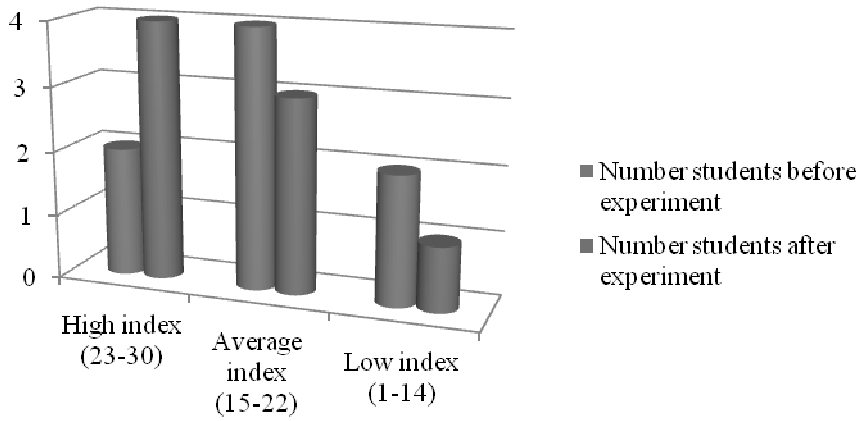

Figure. Analysis of the test for knowledge of problem situations (before and after experiment)

Table 3 presents data from the analysis of interviews on the applicability of problem-based learning at chemistry lessons. The results show the answers that students most often indicated in the interview. The analysis showed that problem-based learning has a great impact on learning skills, life and cognitive skills.

Despite the advantages, problem learning also has disadvantages among which «weak interaction between some students» and «Treating the passive group members equally with the others».

Table 3

Analysis of student interviews about the applicability of PBL

Category	Answers of students	Number of students
Learning skills	PBL encouraged us to do individual investigations	7
	I challenged my phobia of public speaking	4
	We built intragroup and intergroup communication skills and to make presentations	6
Life skills	There was a good communication in our group	5
	Acquired knowledge helped to improve more communication skills	7
	PBL helped students to improve their self-confidence	6
	Group works contributed to the interaction and increased our motivation to learn chemistry	6
	Presentations increased our self-confidence and self-expression	5
	PBL was related to effective use of time	5
Cognitive skills	Problem scenarios were interesting. Therefore, working on it was also interesting	7
	The scenarios had a positive effect on the our curiosity	6
Shortcomings	Weak interactions between some students	2
	Treating the passive group members equally with the others	2

Conclusions

The use of problem-based learning technology in chemistry teaching increases interest of students in the search for new knowledge, provides a special type of thinking, the strength of knowledge acquisition and their creative application in practice. As a result, the students formed the motivation to succeed, develop mental abilities. Diagnostics of educational motivation showed that students increased cognitive and research interest, search features and skills. They became more open to creative cooperation. Testing for knowledge of problem situations showed an increase in the level of knowledge.

However, the technology of problem-based learning, like other technologies, has positive and negative sides. Interviews revealed advantages and disadvantages of the application of problem-based learning. Along with increasing communication skills and research interest, there is a weak control of cognitive activity of students. The technology of problem-based learning requires a lot of time to prepare for the lesson, the necessary starting level of students, and the creative approach of the teacher. Despite the identified shortcomings, nowadays, problem-based learning is the most promising, compared with traditional methods of training, and can be successfully used in teaching chemistry.

References

1 Yoon, H., Woo, A., Treagust, D., & Chandrasegaran, A. Affective Dimensions in Chemistry Education. Berlin: Springer, 2014.

2 Kreke K. Student Perspectives of Small-Group Learning Activities / K. Kreke, M. Towns // The Chemical Educator. — 1998. — Vol. 3, No. 4. — P. 1–23. DOI 10.1007/s00897980232a

3 Senocak E. A Study on Teaching Gases to Prospective Primary Science Teachers Through Problem-Based Learning / E. Senocak, Y. Taskesenligil, M. Sozbilir // Research in Science Education. — 2007. — Vol. 37, No. 3. — P. 279–290. DOI 10.1007/s11165-006-9026-5

4 Robinson J. Project-based learning: improving student engagement and performance in the laboratory / J. Robinson // Analytical and Bioanalytical Chemistry. — 2013. — Vol. 405, No. 1. — P. 7–13. DOI 10.1007/s00216–012–6473-x

5 Larive C. Problem-based learning in the analytical chemistry laboratory course / C. Larive // Analytical and Bioanalytical Chemistry. — 2004. — Vol. 380, No.3. — P. 357–359. DOI 10.1007/s00216–004–2802-z

6 Бадмаева Н.Ц. Влияние мотивационного фактора на развитие умственных способностей: монография / Н.Ц. Бадмаева. — Улан-Удэ: Изд-во ВСГТУ, 2004. — 280 с.

С.Б. Абеуова, Д.Д. Наушабекова, Д.М. Муслимова,
Э.Б. Абеуова, Э.К. Тусупбекова, А.Т. Дюсекеева

Проблемалық оқыту технологиясын «Мектепте химиялық экспериментті жүргізу әдістемесі» пәні сабақтарында қолдану

Мақалада химия сабақтарында проблемалық оқыту технологиясын қолдану бойынша эксперимент нәтижелері келтірілген. Проблемалық оқыту жаңа білім мен іс-қимыл тәсілдерін өз бетімен іздестіруге бағытталған оқыту болып табылады, сондай-ақ мұғалімнің жетекшілігімен жаңа білімдерді белсенді түрде игеріп жатқан студенттерге когнитивті проблемаларды дәйекті және мақсатты түрде алға қоюларын көздейді. Проблемалық оқыту технологиясы үшінші курс студенттеріне «Мектепте химиялық эксперименті жүргізу әдістемесі» пәнін жүргізу барысында қолданылды. Химиядан проблемалық жағдай ретінде екі көрнекілік тәжірибе таңдалды. Тәжірибе алдында білім өзектендірілді. Содан кейін проблемалық жағдайды жасау және мәселені тұжырымдау қажет. Мұғалім химиялық тәжірибені көрсетеді. Студенттер жағдайды саралап, қорытынды жасайды. Студенттердің оқуға деген ынтасын тексеру мақсатында А.А. Реан және В.А. Якунин сауалнамасы қолданылды, проблемалық жағдайларды анықтай білуі тест әдісі арқылы тәжірибе алдында және тәжірибеден кейін алынып, бағаланды. Студенттердің проблемалық оқыту технологиясы бойынша пікірлерін анықтау үшін жеке сұхбат жүргізілді. Проблемалық оқыту технологияларын қолдану нәтижесінде студенттердің когнитивтік және зерттеу қызығушылықтары пайда болды, іздеу ерекшеліктері мен дағдылары артты, сонымен қатар материалды тереңірек, әрі берік ұғынуына ықпал ететін, мұғалім мен студенттердің арасындағы ынтымақтастық қарым-қатынастың пайда болуына жол ашты. Проблемалық оқытудағы студенттердің қажетті «бастапқы» білімінің болуы, көп уақытты қажет ету сияқты кемшіліктерге қарамастан, қазіргі таңда проблемалық оқыту идеялары жаңартылған білім беру жүйесінде ойдағыдай іске асырылуда.

Кілт сөздер: проблемалық оқыту, проблемалық жағдайлар, білім берудің жаңа технологиялары, химиялық эксперимент, химияны оқыту әдістемесі.

С.Б. Абеуова, Д.Д. Наушабекова, Д.М. Муслимова,
Э.Б. Абеуова, Э.К. Тусупбекова, А.Т. Дюсекеева

Применение технологии проблемного обучения на занятиях по дисциплине «Методика проведения школьного химического эксперимента»

В статье приводятся результаты эксперимента по применению технологии проблемного обучения на занятиях по химии. Проблемное обучение направлено на самостоятельный поиск новых знаний и способов действия, а также предполагает последовательное и целенаправленное выдвижение познавательных проблем, посредством разрешения которых студенты активно усваивают новые знания. Технология проблемного обучения применялась на занятиях по дисциплине «Методика проведения школьного химического эксперимента» с учащимися третьего курса. В качестве проблемных ситуаций в нашем случае были выбраны два демонстрационных опыта по химии. Перед проведением эксперимента проводилась актуализация знаний. Затем идет создание проблемной ситуации и формулировка проблемы. Далее преподаватель показывает химический эксперимент. Учащиеся обдумывают ситуации, делают выводы. Для диагностики учебной мотивации студентов использовался опросник А.А. Реана и В.А. Якунина, знание проблемных ситуаций оценивалось методом тестирования до и после эксперимента. Для выявления мнения студентов о технологии проблемного обучения проводилось индивидуальное интервью. В результате применения технологии проблемного обучения у учащихся сформировался познавательный и научно-исследовательский интерес, поисковые особенности и умения, открылись возможности для сотрудничества преподавателя с учащимися, что способствует более глубокому и прочному усвоению материала. Несмотря на минусы проблемного обучения, среди которых большие временные затраты, наличие необходимого «стартового» уровня знаний обучающихся, идеи проблемного обучения на сегодняшний день успешно реализуются в системах развивающего обучения.

Ключевые слова: проблемное обучение, проблемные ситуации, новые технологии обучения, химический эксперимент, методика преподавания химии.

References

1 Yoon, H., Woo, A., Treagust, D., & Chandrasegaran, A. (2014). *Affective Dimensions in Chemistry Education*. Berlin: Springer.

2 Kreke, K., & Towns, M. (1998). Student Perspectives of Small-Group Learning Activities. *The Chemical Educator*, *3*(4), 1–23. DOI 10.1007/s00897980232a.

3 Senocak, E., Taskesenligil, Y., & Sozbilir, M. (2007). A Study on Teaching Gases to Prospective Primary Science Teachers Through Problem-Based Learning. *Research in Science Education*, *37*(3), 279–290. DOI 10.1007/s11165–006–9026–5.

4 Robinson, J. (2013). Project-based learning: improving student engagement and performance in the laboratory. *Analytical and Bioanalytical Chemistr*y, *405*(1), 7–13. DOI 10.1007/s00216–012–6473-x.

5 Larive, C. (2004). Problem-based learning in the analytical chemistry laboratory course. *Analytical and Bioanalytical Chemistry*, *380*(3), 357–359. DOI 10.1007/s00216–004–2802-z.

6 Badmayeva, N.Ts. (2004). Vliianie motivatsionnoho factora na razvitie umstvennykh sposobnostei [Influence of motivational factor on the development of mental abilities]. Ulan-Ude: VSGTU [in Russian].

ҒЫЛЫМИ ЗЕРТТЕУДІ ШОЛУ
ОБЗОР НАУЧНЫХ ИССЛЕДОВАНИЙ
REVIEW OF RESEARCH

DOI 10.31489/2019Ch2/88-104

UDC 544.23+544.6+547.7+662.7+662.8+665.63

Z.M. Muldakhmetov

LLP «Institute of Organic Synthesis and Coal Chemistry of Kazakhstan Republic», Karaganda, Kazakhstan
(E-mail: iosu.rk@mail.ru)

Institute of Organic Synthesis and Coal Chemistry: the present state and development prospects

The article is an overview of the research carried out in the LLP «Institute of Organic Synthesis and Coal Chemistry of RK» in recent years. The application of methods of ultrasonic and microwave chemistry to the processes of oxidation and oxidative modification of coal, activation of the processes of immobilization of humic acids and their derivatives on the surface of burnt rocks, as well as the effect of carbon nanotubes on the processes of obtaining humic-mineral compositions were studied. The properties of new activated forms of humic sorbents were studied and tested as sorbents for wastewater treatment. Composite catalysts based on compounds of VIII (Fe, Ni, Co, Mo) group metals were obtained and their activity was studied in the process of hydrogenation of anthracene and phenanthrene. The optimal parameters of cavitation treatment of fuel oil fractions in the presence of synthesized composite catalysts based on water-soluble metal salts deposited on zeolites and carbon sorbents were determined. Based on aniline-formaldehyde polymer and its mixed compositions with melamine-formaldehyde polymer and polyaniline, new metal-polymer composites with electrocatalytic properties were obtained. Their structure and morphological features were studied by IR spectroscopy, X-ray phase analysis, atomic emission spectroscopy and electron microscopy. Electrocatalytic activity was investigated in the processes of electrohydrogenation of organic compounds. New derivatives of 4-amino-1,2,4-triazole, thiosemicarbazides N-morpholinyl acetic and N-anabasinyl acetic acids were synthesized, their structure, biological activity, reaction mechanisms were studied and optimal conditions for their synthesis were proposed.

Keywords: humic acid, burnt rock, multi-walled carbon nanotubes, humic-mineral composites, composite catalysts, anthracene, phenanthrene, fuel oil, hydrogenation, polymer-metal composites, aniline and melamine-formaldehyde polymers, polyaniline, electrocatalytic properties, 4-amino-1,2,4-triazole derivatives, fulleropyrrolidines, bioactivity.

In 2018, the Institute of Organic Synthesis and Coal Chemistry celebrated its 35th anniversary, the creation of which was associated with the need to expand and deepen basic and applied research in Central Kazakhstan, since the billions reserves of low-energy coals from Shubarkul, Maikubensky and other deposits that are here, also the industrial enterprises of the Karagandaugol and Carbid factories, the coke-chemical production of the Karaganda Metallurgical Plant represented a unique basis for the development of industrial organic synthesis and chemistry of coal. The Institute has carried out a large amount of research, the results of which are published in numerous monographs and rating journals. This article presents the most important results of the last time.

In the field of modification of low-energy coals, the processes of oxidation, oxidative amination, nitration and sulfonation of selected black and brown coals of Kazakhstan were carried out under conditions of ultrasonic and microwave activation. Oxidized coals of the Shubarkol deposit and brown coals of the Kuznetsky and Oi-Karagaysky (Almaty region) deposits were used.

Physical methods using ultrasonic processing (USP) and microwave radiation (MWR), which were first used to intensify the reactions of obtaining a number of coal-chemical products and carrying out chemical modification of coal, are among the poorly studied and promising methods for the intensification of technological processes for the production of humic substances and their compositions. Elucidation of the types of reactions under the influence of ultrasound and microwaves, as well as the prospects for their use, is an important task.

Studies have shown that ultrasound contributes to the accumulation of new acid groups in the coal composition and to an increase in the yield of humic acids from the products of sonolysis. Oxidation processes in coals under the action of ultrasound occur at moderate temperatures for a short time (5–30 minutes) and depend on the nature of the coals. According to the susceptibility of the energy of ultrasound, the coals are arranged in the following row: Oi-Karagai ≥ Shubarkol > Kuznetsky. The effect of various oxidative additives (hydrogen peroxide, nitric acid and sulfuric acid) with modifying ability on the oxidation of coal has been studied. The possibility of introducing nitrogen, sulfur in the form of amino-, amido-, nitro- and sulfogroups, which increase the sorption characteristics of the oxidation products obtained, was proved by the methods of functional analysis and data of the elemental composition [1].

According to the study of sorption and other characteristics of sorbents and comparison with conventional methods for their preparation, the high efficiency of using physical methods of exposure to obtain new humic compositions was noted, including by introducing them into a nonorganic matrix based on burnt rocks that are waste coal mining.

Studies on the activating effect of ultrasound and microwaves on the immobilization of humic acids and their derivatives on the surface of the burnt rock showed that immobilization in USP and MVR conditions showed the promise of using porous aluminosilicate rocks as available and effective sorption-filtration materials. However, to solve the problem of chemical resistance and mechanical strength of humic mineral sorbents, the use of «Taunit» multi-walled carbon nanotubes (MWCNTs) (produced by LLC Nanotechtsentr, Tambov, Russia) allowed.

According to the electron microscopic analysis, the MWCNTs are filamentous formations of polycrystalline graphite, which are predominantly cylindrical. The outer diameter is 20–70 nm, the inner diameter is 5–10 nm. The length is several orders of magnitude greater than the diameter and is 3–10 microns. Modification of the side and end sections of the MWCNTs is often a necessary manipulation when creating materials with improved surface and bulk properties.

Oxidation is the most common method of chemical modification of carbon nanotubes. A mixture of concentrated nitric and sulfuric acids, potassium permanganate, a mixture of ammonia and hydrogen peroxide solutions was used as oxidizing agents. The yield of products using a mixture of concentrated acids was 50–60 %. The highest yield of products (92–95 %) was obtained when potassium permanganate was used as an oxidizing agent. For the first time, the processes of immobilization of humic acid and multi-walled carbon nanotubes on the surface of burned rocks (BR) have been carried out by ultrasonic and microwave activation.

Ultrasonic dispersion and microwave irradiation of components were also used to create humino-mineral compositions modified with carbon nanotubes [2]. For the immobilization processes being developed, an ultrasonic disperser of the IL-100-6/2 brand with an operating frequency of 22 kHz was used. Modification of humic acid with MWCNTs was performed by ultrasonic homogenization of humic acid with MWCNTs. During the study, the influence of various factors (the ratio of initial reagents, the duration of the USP) was investigated. The largest amount of acid groups (4.26 mmol-eq/g) is contained in the sample, which was irradiated with ultrasound for 10 minutes. The product yield was 60–68 %. It was established that the most homogeneous structure, according to microscopic analysis, was achieved with the ratio BR:HA:MWCNT = 50:20:1 and 50:10:1. The yield of products was 94–97 %. The number of acidic groups in the samples is in the range of 2.07–2.38 mmol-eq/g, the largest number of them is contained in humic-mineral composites with activated forms of carbon nanotubes obtained by USP for 10 minutes [3].

The effect of microwave radiation on the immobilization process was carried out in aqueous suspensions at a ratio of the initial components of the BR:HA:MWCNT = 50:20:1 and 50:10:1. The influence of the ratio of the initial components, the duration of MWR-effects and the nature of the modifier on the processes of obtaining humic-mineral nanocomposites has been studied. The number of acidic groups in the samples is in the range of 1.97–2.19 mmol-eq/g [4].

The laboratory tests of humic-mineral nanocomposites during the purification of industrial wastewater from the processing plant Priozersk indicate that humic-mineral sorbents (including those obtained under UZO and MVI conditions) containing nanotubes are highly competitive on the sorption activity with

nanohumic composites. In particular, BR + GA + MWCNT composites purify sewage from the main components: aluminum (by 99.93 %), iron (by 98.02 %), manganese (by 60.58 %), lead (by 97.35 %), strontium (by 67.37 %) and zinc (by 97.98 %). The efficiency of using humic-mineral sorbents containing multi-walled carbon nanotubes as sorbents for wastewater treatment at enterprises has been proven [5, 6].

Thus, for the first time, the high efficiency of ultrasonic treatment on the process of obtaining humic-mineral compositions has been established, and the use of microwave radiation reduces the time of the synthesis process. The composition and structure of humic-mineral samples activated by MWCNTs under conditions of ultrasonic and microwave radiation has been proved by modern physicochemical methods. It has been shown that humic-mineral composites modified by multi-walled carbon nanotubes can be used as sorbents for wastewater purification.

As a result of the research work, a pilot setup was manufactured for testing the developed technologies of humic-mineral sorbents under experimental conditions and the optimization of the technological mode of their production. A draft technical specification for the design of the plant has been drawn up. The calculation of the equipment was done. Two chemical reactors have been manufactured for carrying out processes for the preparation of sorbents [7].

Products of modification of coal and coal waste with various chemical compounds and their applications as sorbents for wastewater treatment, restoration of fertility of depleted and man-made soils, and improving the soil structure are new and have no domestic and foreign analogues. The novelty is confirmed by the patent of the Republic of Kazakhstan [8].

In the field of hydrogenation of heavy hydrocarbon raw materials, studies were carried out to obtain composite catalysts based on compounds of VIII Group metals (Fe, Ni, Co, Mo), and their activity was studied in the process of hydrogenation of polyaromatic compounds. The optimal parameters of cavitation treatment of heavy hydrocarbon feedstock (fuel oil) in the presence of these composite catalysts based on water-soluble salts of iron, nickel, cobalt, and molybdenum deposited on zeolites and coal sorbent were determined.

It has been established that the highly dispersed distribution of the compounds of these metals by the impregnation of active carbon with solutions of their salts and their complex compounds leads to the conversion of metal compounds deposited on the surface of the coal into an oxide form. So it was shown that the impregnation of iron, nickel and cobalt sulfates on a carbon sorbent results in highly dispersed metal-sulfate catalysts on a carbon carrier ($FeSO_4 \cdot 7H_2O/C$, $NiSO_4 \cdot 7H_2O/C$, binary $FeSO_4 \cdot 7H_2O$ — $CoSO_4 \cdot 7H_2O/C$) with a content of active ingredient of 5 % (for metal). High-dispersion catalysts based on iron, nickel and cobalt oxides on a carbon substrate Fe_2O_3/C, NiO/C, binary catalyst Fe_2O_3–CoO/C were synthesized by a thermal modification of the corresponding metal sulfates [9].

The catalytic properties of the synthesized catalysts in the hydrogenation reactions of model polycyclic hydrocarbons — anthracene and phenanthrene — have been studied [10].

In a comparative analysis of the catalytic activity of the obtained composite catalysts with a known iron-chromium catalyst (STK-1), it was found that under the same conditions, Fe_2O_3 and Fe_2O_3/C catalysts give the composition of the reaction products with different ratio of components. It should be noted that, in terms of the active component of the catalysts, iron, the content of the latter in Fe_2O_3/C is 14 times lower than in Fe_2O_3. It was revealed that the replacement of nickel-sulfate by nickel-oxide catalyst leads to a more noticeable increase in the products of hydrogenolysis than on iron-containing analogues, while the content of hydrogenated components in the process of hydrogenation decreases. The composition of gaseous products of anthracene hydrogenation on the catalyst, including methane, ethane and propane, was established by gas-liquid chromatography (GLC). The product of isomerization of anthracene (phenanthrene) on nickel catalysts is formed in larger quantities than on iron ones.

It was established that as a result of the anthracene hydrogenation reaction, two groups of compounds are formed: hydrogenated and hydrogenolysis products. In this case, the transition of the linear form of anthracene to angular phenanthrene and its transformation products is observed [11].

The reaction proceeds according to the scheme:

I anthracene — II dihydroanthracene — III tetrahydroanthracene — IV octahydroanthracene

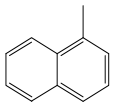

V
1-methyl-naphthalene

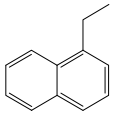

VI
1-ethyl-naphthalene

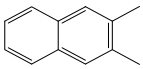

VII
2,3-dimethyl-naphthalene

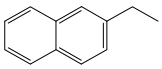

VIII
2-ethyl-naphthalene

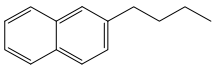

IX
2-buthyl-naphthalene

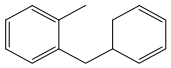

X
1-methyl-2-phenylmethyl-benzene

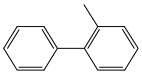

XI
2- methyl-1,1'-diphenyl

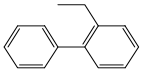

XII
2-ethyl-1,1'-diphenyl

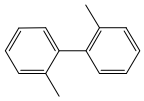

XIII
2,2'-dimethyl-1,1'-diphenyl

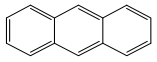

XIV
anthracene

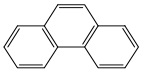

XV
phenanthrene

As a result, two groups of compounds were obtained: hydrogenated II–IV, which include 9,10-dihydroanthracene, 1,2,3,4-tetrahydroanthracene and 1,2,3,4,5,6,7,8-octahydroanthracene, and V–XV hydrogenolysis products: 1-methyl-naphthalene, 1-ethyl naphthalene, 2,3-dimethylnaphthalene, 2-ethylnaphthalene, 2-butylnaphthalene, 1-methyl-2-phenylmethylbenzene, 2-methyl-1,1'-diphenyl, 2,2'-dimethyl-1,1'-diphenyl and 2-ethyl-1,1'-diphenyl. Compounds V, VI, XI–XIII do not belong to the products of destruction of anthracene or its hydro-derivatives. The presence in the reaction mixture of 1-methyl-naphthalene V, 1-ethylnaphthalene VI, 2-methyl-1,1'-diphenyl XI, 2-ethyl-1,1'-diphenyl XII and 2,2'-dimethyl-1,1'-diphenyl XIII can be explained by the result of the destruction of phenanthrene or its hydrogenated derivatives — di- and tetrahydrophenanthrene. In this case, there is a transition of the linear form of anthracene to angular phenanthrene and the products of its transformation:

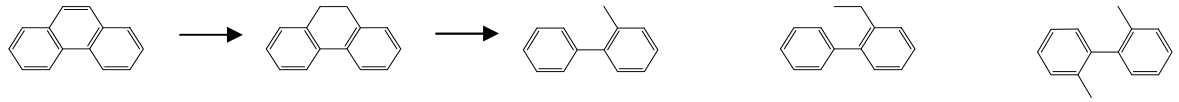

phenanthrene → 9,10-dihydro-phenanthrene → 2-methyl-1,1'-diphenyl → 2-ethyl-1,1'-diphenyl → 2,2'-dimethyl-1,1'-diphenyl

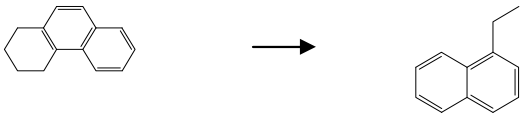

1,2,3,4-tetrahydrophenanthrene → 1-ethyl-naphthalene

The use of zeolite as a carrier was associated with their geometry, porous structure, frame chemistry, and the nature of extra-frame structures. The presence of a large group of microporous crystalline aluminosilicates, the three-dimensional framework of which is permeated with cavities and channels of nanometric dimensions, creates a unique opportunity to modify catalysts. Impregnation of zeolites with aqueous solutions of metal salts, the cations of which are required to be introduced into the zeolite, is the most common method of modifying zeolites.

In order to study the activity of the synthesized iron-containing composite catalysts supported on zeolite, hydrogenation of polyaromatic compounds was carried out.

During the research the following results were obtained:

– by an impregnation of iron, nickel and cobalt sulfate on zeolite, the highly dispersed metal-sulfate catalysts based on synthetic zeolites CaA and ZSM were prepared: $FeSO_4 \cdot 7H_2O$/CaA ($FeSO_4 \cdot 7H_2O$/ZSM), $NiSO_4 \cdot 7H_2O$/CaA ($NiSO_4 \cdot 7H_2O$/ZSM), binary $FeSO_4 \cdot 7H_2O$ – $CoSO_4 \cdot 7H_2O$/CaA ($FeSO_4 \cdot 7H_2O$ – $CoSO_4 \cdot 7H_2O$/ZSM) with the content of the active component 5 % (by metal). By a thermal modification of iron, cobalt and nickel sulfates supported on a carrier (zeolite), the composite catalysts based on iron, nickel and cobalt oxides on a CaA and ZSM zeolite substrate were synthesized: Fe_2O_3/CaA (Fe_2O_3/ZSM), NiO/CaA (NiO/ZSM), binary catalyst Fe_2O_3 – CoO/CaA (Fe_2O_3 – CoO/ZSM) [12].

– the catalytic activity of synthesized catalysts was investigated in the reactions of hydrogenation of anthracene. The chromatographic mass-spectroscopy (CMS) and GLC analysis established the component composition of the hydrogenation products. A method for analyzing the products of anthracene hydrogena-

tion was developed for GLC. The method used a database of component composition, created on the basis of the results of the analysis of standard samples and CMS analysis of reaction products [13].

– it was established that under the same conditions, the synthesis of catalysts Fe_2O_3/CaA and CoO/CaA give the composition of the reaction products of different component ratios. So, with a slight difference in the degree of conversion of anthracene — 95.02 % for Fe_2O_3/CaA and 97.38 % for CoO/CaA, the difference in the content of the products of hydrogenolysis and hydrogenation is more noticeable. In the process of hydrogenation in the presence of Fe-Co/CaA catalyst, hydrogenation products amounted to > 80 %, cleavage products < 10 % [11].

– it was found that the replacement of a cobalt sulfate by a cobalt oxide catalyst leads to a more noticeable increase in the products of hydrogenolysis, in comparison with nickel and iron based analogues (14.12–23.62 % for Ni and 9.01–12.96 % for Fe). At the same time, the content of hydrogenated components decreases (77.67–63.81 % for Ni and 84.95–77.49 % for Fe) [14].

Thus, the synthesized binary catalysts based on compounds of VIII group metals deposited on a coal sorbent and zeolite demonstrate high activity in the process of hydrogenation of model compounds.

In the process of fuel oil hydrogenation, it was established that the conversion and the quantitative composition of the products formed are different and depend on the activity and selectivity of the catalysts, which, in turn, are associated with the surface, dimensionality and porous structure. The use of iron-containing composite catalysts makes it possible not only to increase the conversion of hydrocarbon derivatives, but also to improve the quality of the products obtained, in particular, alkanes of iso-construction with a lower molecular weight (2-methylpentane, 2-methylpentene, etc.) [15].

It was noted a rather significant increase in the content of paraffinic hydrocarbons and a decrease in aromatic, polyaromatic, oxygen-containing hydrocarbons. In the cavitation treatment of the fuel oil fraction in the presence of the composite catalysts Fe_2O_3/C, Fe_2O_3/ZSM and Fe_2O_3/CaA, the content of paraffins with a longer C_{15}-C_{19} chain increases. This is due to the fact that during cavitation treatment in the presence of Fe_2O_3/ZSM, Fe_2O_3/CaA, Fe_2O_3/C catalysts, two coupled processes occur in the mixture — destruction and condensation, however, the destruction of paraffins prevails over condensation processes [16].

Optimal conditions and a number of factors influencing the cavitation treatment of the fuel oil fraction in the presence of the Fe_2O_3/C catalyst are determined. In accordance with the regression equation obtained, the optimal conditions for cavitation treatment are as follows: τ = 90–120 s, the amount of added catalyst is 0.7–1 g and the amount of added water is 1.5–2 ml [17].

Thus, by quantifying the individual composition of the fuel oil fraction, the positive effect of the catalytic-cavitation treatment in the presence of the studied catalysts was established. According to the hydrocarbon conversion, the catalytic systems are arranged in the following order: Fe_2O_3/C > Fe_2O_3/CaA > Fe_2O_3/ZSM.

In the field of electrocatalysis of organic compounds, by a combined chemical and electrochemical method, new polymer-metal catalytic systems were created with the study of their activity in the electrohydrogenation of organic compounds [18–26].

The synthesis of metal-polymer composites based on conductive polyaniline (PAni) polymer with immobilized metal salts (Ni, Co, Cu, Pd, Zn, Ag, Fe), metal oxides (CuO, FeO) without and with further chemical and electrochemical reduction of their cations were carried out [18–23]. The possibility of electrochemical reduction of cations of a number of metals in the composition of the PAni polymer matrix was established when powder composites were deposited on the surface of the Cu cathode (without fixing them), and PAni + M^0 composites possessing electrocatalytic activity were created.

Preparation of polymer-metal composites according to the developed direction was continued with the participation of aniline-formaldehyde polymer (AFP) and its mixed compositions with melamine-formaldehyde polymer (MFP) and PAni with the following monomeric structures:

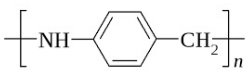

AFP

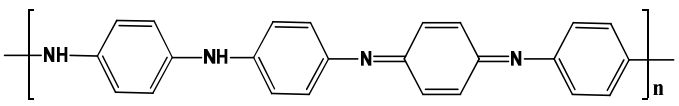

PAni

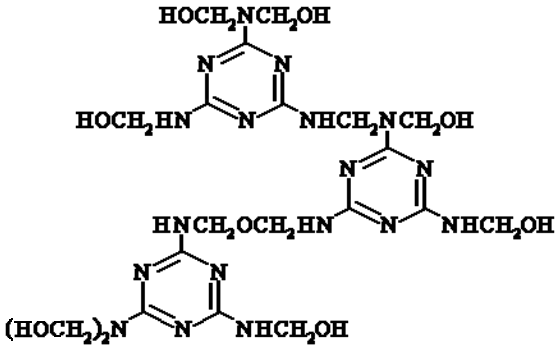

MFP

It should be noted that, unlike polyaniline, AF- and MF-polymers do not have conductive properties and even, on the contrary, are good insulators. The introduction of salt or metal nanoparticles allows to create new materials with semiconductor properties on the basis of individual polymers or their mixed compositions.

Metal-polymer composites with the participation of AF-polymer were obtained by introducing a metal salt ($CuCl_2$, $NiCl_2$, $FeCl_3$, $FeSO_4$) *in situ* polycondensation of aniline and formaldehyde with further thermal treatment (TT), as well as the «impregnation» method by sorbing metal salts with polymer from their aqueous solutions. X-ray diffraction (XRD) analyzes revealed the influence of the synthesis conditions and the nature of the introduced metal (in the form of its salt) on the phase constitution of the synthesized AFP composites. Metal oxides (Cu_2O, CuO, NiO, Fe_3O_4) are formed in composites synthesized *in situ*; $2CuCl_2 \cdot 5Cu(OH)_2 \cdot H_2O$ complex salt, hydroxides and oxyhydroxide ($Ni(OH)_2$, FeOOOH) are present in the composites prepared according to the second variant of the synthesis.

The electrocatalytic activity of the synthesized composites was studied in the electrohydrogenation of *o*-nitroaniline (*o*-NA) in a diaphragm cell when they are deposited on the surface of the Cu cathode (current 1.5 A, 30 ºC, catholyte — 2 % NaOH solution with the addition of ethanol, anolyte — 20 % NaOH solution). The electrochemical reduction of *o*-NA under the same conditions is carried out at a rate (W) of 3.3 mL H_2/min, and a degree of transformation of *o*-NA to *o*-phenylene-diamine (α) is equal to 84 %.

Experiments have shown that Ni- and Fe-containing AFP composites (AFP + $NiCl_2$, AFP + Ni^0, AFP + $FeCl_3$ and AFP + $FeSO_4$) exhibit a weak electrocatalytic activity in *o*-NA electrohydrogenation, which is caused by the inability of the cations of these metals to electrochemical reduction under given conditions. According to the XRD analysis, copper cations are reduced from copper oxides and its complex salt formed during the synthesis and TT, giving copper particles in the zero-valence state in the polymer matrix, which catalyze the electrohydrogenation of *o*-NA [24]. At the same time, AFP + $CuCl_2$ composites obtained by the «impregnation» method showed a higher electrocatalytic activity: *o*-NA hydrogenation rate increases to 5.6–6.1 mL/min, its conversion — to 91–94 % with the formation of one product — *o*-phenylene-diamine having a wide range of practical applications. Preliminary ultrasonic treatment (UST) of these composites contributes to a more complete extraction of copper cations from its aqueous solutions and to a greater amount of their electrochemical reduction.

For the synthesized new polymer-metal composites based on an AF-polymer and salts of metals $CuCl_2$, $NiCl_2$, $FeCl_3$, $FeSO_4$, their electrical conductivity was determined to be about 10^{-6}–10^{-4} $Ohm^{-1} \cdot m^{-1}$, which allows us to classify them as organic semiconductors with promising applications in microelectronics, for the manufacture of various kinds of sensors, etc.

Mixed aniline-melamine-formaldehyde polymers (AMFP) were obtained mainly according to the developed method of synthesis, which consists in carrying out the polycondensation of aniline and melamine with formaldehyde separately for each monomer (with a 1:1 ratio), followed by their combination.

Metal-polymer AMFP-composites were prepared by two methods: *1* — *in situ* by immobilizing metal chlorides (Cu^{2+}, Ni^{2+}, Co^{2+}), their oxides and metal nanoparticles (synthesized by chemical reduction of their cations from aqueous solutions of salts with sodium borohydride and hydrazine hydrate and sonicated) into the polymer matrix, and *2* — the «impregnation» method. By the XRD analyzes of AMFP composites before and after their application in electrohydrogenation of *o*-NA, the electrochemical reduction of copper cations from AMFP powder composites doped with $CuCl_2$, CuO and Cu_2O and the highest electrocatalytic activity of composites synthesized *in situ* were established (Table 1) [25]. As follows from the data presented, the

rate of *o*-NA hydrogenation and its conversion increase with an increase in the copper content in 1 g of AMFP + $CuCl_2$ composites.

Table 1

Electrocatalytic hydrogenation of *o*-NA on the copper-containing AMFP composites

Composites	The copper content in 1 g of composite	*W*, mL H_2/min (α = 0.25)	η, % (α = 0.25)	α, %
Cu cathode	–	3.3	27.7	84.0
AMFP (1:1) + $CuCl_2$ (1:0.5)	0.150	2.4	20.7	80.5
AMFP (1:1) + $CuCl_2$ (1:1)	0.253	4.8	46.7	84.8
AMFP (1:1) + $CuCl_2$ (1:1.5)	0.324	6.1	62.7	98.0
AMFP (1:1) + $CuCl_2$ (1:2)	0.559	8.5	80.3	100
AMFP (1:1) + $CuCl_2$ (1:1) + $NaBH_4$	0.252	4.1	37.2	100
AMFP (1:1) + CuO (1:1)	0.369	4.7	41.7	89.1
AMFP (1:1) + Cu_2O (1:1)	0.209	3.2	30.6	73.7

Mixed AFP + PAni and PAni + AFP polymers were prepared according to the synthesis procedures of AF-polymer and PAni, respectively. Metal-polymer composites PAni + AFP (2:1) with introduced metals (Cu^{2+}, Fe^{3+}, Zn^{2+}) chlorides and their oxides sonicated were produced according to several synthesis options. Their structure, phase composition and morphological features were studied by IR spectroscopy, X-ray powder diffraction, and electron microscopy. The structural-phase changes in the composites under the action of the reaction medium of the oxidative polymerization of aniline and current cathodic polarization are analyzed. It was found that the metal cations in copper (II) and zinc (II) chlorides, as well as in FeO (wustite) (Fig. 1), CuO and ZnO oxides introduced into the polymer matrix undergo electrochemical reduction (on the stage of hydrogen saturation) to form copper, zinc and iron particles in the zero-valent state, which catalyze the electrohydrogenation of *o*-NA.

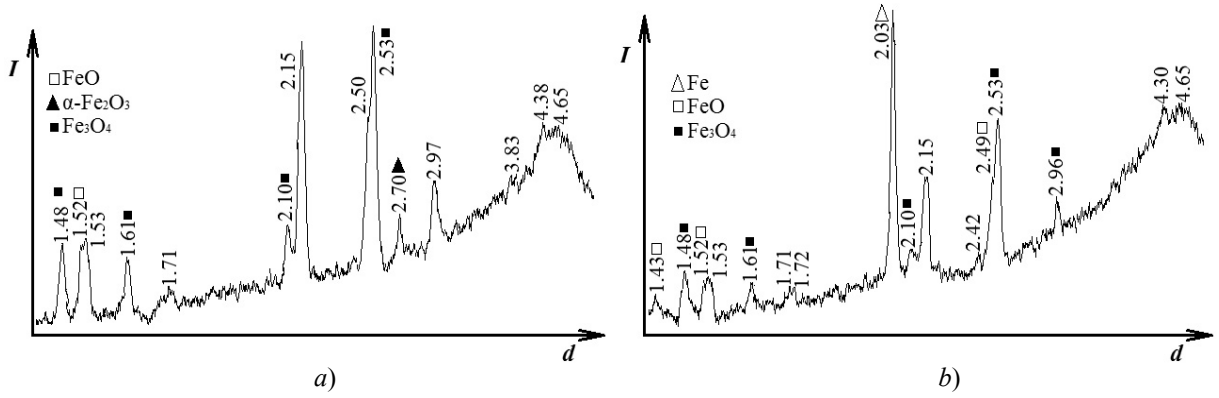

a) *b*)

Figure 1. X-ray patterns of the PAni(2) + AFP(1) + FeO(1:0.6) composite before (*a*) and after (*b*) electrohydrogenation of *o*-NA

Comparison of the electrocatalytic activity of the synthesized composites based on the mixed polymer PAni(2) + AFP(1), doped with metal salt, gives the following series of their activity: $CuCl_2 > ZnCl_2 > FeCl_3$ (not active). The electrocatalytic activity of the PAni(2) + AFP(1) + MeO composites decreases in the following sequence of oxides introduced: CuO > FeO > ZnO.

Table 2 shows the results of experiments on the electrohydrogenation of *o*-NA using Zn-containing composites PAni + AFP, performed under the above described conditions with a current of 2.0 A [26].

Table 2

Electrocatalytic hydrogenation of *o*-NA on the PAni(2) + AFP(1) + $ZnCl_2$ (ZnO) composites

Composites	The zinc content in 1 g of composite	*W*, mL H_2/min (α= 0.25)	η, % (α= 0.25)	α, %
Cu cathode	–	3.5	25.0	71.0
PAni(2) + AFP(1) + $ZnCl_2$ composites				
PAni + AFP + $ZnCl_2$ (1:2)	0.138	3.7	26.7	78.1
PAni + AFP + $ZnCl_2$ (1:2) + NaOH	0.243	4.9	34.4	85.0
PAni + AFP + $ZnCl_2$ (1:2) + NH_4OH	0.270	5.4	39.4	97.7
PAni + AFP + $ZnCl_2$ (1:1) + evaporation	0.085	6.6	47.7	87.6
PAni + AFP + $ZnCl_2$(1:1) + evaporation + TT	0.089	7.0	50.8	92.1
PAni(2) + AFP(1) + ZnO (Zn) composites				
PAni + AFP + ZnO (1:1) + NaOH	0.285	5.1	33.8	99.9
PAni + AFP + ZnO (1:1) + NH_4OH	0.275	4.0	26.7	92.0
PAni + AFP + Zn (1:1) + NaOH	0.384	7.1	52.3	86.4
PAni + AFP + Zn (1:1) + NH_4OH	0.370	7.1	51.6	81.2

It follows from the above data that all synthesized Zn-containing composites based on the mixed PAni(2) + AFP(1) polymer possess electrocatalytic activity in electrohydrogenation of *o*-NA; in their presence electrocatalytic hydrogenation of *o*-NA is carried out at higher rates and more complete *o*-NA conversion than electrochemical reduction at the Cu cathode.

Thus, on the basis of the AF-polymer and its mixed compositions with MFP and PAni, metal salts and oxides, new metal-polymer composites have been created, relating mainly to organic semiconductors and exhibiting electrocatalytic properties depended on the nature of the introduced metal, its content, conditions of synthesis and the influence of ultrasonic treatment. The resulting metal-polymer composites are multifunctional materials and can be used not only as catalysts or electrocatalysts in the synthesis of chemical compounds, but also in other areas of technics, including nanotechnology.

In the field of synthesis of biologically active substances, in continuation of previous studies [27–30] on the basis of heterocyclic compounds, new approaches were proposed to the reactions of interaction of acetoacetic acid anilide with 5-aminotetrazole and substituted aromatic aldehydes, which led to the development of methods for obtaining new series of 7-aryl-5-methyl-N-phenyl-4,7-dihydrotetrazolo-[1,5-α]-pyrimidine-6-carboxamides [31]. Studies are being carried out on the chemical transformation of the structure of fullerene C60 with modified derivatives of alkaloids with obtaining interesting in terms of studying the biological properties of fulleropyrrolidines [32, 33].

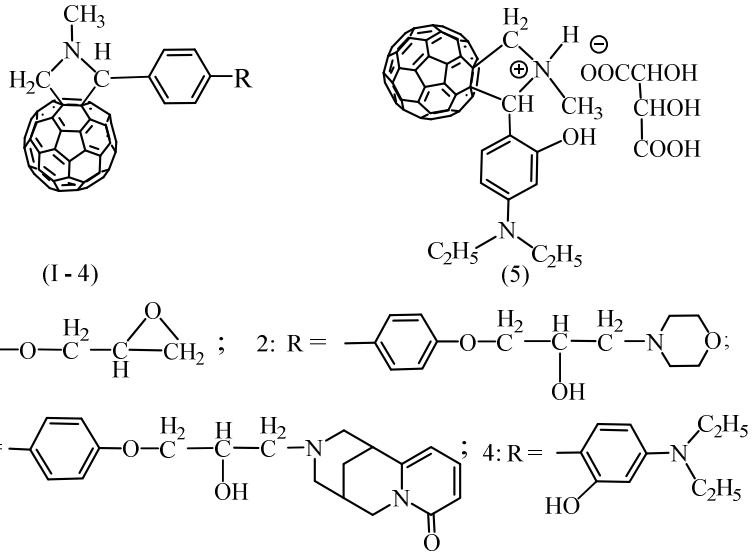

In order to expand a number of polyfunctional 1,2,4-triazoles bearing valuable biologically active groups [34, 35] based on N-morpholinyl acetic acid hydrazide, were synthesized and intramolecular

heterocyclization of thiosemicarbazide derivatives (5) was carried out. These compounds can be widely used in organic chemistry as starting synthons in the synthesis of many nitrogen-containing heterocyclic compounds.

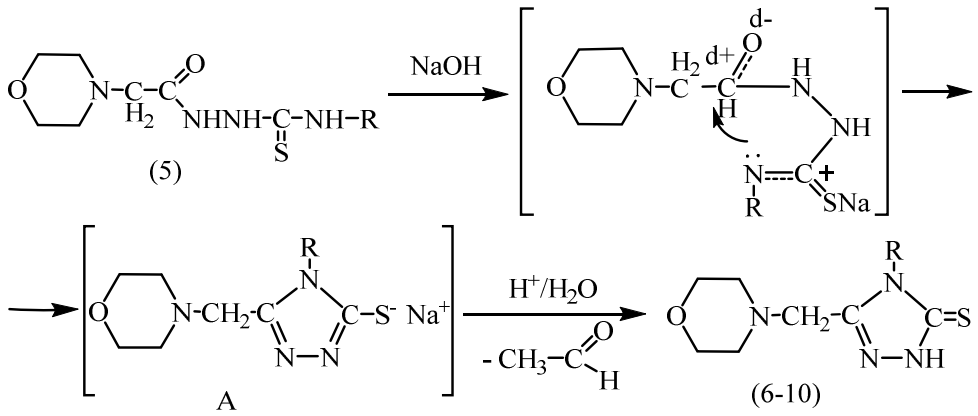

R = CH_2=CH-CH_2- (6); CH_3-CH_2- (7); C_6H_5- (8);
C_6H_5-C(O)- (9); 4-Br-C_6H_4-C(O)- (10)

The cyclization of thiosemicarbazide derivatives (5) was carried out in an aqueous-alkaline medium by heating the reaction medium to 80–85 °C. The starting N-morpholinyl acetic acid thiosemicarbazides were obtained by the interaction of N-morpholinyl acetic acid hydrazide with alkyl and aryl isothiocyanates. In the presence of alkali, N-alkyl(aryl)thiosemicarbazides of N-morpholinyl acetic acid (5) are converted to thiolate, and upon further acidification, 5-(morpholinomethyl)-4-alkyl(aryl)-1,2,4-triazole-3-thions are formed (6–10) [35–37].

In order to establish the spatial structure of 5-(morpholinomethyl)-4-allyl-1,2,4-triazol-3-thione (6), its X-ray structural examination was carried out, the general view of which is shown in Figure 2. From the obtained data it follows that the bond lengths and valent angles are close to normal [37].

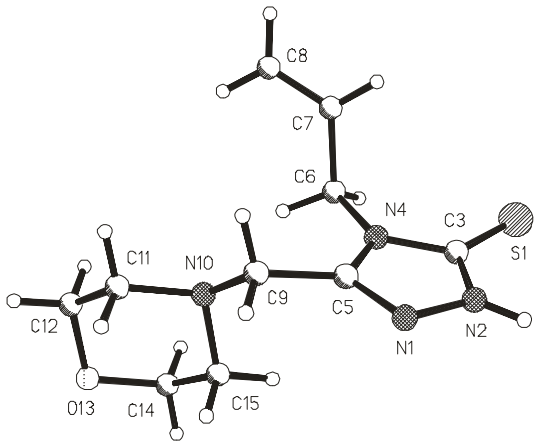

Figure 2. The structure of the molecule 5-(morpholinomethyl)-4-allyl-1,2,4-triazole-3-thione (6)

In continuation of these studies, N-phenyl thiosemicarbazide N-anabasinyl acetic acid (12) was synthesized by reacting N-anabasinyl acetic acid hydroxide (11) with phenyl isothiocyanate in ethanol with a yield of 74 %. It is established that upon acidification of a water-alkaline solution of the obtained phenylthiocarbazide derivative (8), the latter one is subjected to intramolecular hetero-cyclization with the formation of 4-phenyl-5-anabazinomethyl-1,2,4-triazole-3-thione (13) [38].

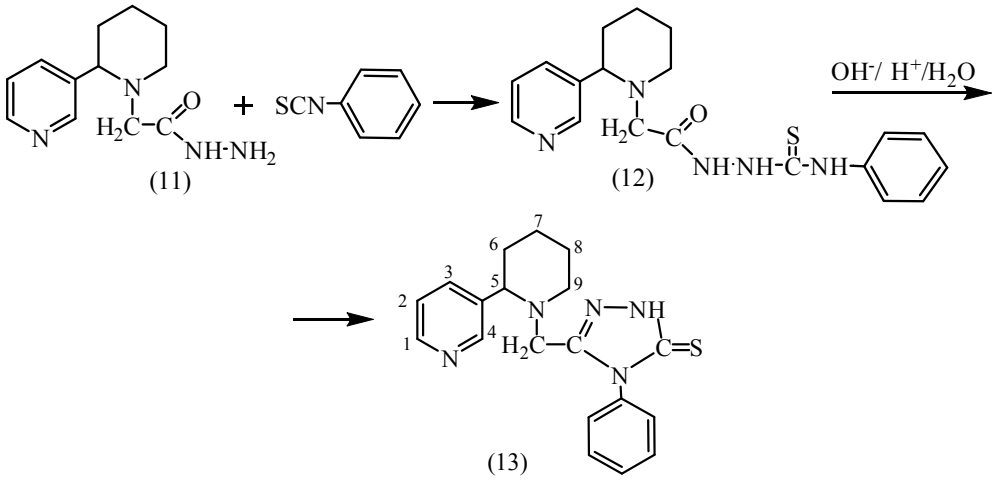

The synthesis of N-allylthiosemicarbazide N-anabasinyl-acetic acid was carried out in a similar way, and further its acidification leads to intramolecular hetero-cyclization with the formation of 4-allyl-5-anabasine-nomethyl-1,2,4-triazole-3-thione.

Among the extensive class of sulfur-containing compounds, an important role belongs to derivatives of dithiocarbamic acids [39, 40]. Derivatives of hydrazides and thiosemicarbazides are known to be important syntons in the synthesis of azaheterocycles [41]. It was established that using various reagents and changing the conditions of the reaction, it is possible to direct cyclization towards the formation of 1,3,4-oxadiazoles, 1,3,4-thiadiazoles or 1,2,4-triazoles.

In order to study the influence of the nature of substituents in the hydrazine component on the structure of condensation products, the interaction of N-morpholinyl acetic acid hydrazide (14) with carbon disulfide in an alkaline medium was studied. It was established that as a result of the reaction, the potassium salt of hydrazinodithiomorpholinyl acetic acid (15) is formed, which was used for further syntheses. The potassium salt of hydrazino-dithiomorpholinyl acetic acid (15) under the action of sulfuric acid (concentrated) at a low temperature easily undergoes cyclization to 5-(morpholinomethyl)-1,3,4-thiadiazol-2(3H)-thione (16) [38, 39]. In order to optimize this reaction, we studied the conversion of N-morpholinyl acetic acid hydrazide to a 1,3,4-thiadiazole derivative in the interaction of hydrazide with carbon disulfide in an alkaline medium under the conditions of «one pot» microwave activation in an aqueous medium [39–42].

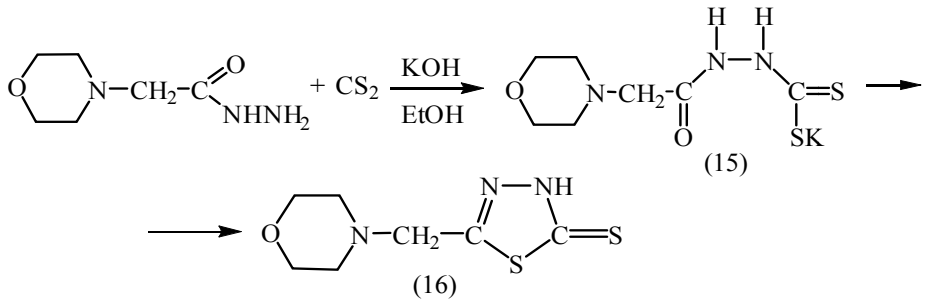

The structure of the substance (16) is confirmed by X-ray structural analysis (Fig. 3).

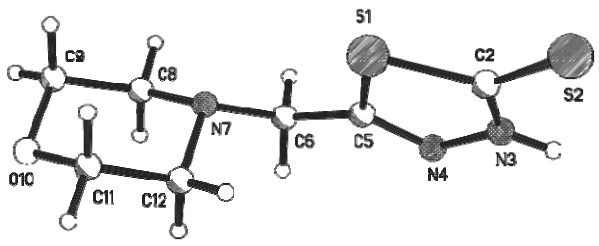

Figure 3. The spatial structure of the molecule 5-(morpholinomethyl)-1,3,4-thiadiazol-2(3H)-thione (16)

In continuation of the ongoing research on dithiocarbamine derivatives, a series of preparatively convenient chemical transformations with the potassium salt of hydrazinodithiomorpholinyl acetic acid (15) was carried out. A study of the hetero-cyclization of the potassium salt of hydrazinodiomorpholinyl acetic acid (15) showed that the nature of the forming substances depended on the conditions of the process [41–43].

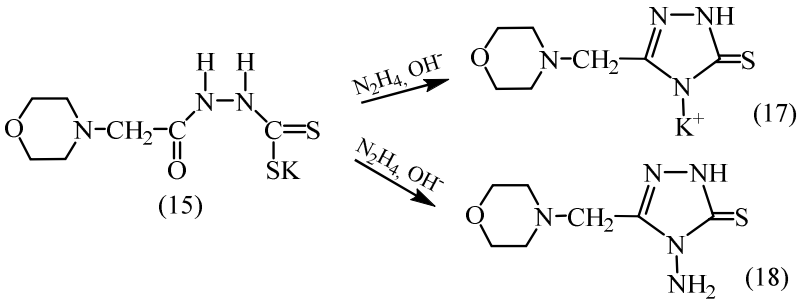

So, by reacting the potassium salt of hydrazinodithiomorpholine-acetic acid (15) with hydrazine hydrate in the presence of potassium hydroxide in absolute ethanol, followed by acidification with hydrochloric acid to a neutral medium (pH = 7), 4-amino-3-(morpholinomethyl)-(1H)-1,2,4-thiazolo-5e(4H)-thione (18) was synthesized [44]. It should be noted that a change in the nature of the reaction medium from absolute ethanol to water-ethanol (1:2) leads to the formation of the potassium salt of 3-(morpholinomethyl) -1,2,4-thiazole-4-thione (17). The structure of the substance (17) was also confirmed by X-ray diffraction [40–43].

As a result of research and experimental works, optimal methods of synthesis were developed and the physico-chemical properties of new potentially biologically active compounds of dithiocarbamate, thiourea, thiazole, and thioamide structures based on N-morpholylacetic acid hydrazides, as well as the known anabasine alkaloid, were studied. The synthesized new substances are of interest as potential objects for studying the biological properties and establishing the regularities of the «structure-bioactivity» relationship.

It should be noted that Institute of Organic Synthesis and Coal Chemistry of RK throughout all the years of its activity takes an active part in the implementation of the most important tasks in the framework of the priority directions of the development of science of the RK. The Institute staff at a high modern level conducts the scientific researches on the development of high technologies for the production of industrially important coal products, including modern approaches based on the use of microwave and ultrasound activation technology in chemical processes for the creation of new natural-synthetic polymers nanostructured catalysts, nanocomposites of various purposes and biologically active substances with the participation of C60 fullerene and nanofibers and other new products.

At the same time, the Institute should pay attention to the issues of commercialization of scientific results, taking into account the experience of promoting a number of developments, namely, the electrocatalytic production of 2,4,5,6-tetraaminopyrimidine and 2,4,5-triamino-6-oxypyrimidine used in the production of the antitumor drug «Methotrexate» and folic acid, introduced at the Shchyolkovo Vitamin Plant (Russia), the creation of the production of the highly effective flotation reagent dimethyl(isopropenyl ethynyl)carbinol (DMIPEK) in Moscow, the release of coal-alkaline reagent from off-balance coals Central Kazakhstan on SJSA «Ekibastuzugol» and LLP «Uglesintez» with capacity up to 1000 tons of products per year.

At this stage, it is necessary to increase the efficiency of implementation works on the basis of the created mini-workshops for obtaining sodium humate and coal-fuel briquettes based on coal screenings from the Shubarkol coal deposit.

It is necessary to ensure further improvement of the created innovative developments of the Institute:

- on the creation of new domestic polymer-humic soil builders and organic-mineral humic fertilizers, coal-alkaline reagent, coagulants and corrosion inhibitors based on coal products;
- on obtaining magnetically controlled nanosorbents for collecting oil spills from the water surface;
- on obtaining valuable chemical compounds (*p*-aminobenzoic acid in the electrocatalytic system, piperidine by electrocatalytic reduction of pyridine, methylphenylcarbonyl by electrocatalytic reduction of acetophenone and etc.), which are the basis of medicinal and fragrant substances.

The results of the implementation of these developments will contribute to the advanced development of high-tech and knowledge-intensive industries that save mineral resources, diversify the economy from raw materials to processing, and also contribute to solving environmental problems in the region.

References

1 Василец Е.П. Продукты химической переработки окисленных углей / Е.П. Василец, Г.К. Кудайберген, О.В. Арнт // Проблемы геологии и освоения недр: материалы XXI Междунар. науч. симпозиума студентов и молодых ученых им. акад. М.А. Усова (3–7 апреля 2017 г.). — Томск, 2017. — С. 379–380.

2 Akkulova Z.G. Surface morphology and sorption characteristics of humates and sulphohumate nanocomposites with natural and synthetic polymers and carbon nanotubes / Z.G. Akkulova, A.K. Amirkhanova, A.Kh. Zhakina, G.K. Kudaibergen, E.P. Vassilets, O.V. Sadykova // Chemical Journal of Kazakhstan. — 2015. — No. 4. — P. 184–188.

3 Аккулова З.Г. Получение и сорбционные свойства гуминоминеральных сорбентов на основе вмещающих пород угольных шахт / З.Г. Аккулова, А.К. Амирханова, А.Х. Жакина, З.М. Мулдахметов, Е.П. Василец, Г.К. Кудайберген, О.В. Арнт // Известия НАН РК. Сер. химии и технологии. — 2016. — № 6. — С. 14–22.

4 Василец Е.П. Исследование влияния ультразвуковой обработки и перекиси водорода на процесс окисления шубаркольских углей / Е.П. Василец, А.Х. Жакина, А.К. Амирханова, Г.К. Кудайберген // Тезисы докл. XXVI Рос. молодежной науч. конф., посвящ. 120-летию со дня рожд. акад. Н.Н. Семенова (27–29 апреля 2016). — Екатеринбург, 2016. — С. 20–21.

5 Жакина А.Х. Влияние ультразвукового метода иммобилизации гуминовой кислоты на горелую породу / А.Х. Жакина, Е.П. Василец, А.Р. Рапиков // Тезисы докл. XX Всерос. конф. молодых ученых-химиков (18–20 апреля 2017). — Нижний Новгород, 2017. — С. 477.

6 Василец Е.П. Влияние термохимических и микроволновых методов воздействия на сорбционные свойства гуминоминеральных композитов / Е.П. Василец, А.Х. Жакина, З.Г. Аккулова, З.М. Мулдахметов, А.К. Амирханова, Г.К. Кудайберген, О.В. Арнт, А.Р. Рапиков // Тенденции развития науки и образования в области естественно-научных дисциплин: материалы Междунар. науч.-практ. конф., посвящ. 70-летию со дня рожд. д-ра хим. наук Б.М. Бутина (7–8 октября 2016). — Алматы, 2016. — С. 87–89.

7 Жакина А.Х. Сорбенты многофункционального назначения на основе углеотходов / А.Х. Жакина, Е.П. Василец, А.К. Амирханова, О.В. Арнт, А.Р. Рапиков, З.М. Мулдахметов. — Караганда: Гласир, 2017. — 104 с.

8 Патент на полезную модель 3157 РК. Способ получения гуминоминерального сорбента для извлечения тяжелых металлов / Жакина А.Х., Мулдахметов З.М., Амирханова А.К., Василец Е.П., Рапиков А.Р., Кудайберген Г.К., Арнт О.В. Опубл. 2018.

9 Baikenov M.I. Effect of new catalytic systems on the process of anthracene hydrogenation / M.I. Baikenov, G.G. Baikenova, A.S. Isabaev, A.B. Tateeva, Zh.S. Akhmetkarimova, A. Tussipkhan, A.Zh. Mataeva, K.K. Esenbaeva // Solid Fuel Chemistry. — 2015. — Vol. 49, No. 3. — P. 150–155. DOI 10.3103/S0361521915030039.

10 Ахметкаримова Ж.С. Гидрогенизация смеси полиароматических углеводородов / Ж.С. Ахметкаримова, М.З. Мулдахметов, М.Г. Мейрамов, А.Т. Ордабаева, Ж.Х. Мулдахметов, А.М. Дюсекенов // Успехи в химии и химической технологии: сб. науч. тр. — М., 2016. — С. 89–91.

11 Мейрамов М.Г. Ангулярно-линеарная изомеризация при гидрировании фенантрена в присутствии железосодержащих катализаторов / М.Г. Мейрамов // Химия твердого топлива. — 2017. — № 2. — С. 42–45. DOI 10.7868/S0023117717020074.

12 Ордабаева А.Т. Изучение процесса гидрогенизации антрацена в присутствии композитного катализатора / А.Т. Ордабаева, М.Г. Мейрамов, В.А. Хрупов, Р.К. Бакирова // Хим. журн. Казахстана. — 2015. — № 3. — С. 338–344.

13 Meiramov M.G. Hydrogenation of model compounds in the presence of iron-containing catalysts / M.G. Meiramov // Solid Fuel Chemistry. — 2014. — No. 2. — P. 50–55. DOI 10.3103/S0361521914020104.

14 Ахметкаримова Ж.С. Влияние нанокатализаторов на процесс гидрогенизации модельного соединения — антрацена / Ж.С. Ахметкаримова, М.И. Байкенов, М.Г. Мейрамов, А.Т. Ордабаева, В.А. Хрупов, Ж.Х. Мулдахметов // Хим. журн. Казахстана. — 2015. — № 4. — С. 219–225.

15 Ахметкаримова Ж.С. Синтез бинарных композитных катализаторов на основе солей металлов VIII группы на цеолитном носителе / Ж.С. Ахметкаримова, З.М. Мулдахметов, Ж.Х. Мулдахметов, А.Т. Ордабаева, М.И. Байкенов, А.М. Дюсекенов // Хим. журн. Казахстана. — 2017. — № 2. — С. 251–259.

16 Ахметкаримова Ж.С. Гидрирование антрацена в присутствии композитных катализаторов / Ж.С. Ахметкаримова, З.М. Мулдахметов, М.Г. Мейрамов, А.Т. Ордабаева, Ж.Х. Мулдахметов, М.И. Байкенов, А.М. Дюсекенов // Известия НАН РК. Сер. химии и технологии. — 2017. — № 1. — С. 33–40.

17 Ахметкаримова Ж.С. Применение катализаторов в процессах гидрогенизации твердого и тяжелого углеводородного сырья / Ж.С. Ахметкаримова, М.Г. Мейрамов, М.И. Байкенов, М.З. Мулдахметов, А.Н. Жакупова, Р.А. Таженова, З.С. Даутова // Известия НАН РК. Сер. химии и технологии. — 2015. — № 3. — С. 116–124.

18 Ivanova N.M. Electrocatalytic activity of polyaniline-copper composites in electrohydrogenation of *p*-nitroaniline / N.M. Ivanova, E.A. Soboleva, Ya.A. Visurkhanova, I.V. Kirilyus // Russian J. Electrochem. — 2015. — Vol. 51, No. 2. — P. 166–173. DOI 10.7868/S042485701502005X.

19 Инновационный патент 29408 РК. Применение композитов на основе полианилина и солей металлов для активации катода в процессах электрогидрирования органических соединений / Иванова Н.М., Соболева Е.А., Избастенова Д.С., Висурханова Я.А., Тусупбекова Г.К. Опубл. 2014.

20 Ivanova N.M. Bimetallic Co-Cu polyaniline composites: Structure and electrocatalytic activity / N.M. Ivanova, E.A. Soboleva, Ya.A. Visurkhanova // Russian J. Appl. Chem. — 2016. — Vol. 89, No. 7. — P. 1072–1081. DOI 10.1134/S1070427216070053.

21 Соболева Е.А. Биметаллические Pd-Cu-композиты полианилина в электрокаталитическом гидрировании фенилацетилена / Е.А. Соболева, Я.А. Висурханова, Н.М. Иванова // Вестн. КазНУ. Сер. хим. — 2017. — № 1. — С. 5–14. DOI 10.15328/cb773.

22 Ivanova N.M. Two-step fabrication of iron-containing polyaniline composites for electrocatalytic hydrogenation of nitroarenes / N.M. Ivanova, Ya.A. Visurkhanova, E.A. Soboleva, S.O. Kenzhetaeva // Electrochem. Comm. — 2018. — Vol. 96. — P. 66–70. DOI 10.1016/j.elecom.2018.09.016.

23 Ivanova N.M. Structure-phase changes in polymer composites doped with silver nitrate and their electrocatalytic activity / N.M. Ivanova, E.A. Soboleva, Ya.A. Visurkhanova, E.S. Lazareva // Russian J. Electrochem. — 2018. — Vol. 54, No. 11. — P. 999–1005. DOI 10.1134/S1023193518130207.

24 Ivanova N.M. Structure and electrocatalytic activity of aniline-formaldehyde polymer doped with copper (II) chloride / N.M. Ivanova, Ya.A. Visurkhanova, E.A. Soboleva, N.A. Pavlenko, Z.M. Muldakhmetov // Chemistry Select. — 2016. — No. 1. — P. 5304–5309. DOI 10.1002/slct.201601101.

25 Ivanova N.M. Structure and Electrocatalytic Properties of Copper-Containing Aniline-Melamine-Formaldehyde Polymer Composite / N.M. Ivanova, Ya.A. Visurkhanova, E.A. Soboleva // Russian J. Appl. Chem. — 2018. — Vol. 91, No. 3. — P. 396–403. DOI 10.1134/S1070427218030084.

26 Ivanova N.M. Structure and electrocatalytic activity of zinc-containing composites of polyaniline with aniline-formaldehyde polymer / N.M. Ivanova, Ye.S. Lazareva, Ya.A. Visurkhanova, E.A. Soboleva // Chemical Journal of Kazakhstan. — 2018. — No. 2. — P. 120–129.

27 Журинов М.Ж. Синтез тиомочевинных и тиазолиновых производных пиразола / М.Ж. Журинов, А.М. Газалиев, М.Б. Исабеков, О.В. Бакбардина, М.К. Ибраев // Доклады НАН РК. — 2010. — № 5. — С. 27–28.

28 Журинов М.Ж. Реакция взаимодействия монотиооксамидов с α-галогенкетонами с образованием тиазолов / М.Ж. Журинов, А.М. Газалиев, О.В. Бакбардина, М.К. Ибраев // Доклады НАН РК. — 2010. — № 3. — С. 44–46.

29 Газалиев А.М. Синтез тиомочевинных производных алкалоидов анабазина, цитизина и *d*-псевдоэфедрина. Кристаллическая структура N-этил-N-анабазинокарботиоамида / А.М. Газалиев, О.А. Нуркенов, Ж.Б. Сатпаева, С.Д. Фазылов, К.М. Турдыбеков, Д.М. Турдыбеков, С.Б. Ахметова, А.С. Махмутова // Хим. природ. соед. — 2016. — № 2. — С. 243–245.

30 Gazaliev A.M. Synthesis and molecular structure of 2-(4-pyridyl)-3,4-dimethyl-5-phenyl-1,3-oxazolidine / A.M. Gazaliev, O.A. Nurkenov, Zh.B. Satpaeva, S.D. Fazylov, T.M. Turdybekov, D.M. Turdybekov, S.B. Akhmetova, A.S. Makhmutova // Chem. Natural Comp. — 2016. — Vol. 52, No. 2. — P. 370–372. DOI 10.1007/s10600–016–1649–9.

31 Нуркенов О.А. Синтез и модификация 5-этокси-6-метил-4-(4-диэтиламинофенил)-2-тиоксо-1,2,3,4-тетрагидропиримидин-5-карбоксилата / О.А. Нуркенов, С.Д. Фазылов, Т.М. Сейлханов, Т.С. Животова, А.Е. Аринова, Ж.Б. Сатпаева, А.Ж. Исаева, Г.Ж. Карипова, А.Б. Мукашев, З.М. Мулдахметов // Изв. НАН РК. Сер. химии и технологии. — 2016. — № 2. — С. 77–84.

32 Фазылов С.Д. Синтез и спектральное исследование строения N-метил-1-[(4-бром-3,5-диметил-1н-пиразол-1)-фенил]-фуллерен-C_{60}-[1,9C]-пирролидина / С.Д. Фазылов, О.А. Нуркенов, А.Е. Аринова, Т.М. Сейлханов, А.Р. Туктаров, А.А. Хузин, Р.Е. Бакирова, Л.Е. Муравлева // Журн. общ. химии. — 2015. — № 5. — С. 751–754.

33 Fazylov S.D. Synthesis and spectral study of the structure of N-methyl-1-[(4-bromo-3,5-dimethyl-1n-pyrazole-1)-phenyl] fullerene-C60-[1,9C]-pyrrolidine / S.D. Fazylov, O.A. Nurkenov, A.E. Arinova, T.M. Seilkhanov, A.R. Tuktarov, A.A. Khuzin, R.E. Bakirova, L.E. Muravleva // Russian J. General Chem. — 2015. — Vol. 85, No. 5. — P. 751–754. DOI 10.1134/S1070363215050072.

34 Nurkenov O.A. Synthesis and structure of condensed biheterocycles on the basis of 3-amino-1,2,4-triazole / O.A. Nurkenov, S.D. Fazylov, T.M. Seilkhanov, A.E. Arinova, A.Zh. Issayeva, Zh.B. Satpaeva, M.Z. Muldahmetov // Bulletin of the Karaganda University. Chemistry series. — 2017. — No. 3. — P. 9–17.

35 Nurkenov O.A. Synthesis and structure of new 1,2,4-triazoles based on *p*-hydroxybenzoic acid hydrazide / O.A. Nurkenov, S.D. Fazylov, Zh.B. Satpaeva, K.M. Turdybekov, G.Zh. Karipova, A.Zh. Isaeva, S.A. Talipov, B.T. Ibragimov // Russian J. of General Chem. — 2015. — Vol. 85, No. 1. — P. 62–66. DOI 10.1134/S1070363215010107.

36 Нуркенов О.А. Синтез, химические превращения и антимикробная активность некоторых тиосемикарбазидов *о*- и *п*-гидроксибензойной кислоты / О.А. Нуркенов, С.Д. Фазылов, Т.С. Животова, Ж.Б. Сатпаева, С.Б. Ахметова, Ж.Ж. Курманбаева, Г.К. Карипова, А.Ж. Исаева // Изв. НАН РК. Сер. химии и технологии. — 2015. — No. 1. — С. 9–14.

37 Nurkenov O.A. Intramolecular heterocyclization of N-allyl-(phenyl)thiosemicarbazide N-morpholinyl acetic acid / O.A. Nurkenov, S.D. Fazylov, Zh.B. Satpaeva, K.M. Turdybekov, D.M. Turdybekov, S.A. Talipov, B.T. Ibragimov // Russian Journal of General Chem. — 2013. — Vol. 83, No. 11. — P. 1879–1881. DOI 10.1134/S1070363213110194.

38 Nurkenov O.A. Synthesis and intramolecular heterocyclization of N-phenylthiosemicarbazide N-anabasinyl acetic acid / O.A. Nurkenov, S.D. Fazylov, Zh.B. Satpaeva, L.A. Smakova // Russian Journal of General Chem. — 2013. — Vol. 83, No. 9. — P. 1581–1582. DOI 10.1134/S1070363213090302.

39 Fazylov S.D. The interaction of thiazolidin-2,4-dione with aromatic aldehydes under microwave irradiation / S.D. Fazylov, O.A. Nurkenov, Sch.K. Amerkhanova, & I.S. Tolepbek // Russian Journal of General Chem. — 2013. — Vol. 83, No. 9. — P. 1577–1578. DOI 10.1134/S1070363213090284.

40 Fazylov S.D. Obtaining 5-(morpholinomethyl)-3,4-thiadiazole-2-thione under microwave irradiation / S.D. Fazylov, O.A. Nurkenov, S.O. Kenzhetaeva, Zh.B. Satpaeva, G.Zh. Karipova // Russian Journal of General Chem. — 2013. — Vol. 83, No. 9. — P. 1579–1580. DOI 10.1134/S1070363213090296.

41 Фазылов С.Д. Внутримолекулярная гетероциклизация гидразидных производных N-анабазинилуксусной кислоты / С.Д. Фазылов, О.А. Нуркенов, Ж.Б. Сатпаева, А.К. Свидерский, А.Н. Жакупова, А.Е. Аринова, Д.К. Макенов, М.З. Мулдахметов // Известия НАН РК. Сер. химии и технологии. — 2015. — № 1. — С. 5–8.

42 Нуркенов О.А. Синтез и свойства производных гидразида изоникотиновой кислоты / О.А. Нуркенов, С.Д. Фазылов, А.М. Газалиев, Ж.Б. Сатпаева, Ш.К. Амерханова, Г.Ж. Карипова // Доклады НАН РК. — 2017. — Т. 311. — С. 68–78.

43 Fazylov S.D. The study of the anti-inflammatory activity of thiosemicarbazide N-morpholinyl acetic acid / S.D. Fazylov, R.E. Bakirova, O.A. Nurkenov, L.E. Muravleva, A.N. Zhakupova // Georgian Medical News. — 2015. — No. 3. — P. 88–102.

44 Нуркенов О.А. Конденсация N-морфолинил-уксусной кислоты с дикарбонильными соединениями / О.А. Нуркенов, С.Д. Фазылов, Ж.Б. Сатпаева, К.М. Турдыбеков, М.З. Мулдахметов, З.Т. Шульгау, Л.К. Салькеева, С.А. Талипов // Известия НАН РК. Сер. химии и технологии. — 2014. — № 2. — С. 3–7.

З.М. Молдахметов

Органикалық синтез және көмірхимия институты: қазіргі жетістіктері мен даму бағдарламалары

Мақалада «ҚР Органикалық синтез және көмірхимия институты» ЖШС-де соңғы жылдары орындалған зерттеулер негізінде шолу жасалған. Ультрадыбыстық және микротолқынды химия әдістерін көмірді тотықтыру және тотығу түрлендіру үрдістеріне қолдану, жанған жыныстың бетіне гумин қышқылдарын және олардың туындыларын иммобилизациялау үрдістерін белсендіру, сондай-ақ гуминминералды композицияларды алу процестеріне көміртекті нанотүтіктердің әсері зерттелді. Гуминді сорбенттердің жаңа белсенді формаларының қасиеттері анықталып ағынды суларды тазарту үшін сорбенттер ретінде сынаулар жүргізілді. VIII-ші топтағы (Fe, Ni, Co, Mo) металдардың қосылыстары негізінде композиттік катализаторлар алынды және антрацен мен фенантренді гидрирлеу процесінде олардың белсенділігі зерттелді. Цеолиттер мен көмір сорбенттеріне қондырылған металдардың суда еритін тұздары негізінде синтезделген композитті катализаторлардың қатысуымен мазут фракцияларын кавитациялық өңдеудің оңтайлы параметрлері анықталды. Анилиноформальдегид полимері және оның меламиноформальдегид полимерімен және полианилинмен аралас композициялары негізінде электркаталитикалық қасиеттері бар жаңа полимер-металды композиттер алынды. Олардың құрылысы мен морфологиялық ерекшеліктері ИҚ-спектроскопия, рентгенофазалық талдау, атомды-эмиссиялық спектроскопия және электрондық микроскопия әдістерімен зерттелген. Электркаталитикалық белсенділік органикалық қосылыстарды электргидрациялауда зерттелді. 4-Амино-1,2,4-триазолдың, N-морфолинилсірке және N-анабазинилсірке қышқылдарының тиосемикарбазидтерінің жаңа туындылары синтезделген, олардың құрылысы мен биологиялық белсенділігі, реакция механизмдері зерттелген және де оларды синтездеу әдістемелерінің оңтайлы шарттары ұсынылған.

Кілт сөздер: гумин қышқылы, жанған жыныс, көпқабатты көміртекті нанотүтіктер, гуминоминералды композиттер, композитті катализаторлар, антрацен, фенантрен, мазут, гидрогенизация, полимер-металды композиттер, анилинді және меламиноформальдегидті полимерлер, полианилин, электркаталитикалық қасиеттер, 4-амино-1,2,4-триазол туындылары, фуллеропирролиндер, биобелсенділік.

З.М. Мулдахметов

Институт органического синтеза и углехимии: состояние и перспективы развития

Статья носит обзорный характер по исследованиям, выполненным в ТОО «Институт органического синтеза и углехимии РК» за последние годы. Изучено применение методов ультразвуковой и микроволновой химии к процессам окисления и окислительного модифицирования углей, активации процессов иммобилизации гуминовых кислот и их производных на поверхность горелых пород, а также влияние углеродных нанотрубок на процессы получения гуминоминеральных композиций. Изучены свойства новых активированных форм гуминовых сорбентов и проведены испытания их в качестве сорбентов для очистки сточных вод. Получены композитные катализаторы на основе соединений металлов VIII группы (Fe, Ni, Co, Mo), и изучена их активность в процессе гидрирования антрацена и фенантрена. Определены оптимальные параметры кавитационной обработки фракций мазута в присутствии синтезированных композитных катализаторов на основе водорастворимых солей металлов, нанесённых на цеолиты и угольные сорбенты. На основе анилиноформальдегидного полимера и его смешанных композиций с меламиноформальдегидным полимером и полианилином получены новые металлополимерные композиты, обладающие электрокаталитическими свойствами. Их строение и морфологические особенности изучены методами ИК-спектроскопии, рентгенофазового анализа, атомно-эмиссионной спектроскопии и электронной микроскопии. Электрокаталитическая активность исследована в процессах электрогидрирования органических соединений. Синтезированы новые производные 4-амино-1,2,4-триазола, тиосемикарбазидов N-морфолинилуксусной и N-анабазинилуксусной кислот, изучены их строение, биологическая активность, механизмы реакций и предложены оптимальные условия их синтеза.

Ключевые слова: гуминовая кислота, горелая порода, многостенные углеродные нанотрубки, гуминоминеральные композиты, композитные катализаторы, антрацен, фенантрен, мазут, гидрогенизация, полимер-металлические композиты, анилино- и меламиноформальдегидные полимеры, полианилин, электрокаталитические свойства, производные 4-амино-1,2,4-триазола, фуллеропирролидины, биоактивность.

References

1 Vassilets, E.P., Kudaibergen, G.K., & Arnt, O.V. (2017). Produkty khimicheskoi pererabotki okislennykh uhlei [Products of chemical processing of oxidized coal]. Proceedings from The Problems of geology and exploration of mineral resources: *XXI Mezhdunarodnyi nauchnyi simpozium studentov i molodykh uchenykh imeni akademika Usova M.A. (3–7 aprelia 2017 hoda) — The XXI Int. scientific symposium of students and young scientists named after academician M.A. Usov (pp. 379–380)*. Tomsk, Russian Federation [in Russian].

2 Akkulova, Z.G., Amirkhanova, A.K., Zhakina, A.Kh., Kudaibergen, G.K., Vassilets, E.P., & Sadykova, O.V. (2015). Surface morphology and sorption characteristics of humates and sulphohumate nanocomposites with natural and synthetic polymers and carbon nanotubes. *Chemical Journal of Kazakhstan*, *4*, 184–188.

3 Akkulova, Z.G., Amirkhanova, A.K., Zhakina, A.Kh., Muldakhmetov, Z.M., Vassilets, E.P., Kudaibergen, G.K., & Arnt, O.V. (2016). Poluchenie i sorbtsionnye svoistva huminomineralnykh sorbentov na osnove vmeshchaiushchikh porod uholnykh shakht [Preparation and sorption properties of humic-mineral sorbents based on the enclosing rocks of coal mines]. *Izvestiia NAN RK. Ser. khimii i tekhnolohii. — News NAS RK. Ser. chemistry and technology*, *6*, 14–22 [in Russian].

4 Vassilets, E.P., Zhakina, A.Kh., Amirkhanova, A.K., & Kudaibergen, G.K. (2016). Issledovanie vliianiia ultrazvukovoi obrabotki i perekisi vodoroda na protsess okisleniia shubarkulskikh uhlei [Investigation of the effect of ultrasonic treatment and hydrogen peroxide on the oxidation process of the Shubarkol coals]. Abstracts of conference: *XXVI Ros. molodezhnaia nauchnaia konferentsiia, posviashchennaia 120-letiiu so dnia rozhdeniia akademika N.N. Semenova (27–29 aprelia) — XXVI Russian Youth Scientific Conference dedicated to 120th anniversary of the birth of Academician N.N. Semenov* (pp. 20–21). Yekaterinburg, Russian Federation [in Russian].

5 Zhakina, A.Kh., Vassilets, E.P., & Rapikov, A.R. (2017*)*. Vliianie ultrazvukovoho metoda immobilizatsii huminovoi kisloty na horeluiu porodu [The effect of ultrasonic method of immobilization of humic acid on the burnt rocks]. Abstracts of conference: *XX Vseros. konferentsiia molodykh uchenykh-khimikov (18–20 aprelia) — All-Russian Conference of young chemists.* (p. 477). Nizhnii Novgorod, Russian Federation [in Russian].

6 Vassilets, E.P., Zhakina, A.Kh., Akkulova, Z.G., Muldakhmetov, Z.M., Amirkhanova, A.K., Kudaibergen, G.K., Arnt, O.V., & Rapikov, A.R. (2016). Vliianie termokhimicheskikh i mikrovolnovykh metodov vozdeistviia na sorbtsionnye svoistva huminomineralnykh kompozitov [Influence of thermochemical and microwave methods of influence on the sorption properties of humic mineral composites]. Proceedings from Trends in the development of science and education in the field of natural sciences, dedicated to the 70th anniversary of the birth of Doctor of Chem. Sciences B.M. Butin: *Mezhdunarodnaia nauchnaia i prakticheskaia konferentsiia (7–8 oktiabria) — Int. scientific and practical conference* (p. 87–89). Almaty, Republic of Kazakhstan [in Russian].

7 Zhakina, A.Kh, Vassilets, E.P, Amirkhanova, A.K., Arnt, O.V., Rapikov, A.R., & Muldakhmetov, Z.M. (2017). *Sorbenty mnohofunktsionalnoho naznacheniia na osnove uhleotkhodov [Coal waste based multi-purpose sorbents]*. Karaganda: Glasir [in Russian].

8 Zhakina, A.Kh., Muldakhmetov, Z.M., Amirkhanova, A.K., Vassilets, E.P., Rapikov, A.R., Kudaibergen, G.K., & Arnt, O.V. (2018). Patent for utility model RK No. 3157. *Sposob polucheniia huminomineralnoho sorbenta dlia izvlecheniia tiazhelykh metallov [The method of obtaining humic mineral sorbent for the extraction of heavy metals]* [in Russian].

9 Baikenov, M.I., Baikenova, G.G., Isabaev, A.S., Tateeva, A.B., Akhmetkarimova, Zh.S., Tussipkhan, A., Mataeva, A.Zh., & Esenbaeva, K.K. (2015). Effect of new catalytic systems on the process of anthracene hydrogenation. *Solid Fuel Chemistry*, *49*(3), 150–155. DOI 10.3103/S0361521915030039.

10 Akhmetkarimova, Zh.S., Muldakhmetov, M.Z, Meiramov, M.G., Ordabaeva, A.T., Muldakhmetov, Zh.Kh., & Dusekenov, A.M. (2016). Hidrohenizatsiia smesi poliaromaticheskikh uhlevodorodov [Hydrogenation of a mixture of polyaromatic hydrocarbons]. *Uspekhi v khimii i khimicheskoi tekhnolihii — Advances in chemistry and chemical technology, XXX(9)*, 89–91 [in Russian].

11 Meiramov, M.G. (2017). Anhuliarno-linearnaia izomerizatsiia pri hidrirovanii fenantrena v prisutstvii zhelezosoderzhahchikh katalizatorov [Angular-linear isomerization in the hydrogenation of phenanthrene in the presence of iron-containing catalysts]. *Khimiia tverdoho topliva. — Solid Fuel Chemistry, 2,* 42–45 DOI 10.7868/S0023117717020074 [in Russian].

12 Ordabaeva, A.T., Meiramov, M.G., Khrupov, V.A., & Bakirova, R.K. (2015). Izuchenie protsessa hidrohenizatsii antratsena v prisutstvii kompozitnoho katalizatora [The study of the hydrogenation of anthracene in the presence of a composite catalyst]. *Khimicheskii zhurnal Kazakhstana — Chemical Journal of Kazakhstan*, *3*, 338–344 [in Russian].

13 Meiramov, M.G. (2014). Hydrogenation of model compounds in the presence of iron-containing catalysts. *Solid Fuel Chemistry*, *2*, 50–55. DOI 10.3103/S0361521914020104.

14 Akhmetkarimova, Zh.S., Baikenov, M.I., Meiramov, M.G., Ordabaeva, A.T., Khrupov, V.A., & Muldakhmetov, Zh.H. (2015). Vliianie nanokatalizatorov na protsess hidrogenizatsii modelnoho soedineniia — antratsena [Effect of nanocatalysts on the process of hydrogenation of the model compound — anthracene]. *Khimicheskii zhurnal Kazahstana. — Chemical Journal of Kazakhstan*, *4*, 219–225 [in Russian].

15 Akhmetkarimova, Zh.S., Muldakhmetov, Z.M., Muldahmetov, Zh.Kh., Ordabaeva, A.T., Baikenov, M.I., & Dyusekenov, A.M. (2017.) Sintez binarnykh kompozitnykh katalizatorov na osnove solei metallov VIII gruppy na tseolitnom nositele [Synthesis of binary composite catalysts based on VIII Group metal salts on a zeolite carrier]. *Khimicheskii zhurnal Kazakhstana. — Chemical Journal of Kazakhstan*, *2*, 251–259 [in Russian].

16 Akhmetkarimova, Zh.S., Muldakhmetov, Z.M., Meiramov, M.G., Ordabaeva, A.T., Muldakhmetov, Zh.K., Baikenov, M.I., & Dyusekenov, A.M. (2017) Hidrirovanie antratsena v prisutstvii kompozitnykh katalizatorov [Hydrogenation of anthracene in the presence of composite catalysts]. *Izvestiia NAN RK. Seriia khimii i tekhnolohii. — News of NAS RK. Chemistry and technology series*, *1*, 33–40 [in Russian].

17 Akhmetkarimova, Zh.S., Meiramov, M.G., Baikenov, M.I., Muldakhmetov, M.Z., Zhakupova, A.N., Tazhenova R.A., & Dautova, Zh.S. (2015). Primenenie katalizatorov v protsessakh hidrohenizatsii tverdoho i tiazheloho uhlevodorodnoho syria [Application of catalysts in the processes of hydrogenation of solid and heavy hydrocarbon of raw materials]. *Izvestiia NAN RK. Seriia khimii i tekhnolohii. — News of NAS RK. Chemistry and technology series*, *3*, 116–124 [in Russian].

18 Ivanova, N.M., Soboleva, E.A., Visurkhanova, Ya.A., Kirilyus, I.V. (2015). Electrocatalytic activity of polyaniline-copper composites in electrohydrogenation of *p*-nitroaniline. *Russian J. Electrochem., 51*, 166–173. DOI 10.7868/S042485701502005X.

19 Ivanova, N.M., Soboleva, E.A., Izbastenova, D.S., Visurkhanova, Ya.A., & Tusupbekova, G.K. (2014). Innovative patent of RK No. 29408. *Primenenie kompozitov na osnove polianilina i solei metallov dlia aktivatsii katoda v protsessakh electrohidrirovaniia orhanicheskikh soedinenii [The use of composites based on polyaniline and metal salts for the activation of a cathode in the electrohydrogenation processes of organic compounds]* [in Russian].

20 Ivanova, N.M., Soboleva, E.A., & Visurkhanova, Ya.A. (2016.) Bimetallic Co-Cu polyaniline composites: Structure and electrocatalytic activity. *Russian J. Appl. Chem., 89*(7), 1072–1081. DOI: 10.1134/S1070427216070053.

21 Soboleva, E.A., Visurkhanova, Ya.A., & Ivanova, N.M. (2017). Bimetallicheskie Pd-Cu-kompozity polianilina v electrokataliticheskom hidrirovanii phenilatsetilena [Bimetallic Pd-Cu-composites of polyaniline in electrocatalytic hydrogenation of phenylacetylene]. *Vestnik KazNU. Seriia khimicheskaia. — Chemical Bulletin of Kazakh National University*, *1*, 5–14. DOI 10.15328/cb773 [in Russian].

22 Ivanova, N.M., Visurkhanova, Ya.A., Soboleva, E.A., & Kenzhetaeva, S.O. (2018). Two-step fabrication of iron-containing polyaniline composites for electrocatalytic hydrogenation of nitroarenes. *Electrochem. Comm.*, *96*, 66–70. DOI 10.1016/j.elecom.2018.09.016.

23 Ivanova, N.M., Soboleva, E.A., Visurkhanova, Ya.A., & Lazareva, E.S. (2018). Structure-phase changes in polymer composites doped with silver nitrate and their electrocatalytic activity. *Russian J. Electrochem., 54*(11), 999–1005. DOI 10.1134/S1023193518130207.

24 Ivanova, N.M., Visurkhanova, Ya.A., Soboleva, E.A., Pavlenko, N.A., & Muldakhmetov, Z.M. (2016). Structure and electrocatalytic activity of aniline-formaldehyde polymer doped with copper (II) chloride. *Chemistry Select., 1*, 5304–5309. DOI 10.1002/slct.201601101.

25 Ivanova, N.M., Visurkhanova, Ya.A., & Soboleva, E.A. (2018). Structure and Electrocatalytic Properties of Copper-Containing Aniline-Melamine-Formaldehyde Polymer Composite. *Russian J. Appl. Chem., 91*(3), 396–403. DOI 10.1134/S1070427218030084.

26 Ivanova, N.M., Lazareva, Ye.S., Visurkhanova, Ya.A., & Soboleva, E.A. (2018). Structure and electrocatalytic activity of zinc-containing composites of polyaniline with aniline-formaldehyde polymer. *Chemical Journal of Kazakhstan*, *2*, 120–129.

27 Zhurinov, M.Zh., Gazaliev, A.M., Isabekov, M.B., Bakbardina, O.V., & Ibraev, M.K. (2010). Sintez tiomochevinnykh i tiazolinovykh proizvodnykh pirazola [Synthesis of thiourea and thiazoline pyrazole derivatives]. *Doklady Natsionalnoi akademii nauk Respubliki Kazakhstan. — Reports of NAS RK*, *5*, 27–28 [in Russian].

28 Zhurinov, M.Zh., Gazaliev, A.M., Bakbardina, O.V., & Ibraev, M.K. (2010). Reaktsiia vzaimodeistviia monotiooksamidov s α-halohenketonami s obrazovaniem tiazolov [Interaction reaction of monothioxamides with α-halogen ketones to produce thiazoles]. *Doklady Natsionalnoi akademii nauk Respubliki Kazakhstan. — Reports of NAS RK, 3*, 44–46 [in Russian].

29 Gazaliev, A.M., Nurkenov, O.A., Satpaeva, Zh.B., Fazylov, S.D., Turdybekov, K.M., Turdybekov, D.M., Akhmetova, S.B., & Makhmutova, A.S. (2016). Sintez tiomochevinnykh proizvodnykh alkaloidov anabazina, tsitizina i d-psevdoefedrina. Kristallicheskaia structura N-etil-N-anabazinokarbotioamida [Synthesis of thiourea derivatives of the anabasine, cytisine and d-pseudoephedrine alkaloids. Crystal structure of N-ethyl-N-anabazinocarbothioamide]. *Khimiia prirodnykh soedinenii. — Chemistry of Natural compounds, 2*, 243–245 [in Russian].

30 Gazaliev, A.M., Nurkenov, O.A., Satpaeva, Zh.B., Fazylov, S.D., Turdybekov, T.M., Turdybekov, D.M., Akhmetova, S.B., & Makhmutova, A.S. (2016). Synthesis and molecular structure of 2-(4-pyridyl)-3,4-dimethyl-5-phenyl-1,3-oxazolidine. *Chemistry of Natural compounds, 52*(2), 370–372. DOI 10.1007/s10600–016–1649–9.

31 Nurkenov, O.A., Fazylov, S.D., Seilkhanov, T.M., Zhivotova, T.S., Arinova, A.E., Satpaeva, Zh.B., Issyaeva, A.Zh., Karipova, G.Zh., Mukashev, A.B., & Muldahmetov, Z.M. (2016). Sintez i modifikatsiia 5-etoksi-6-metil-4-(4-dietilaminofenil)-2-tiokso-1,2,3,4-tetrahidropirimidin-5-karboksilata [Synthesis and modification of 5-ethoxy-6-methyl-4-(4-diethylaminophenyl)-2-thioxo-1,2,3,4-tetrahydropyrimidine-5-carboxylate]. *Izvestiia NAN RK. Seriia khimii i tekhnolohii. — News of NAS RK*, *2*, 77–84. DOI 10.32014/2018.2518–1491 [in Russian].

32 Fazylov, S.D., Nurkenov, O.A., Arinova, A.E., Seilkhanov, T.M., Tuktarov, A.R., Khuzin, A.A., Bakirova, R.E., & Muravleva, L.E. (2015). Synthesis and spectral study of the structure of N-methyl-1-[(4-bromo-3,5-dimethyl-1n-pyrazole-1)-phenyl] fullerene-C60-[1,9C]-pyrrolidine. *Russian J. Gen. Chem., 85*(5), 751–754. DOI 10.1134/S1070363215050072.

33 Nurkenov, O.A., Fazylov, S.D., Seilkhanov, T.M., Arinova, A.E., Issayeva, A.Zh., Satpaeva, Zh.B., & Muldahmetov, M.Z. (2017). Synthesis and structure of condensed biheterocycles on the basis of 3-amino-1,2,4-triazole. *Vestnik Karahandinskoho Universiteta. Seriia khimiia. — Bulletin of the Karaganda University. Chemistry series*, *3*, 9–17. DOI 10.31489/2017Ch3/9–17.

34 Nurkenov, O.A., Fazylov, S.D., Satpaeva, Zh.B., Turdybekov, K.M., Karipova, G.Zh., Isaeva, A.Zh., Talipov, S.A., & Ibragimov, B.T. (2015). Synthesis and structure of new 1,2,4-triazoles based on p-hydroxybenzoic acid hydrazide, *Russian J. of General Chem., 85*(1), 62–66. DOI 10.1134/S1070363215010107.

35 Nurkenov, O.A., Fazylov, S.D., Zhivotova, T.S., Satpayeva, Zh.B., Akhmetova, S.B., Kurmanbayeva, Zh.Zh., Karipova, G.K., & Issayeva, A.Zh. (2015). Sintez, khimicheskie transformatsii i antimikrobnaia aktivnost nekotorykh tiosemikarbazidov *o*- i *p*-hidrobenzoinoi kisloty [Synthesis, chemical transformations and antimicrobial activity of some thiosemicarbazides of *o*- and *p*-hydrobenzoic acid]. *Izvestiia NAN RK. Seriia khimii i tekhnolohii. — News of NAS RK. Chemistry and technology series, 1*, 9–14 [in Russian].

36 Nurkenov, O.A., Fazylov, S.D., Satpaeva, Zh.B., Turdybekov, K.M., Turdybekov, D.M., Talipov, S.A., Ibragimov, B.T. (2013). Intramolecular heterocyclization of N-allyl-(phenyl) thiosemicarbazide N-morpholinyl acetic acid. *Russian J. General Chem., 83*(11), 1879–1881. DOI 10.1134/S1070363213110194.

37 Nurkenov, O.A., Fazylov, S.D., Satpaeva, Zh.B., & Smakova, L.A. (2013). Synthesis and intramolecular heterocyclization of N-phenylthiosemicarbazide N-anabasinyl acetic acid. *Russian J. of General Chem., 83*(9), 1581–1582. DOI 10.1134/S1070363213090302.

38 Fazylov, S.D., Nurkenov, O.A., Amerkhanova, Sh.K., & Tolepbek, I.S. (2013). The interaction of thiazolidin-2,4-dione with aromatic aldehydes under microwave irradiation, *Russian J. General Chem., 83*(9), 1577–1578. DOI 10.1134/S1070363213090284.

39 Fazylov, S.D., Nurkenov, O.A., Kenzhetaeva, S.O., Satpaeva, Zh.B., & Karipova, G.Zh. (2013). Obtaining 5-(morpholino-methyl)-3,4-thiadiazole-2-thione under microwave irradiation. *Russian J. General Chem., 83*(9), 1579–1580. DOI 10.1134/S1070363213090296.

40 Fazylov, S.D., Nurkenov, O.A., Satpayeva, Zh. B., Sviderskiy, A.K., Zhakupova, A.N., Arinova, A.E., Makenov, D.K., Muldakhmetov, M.Z. (2015). Vnutrimolekuliarnaia heterotsiklizatsiia proizvodnykh hidrazida N-anabazinil uksusnoi kisloty [Intramolecular heterocyclization of hydrazide N-anabasinil acetic acid derivatives]. *Izvestiia NAN RK. Seriia khimii i tekhnolohii. — News of NAS RK*, *1*, 5–8 [in Russian].

41 Nurkenov, O.A., Fazylov, S.D., Gazaliev, A.M., Satpaeva, Zh.B., Amerhanova, Sh.K., & Karipova, G.Zh. (2017). Sintez i svoistva proizvodnykh hidrazida izonikotinovoi kisloty [Synthesis and properties of derivatives of isonicotinic acid hydrazide]. *Doklady Natsionalnoi akademii nauk Respubliki Kazakhstan. — Reports of NAS RK, 1*, 68–78 [in Russian].

42 Fazylov, S.D., Bakirova, R.E., Nurkenov, O.A., Muravleva, L.E., & Zhakupova, A.N. (2015). The study of the anti-inflammatory activity of thiosemicarbazide N-morpholinyl acetic acid. *Georgian Medical News, 3*, 88–102.

43 Nurkenov, O.A., Fazylov, S.D., Satpaeva, Zh.B., Turdybekov, K.M., Muldahmetov, M.Z., Shulgau, Z.T., Salkeeva, L.K., Talipov, S.A. (2014). Kondensatsiia N-morfolinil-uksusnoi kisloty s dikarbonilnymi soedineniiami [Condensation of N-morpholinyl acetic acid with dicarbonyl compounds]. *Izvestiia NAN RK. Seriia khimii i tekhnolohii. — News of NAS RK*, *2*, 3–7 [in Russian].

АВТОРЛАР ТУРАЛЫ МӘЛІМЕТТЕР
СВЕДЕНИЯ ОБ АВТОРАХ
INFORMATION ABOUT AUTHORS

Abeuova, E.B. — Teacher of the first category of school-gymnasium No. 102 of Karaganda, Kazakhstan.

Abeuova, S.B. — PhD, Senior lecturer, Department of inorganic and technical chemistry, Ye.A. Buketov Karaganda State University, Kazakhstan.

Ainabayev, A.A. — Researcher of the laboratory of the engineering profile «Physical and chemical methods of research», Ye.A. Buketov Karaganda State University, Kazakhstan.

Arrous, S. — PhD student, Faculty of organic chemistry, Tomsk State University, Russian Federation.

Bakibayev, A.A. — Doctor of chemical sciences, Professor, Tomsk State University, Russian Federation.

Bekturganova, A.Zh. — PhD, Department of inorganic and technical chemistry, Ye.A. Buketov Karaganda State University, Kazakhstan.

Bolde, A. — Master student, Faculty of organic chemistry, Tomsk State University, Russian Federation.

Borsynbayev, A.S. — Researcher of the laboratory of the engineering profile «Physical and chemical methods of research», Ye.A. Buketov Karaganda State University, Kazakhstan.

Boudebouz, I. — PhD student, Faculty of organic chemistry, Tomsk State University, Russian Federation.

Chirkova, V.Yu. — Senior lecturer, Department of physico-chemical biology and biotechnology, Altai State University, Barnaul, Russian Federation.

Dorozhko, Ye.V. — PhD, Associate professor of the Department of chemical engineering, School of natural resources, Tomsk Polytechnic University, Russian Federation.

Dyorina, K.V. — Assistant of the Department of chemical engineering, School of natural resources, Tomsk Polytechnic University, Russian Federation.

Dyussekeyeva, A.T. — Candidate of chemical sciences, Associate professor of the Department of inorganic and technical chemistry, Ye. A. Buketov Karaganda State University, Kazakhstan.

Fazylov, S.D. — Doctor of chemical sciences, Professor, Institute of organic synthesis and coal chemistry of the Republic of Kazakhstan, Karaganda, Kazakhstan.

Gashevskaya, A.S. — Graduate student of the Department of chemical engineering, School of natural resources, Tomsk Polytechnic University, Russian Federation.

Gusar, A.O. — Engineer, Department of chemical engineering, School of natural resources, Tomsk Polytechnic University, Russian Federation.

Iskanderov, A.N. — Master of pedagogical sciences, PhD student, Inorganic chemistry and technical Department, Ye.A. Buketov Karaganda State University, Kazakhstan.

Issayeva, A.Zh. — Master of science, Researcher of the Laboratory of synthesis of biologically active substances, Institute of organic synthesis and coal chemistry of the Republic of Kazakhstan, Karaganda, Kazakhstan.

Ishmuratova, M.Yu. — Candidate of biological sciences, Professor, Ye.A. Buketov Karaganda State University, Kazakhstan.

Kabdrakhmanova, S.K. — Candidate of technical sciences, Chief researcher of the Laboratory of engineering profile, K.I. Satpayev Kazakh National Research Technical University, Institute of polymer materials and technology, Almaty, Kazakhstan.

Kaikenov, D.A. — Researcher of the Laboratory of the engineering profile «Physical and chemical methods of research», Ye.A. Buketov Karaganda State University, Kazakhstan.

Kassenov, B.K. — Doctor of chemical sciences, Professor, Head of the Laboratory of thermochemical processes, Abishev Chemical-Metallurgical Institute, Karaganda, Kazakhstan.

Kassenova, Sh.B. — Doctor of chemical sciences, Professor, Chief researcher of the laboratory of thermochemical processes, Abishev Chemical-Metallurgical Institute, Karaganda, Kazakhstan.

Kasymova, M.S. — Candidate of chemical sciences, Assistant professor of the Department of physical and analytical chemistry, Ye.A. Buketov Karaganda State University, Kazakhstan.

Kenzhetayeva, S.O. — Candidate of chemical sciences, Professor, Organic chemistry and polymers department, Ye.A. Buketov Karaganda State University, Kazakhstan.

Kopylov, N.I. — Doctor of technical sciences, Professor, Institute of solid state chemistry and mechanochemistry of the Siberian branch of the Russian Academy of sciences, Novosibirsk, Russian Federation.

Korotkova, E.I. — Doctor of chemical sciences, Professor, Department of chemical engineering, Engineering school of natural resources, Tomsk Polytechnic University, Russian Federation.

Kuanyshbekov, E.E. — Master of technical sciences, Leading engineer of the Laboratory of thermochemical processes, Abishev Chemical-Metallurgical Institute, Karaganda, Kazakhstan.

Kudaibergenov, S.E. — Doctor of chemical sciences, Professor, Director, Institute of polymer materials and technology, Head of the Laboratory of engineering profil, K.I. Satpayev Kazakh National Research Technical University, Almaty, Kazakhstan.

Lipskikh, O.I. — Associate professor of the Department of chemical engineering, Engineering school of natural resources, Tomsk Polytechnic University, Russian Federation.

Lyapunova, M.V. — PhD student, Faculty of organic chemistry, Tomsk State University, Russian Federation.

Merkhatuly, N. — Doctor of chemical sciences, Professor, Head of the Inorganic and technical chemistry department, Ye.A. Buketov Karaganda State University, Kazakhstan.

Minayeva, Ye.V. — Candidate of chemical sciences, Assistant professor of the Organic chemistry and polymers department, Ye.A. Buketov Karaganda State University, Kazakhstan.

Muldakhmetov, Z.M. — Academician of the National Academy of Sciences of the Republic of Kazakhstan, Honored scientist of the Republic of Kazakhstan, Doctor of chemical sciences, Professor, Director of the Institute of organic synthesis and coal chemistry of RK, LLP, Karaganda, Kazakhstan.

Muslimova, D.M. — MSc, Teacher of the Department of inorganic and technical chemistry, Ye. A. Buketov Karaganda State University, Kazakhstan.

Mustafin, E.S. — Doctor of chemical sciences, Professor, Head of the Laboratory of the engineering profile «Physical and chemical methods of research», Ye.A. Buketov Karaganda State University, Kazakhstan.

Naushabekova, D.D. — MSc, Teacher of the Department of inorganic and technical chemistry, Ye.A. Buketov Karaganda State University, Kazakhstan.

Nikolaeva, A.A. — Postgraduate student, Department of chemical engineering, Engineering school of natural resources, Tomsk Polytechnic University, Russian Federation.

Nurkenov, O.A. — Doctor of chemical sciences, Professor, Head of the Laboratory of synthesis of biologically active substances of the Institute of organic synthesis and coal chemistry of the Republic of Kazakhstan.

Omarova, A.T. — Master of pedagogical sciences, Senior lecturer of Inorganic chemistry and technical department, Ye.A. Buketov Karaganda State University, Kazakhstan.

Pudov, A.M. — Candidate of biological sciences, Researcher of the Laboratory of the engineering profile «Physical and chemical methods of research», Ye.A. Buketov Karaganda State University, Kazakhstan.

Pudov, I.M. — Engineer of the Laboratory of engineering profile «Physico-chemical methods of research», Ye.A. Buketov Karaganda State University, Kazakhstan.

Rustembekov, K.T. — Corresponding member of the Kazakhstan National Academy of Natural sciences (KazNANS), Doctor of chemical sciences, Professor of Inorganic and technical chemistry department, Ye.A. Buketov Karaganda State University, Kazakhstan.

Sadyrbekov, D.T. — Researcher of the Laboratory of the engineering profile «Physical and chemical methods of research», Ye.A. Buketov Karaganda State University, Kazakhstan.

Sagintaeva, Zh.I. — Candidate of chemical sciences, Associate professor, Leading researcher of the Laboratory of thermochemical processes, Abishev Chemical-Metallurgical Institute, Karaganda, Kazakhstan.

Seilkhanov, O.T. — Master physicist, Deputy Head of the Laboratory of engineering profile of NMR spectroscopy, Kokshetau State University named after Sh. Ualikhanov.

Seilkhanov, T.M. — Candidate of chemical sciences, Full Professor, Head of the Laboratory of engineering profile of NMR spectroscopy, Kokshetau State University named after Sh. Ualikhanov.

Shakhvorostov, A.V. — PhD student, K.I. Satpayev Kazakh National Research Technical University, Institute of polymer materials and technology, Almaty, Kazakhstan.

Sharlayeva, Ye.A. — Candidate of biological sciences, Associate professor of the Department of ecology, biochemistry and biotechnology, Altai State University, Barnaul, Russian Federation.

Stas, I.Ye — Candidate of chemical sciences, Associate professor, Department of physical and inorganic chemistry, Altai State University, Barnaul, Russian Federation.

Suleimen, Ye.M. — Candidate of chemical sciences, PhD, Associate professor of Chemistry department, Director of the Institute of applied chemistry, L.N. Gumilyov Eurasian National University, Nur-Sultan, Kazakhstan.

Toleutay, G. — PhD student, K.I. Satpayev Kazakh National Research Technical University, Institute of polymer materials and technology, Almaty, Kazakhstan.

Tussupbekova, E.K. — MSc, Senior teacher of the Kazakh language and culture department, Karaganda State Technical University, Kazakhstan.

Vlasova, L.M. — Candidate of chemical sciences, Associate professor, Karaganda Medical University, Kazakhstan.

Vojtíšek, P. — Associate Professor, RNDr., CSc., Department of Inorganic Chemistry, Faculty of Science, Charles University, Prague, Czech Republic.

Zhanzhaxina, A.Sh. — PhD student, the Institute of applied chemistry, L.N. Gumilyov Eurasian National University, Nur-Sultan, Kazakhstan.

Zhokizhanova, S.K. — Candidate of chemical sciences, Senior lecturer of the Department of physics and chemistry, S. Seifullin Kazakh Agrotechnical University, Nur-Sultan, Kazakhstan.